

S.N.A.K.E.: A Dynamically Reconfigurable Artificial Sensate Skin

by

Gerardo Barroeta Pérez

B.Sc. Electrical Engineering

Instituto Tecnológico y de Estudios Superiores de Monterrey (2002)

Submitted to the Program in Media Arts and Sciences,
School of Architecture and Planning,
in partial fulfillment of the requirements for the degree of

Master of Science in Media Arts and Sciences

at the

MASSACHUSETTS INSTITUTE OF TECHNOLOGY

September 2006

© Massachusetts Institute of Technology 2006. All rights reserved.

Author _____
Program in Media Arts and Sciences
August 11, 2006

Certified by _____
Joseph A. Paradiso
Associate Professor of Media Arts and Sciences
Program in Media Arts and Sciences
Thesis Supervisor

Accepted by _____
Andrew B. Lippman
Chair, Departmental Committee on Graduate Students
Program in Media Arts and Sciences

S.N.A.K.E.: A Dynamically Reconfigurable Artificial Sensate Skin

by

Gerardo Barroeta Pérez

Submitted to the Program in Media Arts and Sciences,
School of Architecture and Planning,
on August 11, 2006, in partial fulfillment of the
requirements for the degree of
Master of Science in Media Arts and Sciences

Abstract

The idea of an *Artificial Sensate Skin* device that mimics the characteristics and functions of its analogous living tissue whether human or animal is not new. Yet, most of the current related work has been focused in the development of either materials, flexible electronics or ultra-dense sensing matrices and Wide Area Sensor Networks. The current work describes the design and implementation of a new type of Artificial Sensate Skin. This Artificial Sensate Skin is implemented as a low-power, highly scalable and mechanically flexible Wired Sensor Network. This Skin is composed of one or many *Skin Patches* which in turn are composed of one or many *Skin Nodes*. Each node is able to measure Strain, Pressure, Ambient Light, Pressure, Sound and Mechanoreception. Each Skin Patch can either work as a stand-alone device or as a data extraction device if this is attached to a Personal Computer through a different type of device referred to as *Brains*. Each Skin Node and therefore each Skin Patch is *Dynamically Adaptable* meaning that they can adapt to external stimuli by either modifying their behavior or by completely changing their code. Construction of a sensate skin in such a modular fashion promises intrinsic scalability, where peer-to-peer connections between neighbors can reduce local data, which can then be sent to the brain by the high-speed common backbone. The current project also involves the design and implementation of the software components needed; these include a PC Graphical User Interface, application software and the firmware required by the embedded microcontrollers. Results show that needed resources like bandwidth are greatly minimized because of the addition of embedded processing power. Results also indicate that the platform can be used as a scalable smart material to cover interactive surfaces, or simply to extract a rich set of dense multi-modal sensor data.

Thesis Supervisor: Joseph A. Paradiso

Title: Associate Professor of Media Arts and Sciences, Program in Media Arts and Sciences

S.N.A.K.E.: A Dynamically Reconfigurable Artificial Sensate Skin

by

Gerardo Barroeta Pérez

The following people served as readers for this thesis:

Thesis Reader_____

V. Michael Bove
Principal Research Scientist
Program in Media Arts and Sciences

Thesis Reader_____

Cynthia Breazeal
Associate Professor of Media Arts and Sciences
MIT Media Lab

Acknowledgments

To **Joe Paradiso** for giving me the opportunity of living two of the best years of my life. For his unquestioning support, flawless technical advice and invaluable friendship.

To **V. Michael Bove**, J. and **Cynthia Breazeal** for providing the necessary extra pairs of critical eyes without which this work would not have been what it is.

To my colleagues: **Ryan Aylward**, **Matt Laibowitz**, **Mark Feldmeier**, **Ari Benbasat**, **Matt Malinowski** and **Josh Lifton**, for their huge help throughout these years.

To all of the Media Lab, especially to **Linda Peterson** for helping me through difficult times and to **Lisa Lieberman** for making things happen.

To my mother for making me what I am. To my father for showing me the path. To my sister for always being there. To my grandparents for constantly reminding me to enjoy the really important things in life.

To my friends a very special thanks, you were the my family away from home. It was only because of you that these two years were the best. Thank you **Rogelio**, **Ricardo**, **David**, **Javier**, **Pepe**, **Federico**, **Fernando**, **Christos**, **Rocio**, **Sendi**, **Vik**, **Ernesto**, and countless others with which I shared one of many, many great moments.

To everybody at the **Graduate Student Council** for giving me so much for so little. Thank you Emmily, Sylvain, Emmi, Shan and everybody else at the Orientation Committee.

To my Media Lab colleagues, **Ernesto Arroyo**, **Ernesto Martinez**, **Ayah**, **Vincent**, and many others for their friendship, sense of humor and brilliant discussions.

To **Pioneer Circuits** for their fabrication expertise

And finally,

To **Telmex**, for making it possible.

Table of Contents

Abstract	3
Acknowledgments	7
List of Figures	11
List of Tables	15
1 Introduction	17
1.1 Problem Definition and Motivation	18
1.2 Synopsis	19
1.3 System Overview	20
2 Artificial Sensate Skins	23
2.1 Artificial Sensate Skins	23
2.1.1 Sensor Networks as Sensate Skins	24
2.1.2 Ultra-dense Sensor Arrays	30
2.2 Flexible Circuits	32
2.2.1 Flex Technology	32
2.2.2 Other Technologies	34
3 Hardware	35
3.1 Design Philosophy	35
3.2 Network Design	37
3.2.1 I2C Backbone	38
3.2.2 Peer to Peer	42
3.2.3 USB PC link	42
3.3 Nodes	43
3.3.1 Substrate Design	44
3.3.2 Power Circuitry	54
3.3.3 Processor	55
3.3.4 Sensing Modalities and Actuation	58
3.4 Brain	73
3.4.1 Processor unit	74
3.4.2 Power unit	75

3.4.3	Communications unit	76
4	Software	79
4.1	Firmware	79
4.1.1	Bootloader	81
4.1.2	Sampling Code	86
4.1.3	Node Application Code	89
4.1.4	Brain	90
4.2	PC Graphical User Interface	92
4.2.1	Network detection	93
4.2.2	Programming	95
4.2.3	Sampling and Display	97
4.2.4	Other Functions	100
4.3	Communications Software	101
4.3.1	I2C Backbone	101
4.3.2	Peer to Peer	103
4.3.3	USB	104
5	Analysis of Results and Evaluation	105
5.1	Mechanical Stability	105
5.1.1	Substrate	106
5.1.2	Connections	107
5.1.3	Pressure Sensors	108
5.2	Sensor Data and Sensing Ranges	109
5.2.1	Skin Patches as Data-extraction Devices	109
5.2.2	Skin Patches as Stand-alone Devices	130
5.3	Performance Metrics	133
5.3.1	Network Performance	133
5.3.2	Power Consumption	136
5.3.3	Cost	139
6	Conclusions and Future Work	141
6.1	Conclusions	141
6.2	Possible Applications	143
6.3	Future Work	144
A	Abbreviations and Symbols	147
B	Bill of Materials	149
C	Schematics and PCB Layouts	151
D	Firmware	167
E	PC Code	183
	Bibliography	207

List of Figures

2-1	Created by MIT Media Lab's Responsive Environments group, Tribble is a Distributed Sensor Network that works like an Artificial Sensate Skin . . .	25
2-2	Leonardo's Hand	26
2-3	Pushpin Computing Platform	27
2-4	Dense sensor arrays as artificial skins	29
2-5	Dense sensor arrays as artificial skins	31
2-6	Types of Flex circuits[46]	34
3-1	S.N.A.K.E. Skin Network Topology	37
3-2	Skin Patch modes of operation	38
3-3	I ² C Routing pattern	40
3-4	I ² C Active pull-up devices	41
3-5	Flex Nodes	43
3-6	Node substrate material stack	45
3-7	Flex circuit cost as a function of fabrication complexity[46]	47
3-8	Rigid node prototype	48
3-9	Skin Patch mechanical terminations	50
3-10	Node with electrical components being flexed	51
3-11	Routing techniques	53
3-12	Power components	56
3-13	Microcontroller with programming header	57
3-14	Strain gage layer prototype	62
3-15	Wheatstone bridge used for Strain gage conditioning	65
3-16	QTC response curve for a QTC pressure sensor[52]	66
3-17	QTC pressure sensors	68
3-18	QTC pressure sensors	69
3-19	Toshiba TPS851/52 Ambient Light Sensors	71
3-20	Brain	74
4-1	Bootloader memory map	83
4-2	Bootloader Flow Chart	84
4-3	Sampling timing example	87
4-4	GUI Components	92
4-5	Automatic configuration of Brains	95
4-6	GUI Programming Environment	96

4-7	Programming packet	96
4-8	Visualization: OpenGL 3D chart transformation modes	99
5-1	Stress concentration points in node microcontrollers	107
5-2	Skin Patch bending profile	108
5-3	Strain Gage electronic calibration for gages 1 and 2 of node #004-3	117
5-4	Real-time 3D visualization control showing offset from each one of the two strain gages of all nodes (no stimuli applied)	118
5-5	Strain gage data plots showing strain gage response	119
5-6	Pressure sensor calibration	120
5-7	Real-time 3D visualization control showing data from each one of the four pressure channels of all nodes	121
5-8	Pressure data plots showing pressure sensor response	122
5-9	Real-time 3D visualization control showing data from different lightning conditions.	124
5-10	Light data plots showing ambient light sensor responses to different stimuli	126
5-11	Temperature sensor response	127
5-12	Raw microphone data with superimposed moving averages. Window size was 32 samples. Each plot corresponds to a vowel spoken in front of the microphone.	129
5-13	Activity sensor results	131
5-14	Patch used as a stand-alone device. LED's light according to the amount of ambient light	132
5-15	Difference in speed for both I ² C lines when active and passive pull-up devices are used.	135
C-1	Node Sensing Suite	152
C-2	Node Processing	153
C-3	Node Dimensions (mils)	154
C-4	Node Full Routing Stack	155
C-5	Node Top Routing Layer	156
C-6	Node Internal Layer 1	157
C-7	Strain Gages (Internal Layer 2)	158
C-8	Node Bottom Routing Layer	159
C-9	Node Top Overlay	160
C-10	Node Bottom Overlay	161
C-11	Brain Processing	162
C-12	Brain Communications	163
C-13	Brain Dimensions (mils)	164
C-14	Brain Top Layer	165
C-15	Brain Bottom Layer	166
D-1	Bootloader Source Code	168
D-2	Node Sampling Firmware	171
D-3	Light Gradients Application	175
D-4	Blinking Application Code	177
D-5	Brain Firmware	179

E-1	OpenGL Control Header File	184
E-2	Resource.h Header File	185
E-3	StdAfx.h Header File	186
E-4	USBtest.h Header File	187
E-5	USBtestDlg.h Header File	188
E-6	OpenGLControl.cpp Source Code	190
E-7	USBtest.cpp Source Code	195
E-8	USBtestDlg.cpp Source Code	196

List of Tables

3.1	Material thicknesses and standards	46
4.1	Bootloader Instructions	83
4.2	Bootloader Status Byte Flags	85
4.3	Sensor sampling rates and resolution	88
4.4	Brain Instructions	91
4.5	GUI Components	93
5.1	Strain gage measured resistances	111
5.2	Resistances needed to simulate 100 microstrain	114
5.3	Emulated strain caused by shunting gages with an $812K\Omega$ resistor	115
5.4	Calibration results	116
5.5	Power consumption of Skin Node components	137
B.1	Bill of Materials	150

Chapter 1

Introduction

“Imagination is the beginning of creation. You imagine what you desire, you will what you imagine and at last you create what you will. ”

– *George Bernard Shaw*

The integumentary system or in other words, our skin is perhaps one of the most versatile organs in the human body. Our skin is not only a protective layer that shields us from the harshness of the environment, it has many other functions that enable us to survive and communicate. These functions include: Interaction with surrounding environment; Regulation of body temperature; Storage of energy as fat; Excretion of body waste through sweat; Absorption of substances like medicines and oxygen and finally, Alert through multimodal sensations and several forms of physical pain[72].

The human skin is also the largest organ in the human body with the average person having over 20 square feet of skin. From a mechanical point of view it is an amazing material: it is able to regenerate itself from wear and tear (cuts), it is flexible, contractible and expandable and it is able to withstand erosion, mechanical stress and swift temperature changes like few other known materials [20],[36].

From a sensing perspective, the human skin is also quite remarkable. By using different kinds of receptors, it is able to sense touch, vibration, pressure, shear, stretching, temperature

(hotness or coolness), mechanoreception by using hair, and several different forms of physical pain[56]. In summary, our skin is much more than a protective surface as it allows us to interact with other people as well as with our physical environment.

If we take into account the aforementioned characteristics and functions of the human skin, it comes as small wonder why people have been trying to emulate it as close as possible. The development of an Artificial Sensate Skin makes economical sense if we consider the huge amount of its potential applications. Some may be evident at first, like using it to increase the autonomy of robots or monitoring a physical quantity in a scientific experiment; others might require more thought, yet the possibilities are endless. Everything from space exploration and aircraft control, to motion capture, patient care, surveillance and even recreation will benefit from a device that closely resembles our skin[43].

1.1 Problem Definition and Motivation

The idea of an Artificial Sensate Skin is anything but new; the literature containing work related to the fields touched on this Thesis, namely Sensor Networks, their associated protocols and Artificial Skins, is vast and broad. It covers the entire span of the technological abstraction layers from microfabrication to software simulations. However, two general trends can be observed as described by Paradiso in [50]: Either they are implemented as dense sensing matrices where individual sensors have to be individually routed to a concentrator or *Central Processing Unit*, or as completely de-centralized Sensor Networks.

This has led to the development of either sensor technologies that are ultra dense in nature such as capacitive fabrics or densely packed VLSI sensor matrices (like CCDs), or extremely distributed like Smart dust that cover areas as large as a city or even more. In the former case, bandwidth can become a problem because of the immense amount of data generated. This kind of sensor must have a dedicated processing unit to be able to operate the sensor matrix. In the second case, because of the distance between nodes and the large areas involved, they are very difficult to use in applications where the stimuli of interest is restricted to smaller areas, probably not larger than a room.

The current project, named S.N.A.K.E Skin or *Sensor Network Array Kapton Embedded Skin*, attempts to attack these problems by having a mixture of both worlds. To do this, two things are done: first, each node is given processing power so that data can be processed locally; second, nodes are brought much closer together, just about enough so that they can be connected to each other to create a skin-like surface that can react to the same kinds of stimuli that our skin encounters.

Furthermore, the addition of processing power enables each node to calculate higher order features, so that if a central unit like a PC needs to extract data from the network, these higher order parameters, like shadow forms and pressure gradients, can be transferred instead of raw data, which saves network resources.

Therefore, the statement of the project goal can be now stated as follows:

To explore and develop a deeper understanding of the different design approaches and technical constraints involved in the fabrication and implementation of a Sensor Network that emulates some of the sensory characteristics and functionality of the Human Skin.

1.2 Synopsis

This work is divided into six chapters. The current chapter gives a general introduction by providing the motivation behind the project, the problem that it is trying to attack, and a general overview of the system developed for such a purpose.

Chapter 2 provides some background work. This chapter will briefly talk about various technologies, projects and ideas in this area that ground the current project.

Chapter 3 describes in detail the Hardware system designed for the project. This chapter is divided into four sections. The first one outlines the design directives followed throughout the entire design of the project. The second one talks about the topology of the S.N.A.K.E. Sensor Network. The third section describes the design of the substrate used for the nodes. The last section describes the design of the Brains.

Chapter 4 talks about the different Software components that had to be developed. This chapter is subdivided into three sections. The first one details the specifics of the Firmware components developed for the embedded processors. The second section describes the PC software that works as a front end to manage the Skin Patches. Finally the last section talks about the details of the communications software.

Chapter 5 details the Results generated by the entire project. This chapter is also subdivided into three main sections. The first one gives the mechanical results of the hardware platform and describes how well they performed. The second presents all the results of the different sensing modalities and modes of operation of the Skin Patches, along with sensor performance and data plots. The last section gives a set of performance metrics under which the entire project performance was judged.

The last part, **Chapter 6**, gives the conclusions derived from the Results Chapter, while also giving some suggestions for possible applications and future work.

1.3 System Overview

Now, a brief system overview of the entire project is provided to give a broad idea of the different components that will make up the S.N.A.K.E. Skin system. For a more detailed treatment of the different components, the reader is advised to read Chapters 3 and 4.

Based on the problem definition and motivations set up before, the current work will therefore focus on the design and implementation of a novel type of sensor network that inherits a subset of the characteristics of the human skin. As such, this Artificial Sensate Skin, will be implemented in a *flexible substrate* as a dense, low-power, and dynamically adaptable Wired Sensor Network. Its design also contemplates that it will be highly scalable and portable, so that it can be formed and “grown” to cover surfaces of different shapes and sizes.

Hardware

Each *Skin Patch* is composed of one or many *Skin Nodes*, each of which is capable of sensing six different physical quantities. Each node is also given processing power, a direct connection to its immediate neighbors, and a connection to a fast backbone bus. Finally, nodes are capable of actuating through the use of an on-board, multi-color LED. This means that each node is an independent and autonomous entity within the Sensor Network.

Data extraction and network management is done through a different entity: the *Brains*. These devices ensure the reliability of the network and deal with administrative tasks like network re-programming, data collection, and overall synchronization. They also arbitrate the use of the backbone bus.

Software

Several different Software components were also created to control the network. First, since each node is capable of changing its behavior by changing its code, application software and a simple Operating System were created. Second, application firmware was developed to indicate the nodes when and how to obtain data from its sensing channels. Finally, a graphical front end was developed so that a personal computer can be used to gather data and control the network.

Chapter 2

Artificial Sensate Skins

“We stand on the shoulders of giants.”

– *Bernard of Chartres*

Following the Introduction, the current chapter talks about several previous projects that in some way or another, inspired or contributed to the idea on which this project is based. Given the Sensor Network nature of the project, the design choices draw heavily upon several different types of technologies that are briefly outlined in this chapter. The first section highlights some of the similarities and differences of several types of Sensor Networks. These were subdivided into two different types according to the level of integration of their sensing elements into *Sensor Networks as Sensate Skins* and *Ultra-dense Sensor Arrays*. The second section talks about other technologies that are also related to this project but had much less influence. These are mentioned so that the current project can be then established within the broader context of its technological field.

2.1 Artificial Sensate Skins

The concept of “Artificial Sensate Skins” refers to a very specific type of device that in some way or another, try to copy either the functionality or appearance (or both) of its analogous

living tissue. Particularly in the projects from the Media Lab’s Responsive Environments Group, these devices are generally implemented as a Sensor Networks in which several smart sensing elements or nodes are capable of extracting information from the environment.

Although there have been several projects that have attempted to do this, their approaches have been extremely different from each other, the main difference being the amount of integration between sensing elements, and their density. Let us now describe each one of them in detail, so that their relationship to the current project can be better understood.

2.1.1 Sensor Networks as Sensate Skins

The main characteristic of these devices is that the level of integration of their sensors and their density is not as high as with Dense Sensor Arrays but it is much greater than for typical Wireless Sensor Networks. Much of the work related to these Artificial Sensate Skins was either pioneered or heavily developed by faculty and students at the MIT Media Lab. In fact there are three projects that are very closely related to the one presented in this document, and therefore, not only served as major sources of inspiration, but were valuable sources of experience from which this project drew from.

This section will then attempt to summarize the contributions of these three projects along with a selected few from outside of the Media Lab by emphasizing their relative strengths and weaknesses compared to the proposed ongoing work.

Artificial Sensate Skins at the MIT Media Lab

Paintable Computer: Perhaps the starting point of the big interest in Artificial Skins and dense Sensor Networks at the Media Lab, was the work of William Butera[6]. In his Ph.D thesis, Butera presents a new programming paradigm for ultra-dense and ultra-miniaturized computing particles, called *Paintable Computing*. He defines Paintable Computing as: “an agglomerate of numerous, finely dispersed, ultra-miniaturized computing particles; each positioned randomly, running asynchronously and communicating locally”. In other words, he

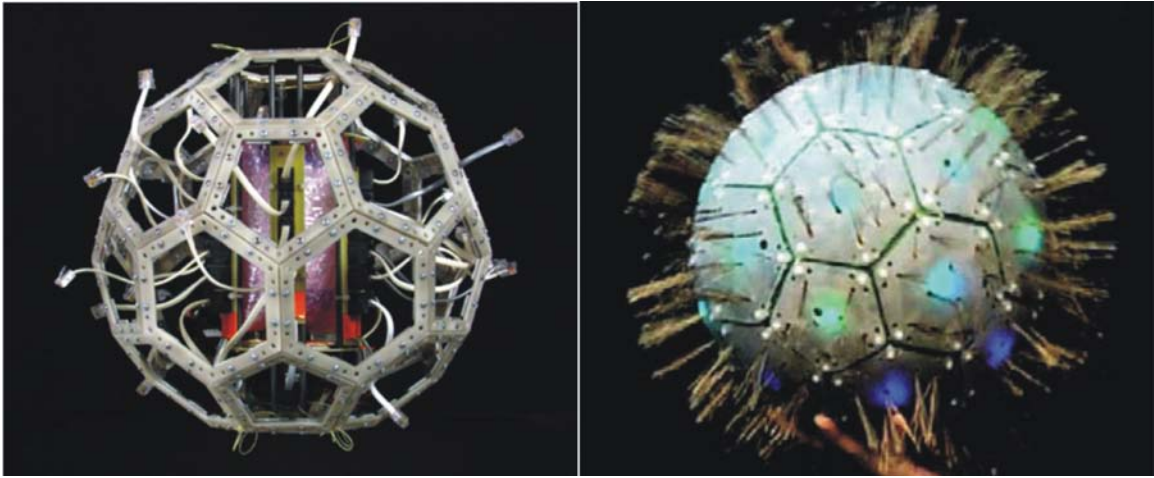


Figure 2-1: Created by MIT Media Lab’s Responsive Environments group, Tribble is a Distributed Sensor Network that works like an Artificial Sensate Skin

presented a plausible processing and communications method for programming an otherwise seemingly chaotic computing platform, and therefore enabled much of the future work that would be developed by other groups at the lab.

Tribble: Based on Butera’s work, and perhaps the most relevant to the work described here was developed at the Responsive Environments Group by Lifton[41] with the name Tribble or *Tactile Reactive Interface Built By Linked Elements*. Tribble is a dense, multi-modal and peer-to-peer Sensor Network assembled as a plastic sphere that is made up of tiles or Skin Patches resembling a soccer ball. Tribble is shown on Figure 2-1. This was

Each of its nodes is capable of routing data to its neighbors, and it was created as a completely decentralized Sensor Network. Moreover, each one of the nodes is capable of processing its own generated data without the need of a centralized processing unit. It has however, several design characteristics that make it somewhat inflexible and difficult to adapt. First of all, its shape is fixed to that of a sphere-shell-like object, which obviously prevents its from being used to wrap arbitrarily shaped objects.

The second design problem is that even its smaller node is somewhat large, which means that it is difficult to achieve high sensing density. It is also power hungry, heavy and stiff; yet Tribble not only set the standard by which this project is measured, but it was also a



Figure 2-2: Leonardo's Hand

great hardware test-bed in which some of the already existing sensor network algorithms were tested. In short, Tribble is the foundation of the current project and in fact many of the design characteristics that will be outlined in Chapter 3 section will heavily draw upon the experience gained from this project.

Sensate Skin: Another Media Lab project that relates to this research was the work done by Daniel Stiehl regarding Sensate Skins for robots[65]. In his Masters Thesis, Stiehl describes a method to give a robot the ability to sense pressure through a silicon skin. Although the goal of his work is similar to that of the current project, Sensate Skin was more concerned with the mechanical and morphological aspects of the skin, so that this could be adapted to the body parts that make up their test robot Leonardo. It can also only sense pressure, and every sensor must be routed to a central processing unit. This can be seen in Figure 2-2.

Pushpin Computing: Also by Lifton [40],[39], at the Responsive Environments group, a Sensor Network platform with the name of *Pushpin Computing* was created. Its intention was to approach the sensor network world from a ground-up perspective by making a testbed with over a hundred peer-to-peer wireless sensor nodes freely distributed across a table-top as opposed to the more typical top-down approach proceeded by software simulations. The

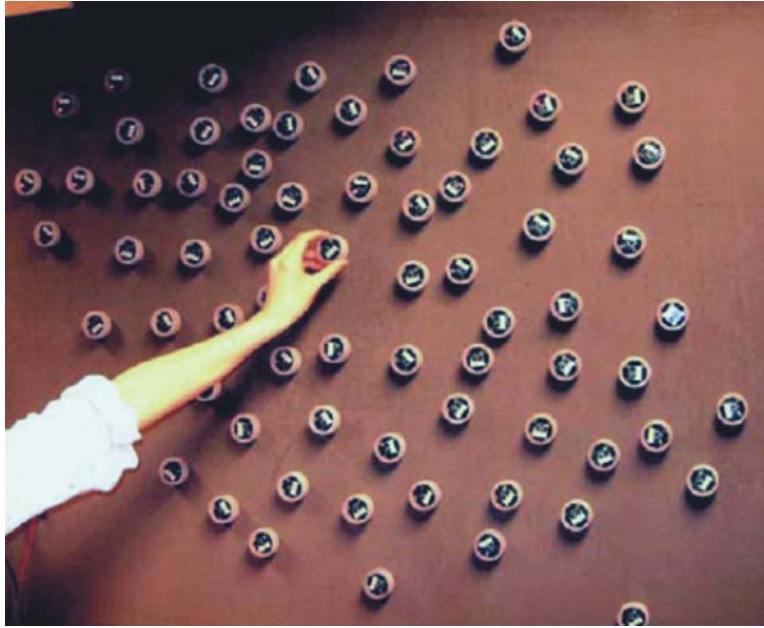


Figure 2-3: Pushpin Computing Platform

Pushpin computing platform is presented in Figure 2-3

This project however, is quite different from that proposed in the current work as it is centered on Sensor Networks and the possible algorithms that can run on the developed platform, rather than on Artificial Sensate Skins. It is also constrained to a fixed rigid substrate and nodes are not directly connected to each other. Still, it is relevant in the sense that it has been a successful attempt to create a dense distributed computing platform in which real applications like shadow tracking and accounts time of flight have been implemented.

Although the S.N.A.K.E. Skin project is not intended to work entirely as a Distributed Sensor Network like the Pushpin platform did, it does attempt to combine the advantages of distributed and centralized processing, so the Pushpin platform proved to be an invaluable source of experience from which the new platform greatly benefited.

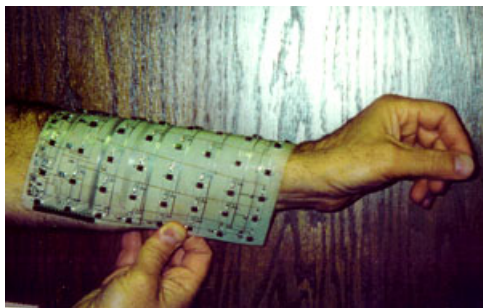
Artificial Sensate Skins elsewhere

The MIT Media Lab is not the only institute interested in such ideas though, and several other similar projects have been created by people outside of the Lab. But perhaps the main supporter of this concept is Dr. Vladimir J. Lumelsky from the University of Wisconsin-Madison. His 2002 article “Sensitive Skin” [43] is essentially a call-to-arms to generate interest in the scientific community, so that devices with characteristics similar to those of the human skin are created. To demonstrate their idea, they created a prototype of a Skin Patch with infrared lights and receivers that were used as proximity sensors. The prototype presented in the article is shown on Figure 2-4(a).

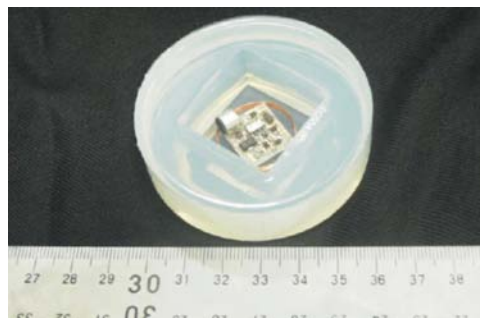
This is not the only recent work outside of the Media Lab though, as many others have attempted different ways to recreating our sense of touch[37][45]. Some of the most relevant works are mentioned in the following list and they can be seen in Figure 2-4.

- Hakoziaki[17] proposes a method to create a flexible robot skin to cover wide robot surfaces (fig. 2-4(b)).
- Yamada[75] shows a way of detecting deformations in a rubber membrane by optical means (fig. 2-4(c)).
- Hritsu[22] proposes a similar way of tracking deformations in a finger-like structure (fig. 2-4(d)).
- D. Um presents in [69] a very similar Sensitive Skin to Tribble, however it lacks local processing power (fig. 2-4(e)).
- Rekimoto introduces a capacitive “Smart Skin” sensor in [58] for its use in interactive surfaces (fig. 2-4(f)).

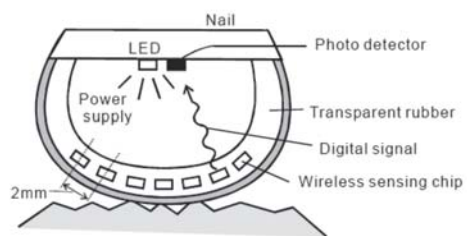
Unlike the work presented earlier, all of these examples rely on a centralized processing unit to process the data extracted from the sensors.



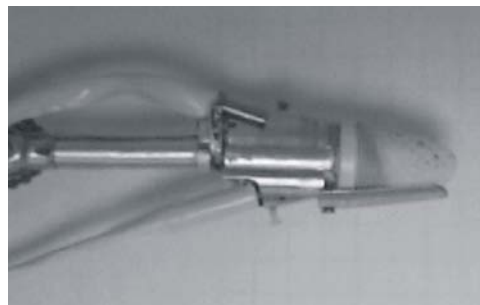
(a) Sensitive Skin by Lumelsky



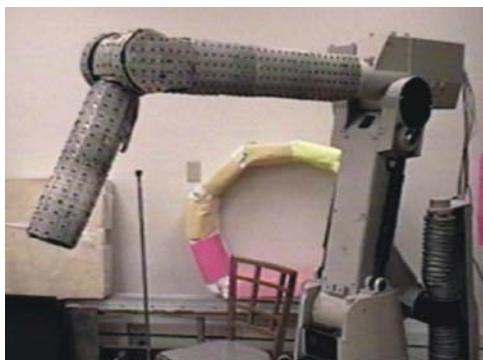
(b) Flexible robot skin by Hakoziaki



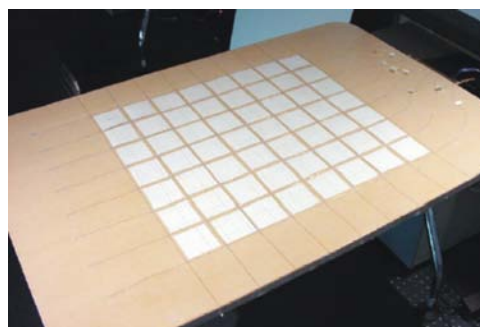
(c) Tactile sensor by Yamada



(d) Tactile sensor by Hritsu



(e) Modularized Sensitive Skin by D. Um



(f) Smart Skin sensor by Rekimoto

Figure 2-4: Dense sensor arrays as artificial skins

2.1.2 Ultra-dense Sensor Arrays

This second category of Artificial Sensate Skins differs from the previous one because of their ultra-high sensor density. The other main difference is that these are also never implemented as sensor networks but rather as sensor matrices. This means that each sensor must be individually routed to a central processing unit. There are numerous works that have developed high-density sensing arrays for their use as Artificial Skins some of which are presented in the following list:

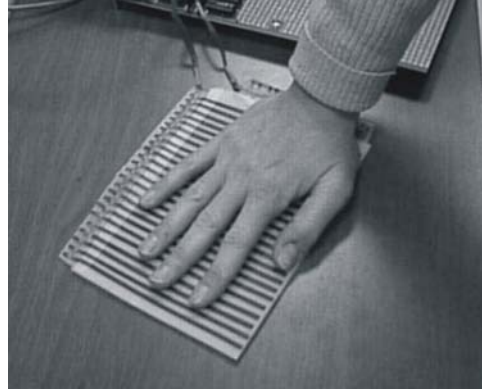
- Takao Someya in [62] presents a large-area flexible sensor matrix with organic field effect transistors (fig. 2-5(a)).
- M. Sergio describes a textile-based capacitive sensor array that can be used as sensitive skin[44] (fig. 2-5(b)).
- Yong Xu, reports an IC-integrated flexible sensor skin that can sense shear stresses for a possible aerospace application[74] (fig. 2-5(c)).
- Papakostas talks about a large-area printable force sensor for smart skin applications based on a piezoresistive effect[49] (fig. 2-5(d)).
- Engel and others[11] talk about a multi-modal flexible skin fabricated with polymer micro-machining methods (fig. 2-5(e)).
- Darren Leigh presents DiamondTouch, a technology to create table-top input devices based on capacitive sensing (fig. 2-5(f)).

The problem with these approaches though is that as sensor density increases, so does the bandwidth required to retrieve information from the sensors. Moreover, a central processing unit is forcefully required because the sensors can't do anything by themselves. In spite of this, these devices are currently the ones that have the greatest physical and functional resemblance to our skin.

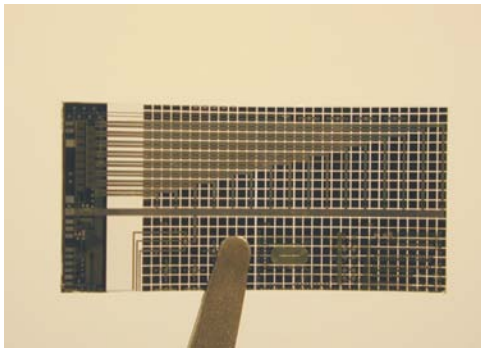
It is also necessary to say that there are several other projects with similar characteristics, however, the previous list only presents a few as a way to exemplify them.



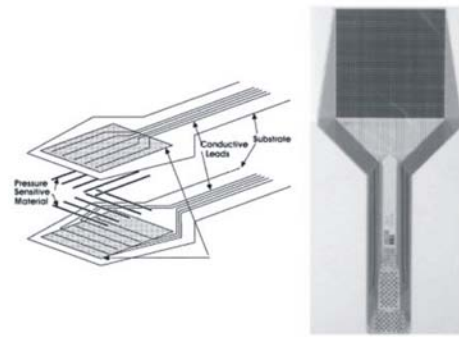
(a) Sensor Matrix by Someya



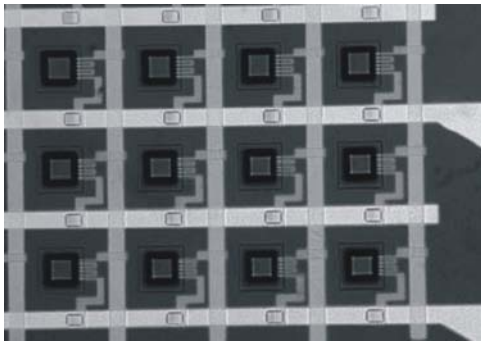
(b) Capacitive-based textile sensor by Sergio M.



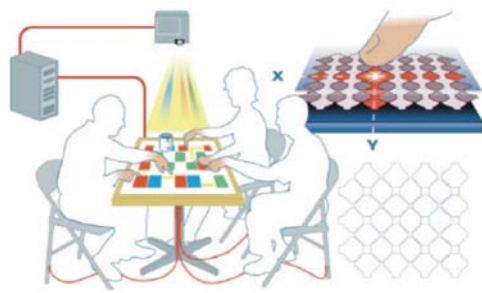
(c) IC-integrated flexible skin sensor by Xu



(d) Large-area force sensor by Papakostas



(e) Engel's Multi-modal flexible skin fabricated with polymer micro-machining techniques



(f) Table-top capacitive input device by Leigh

Figure 2-5: Dense sensor arrays as artificial skins

2.2 Flexible Circuits

Although, not exactly Artificial Skins, the subject of flexible circuits is relevant because of two main reasons: first, most of the reference works presented before use some kind of flex circuit technology, because of its ability to bend and in some cases stretch, in analogy to animal skin. Second because this project will be based on a Sensor Network implemented in flexible nodes fabricated with this technology.

The concept of flexible circuits is not new, actually the concept dates back to 1904[13]. Yet, in spite of their favorable physical characteristics, it wasn't until recently that the use of Flex circuits became more widespread, mainly because the level of integration in today's electronic devices would be impossible without its use. This section is subdivided into two parts. The first one gives a broad overview of the elements of Flex circuit technology. The second one describes other similar technologies that have been recently proposed.

2.2.1 Flex Technology

First of all, what exactly is Flex Technology? From the Handbook of Flexible Circuits by Ken Gilleo[13]: "Flexible circuitry is a patterned array of conductors supported by a flexible dielectric film."

This of course is a very broad definition but it generally refers to any circuit patterned on top of a flexible substrate. It can be as simple as a cable or as complex as the motherboard of a portable computer with several layers made up of different materials. They all however, share some common characteristics, like the thinness of the dielectric materials used for their construction (about $12\mu m$) and their remarkable ability to flex and bend.

The construction of flexible circuits is very different from typical rigid circuits because many different materials can be used for their construction. The following list shows the components that go into the construction of flex circuit boards:

Dielectric Base Film: this is the most important component of a flexible circuit because

it will determine its final mechanical, electrical and chemical properties. These are usually very thin layers of a heat-resistant polymer which serves as the circuit substrate

Conductors: since the mechanical properties of flex circuits are determined by the materials they are built with, several different metal alloys can be used if different mechanical properties of the typical copper films are desired.

Adhesives: if the metal is not electro-deposited onto the substrate, adhesive layers must be used to bond the conductor films to the backing base films.

Platings and Finishes: sometimes conductors are treated with special finishes to keep the conductors from oxidizing and maintain good solderability. Gold platings are also common to increase the overall performance of the conductors.

Protective Surfaces: the majority of circuits are usually covered with protective layers to insulate the conductors from the environment. Other covering finishes like soldermasks are used to keep solder only in the specified areas. In the case of flexible circuits though, special covering layers have to be used so that these don't crack when the circuit is bent.

Material selection is not the only different thing between Flex and rigid circuits. Since Flexible circuits can be conformed to the shape of its container or even constantly flex¹, they are generally constructed very differently than their rigid counterparts. Some of the construction types are shown in Figure 2-6²

These are only a few of the vast amount of fabrication options available. In fact, every manufacturer offers specialized capabilities that can be used to further enhance the functionality of the Flex circuits. Chapter 3 will describe in more detail some of the other fabrication options and the details of the design choices used for the current project.

¹This is generally referred to as Dynamic Flex

²Extracted from Minco's design guide

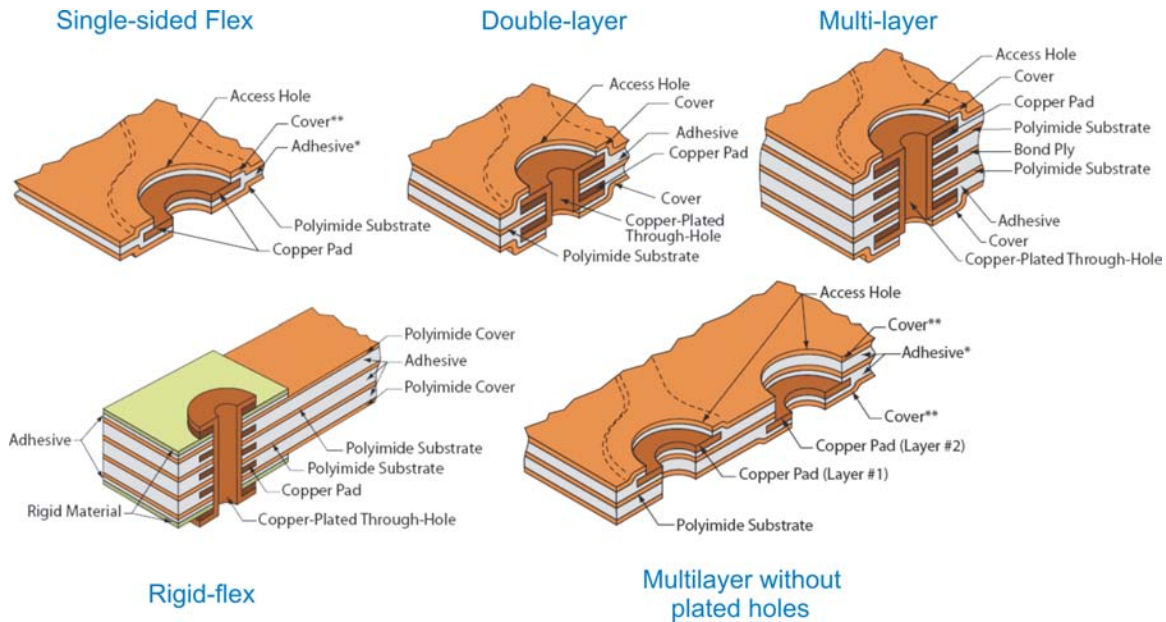


Figure 2-6: Types of Flex circuits[46]

2.2.2 Other Technologies

Flex technology is not the only form of flexible circuitry, however. There are other types of flexible circuits that have been developed for other specific applications, and could be applied to develop an Artificial Sensate Skin.

The most prominent example is perhaps the work done by Stéphanie Lacour[35]. By depositing an ultra-thin gold layer on top of a PDMS substrate she has created a new conducting material that can be stretched much like our own skin.

Other types of flexible circuits are much less related to the area of Artificial Skins like Jacobson's E-paper[33] and printable electronics, but the technologies used to create them might one day also be applied to fabricate an Artificial Sensate Skin. These projects though, are still under research and thus would be better suited for future applications.

Finally, two special issues of IEEE Proceedings (July and August 2005) were devoted to Flexible Electronics.

Chapter 3

Hardware

“Inanimate objects can be classified scientifically into three major categories; those that don’t work, those that break down and those that get lost.”.

– *Russell Baker*

The current chapter describes the hardware system which is the foundation of the project. The System is based on a set of design directives which are outlined first so that the reader can have a better understanding of the design choices made throughout this and upcoming chapters. Once these directives are mentioned, a thorough description of the hardware components along with their selection criteria will be provided. The chapter ends with a brief description of the three different communications channels used by the three hardware devices that make up the system: the *Skin Network*, Network Hubs or *Brains* and an associated Windows[™]based Personal Computer.

3.1 Design Philosophy

As it was mentioned in the previous chapter, the main goal of this project is to create a Sensor Network that emulates some of the functions and mechanical characteristics of the

human skin. The following design principles thus provided the criteria for the selection of materials and electrical components with which the project elements were created:

Scalability: crucial for covering large surfaces, especially if the node size is small.

High Sensor Density: necessary to achieve high sensor resolution.

Sensing Variety: to allow a broader range of applications and to enable the study of the impact that different sensor types would have on available resources.

Robustness: given that the Artificial Sensate Skin was implemented as a Wired Sensor Network, reliability of network components and communications links are essential for good operation of the system.

Low Maintenance: this is so that the Artificial Skin can operate as a “black box” device and to keep the administrative tasks to a minimum.

Mechanical Flexibility: a key point in the design of the Artificial Skin was to make it flexible so that it can be bent and wrapped around arbitrarily shaped objects.

Ultra-low Power Consumption: ultra-low power is also highly desirable, given that as the network grows, the number of network nodes grows quadratically and so potentially does power consumption.

Small Node Footprint: goes hand by hand with high sensor density; the smaller the footprint with the same number of sensors per node, the higher the density and therefore resolution for a given covered area.

It is important to note that even though the *Skin Network* contains a high speed serial communications backbone, “high speed” is not mentioned as a main design point because of two reasons: first, one of the goals of the project *is* to prove that it is possible to limit the network traffic¹ by including processing power into every node in the Skin. And second, the project will also try to provide clues that will help to understand how the inclusion of

¹And therefore reduce the overall resources needed to manage a large Skin Network

different sensing modalities will affect the necessary bandwidth that such a system would require.

3.2 Network Design

The high-level design for the Skin follows that of a Sensor Network based on a star network topology. Each spoke of the star is composed of a concentrator node or *Brain* that manages a *Skin Patch* made up of n nodes. The Skin Patches or sub-networks are based on a mesh topology with the addition of a backbone bus. Figure 3-1 shows the Skin Network Topology.

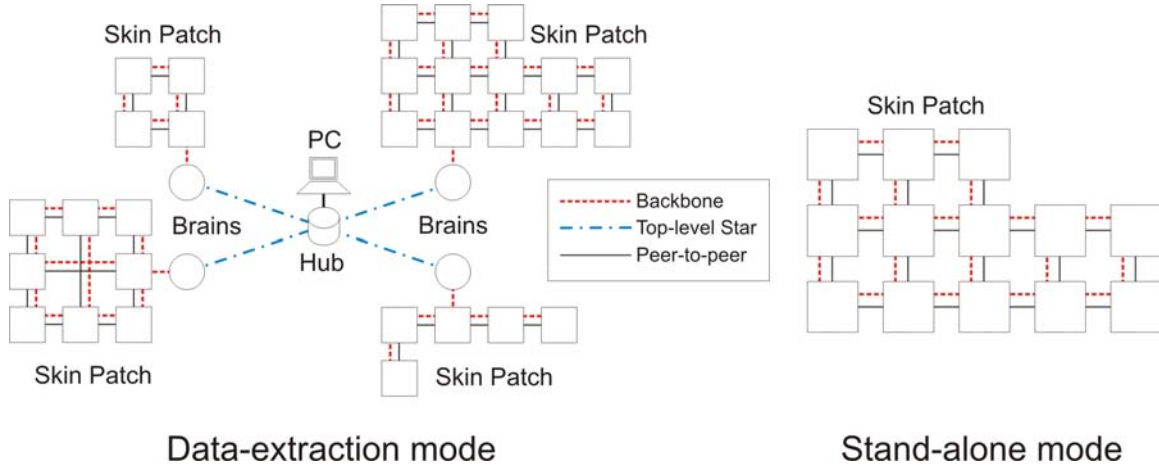
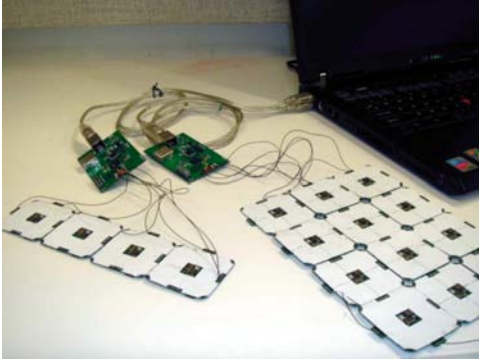


Figure 3-1: S.N.A.K.E. Skin Network Topology

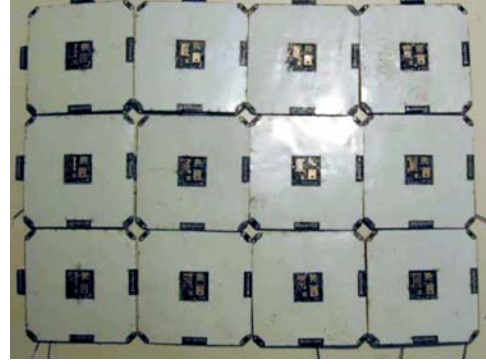
This approach guarantees the scalability of the system at both network levels. Each patch of skin can be made of any arbitrary size² without affecting other patches, and at the same time multiple patches of skin can be connected together through their brains to a PC.

This in no way means that a Skin Patch can't be used without a PC connected or even a Brain. Having processing power in each node gives them the ability to process data locally without the need to relay it to a centralized processing unit as in the works presented in [69], [11] and [43]. This also means that skin patches can be used either connected to a

²Up to the limit of the backbone bus



(a) Skin Patches as data extraction devices



(b) Skin Patch in stand-alone mode

Figure 3-2: Skin Patch modes of operation

PC with a brain in a data extraction scenario, or by themselves as a stand-alone sensing-processing-actuation distributed platform. The former may be useful to monitor pressure gradients on an airplane's wing, when this is tested inside of a wind-tunnel for example. The later would be better suited if the material is to be used as an interactive architectural material³. Figure 3-2 shows the two ways the Skin Patch Network can work.

We now describe the different communication links that the project contains. Although these links are designed according to the specific needs of the involved elements, many of the points described above are observed during the design of these communications channels. Reliability, for example, is a key issue because the integrity of the network depends on the stability of the communications links. For this reason, several redundant links are provided for the backbone network. Scalability is also observed and specific measures were taken to ensure this. We will come back to these points though when the links are individually described.

3.2.1 I2C Backbone

According to the previous section, the Skin Patches are equipped with a network backbone. There are of course many ways of implementing it, but which is the adequate for the project?

³More on this point is provided in the Actuation and Sound sensing sections

It is clear that a serial protocol must be used to avoid the high number of lines that a parallel port would require, but then again, which one is the right option? There are a multitude of serial protocols for embedded systems to choose from: SPI, I²C , Microwire, UART, RS-232 and others. To make the right choice, we have to start from what we know:

- The Skin Patch network can be made up of tens up to a few hundred nodes.
- One of the goals of the project is to minimize bandwidth through local processing of data.
- If the skin is working as a stand-alone device, it would be desirable to use the backbone as a multi-master, multi-slave bus.
- If the skin is connected to a computer, it would be desirable to have only one master (the Brain) and multiple slaves (the nodes), depending on whether multiple patches are needed
- Number of communications lines should be minimized to decrease wiring complexity.

By taking this into consideration, we can easily discard SPI because it can't be used as a multi-master bus and needs four lines plus a common ground; we can also discard UART, RS-232, and Microwire, because they can't handle more than 2 devices without multiplexing. I²C on the other hand is capable of doing everything outlined above and it can be run at up to 400Kbps in fast mode and up to 3.4Mbps in high-speed mode. Moreover, the chosen microcontroller has an I²C hardware module so it does not even need to be implemented in software and it also requires only 2 lines: Serial Data (SDA) and Serial Clock (SCL).

Running I²C at the higher speeds requires special considerations, however. The I²C bus can allow multiple devices to be connected connected to the data lines, because it uses what is referred to as a *wired and*, which means that the lines can be pulled down, but not up to avoid short circuits. This is accomplished by using either open collector devices or by alternating the states of the connected devices between high-impedance and a permanent pull-down.

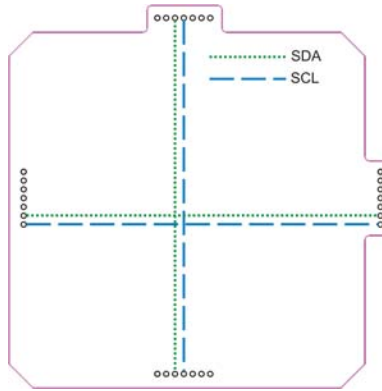


Figure 3-3: I²C Routing pattern

The bus is then limited only by the rise and fall times specified by the I²C standard [54], which also means that the bus is limited by its allowed maximum capacitance.

Since there are no devices pulling up the lines of the bus, this has to be done by pull-up devices, generally resistors that connect the bus lines to the power supply. Whenever the bus lines are unused, the bus idles by staying equal to the supply voltage. The problem with this situation though, is that when a device transitions either line from a logical 0 to a logical 1, it must release the line and let the pull-up device drive the line to the supply voltage; if this is done with a resistor, then the line will behave like an RC circuit with a typical exponential response. In other words, it will be slow.

To ensure the reliability goals and scalability that we mentioned before, we have to ensure that the bus can support as many devices as possible and that there are redundant connections so that communications are not lost. The first objective is ensured by routing both I²C lines to all adjacent neighbors in a + shape shown in Figure 3-3⁴. The second objective, scalability is more difficult to guarantee because the I²C standard dictates that there should not be more than 400pF in either bus line to ensure the correct operation of the bus. This puts a severe limit on the amount of devices and bus length that can be used. There are, however, two ways around this limitation: the first one requires the use of I²C expanders like the Philips P82B715 and P82B96 chips, which increase this limit up

⁴Actual routing is shown on Appendix C

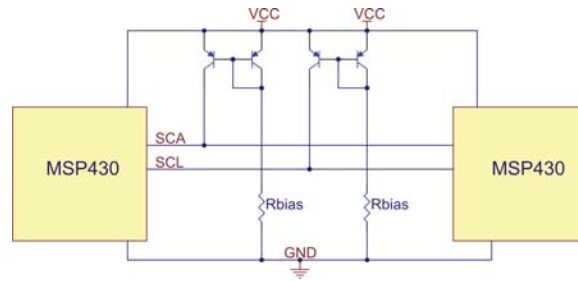


Figure 3-4: I²C Active pull-up devices

to 4000pF; the second one involves using an active pull-up device. The first option involves adding more components to the nodes, which is something we want to avoid, but the second option involves only the modification of the pull-up devices, of which there is only one per patch

Active pull-up devices charge up the bus lines faster than a resistor. The most typical kind is a current-mirror. Current mirrors work as current sources injecting current into the bus lines and thus charging up the capacitance with a linear instead of inverse exponential response. The slope of this line is controlled by the source biasing and it can be made as fast as the current capacity of the transistors used will allow. The schematic of in Figure 3-4 shows this configuration.

This approach is used by the project, and it will be described in more detailed when the hardware of the Brains is mentioned; the actual gain in speed, however, will be shown in the Results Chapter. One last thing to mention is that whenever the skin is working in stand-alone mode, no active pull-ups are used because these are placed in the Brain. This could mean that if there is no Brain connected to the network, the backbone will not work. This is not the case, however, because each node provides a footprint to add a pull-up device if needed. Another option would be to designate a central node in the Skin Patch and add active pull-up devices to it. The backbone is not however meant for node to node communications, this is done through another communications channel which will be described next.

3.2.2 Peer to Peer

As we already mentioned, node to node communications has a different design. What is the reason for this and what kind of communications link is used? The inclusion of a communications link that allows each node to directly communicate to its adjacent immediate neighbors is inspired from the fact that cells in our skin do this to adjust their sensitivity to foreign stimuli. When cells are stimulated they generate an electrical pulse that informs our brain of the event, however when doing so, they release neurochemical transmitters that are received by neighboring cells. This is also used by our eyes to adjust to different amounts of light, and our noses when they become accustomed to certain smells[68],[32].

The addition of a communications link that allows nodes to have peer-to-peer communications is not then responding just to a technical need, but is in fact an emulation of a biological effect observed in living tissues. With this feature, it is expected that the Skin Nodes, will be capable of combining data sensed by their neighbors with that of their own, thus extracting more meaningful information about stimuli events. It will also decrease or eliminate traffic on the backbone bus for inter-node communications.

Peer-to-peer communications is realized by using a custom-created serial protocol similar to Microwire, which uses three lines plus a common ground to transfer information back and forth between nodes. These lines are Serial Transmit (STX), Serial Receive (SRX) and Flow Control (FC). Each node is then connected with three different lines to their four closest neighbors, needing a total of 12 interrupt-capable processor pins. More on the serial protocol will be mentioned in the Software chapter that follows. Also, the full routing of the nodes is presented in Appendix C, which show how these lines are connected.

3.2.3 USB PC link

The last communications link included in the project is a USB PC link. As we have seen before, scalability looms large in the design of the project. USB allows the top level of the network topology to keep with this design philosophy because of its inherent design. USB

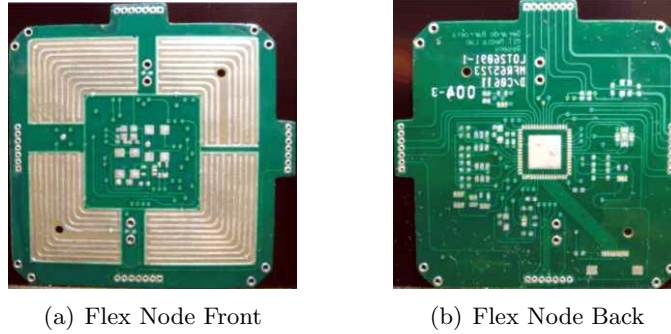


Figure 3-5: Flex Nodes

has a physical bus topology, but a logical star topology which allows multiple Brains to be connected together. USB also provides enough bandwidth to handle the data requirements that connecting multiple brains would involve.

USB is also an industry accepted protocol that has proved to be successful for practically any electronic device created in the last few years from cellphones to portable cameras. It is easy to implement and there are a wide selection of readily available devices that easily add USB functionality to practically anything. A full description of the devices used here will be provided in the Brain section further ahead on this chapter.

3.3 Nodes

Every *Skin Patch* is a Sensor Network composed by one or many *Sensor Nodes*. Each node is composed of a multi-layer, *flexible circuit substrate* or **PCB** that is capable of sensing six different physical quantities:

1. **Strain/Bending:** by using two orthogonal custom-made strain gages
2. **Proximity/Activity:** by using a piezoelectric cantilever
3. **Absolute Pressure:** by using a Quantum-tunneling effect material
4. **Ambient Light:** by adding an integrated sensor

5. **Audio:** by adding a MEMS microphone

6. **Temperature:** by using an integrated temperature sensor

In addition to the sensors, an ultra-low power microcontroller, programming header, external crystal and **RGB LED** are also included. This means that each node is capable of sensing, processing and actuating independently from each other. This approach, not only makes the Network more reliable and robust, in accordance with one of the design principles, but it also provides each node with the processing power required to eliminate the need to route signals from every sensor to a Central Processing Unit, typical of dense sensor arrays like the ones presented in Haris[18] and Papakostas[49].

3.3.1 Substrate Design

The Nodes were built using Flex Circuit Technology following the recommendations found in Gilleo[13] and Harper[19]. Flex technology was chosen on top of other technologies described in the previous chapter, because it is a well established technology that has proved to be successful in many commercial products[47]. It also has many of the mechanical properties that conform to the project specifications: flex can be conformed to any arbitrarily shaped container, flexed continuously and virtually indefinitely, is stress compliant, extremely thin and it withstands high temperatures. It is also widely available through several manufacturers, and there is a vast amount of reference information about it[64][13][19]. Choosing a newer technology like the one proposed by Lacour[35], for example, would have created numerous constraints on the project and, because of lack of technological maturity, place the emphasis of the research in the fabrication techniques rather than in the mentioned goals.

Flex circuits are different from regular rigid PCB's because they can be manufactured with a very wide selection of materials, and unlike their rigid counterparts, a material stack-up must be provided to the manufacturer as part of the design process. Flex circuits are composed of four major parts: one or many *dielectric base films* whose properties depend on the

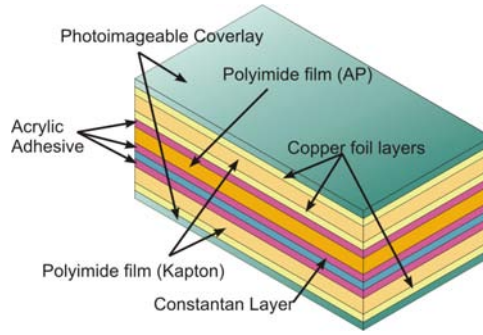


Figure 3-6: Node substrate material stack

material⁵, one or more *conducting layers*, their respective *adhesive layers* and any necessary *finishing layers*. However, even though the material selection and the combination between possible elements is very broad, there are typical standardized combinations of adhesives, base materials and conductive layers. Perhaps the most popular combination is Copper film over a Polyimide base because of its low cost and favorable electrical properties. The Skin Nodes are based on this basic material combination with a few necessary modifications.

Lets now describe the material stack-up and design options selected for the project. Figure 3-6 presents the entire material stack layer by layer. First, there were two main options to choose from for the base material: Mylar® (Polyester film) and Kapton® (Polyimide film). According to Gilleo, Mylar is about 20 times cheaper than Kapton, has excellent flexibility, moisture resistance and electrical characteristics but it has very low tear resistance and it can't withstand the high temperatures required for soldering. Kapton films are much more expensive and moisture absorbent than Polyester films but they are easier to prototype with because they can support the temperature used for soldering electrical components. A 2mil ($50.8\mu m$) Kapton layer was therefore chosen as the Node substrate.

The Skin Nodes also contain 4 conductive layers, three of them made of 1oz ($35.5\mu m$) copper and one of a special copper and nickel alloy called **constantan**(Cu55Ni45). Constantan is not as good a conductor as copper, but it has some properties that make it ideal for other purposes [23]. This will be explained in one of the following sections when the different node sensors are explained. Again, there are several options when choosing the right kind

⁵Usually Polyimide or Polyester films but can also be epoxy-glass, glass-resin or others

Thickness (mils)	Layer	IPC Standard
0.001	Photoimageable Coverlay	IPC-SM-840C
0.0014	Top Layer (1 oz Rolled Annealed Cu)	IPC-4204/11 E1E2 M0 W71S/1S
0.002	Polyimide Film (Kapton)	
0.0014	Inner Layer (1 oz Rolled Annealed Cu)	
0.001	Acrylic Adhesive (Pyrалux)	IPC-4203/1 E1E2 M2/2
0.002	Polyimide Film (AP)	
0.001	Acrylic Adhesive (Pyrалux)	
0.001	Inner Layer 2 (Constantan Foil)	ASTM B267-90, ALLOY 5B
0.001	Acrylic Adhesive (Pyrалux)	IPC-4203/18 M2
0.002	Polyimide Film (Kapton)	IPC-4204/11 E1E2 M0 W71S/0
0.0014	Bottom Layer (1 oz Rolled Annealed Cu)	
0.001	Photoimageable Coverlay	
0.0162	Total thickness	

Table 3.1: Material thicknesses and standards

of conductor. Gold and silver are better options than copper, but they are evidently more expensive. Polymer Thick Film conductors are also widely used in flexible circuits because they can be applied as inks, but they tend to be more resistive than copper. As with rigid circuits, copper offers the best tradeoff between cost and performance but in the case of flexible circuits, the metal can be either electro-deposited onto the substrate or glued as thin *rolled annealed copper laminates*. Rolled annealed copper has the advantage of supporting virtually infinite flexing cycles, while electro-deposited copper tends to crack under these circumstances. Since the idea of the project is to emulate the way a skin would behave, RA copper was chosen in spite of a marginal increase in cost.

Finally, both sides of the nodes had to be covered by a protective layer to isolate the conductive traces from the environment, and to serve as a solder mask. There are four main options: coverfilm, screened solder mask, photoimageable solder mask or dry film solder mask. Coverfilm is the cheapest, but it has to be machined like any other layer which limits the pad size and hole sizes. Photoimageable solder masks or coverlays are flexible versions of their FR-4 cousins; they are a bit more expensive but they allow for pads and vias of practically any size, plus they offer the advantage of being re-workable [73] which is essential for prototyping.

An acrylic adhesive (Pyrалux) was used to join the different layers together and make up the stack. All of these materials, along with their exact thicknesses and specifications are included in the IPC-4203[29] and IPC-4204[30] industry standards that can be obtained from

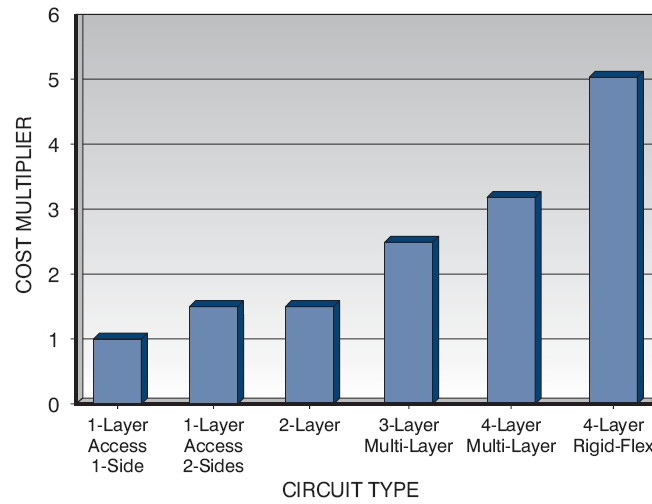


Figure 3-7: Flex circuit cost as a function of fabrication complexity[46]

www.ipc.org. Table 3.1 lists the thicknesses and fabrication standards used to fabricate the substrate⁶.

Cost Considerations

Material selection however, is only the first step when designing a flexible PCB. There are many mechanical considerations to make that have a big impact on cost: circuit size, shape, overall thickness, minimum bend radius, mechanical fittings and circuit terminations must all be included into the design phase as well. But before going into these in detail, a brief cost analysis is necessary to illustrate why some design decisions were made.

Flexible circuits are broadly classified depending on the types and number of layers used for their construction⁷, and the type chosen will affect the cost, mechanical flexibility, and mechanical stability. Generally speaking, the greater the number of layers per circuit, the greater the fabrication complexity and therefore cost. Layers should be added sparingly then, to keep design/fabrication complexity and costs to a minimum. Keeping the layer count low also increases the flexibility⁸ and compliance of the material, which in the case

⁶Courtesy of Dan Hansler of Pioneer Circuits, Inc

⁷Classified as Single-sided, Back-bared, Double Sided, Multilayer, and Rigid-Flex

⁸Characterized by the maximum bend radius

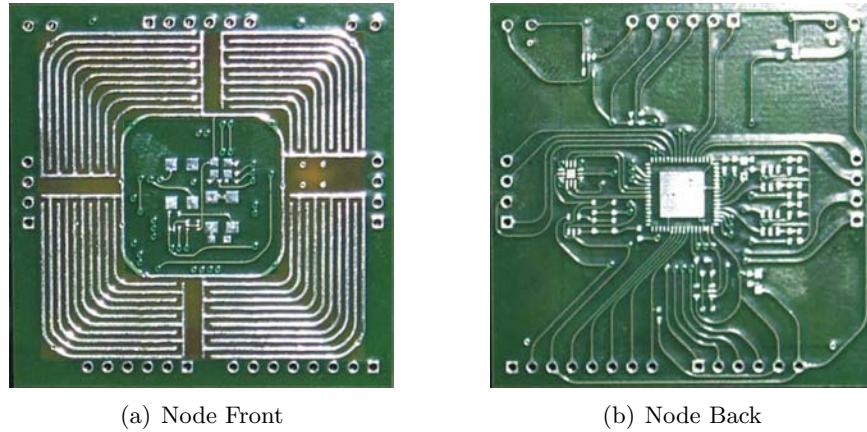


Figure 3-8: Rigid node prototype

of this project are crucial. Figure 3-7⁹ shows the relative cost increase for different types of flex. There are several other factors that also increase cost, but analyzing all of them in detail would be beyond the scope of this document; the reader is welcome to check the provided references if further information is needed.

It is clear that multi-layer boards cost more than twice than the average double-layer flex board and more than thrice that of single-layer boards. Yet, it is necessary to resort to the more expensive multi-layer flex boards in order to have enough layers to route all the electronic components required by the goals of the project. Manufacturing the final boards is not the only costly part, though, as they must be first prototyped. A typical four-layer rigid board of this size can be prototyped for less than \$50, the same prototype on flex usually costs between \$800 and \$1,200 because of the labor involved. For this reason, prototyping of the Skin Nodes was done on regular rigid boards, and only the “final” version was fabricated on flex. Not all of the functionality could be tested in the rigid prototypes, but they were essential for the design, debug and first tests. These boards are shown on Figure 3-8.

⁹Courtesy of Minco™: http://www.minco.com/uploadedFiles/Products/Flex_Circuits/aa24-flex_design.pdf

Mechanical Design

Once cost issues have been addressed, we can proceed to describe some of the mechanical aspects behind the design of the Skin substrate. Again, things like mechanical terminations and fittings, shape, size, number and types of layers, overall thickness and minimum bend radius all have to be taken into account when designing the circuit.

The **shape of the Skin Node** was chosen to be roughly square with two overhanging flaps to create mechanical connections to adjacent nodes. This can be seen in any of the layouts of Appendix C or Figure 3-5. Making the nodes square has several advantages: first, unlike complex tiling of polygonal-shaped nodes, square nodes can be made equal to each other avoiding the need to make distinctions between them in the network and thus simplifying the coding of applications; second, they can be easily tiled to form any arbitrary shape, like pixels in a monitor; third, one of the characteristics of the network communications scheme is that every node can communicate directly to its adjacent immediate neighbors, which in the case of a quadrilateral shape is a maximum of four¹⁰ (except for edge and corner nodes). This not only helps to keep the routing and wiring simple but it helps to keep the necessary available processor port-pin-count low, which is important to maximize functionality.

Mechanical terminations are another big design choice. There are many possible ways to connect flexible boards to each other many of which are outlined in Minco’s design guide[46]. For the first Skin Network revision, *Physical Reconfigurability* was not included as a design point because of its increased complexity both in hardware and in software. Basically, network reconfigurability in the context of the project means that nodes can be easily rearranged, which would have many advantages over a fixed network configuration, but it requires a type of connector/mechanical terminator that can allow nodes to be easily plugged and unplugged while maintaining a high enough degree of mechanical stability so that communication links (backbone and peer-to-peer) are not frequently lost. None of the evaluated mechanical terminators could achieve this with ease, so a semi-permanent termination method was chosen instead. The chosen Node connection scheme is similar to that presented by Um in [69], and it was implemented with header holes that can be joined

¹⁰North, South, East, West

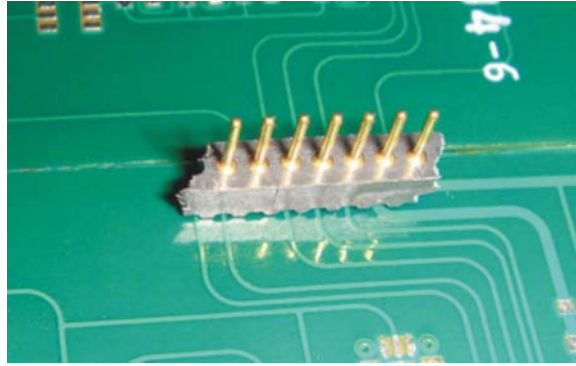


Figure 3-9: Skin Patch mechanical terminations

together by soldering single in-line, break-away headers, which can be seen in Figure 3-9. Header holes are located in the overhanging flaps so that nodes can be tiled without much overlap.

Size was another major consideration; all circuit dimensions can be seen in Figure C-3. How big should the Nodes be such that there is enough space to accommodate all the necessary components, while keeping an acceptable level of sensor density per covered area? This is essentially a cost problem since more expensive fabrication techniques like *blind and buried vias* are needed to increase the component and routing density of the Skin Nodes since there is virtually no space left for compacting the layout. This can be observed in Figure C-4 included in Appendix C. However, given that costs are already high and that these are pricey options, the costs would have become prohibitively expensive. Accordingly, these options were then left for a possible second revision. Finally, Some extra space was needed for to allow bonding of a special material used for the pressure sensors; this is why the Nodes are not routed close to the edges.

Yet the most important mechanical characteristic, and the one that separates this design from rigid PCBs is its ability to bend and flex. Flexibility of the board is influenced by many things, but the three main ones are **material selection, final substrate thickness and routing techniques**. Material selection was already described, but in terms of flexibility, rolled annealed thin films are the best for applications that require constant bending. One could arbitrarily choose extremely thin (up to about $9\mu m$ thick) films, but they are not good



Figure 3-10: Node with electrical components being flexed

at withstanding large stresses which lead to *hairline* cracks on the conductors that cause faulty electrical connections. For this case, standard 1oz copper was chosen. Final substrate thickness simply depends on the number of layers on the material stack; the more layers, the smaller the minimum bend radius that the substrate can take without permanently deforming or cracking. The thicknesses of the entire stack and each layer are shown in Table 3.1. A good rule of thumb is that the minimum bend radius should be at least 24 times the total thickness of the substrate, however this is best defined in IPC's document IPC-2223 [31]. Figure 3-10 shows an example of a fully-assembled node being flexed

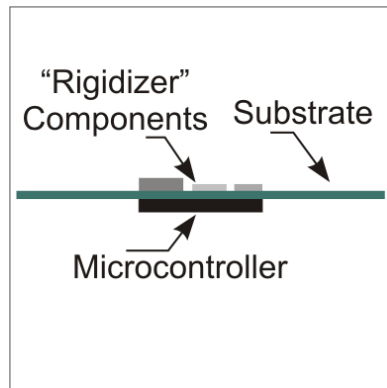
Routing and Component Placement Issues

The routing of the board requires special mention. There were several issues that either limited or complicated the electrical routing of the board. First of all, there are only two layers available for electrical components, as the inner layers are only for routing and sensing. The top or *outer skin layer* was rendered almost useless for component placement because the real estate was used up by the electrodes required for the pressure sensors; the only available space was occupied by the ambient light sensor, LED, and microphone, which by necessity *had* to be on the outer layer. Second, as it was seen before, layer count must be kept low because of cost and flexibility issues, so *power and ground planes* could not be

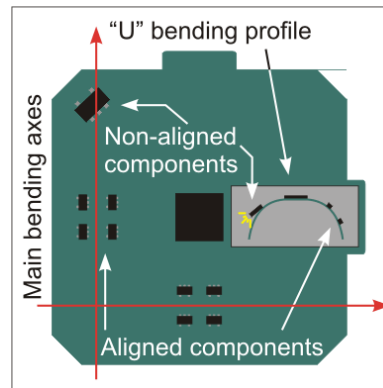
used, which only further complicate the routing. Third, including a microcontroller on a flex board is difficult because the bending can cause it to pop out. One solution for this is to wire bond the processor chip as thinned bare-die silicon but this is well beyond the scope of the current project.

A more conventional workaround for this is using either *rigidizers* or rigid-flex, but the former can't be used if components have to be placed directly underneath the area to be rigidized, and the later would have been prohibitively expensive. Several routing and component placement tricks, which are shown on the following list, had to be used to reduce overall stress points; these are shown on Figure 3-11.

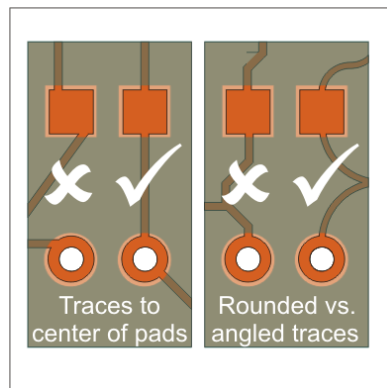
1. The microcontroller was placed in the center of the bottom layer, and the components that had to be on the top layer plus the crystal were placed directly opposite of the microcontroller on the top layer so that their large bodies worked as rigidizers.
2. Because the node footprint is small, and the center of the board was now somewhat rigid, bending was mainly constrained to the outer regions of the board, so every component that had to be placed in the outer region of the bottom layer was aligned to the bending axis so that stress points at its pins are minimized.
3. Whenever possible, traces were routed so that they would meet at pads/vias through the center, except for those cases where this would create unnecessary extra curves and corners.
4. The *Ibeam* effect shown on Figure 3-11(d), limits bend radius, and is therefore minimized throughout the layout of the circuit. This also helps to keep crosstalk between routed signals to a minimum, which is good for speed as well.
5. Routing Corners are natural stress points, so they were routed underneath components whenever possible.
6. Rounded corners were also used to increase the bending life of the nodes.
7. Sharp corners create stress points so the curvature radius of the corners was kept large when possible.



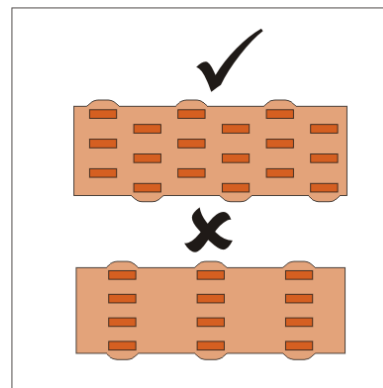
(a) Rigidized center



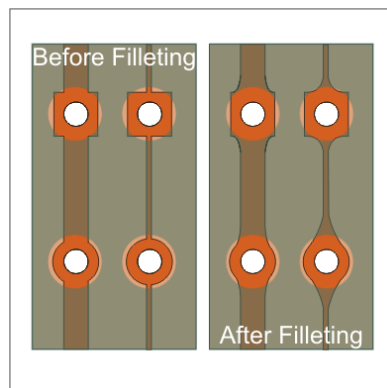
(b) Aligned components



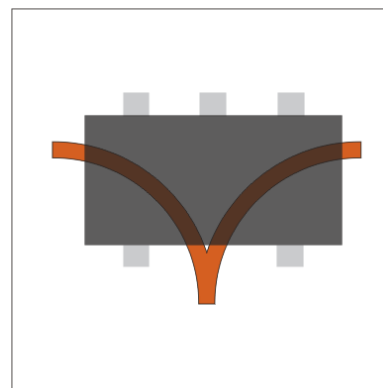
(c) Rounded routing and Centered Routing



(d) IBeam Effect



(e) Teardrops and Fillets



(f) Corners routed under components

Figure 3-11: Routing techniques

8. *Teardrops* and *filleting* were added to all pads and vias.
9. Components were also chosen to be as small as possible, so that bend radius is not limited by this. If components are large, then the substrate will not be able to bend without components breaking off.

There is one last thing to mention. Because of the necessary number of layers and the presence of surface mount components on both layers of the board, the nodes will certainly not be as flexible as a natural skin, plus are not, of course, elastic and 3-axis conformable. These and other results will be mentioned in Chapter 5.

3.3.2 Power Circuitry

As we mentioned in the previous subsection, component selection was made in such a way so that component size and orientation would not much hinder the bending of the circuit. In general, this means selecting components as small and compact (not elongated) as possible, otherwise there would be a risk of components breaking off the substrate as shown in Figure 3-11(b).

Referring back to the design principles of section 3.1, one of the key points is to have a reliable network. Reliability in the case of network power distribution is gained by providing each node with their own power supply or individually wiring each node to a centralized one. Connecting each node to a central power supply would be a step back in the design, because it would mean that each node has to be wired, which is exactly what we are trying to avoid by having processing power in each node. The other option would be to have a coin-cell battery in every node, but these are generally not rechargeable, bulky in relationship to node size and would hinder flexing motion.

The next best option is to provide as many redundant power and ground connections throughout the network as possible. This is the option implemented in the SNAKE project, and therefore every node has a power and ground connection to each one of their immediate neighbors (North, South, East, West). Since the Skin Network topology is dictated by the

shape in which the nodes are connected, the nodes at the edges of whatever network shape is chosen would obviously have less than the four maximum redundant power links. The worst case scenario here, would be when the network topology is a straight link of nodes connected in a line, which provides no redundancy. Power to the network is therefore distributed from a centralized unit, but no individual wiring is necessary, because each node provides power its adjacent neighbors.

Each node is provided with a NCP553SQ33T1 linear voltage regulator that provides a constant 3.3V supply to each node. This regulator is ideal because not only does it come in a ultra-small and compact SC-70-4 package, but it also does not need any external components except for an optional output capacitor. It is an ideal regulator, because it has a 12V maximum input voltage, which allows for a very wide range of power supply voltages; it has an output current capacity of up to 180mA with a 650mV dropout, more than enough for the node circuitry, and it only consumes $2.8\mu\text{A}$ of quiescent power, which suits our goal of low power consumption.

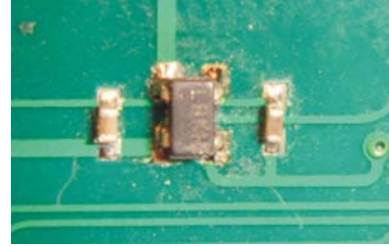
Power requirements of the network vary widely, mainly because the size of the Skin will change, depending on the number of nodes connected. Either a large battery or a bench-top power supply can be used, but for the specific case of the skin patch built to test the project, a Rose Electronics LI-2S1P-2200 7.4V Lithium-ion battery pack was chosen, mainly because they were available from previous projects but also because they have a high-discharge rate of 2.20A/h. This means that if each node consumes an average of 15mA, one battery can provide enough power to operate roughly 140 Nodes for about an hour. Actual power consumption is much less than 15mA, but this and other results will be mentioned in Chapter 5. Figure 3-12 shows the power components.

3.3.3 Processor

Microcontroller selection was also a critical part in the design of the Node Hardware. Following with the established design principles, the chosen microcontroller should be capable



(a) 7.4V, 2.2mAh Li-ion Battery



(b) 3.3V Regulator in each node

Figure 3-12: Power components

of processing all data generated by the node's 11 sensing channels¹¹ and still have enough processing power remaining to handle the two communications channels provided (I2C and P2P). It should also be capable of ultra-low power operation and have enough ports and peripherals (timers, ports additional hardware) to handle data and tasks efficiently. Finally, it needs to include a relatively large amount of **RAM** ($> 10KB$) on die, to handle sampled data and data packets, and come in the smallest possible package.

There are hundreds of microcontrollers available, however only a few manage to have the required characteristics. The PIC24H family of microcontrollers for example, would be an excellent choice, if it wasn't for their large size. Others like the PIC18, Atmel's AVR's, and 8051-based families (Silicon Labs, Intel, Atmel) come in a broad variety of memory sizes, hardware peripherals and special features, however they are all 8-bit microcontrollers, which complicates the handling of large quantities of data, and they are also generally power-hungry, requiring an average of $300\mu A$ per MHz.

The **MCU** with the most adequate balance of characteristics for the project was a Texas Instruments MSP430F1611. The MSP430 family of microcontrollers has the best-in-class power management modes and ultra-low power consumption [26]. With five different low power modes, 16-bit native operation, less than $6\mu S$ standby wake-up time, and a 300nA deep sleep mode, the MSP430 has the most flexibility when low power is needed [27]. MSP430's can run up to 8.000Mhz with an optional external crystal and up to 5.000Mhz

¹¹2 Strain/Bending, 2 Motion sensors, 4 Pressure sensors, 1 Ambient Light sensor, 1 Microphone, 1 Temperature sensor

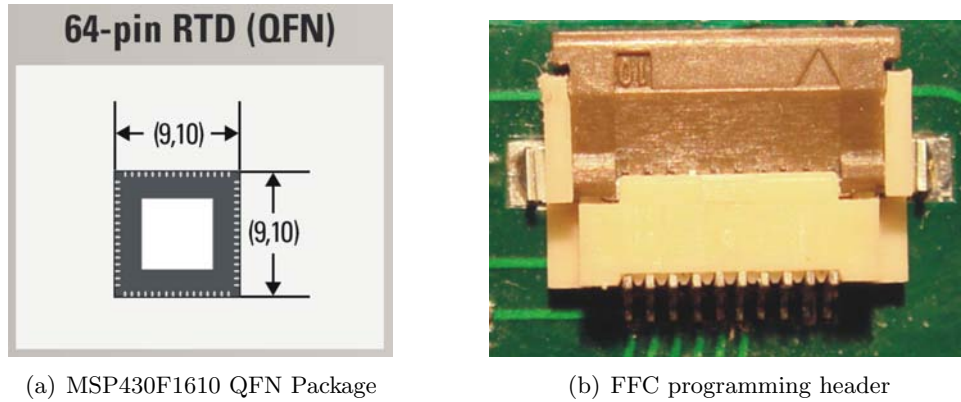


Figure 3-13: Microcontroller with programming header

with the internal **DCO**. For this case, an external ABMM2-8.000MHZ-E2-T 8.000Mhz **SMD** Crystal which was included to mainly drive the serial backbone at a higher speed.

The MSP430F1611 comes in a very compact 9mm-by-9mm leadless 64-**QFN** package with 48 general purpose **I/O** pins and two hardware serial modules that can be configured as either **USART**, **SPI** or **I²C** ports. It also includes 10KB of RAM and 48KB of Flash, a hardware multiplier, a **DMA** controller, two timers, a supply voltage supervisor, and a 10-input channel, 12-bit **ADC** module. Although features like the hardware **I²C** controller, **DMA** and hardware multiplier are not absolutely necessary for the system, they are highly desirable because the network backbone uses an **I²C** protocol; **DMA** can be used to transfer sampled sensor data to RAM leaving the processor free for other tasks; and the hardware multiplier greatly speeds many of the calculations.

Probably the only drawbacks to selecting this microcontroller were its relatively big size compared to other MCUs of the same and other families¹² and its price, which at the time this project was created was of roughly \$12.0. These microcontrollers went also unexpectedly out of stock of all major providers when the flexible boards were already created, and the restocking date was beyond the project time frame, so MSP430F1610 had to be used instead with the minor disadvantage of having only half of the RAM. Fortunately, this had no major impact on the operation of the network, but then again this will be mentioned

¹²64-QFN is almost 4 times larger than a 32-QFN used by the MSP430F123

in more detail in the Results Chapter. Finally, since this is a first revision prototype, an FH12-10S-0.5SH **FPC** programming header was included for debugging purposes. Both, processor and header are shown in Figure 3-13

3.3.4 Sensing Modalities and Actuation

The human skin is capable of sensing many different physical quantities. Every square centimeter of skin is filled with hundreds of nerve fibers sensitive to temperature, light, vibrations, pressure, mechanoreception, and many different forms of pain¹³. This subsection, describes some of the available sensing technologies with which it is possible to emulate some of the sensing capabilities of the human skin while comparing their characteristics to illustrate why one was chosen over the others.

The sensor subsystem of the Skin Nodes is composed of the actual sensors themselves, their associated analog signal processing, and the ADC module of the chosen MSP430 microcontroller. Although they are all independent of each other and use very different sensing technologies, they all share the same selection criteria, and follow the previously mentioned design points. Sensor technologies were selected in such a way so that:

- a. Analog-processing component count is minimized.
- b. Sensors can be integrated into the substrate if possible.
- c. They observe ultra-low power operation.
- d. They are analogous to a sensor present in human skin.

Unless otherwise noted, all of the signal conditioning circuits use the same amplifier from Maxim IC: MAX4400AXK which comes in a tiny SC-70-5 package, and consumes only $320\mu\text{A}$ of quiescent current. Although there are other devices that consume considerably less power, like the Texas Instruments OPA347 or TLV2252, the former was chosen because

¹³Depending on the part of the body, fingertips for example, have up to 2,500 receptors

its better balance between Gain-Bandwidth product and power consumption. These could not be used for the Strain/bending sensors, because a differential amplifier is needed. Other sensors already come pre-amplified and no external amplification was needed. We'll come back to this point when we individually describe each sensor.

Each sensor type is sampled at a frequency high enough to capture the necessary information, but low enough to keep power consumption down and also to avoid saturating the RAM before the processor can extract higher-order features from raw data. In the case that data needs to be extracted from the nodes, these higher-order features are what is generally transferred, thus bandwidth requirements are minimized. This will be described in more detail when we mention some of the applications that run on the Skin Network and again in the Results Chapter.

Before heading on to the sensor suite description, it is important to note that even though receptors in the human skin are capable to sense different types of sensations at once¹⁴ [56], in the world of electronic sensing it is generally easier to use a different sensor for a specific physical quantity. Otherwise effects like temperature drift, electrical coupling and other effects can disturb many measurements and cause ambiguousness in the readings. For this reason, strain was separated from pressure and vibration and a separate sensor with a different technology was chosen for each modality.

Actuation

Due to the nature of the project and the limited amount of node surface real estate, actuation was limited to light response. Skin Nodes are provided with a LTST-C17FB1WT RGB LED. This small 2.4mm-by-2.0mm RGB LED can be easily driven by the 3.3V outputs of the MSP430 MCU without needing a special driver. The LED has a common cathode so the anodes of each LED were connected to three different MCU I/O pins through a current limiting resistor. Since the blue and green LEDs have a **DC** forward current of 20mA with a forward voltage of 3.5V, a 100 Ω resistor was used to limit the current. The red LED

¹⁴Some examples include: Meissner's corpuscles are sensitive to vibrations and light touch; Pacini's corpuscles are sensitive to pressure and vibration; Merkel's disks, Pincus domes to touch and pressure

has a 30mA forward current with a forward voltage of 2.0V so to keep brightness levels roughly equal a 150Ω was used instead. Moreover, the microcontroller pins to which the LEDs are connected are timer outputs which allows them to be pulse-width modulated and thus generate practically any color.

Although the LED was added mainly for debugging purposes, it turned out to be a very useful tool for demonstrating the capabilities and functionality of the assembled test network. An interesting thing to note here is that the Skin Network generated some interest for its possible use as an architectural material, so having LEDs makes sense to give the skin a certain type of “chameleon-like” expression.

Strain and Bending

The idea of providing the Skin Nodes with the ability to sense strain and/or bending amount, and its direction was derived from the fact that our human skin is perfectly capable of doing this. The idea is clearly not new, and several ways of achieving this result have been proposed: the works presented by Banks[2], Yamada[75] and Hritsu[22] for example, describe similar optical ways to track the strain and deformation of a skin-like material. In Yamada[76] et al, a vibrotactile strain-sensitive device is used to detect textures. Still, perhaps the example that best demonstrates this emulation are the so-called eFabrics or Smart Fabrics that have been presented in numerous articles describing similar methods to sense the deformation of conductive fabrics and plastic films [61], [71], [44].

Transducer Selection There are indeed, many ways of measuring the strain and/or bending of a material, but as we already saw, the ideal choice for this project will be one that can be integrated into the node substrate while requiring minimal signal conditioning so as to keep power consumption and component count low. Yet, even with these constraints there are still multiple viable options: *FSRs*, *Strain Gages*, and *Piezo-resistive films* are all good candidates.

Taking a closer look though, we find that FSR bend sensors can’t be easily integrated into

the substrate at the time of fabrication or are difficult to fabricate with any accuracy[34]. because they are made of special, proprietary materials which can't be easily obtained¹⁵; instead then, they must be added at the time the skin is assembled, which complicates the Skin Node layout and assembly. FSRs also delaminate pretty easily and are not good at resisting high humidity environments. Piezo-resistive (PVDF) films are very good for transducing changes in strain, but they can't be used for cases where static strain is needed; there is also no easy way to integrate them into the fabrication process. Strain gages on the other hand, can be easily customized and streamlined into the fabrication process, they add only one extra layer into the material stack and incurs only a marginal increase in cost. Two orthogonal axes of strain sensing were therefore included into each node.

Strain gages are long traces of a resistive metal for which a change in strain results in a change in electrical resistance[10]. This change can be then amplified and read by a microcontroller. The change in resistance is represented by the equation:

$$\frac{dR}{R} = S \cdot \varepsilon \quad (3.1)$$

Where R is the resistance, ε is the strain, and S is the strain sensitivity “gauge” factor of the material. This sensitivity factor is what determines the effectiveness of a strain gage design and it is highly dependant on the materials and fabrication methods chosen. Another interesting point is that strain can be compressive or tensile, which means that not only the amount of the strain can be extracted but also its direction. As a result, strain gages can be used as bend sensors for the skin.

Strain gages are manufactured by adhesively bonding a thin foil of metal to a flexible plastic substrate like Kapton. The gage is then glued to a surface of the object for which a strain measurement is needed. Ideally, the gages should only change their resistance due to mechanical deformations, however in real applications, factors like the adhesive used to install the gage, temperature, and the gage material, all have an effect on the measurements

¹⁵Like Tekscan's Flexiforce sensors

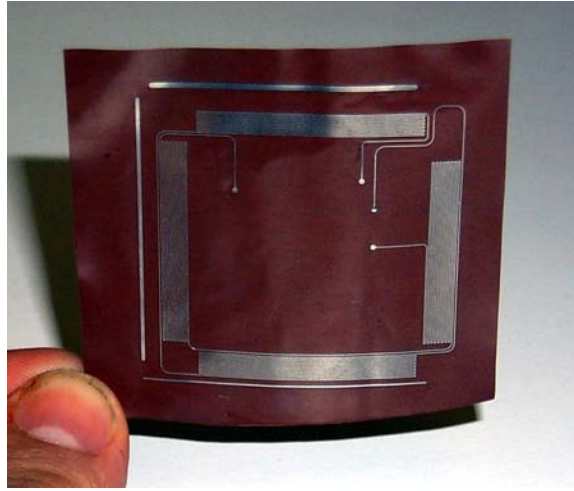


Figure 3-14: Strain gage layer prototype

[48]. Because of this, strain gages are built from special alloys for which the gage factor S is much less sensitive to temperature variations than for regular metals.

Strain Gage Design Material selection directly affects the mechanical properties of the gage, like fatigue life, flexibility, sensitivity and stability. However, even though the materials selection available for fabrication is very broad, constantan has constantly been the most widely used alloy for strain gage applications, and was therefore selected. Constantan has a relatively high sensitivity, high resistivity and high drift temperature which make it ideal for this project.

There are five other variables that have to be taken into consideration when custom-designing a strain gage: gage length, gage width, overall resistance, grid pattern and backing material. In the specific case of our project, backing material was not an issue because the skin is actually made from Kapton, which is the most typical backing material for constantan foil. Here, the length of the sensor grid determines the “active area” of the sensor, and therefore must be adequately fit to cover enough node area so that dead zones¹⁶ are minimized. The width of the gage traces, on the other hand, is the main determinant of the overall resistance of the gage, which translates into its ability for dissipating heat and

¹⁶Skin areas insensitive to bending

therefore defines its stability. Overall resistance is an issue if the amount of current flowing through the gage needs to be controlled. Finally, The grid pattern is important because it determines the axis of the strain to be measured; grid patterns can be either one of the typical ones (uniaxial, biaxial rosettes, multiple-axis rosettes, radial rosettes) or a customized design. This is provided, however, just as an overview of the available design choices that must be made; for a detailed explanation of these the reader can try Vishay's tech note TN-505-4[24].

For the more specific case of the current project, the strain gage design can be seen in Figures 3-14 or C-7. An observant reader may notice that there are actually four sets of traces, however, these are considered as two gages because the top and bottom sets of traces are connected so they actually make one sensor; this is also the case for the left and right sets. Their design characteristics are outlined in the following list:

Length: designed to cover as much area as possible to diminish dead zones.

Trace width: made as thin as possible; the manufacturer imposes a 5mil trace width limit without imposing a price increase, so this width was chosen.

Overall resistance: determined by trace length and material properties. Although trace length was controlled to make both gages in each node have the same resistance, fabrication variations caused them to have a variation from node to node of up to 20 Ω s. The total gage resistances are then in the range of 168 – 188 Ω .

Grid pattern: 90-degree T-rosette style with redundant traces (2 sets of traces per strain axis) which gives a resolution of 2 sensors per node.

Strain gages, however, produce very reduced output voltage swings¹⁷ because the changes in resistance due to strain are small. For this reason, they need to be conditioned by a very high-gain amplifier in order to be adequately sampled by the microcontroller. The way this is usually accomplished, and the way it was actually done in the project, is by using

¹⁷Tens of millivolts

an unbalanced *Wheatstone bridge*, from which a differential output is taken and fed to an instrumentation amplifier. An unbalanced Wheatstone bridge can be seen as nothing more than two independent voltage dividers, from which one of the resistive elements has been replaced by the strain gage. As the gage undergoes some strain, its resistance changes, and the voltage seen at the divider node correspondingly changes¹⁸. Since one of the voltage divider branches is composed of regular resistors, the voltage seen at its divider node will always be set at $V_{CC}/2$, so when these two bridge outputs are fed to an instrumentation amplifier, this will amplify the difference seen at the divider nodes, causing the output of the amplifier to swing positively or negatively from the bias point, depending on the type of strain experienced by the gage (either tensile or compressive). This arrangement is shown on Figure 3-15.

The resistors that make up each one of the bridge divider branches are generally picked to be of the same value so that the excitation voltage is divided equally among the two resistors, giving the widest possible output swing. However, this configuration has a problem that, although not evident at first, could potentially cause the amplifier to saturate. Since the resistance change of the gages is so small even at their full bending range (around 3Ω maximum change), and given that large gains are needed for the signal to have a noticeable swing at the amplifier output, any minuscule mismatch between the resistance value of the strain gage and its adjacent voltage-divider resistor will cause the amplifier output to saturate. This is never a problem with commercial-grade strain gages, because they are fabricated in such a way that their resistances are within 1% of a commercially available resistor. This is possible because they are mass-produced, which keeps the costs of stringent quality control measures low. Doing this with a multi-layer flex PCB in a custom application is not possible because it would be extremely expensive.

The solution to this problem was to add a matching resistor in series with the strain gage, so that the resistances could be matched to that of the closest commercially-available resistor value. Thus if, for example, the measured effective strain gage resistance was of 166.9, placing a matching 2Ω resistor in series would add enough to the measured value to almost

¹⁸Since strain can be tensile or compressive, the difference in resistance can be either positive or negative

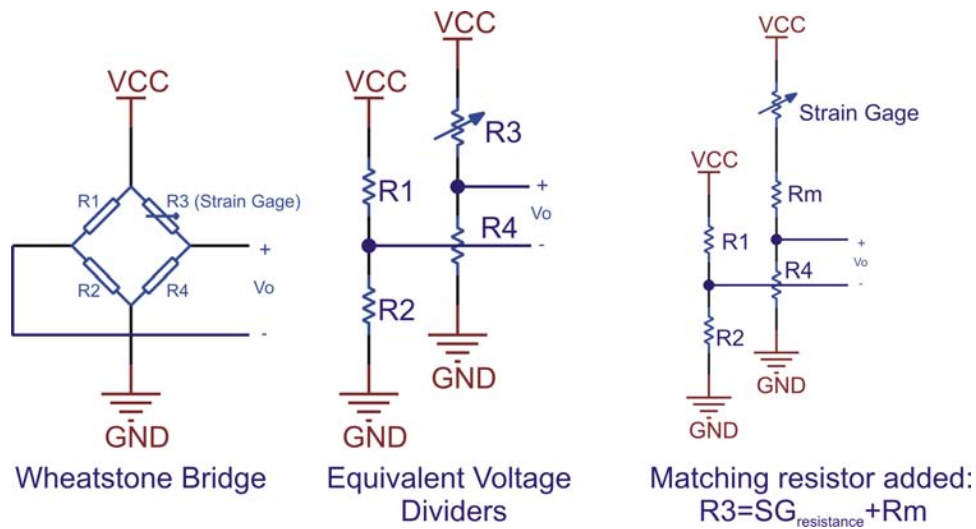


Figure 3-15: Wheatstone bridge used for Strain gage conditioning

perfectly match a 169Ω resistor, which can be obtained commercially. This matching then ensured that the amplifier would not saturate for resistance mismatches, at the expense of manually matching each gauge on each node.

Only the hardware selected for signal conditioning is left to be mentioned. As it was previously said, the Wheatstone bridge output nodes are fed to an instrumentation amplifier. The selection of the amplifier followed the same principles we have been mentioning throughout the document. It was rather difficult to locate an instrumentation amplifier small enough and with a sufficient gain for the required application. Fortunately enough, the MAX4462HEUT from Maxim IC Inc. comes in a small SOT-23 package, and is precisely designed for bridge applications. It even includes a reference input signal for correctly biasing the output voltage of the amplifier¹⁹. Probably its only drawback is that it comes with fixed gains of 1, 10 and 100, but even with a gain of 100, the output swing for moderate Skin Node bending is of at most 1 volt, which was enough for the requirements of the project. Having the full 0–3.3V swing accepted by the microcontroller would have required a second amplifier stage, which would have been impossible to include, given the already lacking component real estate. Possible ways to improve this and other parts of the design

¹⁹All amplifiers are actually biased at 1.5V using the external voltage reference provided by the MSP430. This is done so that they have roughly equal voltage swings

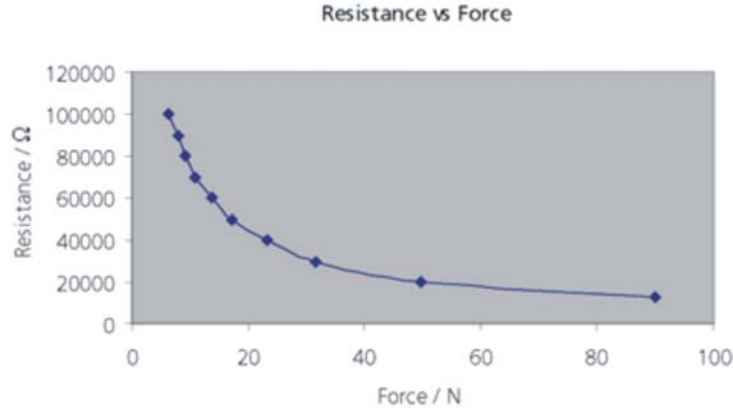


Figure 3-16: QTC response curve for a QTC pressure sensor[52]

are provided in the final chapter.

One factor that has not been mentioned so far about the hardware is its power consumption. This is observed through the entire design of the sensor systems by adopting three measures: use of instrumentation amplifiers that have a low quiescent current, the resistance of the traces is made as high as possible, and gages are gated. Sensor gating is done by pulling down the Wheatstone bridge using a FDG6301N Dual N-channel MOSFET, with the gate connected to a microcontroller output pin. These transistors come in a neat and compact SOT-23-6 package, and allow the microcontroller to turn on the gages only when a measurement needs to be taken greatly reducing the current consumed.

Pressure

Pressure sensors were also custom-made for this application. The reason for this is that even though most of the technologies evaluated before for strain sensing can be also used for pressure, they had to be discarded for same reasons described above and instead a QTC sensor from Peratech was used.

QTC sensors can be obtained as thin films bonded to a paper-like polymer, and can then be therefore easily bonded to the Skin Node substrate. Using these sensors also allows the entire surface of the node to work as a pressure sensor, unlike solid-state pressure transducers,

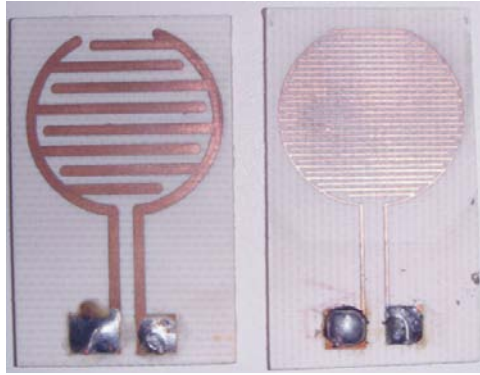
which are localized. QTC sensors are made of metal particles bonded to a thin polymer. These particles are isolated, but as pressure is applied to the material they come closer to each other. As this happens, electrons start to “tunnel” between the isolated material gaps, and increase the conductance of the material. This behavior is not linear though, as it can be seen in Figure 3-16.

This curve is almost an inverse exponential, meaning that a pressure sensor fabricated with this material will be extremely sensitive to relatively light touches, and have a lesser sensitivity to higher pressures. This can be adjusted with a good signal-conditioning circuit design.

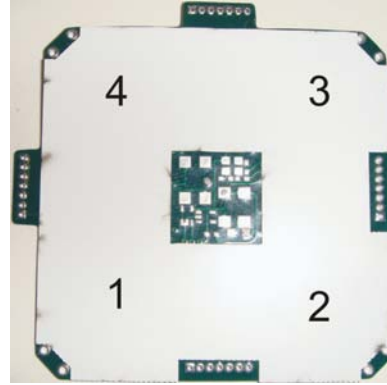
According to Peratech’s integration guidelines [53], the sensor requires the use of electrodes over which the material must be placed, free-floating with the coated side facing them. Accordingly, electrodes were placed on the top or external facing side of the Skin Nodes, and cover almost their entire surface except for the center and edges. The center could not be used, because it was needed for mounting all the electrical components that also need to be on this layer. The edges were left blank because they were used to glue the material to the substrate.

These electrode layouts have two parameters that must be controlled: electrode spacing, and trace width. The right balance between these two will dictate the resolution of the sensor. To ascertain these parameters, several prototype layouts were tested. Some of these are shown on Figure 3-17(a). From these two, conclusions were obtained. First, the width of the traces determines the base resistance of the sensor, which is an important quantity for the circuit design. And second, although electrode width has nonnoticeable effects on the sensitivity, slimmer traces give more flexibility and resolution to the sensor. For the Skin Nodes, an electrode width of 20mils was chosen.

The entire surface of the node substrate was subdivided into four corners, so that four separate pressure sensor areas could be created as shown in Figure 3-17(b). These four electrodes were then multiplexed using a Maxim MAX4734EGC 4:1, multiplexer and the output of the multiplexer was amplified using the circuit shown on figure C-1. This is



(a) Prototype boards used to calibrate sensors

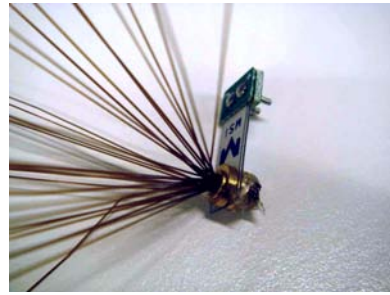


(b) A node covered with QTC material. Each node has four channels of pressure sensing as shown

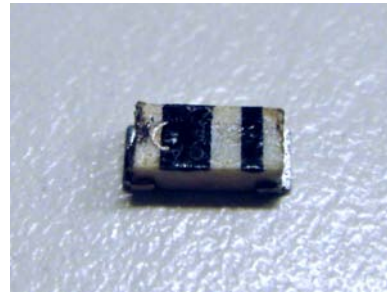
Figure 3-17: QTC pressure sensors

nothing more than a non-inverting amplifier biased at mid-range by the voltage divider created by the sensor selected by the multiplexer and a resistor. Whenever the pressure sensor is not pressed, it has a resistance in the order of mega ohms. As pressure is applied to the sensor however, the resistance decreases, and the voltage divider voltage changes, which causes the output voltage to swing. One advantage of this circuit is that the sensitivity range of the pressure sensor can be adjusted by changing just one resistor, in this case the pull-down resistor used in the voltage divider.

Finally, there are some mechanical design aspects to consider. Gluing the QTC films onto the substrate only by the edges causes the material to warp and bubble when the substrate is bent. There are work-arounds to avoid this: the first one would be to selectively apply an adhesive around the metal electrodes so that only the parts with no metal stick to the coated side of the sensitive material. A second option would be to encase the entire skin into a silicone rubber; this has the added advantage of evenly distributing the pressure among the four corners of the node, so gradients are better observed.



(a) Mini-sense cantilever with whiskers glued to end mass



(b) Kyocera's PSAC piezo shock sensor

Figure 3-18: QTC pressure sensors

Proximity/Motion Sensing

Proximity sensing or mechanoreception (motion sensing) was added to the nodes to copy the ability that our skin has to perceive close activity through hair. As with any other sensing modality, there are several different ways to convert the whisker vibrations into electrical signals that can be then sampled by the microcontroller. Two different options based on piezoelectric cantilevers were tested.

The first option was based on the design presented by Lifton in [41]. Taking advantage of piezoelectric film's ability to turn bending strain into high voltages, nylon fibers were glued to the end of a Measurement Specialties MSP6915-ND Mini-Sense piezo cantilever to make up a vibration/mechanoreception sensor. This sensor has a mass attached to the end of the cantilever which also gives significant sensitivity to inertial forces. This design is shown on Figure 3-18.

The second option was based on the same principle of the first one, however instead of using a large piezo cantilever, two different Kyocera PZT vibration sensors, the PSAC380A and PSLC382S, were tested. The only difference between these two sensors is the axis of maximum sensitivity. These sensors have the advantage of being surface mountable, and are very small and sensitive. The only minor drawback is that the sensitive part is located inside of the small package and the whisker can't be directly glued onto it. Fortunately though, these sensors are sensitive enough that they are able to pick up vibrations if the

whisker is epoxied to the package of the sensor. For this to be possible the whiskers have to strain the package enough for the sensor to respond, which is easily obtained if the whiskers are thick and stiff enough, and enough gain is given to the amplifier.

The circuit necessary for its signal conditioning depends directly on the type of information that is desired. Vibration, strain, shock or simply activity can all be derived from this sort of sensor depending on the signal conditioning and sampling chosen. A very detailed review of possible circuit options are shown in the Measurement Specialties Piezo Film Technical Manual [63]. Since the idea of including whiskers was mainly to detect the presence of close activity, a very simple circuit was used to generate vibration pulses, which are then connected to an input pin of the microcontroller, which can then either extract the vibration frequency, or simply report if there was or no activity for a certain period of time. This is also shown in Appendix C.

Ambient Light

Although one might not notice the fact that our skin is indeed capable of sensing ambient light, this becomes clear if we take into consideration that it is light and not heat which causes the familiar melanin concentration change in the skin when we spend long times under the sun; in other words we get tanned because of the amount of light received by our skin. Some animals (e.g. Cattlefish have optical sensors distributed in their skin).

Including an ambient light sensor into the nodes would allow several applications to be developed with the network. Some possibilities include the retina-like light edge detection system presented by Lifton in his push-pin distributed-computing-platform [39], and light gradient and source direction detection, and longrange proximity detection by cast shadows.

This capability was implemented by adding a Toshiba TPS851/52 ambient light sensor, shown in Figure 3-19. This tiny device was created as an illuminance sensor for brightness control of mobile device displays, and it is based on a current-amplified photodiode. It is an ideal option for the Skin Nodes because it doesn't need any external amplification, which reduces component count. It also has a low supply-voltage and power consumption that

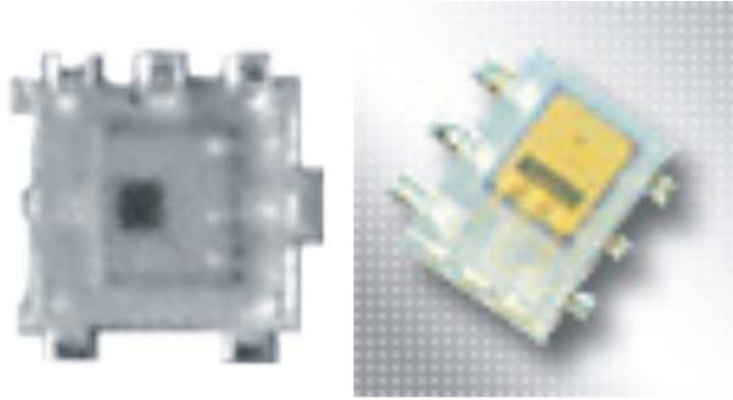


Figure 3-19: Toshiba TPS851/52 Ambient Light Sensors

makes it compatible with the rest of the circuit, it is very sensitive, and it includes a built-in Luminous Efficiency Correction, which adapts to different light sources (incandescent or fluorescent). On top of this, the ambient light sensor has infrared sensitivity suppressed, and has a spectral response close to that of the human eye with a relative sensitivity peak located at 600nm [67].

This sensor has the added advantage of coming in a tiny package that can be surface mounted. There was only one design problem that had to be overcome when mounting the sensor into the nodes. Since both the ambient light sensor and RGB LED have to be placed in the *outer* Skin Node layer, they have to be carefully placed to avoid interference with the sensor measurements. This was accomplished by placing them as far from each other as possible. In actual results, it was seen that some coupling still exists but, is minimal.

Finally, since the sensor outputs current, a resistor was connected at the output to turn it into a voltage that can be then sampled by the ADC. This is the only component needed to condition the signal, which again helps to keep component count low, and it allows the sensitivity of the sensor to be changed by tuning the resistor value (currently $8K\Omega$ s).

Sound

The only sensing modality added to the nodes that is not present in the human skin is sound²⁰. The reason for doing this is that sound sensing requires a much larger amount of bandwidth than the other sensors, and was therefore useful for pushing the limits of the hardware used, and testing how much data could be processed locally. Having a microphone on each node also enables several exciting applications, such as using differential time of flight to determine sound localization and sound directionality; beamforming is also possible since the skin becomes a conformal microphone array. Moreover, it allows for greater interaction if indeed this material is used as an architectural material.

Sound sensing is realized through a Mini-SiSonic™ Knowles SPM0102NE3 **MEMS** Microphone. This microphone is usually used for mobile phones and PDAs, because unlike electret-based microphones, which can't be subjected to high temperatures and therefore surface mounting, MEMS microphones can be easily soldered and don't require special assembly processes. This was one of the reasons for picking this model. Other reasons include its good frequency response, omni-directionality, and very low current consumption. It can also work with the low voltages used by the microcontroller and other sensors.

The microphone signal conditioning circuit is shown also in Appendix **C**, and it consists of a capacitor that couples the microphone output to a second-order, low-pass anti-aliasing filter. The amplifier used is the previously-mentioned MAX4400 that has a Gain-Bandwidth product of 800Khz, high slew-rate and low noise. Biasing for the amplifier was accomplished by connecting a 1.5V voltage reference generated by the microcontroller which causes the output voltage of the amplifier to swing across the desired 0–3.3V range. Analog component selection was done to have a cut-off frequency of 4Khz, enough to sample human voices and low-quality audio. The low cutoff frequency chosen responds to the fact that high sampling frequencies need more processing power, and the microcontroller used only has a maximum of 12 **RISC MIPS**, that has to be divided among sensing, data transfer, and processing

²⁰The inclusion of sound sensing into the sensor suite of the Skin Network, is one of the reasons for which the project acronym was chosen as S.N.A.K.E or *Sensor Network Array Kapton Embedded*. Snakes as we know, have the capability of perceiving vibrations and sounds through their skin. The final appearance of the Skin Network when finally assembled was also scale-like like a snake skin

tasks, one of the inherent design tradeoffs that will be mentioned in the software section.

Temperature

For temperature sensing, there was the option of integrating an **RTD** film into the substrate, however this would have required another Wheatstone bridge for signal conditioning, and a current source to excite it, which translates into a high component count. Including it into the substrate also complicates the fabrication and further increases cost. This option then was discarded and instead a National Instruments LM20CIM7 temperature sensor was chosen. The LM20CIM7 is a precision, low-voltage and low-power, micro SMD temperature sensor. It operates over a -55°C – $+130^{\circ}\text{C}$ temperature range and has a predominantly linear response with a slight predictable parabolic curvature. Its best feature though is that it outputs an analog voltage that can be directly sampled by the ADC without need for signal conditioning.

Using an integrated temperature instead of a film that can be distributed across the whole substrate has the disadvantage that only the temperature directly affecting the component can be measured instead of that of the bulk substrate, however this can be minimized by encasing the skin in a heat-conductive silicon. This not only helps to average the temperature along the entire surface of the nodes, but also pressure, which as we previously mentioned, had a similar problem.

MSP430 microcontrollers include an internal temperature sensor, but this was not used because it is used to measure the internal core temperature rather than ambient temperature.

3.4 Brain

As outlined in the Network Design section, if a Skin Patch is to be used as a data extraction device, then it must be connected to a PC through a Brain. Brain design did not require much of the previously mentioned design points, because the Brains were implemented with

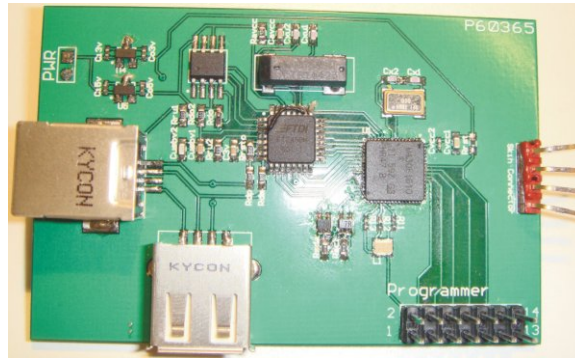


Figure 3-20: Brain

regular PCB fabrication techniques, and their mechanical properties were of no relevant significance. Brains, as opposed by Nodes, need to have the ability of quickly and efficiently relaying information back and forth between the Skin Patches and the PC, while allowing other brains to do so as well.

Given that Brains are not required to do any major data processing, the processing power is not a direct requirement, however larger and more powerful processors are generally needed to handle large amounts of data. In the specific case of this project though, data is locally processed at the nodes and higher-order features rather than pixelated data are transferred to the Brain by the nodes, which allows the Brains to concentrate more on administrative tasks of the network, rather than relaying data back and forth, and it also minimizing the bandwidth required.

Brains are composed of a microcontroller unit, power unit and communications unit; one is shown in Figure 3-20. The schematics and layouts of the brain, which will be briefly outlined in the following subsections, are shown in Appendix C.

3.4.1 Processor unit

The processor unit of the brain is composed by the microcontroller, crystal, programming header and output devices. Having a faster MCU than the one used in the nodes could in theory, transfer data faster. This would be true if the MCU could extract information from

the nodes faster than what the bus can provide. However, since the Brain is connected to the Skin Patches using a shared common serial bus, the factor that dictates the transfer speed is the bus and not the microcontroller.

An MSP430F169/10/11 was therefore chosen, which had several advantages. First, it has the same hardware I²C peripheral that nodes have, which makes it easy to interface; second, this is also an ultra-low power microcontroller which is consistent with the overall design goals of the project; and third it is widely available, inexpensive and compact. Keeping in the MSP family also eased potential development overhead

Also part of the processing unit are a **JTAG** programming header needed for debugging, a crystal, and RGB LED, the same as those used in the nodes. It was considered at some point to add a speaker and other output devices besides the LED to the Brains, however this was discarded because it was decided to use them only as administrative devices to control the flow of data between the nodes and a PC.

3.4.2 Power unit

The power unit is made up of a power supply and power regulators. The batteries used were already mentioned when the node's power unit was described. In fact, the Brains use the same batteries, because power is actually distributed to the Skin Patch from the Brains. This was done because Brains can be encased into a box along with the batteries, as opposed to the Skin patches, which have to be either wrapped around objects or allowed to freely flex and bend.

Two power regulators are needed in the Brains because the processor circuitry requires 3.3V DC, while the chip used for **USB** communications with the PC needs a 5V power supply. Two SOT-23 Zetex regulators, were chosen: the ZMR500FTA for 5V and the ZMR330FTA for 3.3V. The power provided to the network is unregulated because the nodes already have their own regulators, and is carried by thick traces on the PCB that can withstand higher current loads.

3.4.3 Communications unit

The Communications unit is made up by the I²C bus that connects it to a Skin Patch, and the USB link that connects it to a PC. Furthermore, the I²C module is composed of the active pull-up devices described before, a header to connect the brain to a Skin Patch, and the I²C module of the MSP430 microcontroller. The USB module is formed by the USB controller circuitry, the USB headers, and an external crystal.

Active pull-up devices were created with two XP02401 dual PNP transistors connected as a current mirror, and a biasing resistor. The biasing resistor was chosen so that the current injected by the current mirror to each one of the two I²C lines was not over the allowed maximum input current of the MSP430 microcontroller (2mA). This can be easily calculated as follows:

$$I_{max} > \frac{V_{cc} - 0.6V}{R_{min}} \quad (3.2)$$

$$R_{min} > \frac{3.3V - 0.6V}{2ma} \quad (3.3)$$

$$R_{min} > 1350\Omega \quad (3.4)$$

A 1.5K Ω resistor was then used for biasing the current mirror.

USB communication was achieved thanks to FTDI's FT245BM USB chip. This device is a USB to FIFO interface chip, that allows any microcontroller to easily have USB connectivity. The device requires its own clocking source, so a 6.000Mhz crystal is also included. Also, if the device is to be named and given a serial number²¹ then an EEPROM must be used, and so a 93LC46B EEPROM chip from Microchip was also included. FTDI provides a very detailed design guide[12] for their chips, the Brain's USB circuitry is based on their "self powered 3.3V example".

Finally, it would be prudent to mention that if multiple Brains will be connected to a PC,

²¹This is usually done so that multiple devices of the same type can be later identified

a USB hub is needed. Although in this case the USB controller from the PC was used as the USB hub it is also possible to make each brain a USB hub, itself and daisy chain them one to one another.

Chapter 4

Software

“A Scientist discovers that which exists. An Engineer creates that which never was ”.

–Theodore Von Karman

After having described the hardware platform of the S.N.A.K.E. Skin, we now pass on to describe the Software that glues all pieces together and makes it run. The current chapter is divided into three main sections. The first section will describe the embedded firmware that goes into each one of the *Skin Nodes*, and that of *Brains* themselves. The second section outlines the characteristics of the Software necessary to use the Skin Patches as data extraction devices. We end the chapter with a mention of the communications protocols and their associated algorithms, metrics and necessary adaptations.

4.1 Firmware

Given the relatively large amount of embedded processing present in the entire project, a big part of the total Software developed is in fact Firmware. There were four main different firmware components that had to be created for the platform: Node Bootloader, Node Applications, Node Sampling and Brain Firmware.

A key point in the design of the Overall Software and Hardware Systems, has been *Dynamic Reconfigurability*. This term was already mentioned in the previous chapter when we mentioned the mechanical connectors. In the case of the Software System though, this refers to the ability of the Sensor Network to update, change or modify its behavior by modifying its software. This is represented here in two different ways: first, the nodes in the Skin Patches can be reprogrammed at will and second, the application code can dynamically change the sampling rate of the sensors to adjust itself to different stimuli events. We will come back to the later feature when we describe the sampling code in more detail.

Sensor Networks are composed of usually tens or hundreds of nodes; and the current project is no exception¹. This fact makes our current method of manually loading code to each one of the nodes using the included programming header very impractical, and we therefore need to look for another option.

Several ways of distributing code in Wireless Sensor Networks have been proposed: Reijers[57], for example, proposes a way to wirelessly reprogram the nodes by only transmitting changes and therefore conserving energy; Boulis[5], in the other hand says that distributing executable images of code to each and every node is inefficient and that having an approach that programs the network as a whole is better suited to large networks; other approaches like the one presented by Lifton[40] use a method called algorithmic self-assembly, in which different algorithms are built with smaller fragments of code.

On top of this, there are even multiple Operating Systems that can be implemented into the MSP430 microcontrollers. Some examples include TinyOS[38], Contiki[9] and FreeRTOS[3]. Which then would be the appropriate combination of code distribution and management technique for our network?

Before answering that question, we have to take into account a fundamental difference between the characteristics of the present project and those of the works presented above, and even further, those of the majority of the literature that is available on the subject: Skin Patches are *Wired Sensor Networks*, and those references specify to Wireless Sensor

¹A more detailed calculation for the theoretical limit of nodes per Skin Patch will be mentioned in the Communications Software subsection later on this chapter

Networks. Why is this relevant? Mainly because the energy requirements for our project are not as stringent as those for Wireless Sensor Networks. With this in mind, a customized approach was taken: each node was provided with a bootloader capable of dynamically reprogramming application code using the available backbone bus.

4.1.1 Bootloader

Generally speaking, a bootloader is a process that loads programs into memory. These can be one of either an Operating System or an application code. In the more specific case of embedded processors or microcontrollers, however, a bootloader is simply a process that receives a program through a communications channel, writes it to program memory and then executes it. This allows the system to be updateable or upgradeable without the need of special hardware to reprogram the microcontroller.

It is important to note that even though the MSP430 microcontrollers already include a *Bootstrap Loader*[\[14\]](#), this could not be used because it needs to have five lines to be individually routed to every node in the network. So, given the already tight routing of the node layers, making this possible would have entailed adding an extra layer to the material stack. Doing so was highly undesirable because of its impact on cost and mechanical flexibility. On top of this, the MSP430 bootstrap loader would have needed special hardware to be added to the network Brains. Therefore, taking advantage of the MSP430 in-system flash programmer, a customized bootloader was implemented.

Design

There are many things to consider when designing a Bootloader:

- What will be the format of the uploaded code?
- How will this program will be transferred to the microcontroller?

- How much memory is there available for the bootloader and where should this reside in memory?
- Will the bootloader need to relocate or in other way modify the uploaded code?
- Will the bootloader interact with a user or other processors?

But for the particular case of this project, it was decided that:

- Code will be presented in Intel HEX format
- Given that no extra lines can be routed to the nodes, the I²C Backbone has to be used to upload the code to the nodes
- MSP430F1611/10 have at least 48KB of Flash memory, so the Bootloader should take less than 10% of the memory
- It would be highly desirable if the use of the bootloader is transparent to the user so no changes need to be made to programs for them to work properly
- Since the user will have control over the operation of the Hardware platform, the bootloader will directly interact with a user

The most important aspect to consider though is: Where in memory will the bootloader be located? This is important because the bootloader needs control of the microcontroller after a reset, so it will need to use the reset vector. Interrupt vectors are located at the start of memory, so if the bootloader is placed here, it would then need to redirect the entire interrupt vector to the downloaded program. This would add complexity and latency to the interrupt vectors, so the bootloader was placed at the end of memory instead. Figure 4-1 shows the memory arrangement on the MSP430 once the bootloader has been programmed.

Implementation and Operation

The bootloader was coded using IAR's Embedded Workbench IDE completely in Assembly language. The main reason for choosing ASM over C was purely philosophical, although it

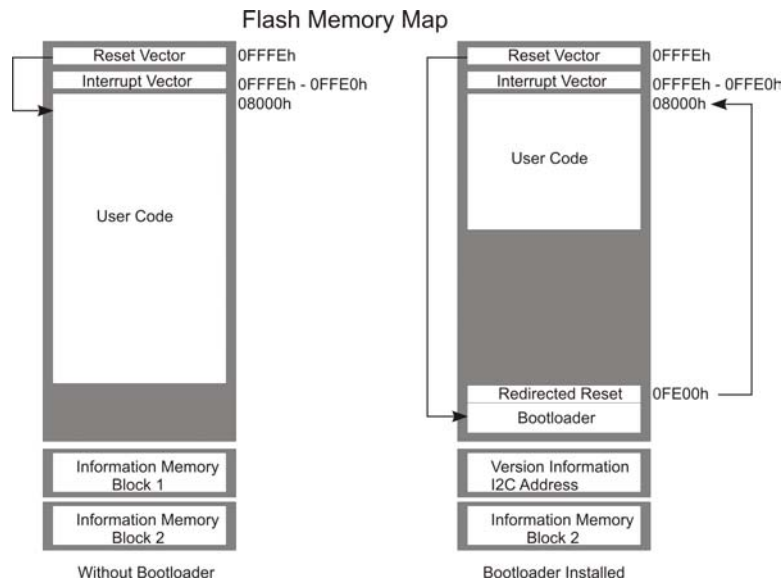


Figure 4-1: Bootloader memory map

Code	Instruction	Description
0xA0	REFLASH_INSTRUCTION	Reflashing instruction, awaits for code
0xA4	RESET_NODE_INSTRUCTION	Issues a Watchdog timer fault to reset the node
0xA6	EXECUTE_CODE_INSTRUCTION	Executes programmed code if any is present

Table 4.1: Bootloader Instructions

has the added advantage of better timing control and less overhead. The total size of the Bootloader HEX file is 794 bytes, which is assembled into the last available flash page.

The Bootloader is started every time a Power-on reset is generated. Once the Bootloader is executed, it instructs the microcontroller to use the external 8.000Mhz crystal, turn on the Supply-Voltage Supervisor and deactivate the Watchdog timer. It also configures the I²C port as a slave device. The Bootloader then waits indefinitely for an instruction, which can be any of those listed in Table 4.1:

The program flow can be observed in Figure 4-2, and the full listing of the code is included in Appendix D. Once a `Reflash_Instruction`, is received, the bootloader will expect a file that contains the length of the transmission, the version of the code, and the code itself in a stripped-down version of the Intel HEX format (the start code and type fields are eliminated). If the file is correctly received, and it does not exceed the maximum file size

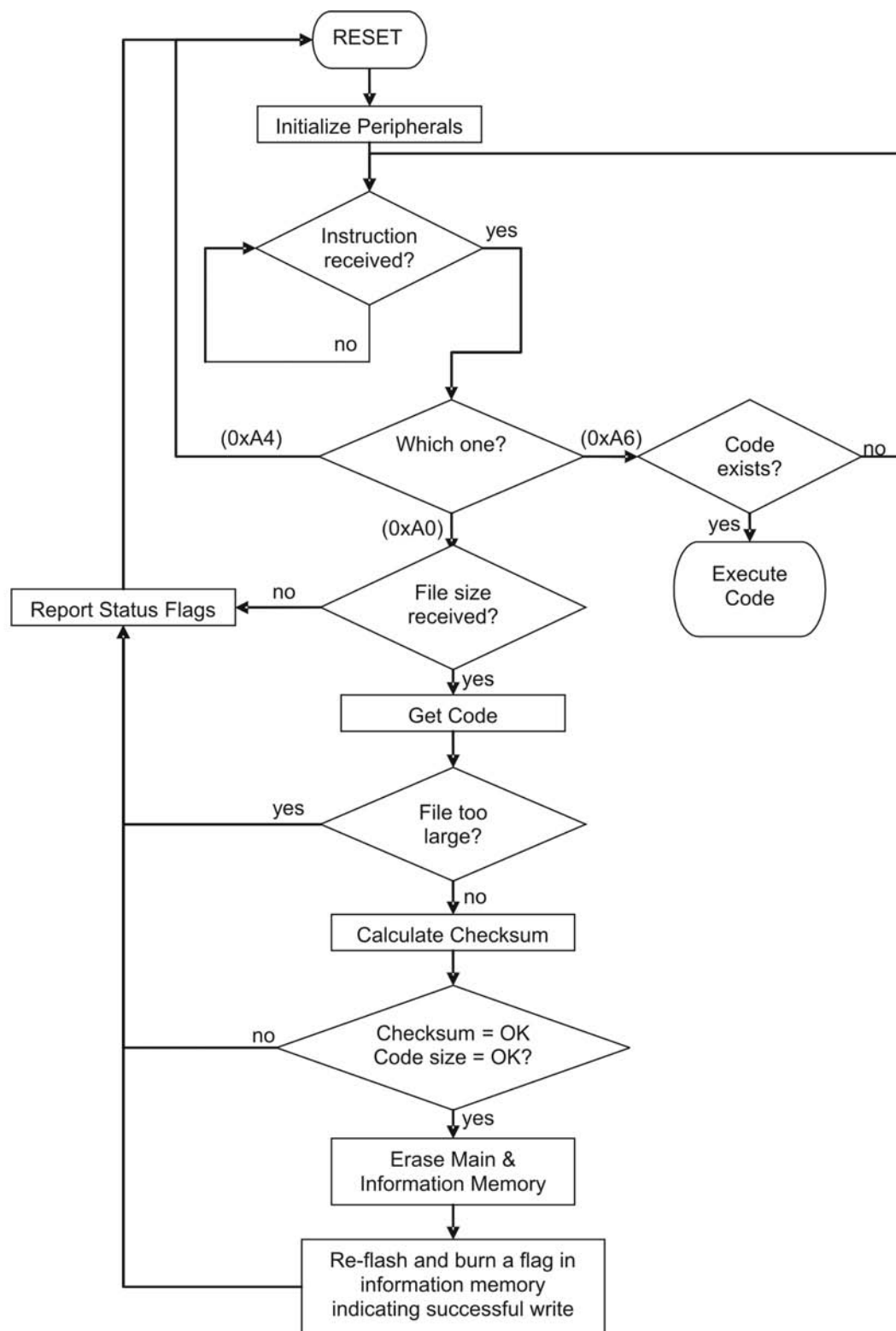


Figure 4-2: Bootloader Flow Chart

Bit	Flag Name	Description
0x01	FILE_RECEIVED_OK	Code file successfully transmitted
0x02	TRANSMISSION_ERROR	I ² C Transmission error
0x04	TRANSMISSION_OVERFLOW	File larger than available RAM
0x08	CHECKSUM_ERROR	Code invalid because of checksum fail
0x10	FILESIZE_OVERFLOW	Code file too large
0x20	INVALID_ADDRESS	Invalid address caused by an address conflict
0x40	FILESIZE_UNDERFLOW	Receiver expects more bytes than actually received
0x80	REFLASH_OK	Device reflashed successfully

Table 4.2: Bootloader Status Byte Flags

allowed, the bootloader will calculate a checksum for every Intel HEX line, and compare it to the one received. If the checksum succeeds, then it proceeds to erase the main and information memories, and burn each line of code into its specified address. The process will only succeed if all the lines were successfully copied into flash, and no invalid addresses were found². The only case in which the code is modified before burning it into flash, is when the reset vector address is detected within a line, in which case the bootloader will redirect it to the first address specified in the received code. A flag byte is always reported back to the Brain indicating the status of the operation; if the code was received as a broadcast message, the status byte is not reported until the Brain polls each node, otherwise it is sent back after programming is complete or an error found. Table 4.2 lists the different flags encoded into the response byte

Flag 0x01 means that the node correctly received the file, but it does not necessarily mean that it was burned into flash. Flag 0x02 might be reported if there were problems in the I²C bus. There are two flags that indicate an overflow; this is because to make efficient use of the I²C bus, the code file is not transferred (Intel HEX) line by line, but 4KB blocks are sent at once. Flag 0x04 indicates that a block was larger than 4KB and it can't be accommodated into RAM, while flag 0x10 means that the code file can't fit into flash³. Flag 0x08 is reported if any line fails the checksum. Flag 0x20 will be set whenever a line has an address occupied by the bootloader which prevents it from being overwritten. Flag 0x40 is set if the transmission file indicates a transmission larger than was actually received, and

²An invalid address will be any address that conflicts with the bootloader code space

³This might be due to either the code size being larger than the actual Flash, or that it is larger than the Flash minus the size of the bootloader itself

flag 0x80 indicates a successful write to flash.

As previously noted, the Bootloader will wait indefinitely for an instruction, but it could be easily changed to start execution of a program after a determined amount of time. Once execution starts though, the bootloader can't be invoked again unless a reset is generated (hardware or software initiated) or the application code explicitly includes a mean to invoke it. This can be easily accomplished by generating either a Watchdog timer timeout or an invalid write to its counter register.

4.1.2 Sampling Code

The second large firmware component is the application code that deals with sensor sampling. This is probably, the principal software component, given that it is mainly where the *Dynamically Reconfigurable* feature of the Skin Patches lies⁴. As the reader may recall, one of the main goals of the project is to demonstrate that the amount of required bandwidth and other resources can be minimized if each node is given processing power. By doing this, the need to route pixelated data to a centralized processing unit is practically eliminated.

Although this code could be used if the Skin Patches are used as data extraction devices, it is mainly intended for the case when the Skin Patches are being used as stand-alone devices. Its main purpose is to set the rate at which the sensors are sampled, process the generated data, calculate higher order features and possibly transfer these to a PC through a Brain if further processing is needed. Concurrent sampling and processing is possible because the sampling and timing of the application is carried out by the microcontroller peripherals, so the processor core is left free to process the generated data. This is shown in Figure 4-3.

Lets now describe what the microcontroller does after starting up. After a reset, the application configures the clocking unit to run at 8.000 Mhz, initializes the I²C module as a slave device and designates an ADC memory channel for each one of the sensor modes⁵.

⁴The other one being its ability to be reprogrammed

⁵The MSP430 ADC module is equipped with 10 sampling channels each one of them with a 16-bit conversion result register

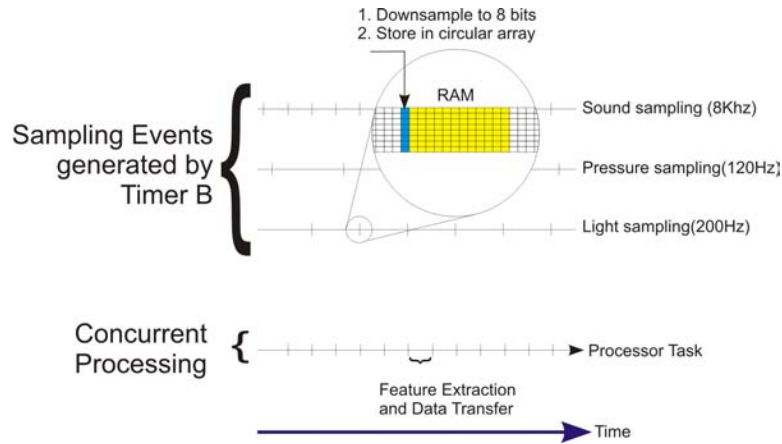


Figure 4-3: Sampling timing example

Then, the Timer B peripheral is configured to generate 6 different timing intervals which trigger the sensor sampling events. With this approach, each sensor can be sampled at a different rate according to its needs. Once a sensing event is generated, its associated sensor is sampled and the result is stored in its assigned memory register. Depending on the sensor type, some additional tasks are sometimes performed before their information is stored, and higher-order features can be then calculated. Sensors that need additional tasks are mentioned in the following list:

Pressure sensing: since there are four pressure sensors controlled by a multiplexer, every time a sampling event is generated (120Hz), the multiplexer address is changed, and a different sensor is sampled. This effectively reduces the sampling rate of each one of the four pressure sensors to 30Hz. After sensing, pressure samples are downsampled to 8-bits, and stored in a 4-byte array, one for every sensor.

Sound sensing: sound is the only sensor which is not downsampled for signal fidelity reasons. It is also the sensor with the fastest sampling rate (8KHz). The result of the samples is stored in a 1Kb circular array that uses 2 bytes per sample.

Strain/Bending: strain gages are gated through a MOSFET transistor so that the Wheatstone bridge used for both strain gages doesn't waste energy when not in use. When a sampling event is generated for either one of the strain gages, they are first turned on,

Sensor Type	Sampling Rate	Bit Depth
Strain/Bending	60Hz	8-bit
Proximity/Activity	120Hz	1-bit
Pressure	120Hz	8-bit
Ambient Light	200Hz	8-bit
Sound	8Khz	12-bit
Temperature	80Hz	8-bit

Table 4.3: Sensor sampling rates and resolution

and once sampling is done, they are turned off to conserve power. Only one sample is stored per sensor.

Whiskers: whiskers are the only sensors that are not sensed through the ADC. The reason for this is that it is mainly the presence or absence of activity that interests us. So instead they are connected to an interrupt-capable input pin, so that they generate one or many interrupts whenever they are stimulated.

Now, as we may recall from the previous chapter, there are a total of six different sensing modalities, but a total of 11 sensing channels (4 pressure, 2 whiskers, 2 strain gages, 1 microphone, 1 ambient light, 1 temperature). The interesting thing is that each one of them can be individually configured to detect different kinds of stimuli. And, even though sensor sampling rates and resolutions are set at start-up, these can adapt and go to nearly zero or increase depending on the history of samples and the current stimuli. Table 4.3 summarizes the default sampling rates and bit depths for the different sensors.

These sampling rates and resolutions may seem arbitrary, however they were chosen so that enough information could be extracted from each sensor to divine some higher order features, but at the same time sampling as low as possible so that the processor can keep up with the generated data. The reader may notice that some sampling rates, like the one for temperature, could be made much lower indeed. This was deemed unnecessary because only processing speed and not sampling speed has an impact on performance. For these cases data was just simply overwritten. Furthermore, having a higher temperature sampling rate may allow to detect human touch.

We also mentioned before that there is an inherent tradeoff in the system as processing power must be divided between sampling, data processing and data transmission. As previously mentioned, these rates, can be changed at any time by either modifying the application code and reprogramming the network or by modifying the code so that it can be dynamically changed without the intervention of a Brain. This is where the beauty of the system lies: it can either statically (through instructions received from a PC or Brain) or dynamically (using data history and neighbor data) adapt to external stimuli based on the needs of the task at hand.

Finally, we have mentioned that sensor data is used to calculate higher-order features, but none have been described so far. There are, however, some features calculated for sound, activity, pressure and bending (strain gages). In the case of sound, a history of 1024 samples is stored (about a quarter of a second) in a circular array, which is then used to calculate the mean and variance of the signal. In the case of the whiskers, a counter stores the amount of positive interrupt edges generated over a second. Strain gages are used as bend sensors, so the reading is converted to an approximate bending angle⁶.

Although these are just a few limited examples meant as a proof-of-concept, there are many others that can be calculated and were left for future revisions of the system. These will be mentioned in the last chapter, along with some other future work suggestions.

4.1.3 Node Application Code

The third large firmware component is made up of several other smaller applications that were meant to demonstrate some of the hardware capabilities of the system. They are basically different ways of mapping sensed data to the LEDs and making use of the two available communications channels: I²C and P2P. These applications, served to test the functionality of the Skin Patches as data extraction devices.

The first application uses the light sensors to create a negative feedback loop that turns on the green LED based on the amount of light in the environment. The more light in

⁶An approximation was used based on the data extracted from experimental measurements, which will be shown in the Results chapter later on

the environment, the less active the LED is. This was done by using the timers of the microcontroller for Pulse-Width Modulating the LED light intensity. This application in fact resembles the Retina PFRAG presented by Lifton in his pushpin computing platform[40], which illustrates how this is indeed a Sensor Network, similar to many of those already available. If the Skin Patch is connected to a Brain and an instruction is received to start sending data, data is constantly sent to a Brain every time the node is polled. The interesting thing about the application is that by simply changing the sensor type, any sensor can be constantly monitored on screen in real time for an entire Skin Patch. More on this, however, will be mentioned once the visualization software is described.

The second application was intended to be used as a test for the pressure sensors. This was done by blinking LED lights based on the amount of pressure detected from the pressure sensors. Different corners of the nodes were mapped to different colors of lights.

The third application made use of the P2P communications to transfer a token that could be interchanged between nodes if the pressure sensors were stimulated. This application, however, is only mentioned, and will not be shown but because of its early development phase. Full code listings for applications one and two are shown in Appendix D. Again, the code for the third application was not included because it was not completely debugged and tested.

Just before going on to describe the Brain's firmware, it is important to mention that all application code must be executed explicitly by the user by issuing an **Execute Code** instruction. This is because, as we previously mentioned, after a reset, the Bootloader always has control over the processor, and it will wait indefinitely for an instruction.

4.1.4 Brain

The fourth and last firmware component is that of the Brains. Brains are the bridge between Skin Patches and a personal computer for the case when the skin is to be used as a data extraction device. Brains were already mentioned in the hardware section, where they were described as Skin Network administration and data relay devices. Brains not only arbitrate

Code	Instruction	Description
0xA0	REFLASH_ALL	Receives code and broadcasts it to the Skin Patch Network
0xA2	RESET_BRAIN	Issues a Watchdog timer fault to reset the brain
0xA4	RESET_SKIN	Broadcasts a reset instruction to the Skin Patch Network
0xA6	EXECUTE_CODE	Issues an execute instruction for the addressed node
0xA8	REFLASH_DEV	Receives code and forwards it to the addressed node
0xAA	RESET_DEV	Issues a reset instruction to the addressed node
0xAC	START_SAMPLING	Indicates the network to start sampling and sending data
0xAE	RESET_NODE	Stops sampling and data transfer
0xB0	DEEP_SLEEP	Hibernation mode (ultra-low power consumption)

Table 4.4: Brain Instructions

the flow of information between the PC and a Skin Patch, they also configure, synchronize and maintain a stable network.

PC software directly interfaces with the firmware of the Brains, so a set of instructions had to be implemented so that the user can communicate to the Brain what needs to be done. Many of these are explicitly requested by the user, while others are internal instructions that usually need to be executed by others. Table 4.4 lists the available instructions of the brain:

As it can be seen, the brains can selectively reprogram⁷ or reset a single node in a Skin Patch Network, or do so for the entire network depending on the command received from the computer. They can also indicate nodes to start/stop execution of application code or sampling code, and/or send a patch of skin to deep-sleep mode to conserve power. An extra instruction was also added to reset the Brain in case this gets stuck.

These are not, however, all tasks carried on by Brains. In fact, most of their tasks are executed automatically and thus are transparent to the user. This was done so as to facilitate their use and minimize the need for administrative tasks. Some of these include: management of both communications channels (USB and I²C), data flow control and buffering, and synchronization.

⁷If all nodes are programmed at once, programming code is sent to the I²C broadcast address. This activates the **General Call** flag in the MSP430 microcontroller, which allows it to differentiate if code was sent only to it or to all of the nodes in the network. This is useful because a status byte is transferred back to the brain. If the code was only sent to one node, this status byte is transferred right away, otherwise each node will wait until polled by the Brain.

4.2 PC Graphical User Interface

The second software component developed for the project, is the **GUI** that serves as a front end to the Skin Patch networks. As the reader may recall, this application is mainly intended for the case in which the Skin Patches are used as data extraction devices, however it could also be used to reprogram a Patch of Skin that is being used as a stand-alone device. The user interface has three main purposes: Network Discovery, Network Programming and Data display and logging. Figure 4-4 shows the application window indicating its components, and Table 4.5 gives a quick description of these.

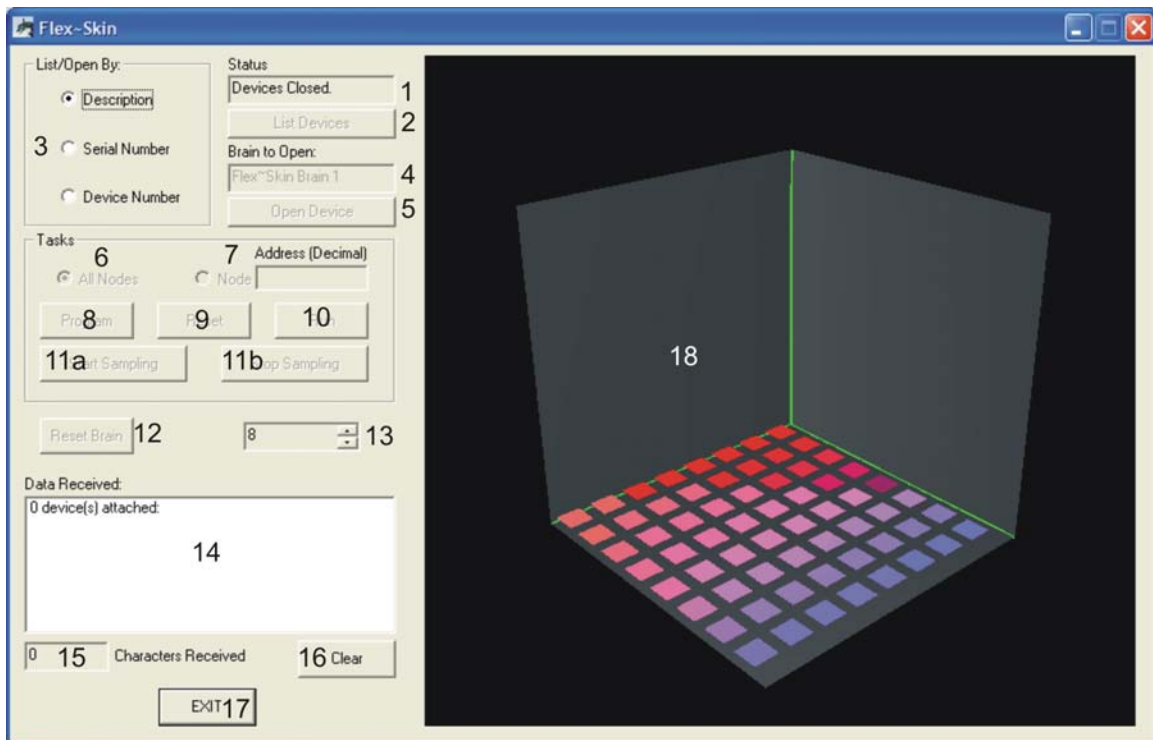


Figure 4-4: GUI Components

These functions along with others will be described in more detail in the following sections.

Component	Description
1	Indicates the current network status
2	Lists the currently connected Brains
3	Brains can be either listed by any of these three options
4	This box is used to specify which Brain to work with
5	Opens a new device to work with
6	Specifies that all nodes will be affected
7	Specifies that only the node with the typed address will be affected
8	Programs the specified node in the network (affected by 6&7)
9	Resets the network (affected by 6&7)
10	Starts execution of code (affected by 6&7)
11	11a starts network sampling; 11b stops network sampling (affected by 6&7)
12	Resets the currently opened brain
13	Changes the amount of <i>Display Nodes</i> in 18
14	Displays messages and echoes received data
15	Displays the number of bytes received
16	Clears 14&15
17	Exits the application
18	Displays received data from the network (size determined by 13)

Table 4.5: GUI Components

4.2.1 Network detection

The reader may recall that one of the design directives of the system was to make it scalable. Software plays an important role in this regard because it has to be able to manage networks of any arbitrary size and shape⁸. With this in mind, the software was designed in such a way that it can work with several different Skin Patches by allowing numerous Brains to be connected concurrently to the system. The ability of FTDI’s FT245BM USB chip to allow several identical devices to be operated in the same bus, and its very simple **API** were in fact the two reasons for which this device was chosen. Before explaining the way that the GUI manages the Brains though, it is necessary to provide a quick overview of the low-level interface between the OS and the device drivers.

Windows requires all hardware devices to have a device driver installed so that the Operating System can understand how to handle it. FTDI provides two different drivers: A **VCP (Virtual COMM Port) driver** and the **D2XX Direct Driver**[28]. The first one turns

⁸Up to the limits set by hardware

the USB device into a regular serial COMM port that can be accessed using Windows COMM API. The problem with this approach though, is that it needs to install a different driver for every device; so if 10 Brains are connected at once, there will be 10 different Virtual COMM Ports, which is highly undesirable. The second driver, however, allows the device to be accessed through a dynamic library or DLL, and therefore allows multiple devices to be operated concurrently. This was the driver used by the application.

Once Windows detects that a Brain has been connected, it automatically loads its driver. If multiple Brains are connected, however, Windows can't address them individually because the driver has no way of recognizing one Brain from the other because their chips are identical. To get around this, the USB chip uses an EEPROM chip that can be loaded with a serial number so that Windows can differentiate them. This was done using a special application provided in FTDI's website (MProg 2.8a).

Going back to our application, for it to be able to work with a Brain, they have to be successfully *enumerated* and *opened*. Enumeration has to be done in order for the driver to recognize the specifics of the devices connected to the bus. Once devices have been enumerated, the application must open a handler to the device through which communications can then be established. Enumeration is always carried out automatically by the application, but the user must manually open the device⁹ with which he wishes to work with; this is done by typing-in either the name, serial number or device number (depending on the selected option) into the edit box (number 4 on Figure 4-4) and then clicking the **Open Device** button. The only case when a device is automatically opened is when the application detects that only one Brain is connected. This behavior is shown on Figure 4-5.

Automatic Enumeration is done by registering the application so that it can receive notifications whenever hardware changes. This is done by registering the application with a device filter so that it is only notified by Windows whenever a USB device insertion/removal event is generated. Since Brains are therefore detected and enumerated automatically, the system is to a certain extent “plug and play”; it is not fully plug and play because nodes in a skin Patch are not currently automatically detected. This point will be covered in the

⁹In this context, *device* refers to a Brain with an attached Skin Patch

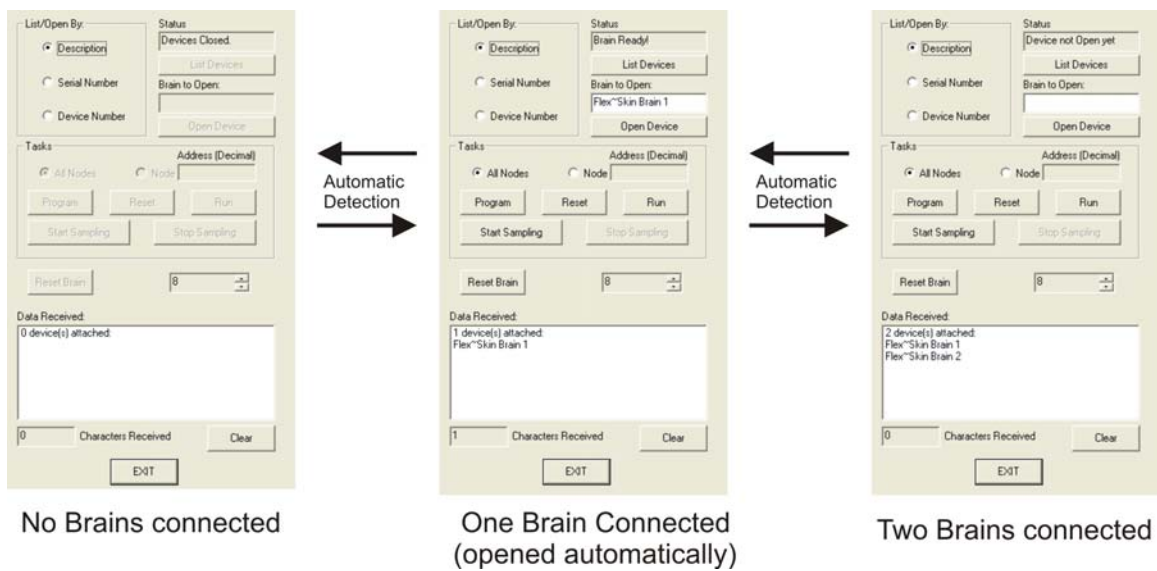


Figure 4-5: Automatic configuration of Brains

last chapter.

Two other things are left to mention: first, all functions will be disabled until a successful enumeration/opening sequence is executed. And second, enumeration can be always be carried out by selecting an enumeration option in the radio buttons (component number 3). This is useful if several Brains are connected, and their ID's or serial numbers need to be extracted.

4.2.2 Programming

The second major task, and perhaps the most useful one of the PC software is its programming functionality. This has been mentioned before, but what is the role of the GUI? It is actually a really simple one, since the complexities of programming the nodes are mainly carried out by the brain firmware.

There are two ways in which the GUI can program a Skin Patch: programming a single node or the entire Patch. These options are specified by components 6 and 7 (the two radio buttons) shown in Figure 4-4. When the program button is pressed, a modal File Open

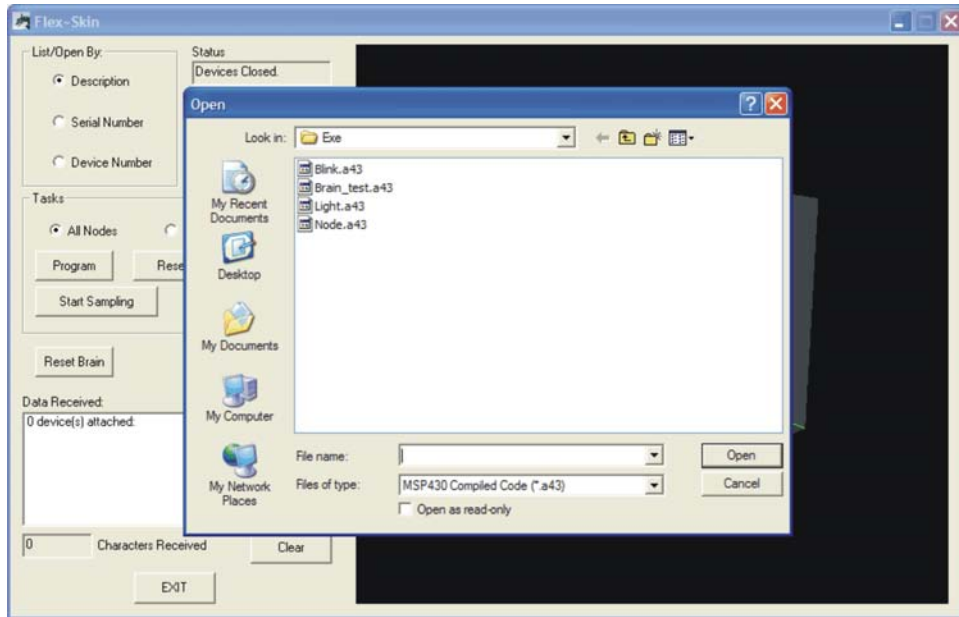


Figure 4-6: GUI Programming Environment

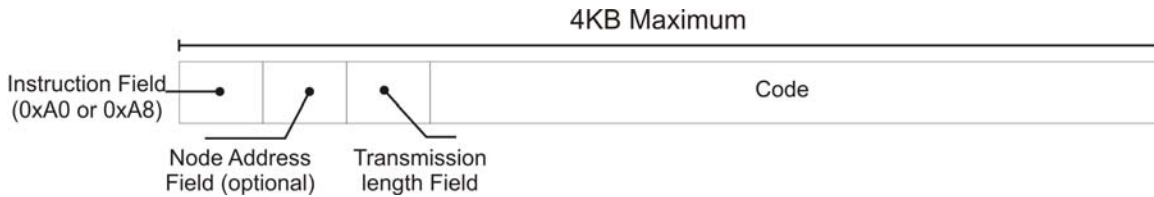


Figure 4-7: Programming packet

dialog box is opened so that the user can select the code file that will be used to reprogram the network. This is shown in Figure 4-6.

If no file is selected, the operation is cancelled, otherwise the application will assemble a code package of up to 4KB in length by parsing the file to remove its unused fields (leading colons and field type) and appending extra needed fields. These fields are the appropriate instruction, (either 0xA0 or 0xA8), depending if it is a single node or the entire Patch, the node address in case this is a single node operation, and the total transmission length. This is then transferred through USB to the currently opened Brain, and then forwarded by this to the appropriate recipients. This can be seen in Figure 4-7

An important point to stress is that the code has to be in Intel HEX format. This can be generated in several different ways. In this case, IAR's Linker was used to generate an output file in this format. The application can be either coded in MSP430 Assembler or C, but it will ultimately depend on the capabilities of the compiler used.

4.2.3 Sampling and Display

The next component of the GUI software is the Sampling and Display sub-unit. This is conformed of components 11a, 11b, 13, 14, 15, 16 and 18 and it allows the user to visualize extracted data in real time, as well as store the information for further processing. These functions can be used in either single node or full patch modes. Visualization and Data logging are always started and stopped at the same time, however they are two separate functions and each will be described separately.

Data visualization is done by embedding an OpenGL picture control into the application window. OpenGL is probably the most widely used graphics programming language because it easily allows 2D and 3D images to be created. The OpenGL control was then used to create an array of 3D-bars to plot data values read from the sensors. Whenever a data value is received, it is mapped to the height value of its corresponding 3D bar, so the sensor value can be visualized in real time by observing how the 3D plot changes.

Several additional effects and controls were added to allow the user to easily change the perspective of the image, and to enhance the visual aspect of the displayed data. The chart can thus be rotated around its X and Z axes, panned (up, down, left and right) and zoomed (in and out), all in real time using the mouse pointer; this was done so that data that may be obstructed by other bars, can be easily visualized. Picture quality was enhanced because in 3D rendered scenes, this depends heavily on the lightning effects used, so a full shading and lightning model was also included in the rendering pipeline. Finally, since the necessary amount of display units (3D bars) can vary according to either Skin Patch size, the type of sensor being monitored¹⁰, or the sampling mode selected (single node or full patch) a spin

¹⁰Skin Patch size affects the number of necessary display units because it affects the number of nodes that

control was added to change the number of bars that make up the 3D chart. Figure 4-8 shows how these controls affect the chart area¹¹.

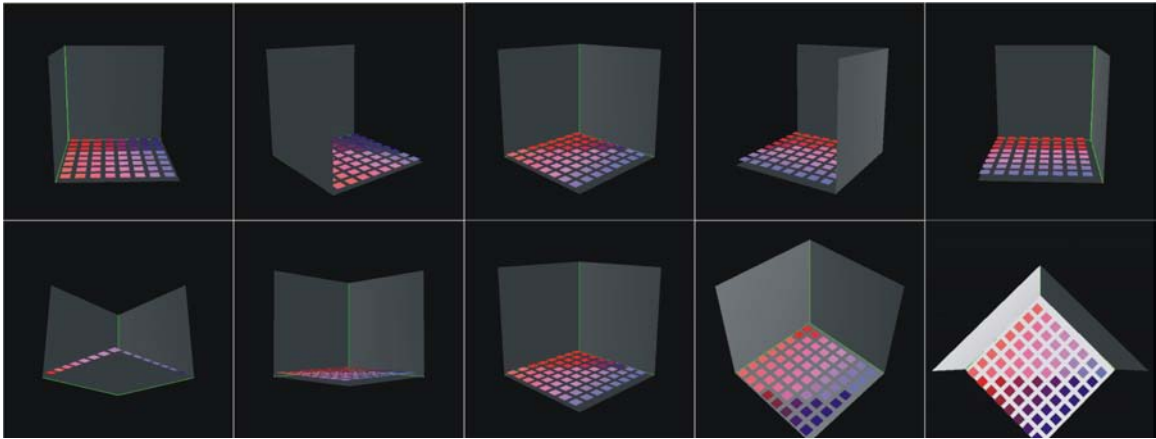
The reader may notice that there is a color gradient in the different columns that make up the plot. This is merely a cosmetic change that was done to better visualize the different bars, because visualization was a bit difficult when bars were all the same color. Yet, this may be used as an extra degree of freedom in case a physical quantity has to be mapped to a display value.

The second function of this sub-unit is data logging. Every time the start sampling button is pressed, a modal File Save dialog box is opened to ask the user for a file name. If this is not provided, then sampling does not start, otherwise, several things will happen:

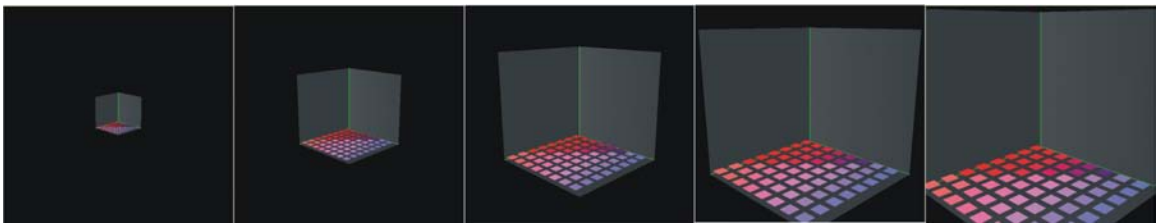
1. The file specified by the user will be opened or created if it does not exist
2. All buttons except for **Stop Sampling** become disabled
3. An **Execute Code** instruction is issued to ensure that the nodes are executing the code
4. A thread is started to handle the sampling process
5. If **All Nodes** is selected, the entire Skin Patch will be scanned for new sensor data by issuing instruction **0xAC** for every node in the Patch. Otherwise, if a node address is specified, only this sensor will be sampled
6. Data from each sensor is then converted to a decimal number, and stored in a different column for every sensor
7. Data is sent to the OpenGL control for visualization
8. The cycle continues until the **Stop Sampling** button is pressed

have to be monitored. The type of sensor affects it because the amount of sensing channels varies according to the sensing modality being monitored, 4 for pressure, 2 for strain and whiskers, 1 for temperature, ambient light and sound

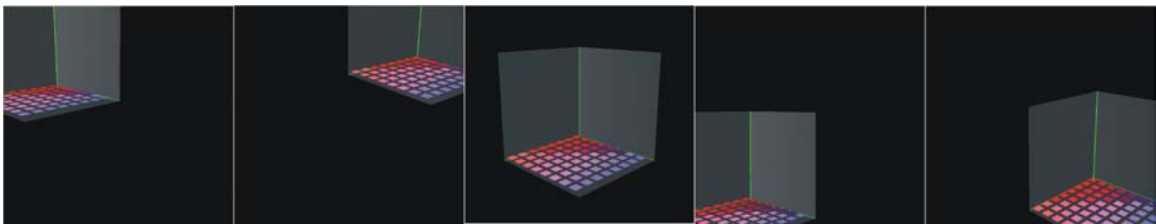
¹¹These charts are shown without any data so that the effect of the transformations can be seen. Other plots with data will be shown



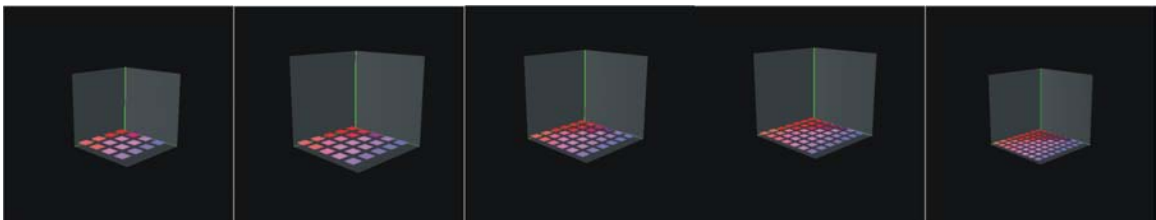
(a) Rotation control



(b) Zooming control



(c) Panning control



(d) Sizing control

Figure 4-8: Visualization: OpenGL 3D chart transformation modes

Once the process is stopped, the file is closed, the thread is finished and all buttons are now enabled (except for the **Stop Sampling** button). The file is stored in a Microsoft Excel readable format so that further processing/plotting can be done.

It is important to mention that although the application is capable of showing the data from any one of the sensor modalities in the Skin Patches, the functionality to extract data from all sensing modalities at once has not been implemented so far¹² because of the complexity involved in displaying data from many different sensing modalities effectively. Sampled data is also controlled by the installed application on the nodes, therefore if a different sensor needs to be sampled, the application on the nodes has to be changed. Data extracted from all types of sensors will be shown in the results chapter.

4.2.4 Other Functions

Finally there were some other minor functions that were not mentioned before, but that are also useful to have. These are summarized in the following list:

- Resetting Brains (Button 12): useful if either the Brain or the I²C bus gets stuck
- Executing node applications (Button 10): to indicate the Bootloader to start execution
- Resetting nodes (Button 9): resets either a single node, or the entire patch.
- Amount of bytes received (component 15): useful to debug the network.
- Address validation (component 7): The node address must be in the valid range (0-1023) or the task buttons will not be enabled

Many other functions of the software were left unmentioned intentionally, however the reader is welcome to check the full listing of the different project files in Appendix E.

¹²This means for example that temperature readings and light readings can't be sampled at once, but *not* that several nodes can't be sampled at the same time which as it was previously noted is indeed possible

4.3 Communications Software

The last part of the software section corresponds to the specifics of the communications channels used in the entire project. This will briefly outline some of the necessary design choices that were taken along the whole process.

4.3.1 I²C Backbone

We have talked about the hardware considerations of the I²C backbone, but nothing has been mentioned about the software that runs the bus. The I²C bus requires two lines to be routed among all devices which are to be connected to it plus a common ground. This means that whenever a device needs to talk to another one in the bus, it needs a way to address it. In fact the I²C bus has two different addressing schemes: 7-bit and 10-bit.

The addressing scheme is actually the theoretical limit to the number of devices that can coexist in the same bus. The first one allows a maximum of $2^7 - 1 = 128$ devices while the second one allows $2^{10} - 1 = 1023$ devices. Naturally, the second one was chosen to allow a larger number of devices to be connected to the bus. These numbers are not the actual allowed limit, because the input capacitance of all pins connected to the bus add to the total, which as we already mentioned cannot exceed 400 pico-farads. We already mentioned some ways to get around this limitation, however for the case of the current project, the real limit to this will be presented in the Results Chapter.

There are however several questions that must be answered though: How are these addresses assigned? Is it the Bootloader which assigns the address or is it the application code or both? What happens if there are more than one device in a Skin Patch with the same address? How is the bus arbitrated?

First of all, the scope of an I²C address is limited to the Patch of Skin to which the node is connected. So although there can't be two nodes with the same address in the same Patch of Skin, addresses can be reused if a different Brain is used. In other words, as long as there are not two nodes with the same address on the same Skin Patch, addresses can be

arbitrarily assigned. In the specific case of the Skin Patch assembled to test the project, 12 nodes were connected and addresses 0x100–0x10A were assigned, to consequent nodes.

Now, all nodes are first loaded with the Bootloader program described before, however what was not mentioned before is that when the Bootloader is programmed using the JTAG debugger, the I²C address assigned to the node is assembled into location 0x1080 in flash memory. This is done so that I²C addresses are only assigned once in the programming lifetime of the nodes, and no conflicts are created in the bus. If two nodes with the same address are placed on the same bus, the system will eventually reach a deadlock state which must be manually reset, which is why it is so critical to avoid this situation.

The solution to the last question, "How is the bus arbitrated?" is actually really simple: the MSP430 does it. The I²C hardware module of the MSP430 microcontroller, can detect collisions in the bus and has a method to resolve contentions. Whenever a collision is detected, the device that first takes the data line to ground loses arbitration and an interrupt flag is generated. Processing this interrupt flag allows communications to remain reliable. These cases are rare though, as only one master exists in every Skin Patch: the Brain.

The last consideration to make about the I²C backbone bus is the speed at which it is run. This is the second parameter that limits the amount of nodes that can be connected to the same patch. Although bandwidth requirements are supposed to be brought down with the addition of processing power into each node, there is still the need to transfer either higher-order features into a PC, or simple raw data if the Skin Patch is to be used as a data extraction device. The amount of bandwidth needed will depend on a variety of factors, like the number of nodes, the sampling rates, and the resolution at which each sensor is sampled. Making the bus run at fast-speed (3.4Mbps) would have placed huge constraints on the length of the bus lines, and running it at the standard speed of 100Kbps would not have been enough for more than a couple of nodes. Therefore high-speed mode was chosen, and the bus is then run at 400Kbps¹³.

¹³Although these are the standard speeds of the I²C standard, the I²C module of the MSP430 can run the bus at any arbitrary speed, up to a limit of close to 500Kbps

4.3.2 Peer to Peer

Peer to peer communication was added to every node so that data could be exchanged between them without the need to use the backbone bus, which is only to be used for data transfer between a Brain and the Patch Network. With this, it is possible to combine data from each node's own sensors with that of adjacent ones so that more information can be extracted across the footprint of a stimulus event, and either sampling rates can be adjusted, or features like center of mass and sound directionality can be calculated.

No application currently developed for the system utilizes this capability, however this is mentioned before for two reasons: first, because it is part of the design of the system, and second because it sets the basis for future applications and algorithms.

One of these possible algorithms is precisely a Network discovery algorithm, which is critical for a Skin Patch that can be assembled and disassembled. Our current project has a fixed number of nodes in a known topology, so all the software developed for the PC and most of the firmware was created knowing beforehand the configuration of the Skin Patch network. Yet, for the more general case in which the number of nodes, and the way they are connected is not known a priori, a method must be provided so that the Brain firmware and PC software can identify how a particular Skin Patch is connected. The algorithm may look something like this:

1. Every Brain should ping all the addresses to find out which nodes are present
2. For every node in present, the brain will obtain a neighbor list
3. Once a list with all nodes is created, a routing table is generated
4. With the routing table generated, all P2P links can be established and the topology of the Skin Patch Network is found

An alternate way of doing this would be to have each node report itself to the Brain once it is connected, however this would need the I²C bus to work as a multiple master bus. This is actually possible but, once again it is left as a future enhancement to the project.

4.3.3 USB

The last part of the communications software is that of the USB link. As previously mentioned in the Network detection subsection, all USB communications are handled by the D2XX driver. Not much else can be mentioned about it, as most of this was extracted from FTDI's programming guides. For a full reference of the D2XX API the reader is welcome to check FTDI's Programming guide[\[28\]](#), or the full listing of the code in Appendix [E](#).

Chapter 5

Analysis of Results and Evaluation

“No amount of experimentation can ever prove me right; a single experiment can prove me wrong”.

– *Albert Einstein*

Once hardware and software components have been described, we proceed to show in the current chapter the obtained results. First, the mechanical performance of the system is presented. Then, the second section will analyze each sensing modality and show data plots for each one. The third section analyzes both communication links, and evaluates the actual operation speeds, data throughput and overall system scalability. The fourth section of the chapter describes how well the system performed as an ultra-low power device under several conditions, so that it can be then evaluated against the design goal. Finally, the last section presents a brief analysis of the involved costs.

5.1 Mechanical Stability

The first of the Results subsections will talk about experience with the mechanical characteristics of the system. These are mentioned first, because several mechanical characteristics

of the design greatly affected several of the results presented in this chapter. There were three main characteristics of the mechanical design that affected the overall system performance. The first was related to the substrate, the second to mechanical connections and the third to pressure sensors.

5.1.1 Substrate

Given that the prototyping phase is so expensive it was nearly impossible to exactly know how flexible the material would be until the final design was fabricated. When the nodes were fabricated, the final substrate thickness was actually less than the one specified by the project, however its flexibility and compliance to conform to the shape of the soldered components was far below what was expected. This means that instead of having a substrate with mechanical characteristics similar to that of a thick sheet of paper, it ended up being almost like a credit card. The problem with this is that the substrate does not conform to the body of large components soldered to it like the microcontroller, so whenever the substrate is bent, these components easily break off. This ultimately had an enormous impact on the Skin Patches because they now had to be handled with extreme care to avoid breaking off the microcontrollers. For this reason, the data plots and snapshots extracted for sensing modalities that require physical warping of the Skin Patch like strain and pressure are only shown for a single node to avoid any excess strains.

The fact that components may eventually break off because of skin patch bending was actually expected, however this problem was much worse than was expected in the case of the microcontroller. Not all was a total failure in this regard though, because amazingly enough, none of the other components presented this problem. In fact, all the other components were remarkably resistant to even sharp bending angles; even the larger ones like the MEMS microphone and crystal. What was the difference? Footprint size and type. The microcontroller comes in a 64-pin $9mm \times 9mm$ QFN leadless package which means that when the node was bent all the stress was absorbed by the microcontroller pins. Since there is nothing but a really small amount of solder holding the microcontroller pin to the substrate pad, these break off very easily. This does not happen with other components

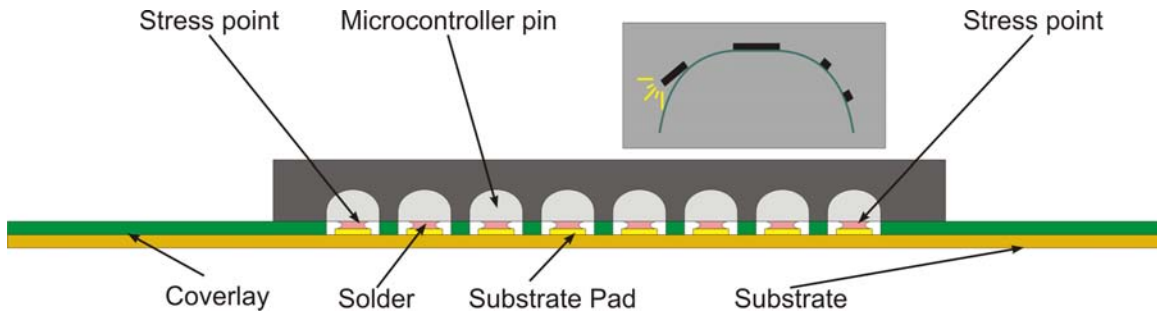


Figure 5-1: Stress concentration points in node microcontrollers

because the pin leads can absorb some of the stress and because they are so small that even sharp bending angles don't stress the soldered connections enough to break them. This effect is shown on Figure 5-1. There are several ways around this problem, some of which will be mentioned in the Conclusions chapter.

5.1.2 Connections

The second mechanical aspect to evaluate was the mechanical terminations used. We mentioned before that mechanical terminations were critical to maintain good network stability, yet there were two problems with the ones chosen in the design: header hole size and connection flap size.

Something that was not foreseen at the design stage of the project is that header holes were so small that they actually caused connections to easily crack when the node was bent. This generated numerous connection flaws which sometimes prevented the correct operation of the I²C network in the Skin Patches.

The other thing that was not well thought when the design was made is that since headers were placed on a flap that protrudes from the body of the Skin Nodes, whenever a Skin Patch experienced some bending, all the bending happened mainly at the flaps and not at the node body. This was actually a good thing to relieve some of the stress that could concentrate on the microcontroller pins, however it was detrimental to the performance of the strain gages. This is shown on Figure 5-2. Because of this, even if the patch is bent,

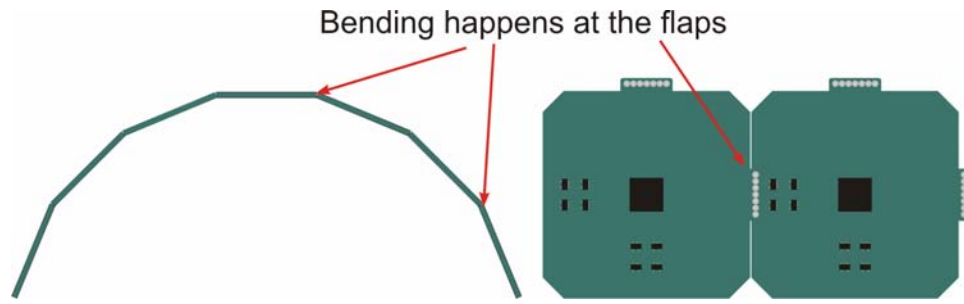


Figure 5-2: Skin Patch bending profile

the strain gages are only minimally stimulated. For this reason, data plots shown for strain gages are not shown for the entire Skin Patch, but rather for individual nodes so that the reader can have an idea of their actual performance.

5.1.3 Pressure Sensors

The third mechanical characteristic that had a deep effect on the sensing behavior of the nodes is related to the pressure sensors. Pressure sensors use a special material that has to be bonded to electrodes placed on the surface of the nodes. However since the electrodes must be in direct touch with the sensing material, no glue can be placed in the active sensor area. Moreover, Skin Nodes had to be very small to maintain a good sensing density, which left very little space that could be used to glue the material to the substrate.

To bond the QTC material to the substrate, a 3M 77 Super Spray Adhesive was used. This glue was applied to the nodes with a mask, so that the sensor electrodes were not coated. However, this glue is semi-liquid when first applied, and because the area available for bonding was so reduced, even if the sensor electrodes were masked, some of the glue was spilled on them making some sensors more sensitive than others and some not sensitive at all.

A way better way of bonding the QTC material to the nodes would have been to use adhesive tape instead of glue, which is easier to correct, cleaner and easier to handle. This lesson was learned later in the assembly process though, and therefore some of the sensors

of the assembled skin patch don't work as well as they should. So when these are analyzed, only data plots of the sensors that were not affected will be shown.

Finally, it is important to remark that even though pressure sensors and strain gages were affected by these mechanical flaws, they were actually more sensitive than actually expected, when they were first tested before the entire patch was assembled. Other sensing modalities that did not depend on the mechanical characteristics of the system design were obviously not affected by these problems, so the entire Skin Patch could be easily scanned by the PC sampling application as it was originally intended.

5.2 Sensor Data and Sensing Ranges

Several experiments were carried out to test the functionality of the designed platform. Two patches of skin (one with 12 nodes and another one of 4) and two Brains were fabricated and assembled to test both modes of operation of the Skin Patches: stand-alone mode, and data-extraction mode. This section is divided into two subsections: the first one will show how each one of the sensing modalities performed along with data plots extracted for each one of them using a skin patch as a data extraction device; the second one will demonstrate the functionality of the same patch used in stand-alone mode.

5.2.1 Skin Patches as Data-extraction Devices

To analyze how well each one of the sensing modalities performed, they were first calibrated if necessary and then data was extracted from them. Since each one of the sensing modalities was analyzed separate from each other, results will be presented according to the sensing modality they were obtained from. Although only one data set was extracted for each sensing modality, the extracted information will be shown in two different ways: the first will show some snapshots taken from the real-time 3D OpenGL control from the GUI application when the sampling process started to illustrate its functionality; the second set corresponds to plots created with the data saved by the application at the moment of

sampling, along with some images of the stimuli events that generated them. Additionally, there will be a brief evaluation of the performance of the sensors.

Strain and Bending Results

Much was mentioned about strain gages in the hardware section, as they were one of the two sensing modalities that had to be custom-designed. How well did they perform though? To answer this question, we must first calibrate them; this was done by the method of *Shunt Calibration*[15]. Shunt calibration is an indirect way of calibrating strain gages that consists of simulating a strain by changing the resistances of the Wheatstone bridge. This is a popular method because it can be used whenever the required instruments to conduct a direct calibration are not available. This is a tricky exercise though, as the gage factor and total resistances of the gages must be known. Gage factor being an intrinsic property of the used material it is easily obtained from the manufacturer or material property tables; in the other hand, resistances had to be manually measured.

Calibration

Referring back to Chapter 3 when strain gages were mentioned, it was said that it is critical to match the resistances of the strain gages so that the amplifier is not saturated by a resistance mismatch. Table 5.1 shows the actual measured resistances of each one of the two strain gages contained in every one of the 32 fabricated nodes along with the proposed matching and bridge resistors that were used.

The first column is just an index while the second one refers to the serial code imprinted on the node and it was used as a reference. The third and fourth columns indicate the actual measured resistances in Ohms for each one of the two strain gages included in every node. The fifth and sixth columns list the commercially available resistors with the closest resistance values to those listed in the previous two columns. Columns seven and eight show the difference between these two. The next two show the necessary resistor to use in series

	Node	SG1	SG2	R(X)	R(Y)	$\Delta(X)$	$\Delta(Y)$	Rb(X)	Rb(Y)	$\Delta(Xc)$	$\Delta(Yc)$
1	001-1	168.9	173.3	169	174	0.1	0.7	0	0.5	0.1	0.2
2	001-2	161.4	165	162	165	0.6	0	0.5	0	0.1	0
3	001-3	169	173	169	174	0	1	0	1	0	0
4	001-4	178.2	182.2	178	182	-0.2	-0.2	0	0	-0.2	-0.2
5	001-5	175.9	176.5	178	178	2.1	1.5	2	1.5	0.1	0
6	001-6	166.9	167.5	169	169	2.1	1.5	2	1.5	0.1	0
7	001-7	167.2	167	169	169	1.8	2	2	2	-0.2	0
8	001-8	173.5	176.7	174	178	0.5	1.3	0.5	1	0	0.3
9	001-9	171.1	173.9	174	174	2.9	0.1	3	0	-0.1	0.1
10	001-10	165.5	166.1	169	169	3.5	2.9	3.6	3	-0.1	-0.1
11	002-3	184.5	184.7	187	187	2.5	2.3	2.4	2.4	0.1	-0.1
12	002-5	180.8	183.4	182	187	1.2	3.6	1	3.6	0.2	0
13	002-6	183.1	184.7	187	187	3.9	2.3	3.9	2.4	0	-0.1
14	002-10	181.5	182.3	182	182	0.5	-0.3	0.5	0	0	-0.3
15	003-7	173.4	174.3	174	174	0.6	-0.3	0.5	0	0.1	-0.3
16	004-1	172.9	174.7	174	178	1.1	3.3	1	3	0.1	0.3
17	004-2	175.7	179.8	178	180	2.3	0.2	2.4	0	-0.1	0.2
18	004-3	167.8	174.2	169	174	1.2	-0.2	1	0	0.2	-0.2
19	004-6	171	174.9	174	178	3	3.1	3	3	0	0.1
20	004-8	170.3	171.4	174	174	3.7	2.6	3.6	2.4	0.1	0.2
21	004-9	166	171	169	174	3	3	3	3	0	0
22	004-10	173.5	178	174	178	0.5	0	0.5	0	0	0
23	005-1	171.2	177.2	174	178	2.8	0.8	3	1	-0.2	-0.2
24	005-2	170.4	177	174	178	3.6	1	3.6	1	0	0
25	005-3	172.5	177.8	174	178	1.5	0.2	1.5	0	0	0.2
26	005-4	174.6	178.8	178	180	3.4	1.2	3.6	1	-0.2	0.2
27	005-5	178.5	179.8	180	180	1.5	0.2	1.5	0	0	0.2
28	005-6	177	180.3	178	180	1	-0.3	1	0	0	-0.3
29	005-7	175.9	180.9	178	182	2.1	1.1	2	1	0.1	0.1
30	005-8	176.4	180.7	178	182	1.6	1.3	1.5	1	0.1	0.3
31	005-9	176.1	181.4	178	182	1.9	0.6	2	0.5	-0.1	0.1
32	005-10	177.3	183.1	178	187	0.7	3.9	0.5	3.9	0.2	0

Table 5.1: Strain gage measured resistances

with the strain gages to match their resistance values to those listed in columns five and six. The last two columns show the actual measured difference between the resistance of the matched strain gage, and the resistor used in the bridge. It can be seen that the largest difference is of 0.3Ω which is negligible. It is also important to point out that trace lengths for gages one and two of each node were designed to be equal to keep resistance variations to a minimum. Yet as it can be seen, there is still a considerable variation within nodes and from node to node.

With these resistance values it is now possible to calibrate the strain gages. If we refer back to Figure 3-15, the following relationships can be extracted:

$$\begin{aligned} V_{R2} &= V_{CC} \left(1 - \frac{R_1}{R_1 + R2} \right) \\ V_{R3} &= V_{CC} \left(1 - \frac{R_3}{R_3 + R4} \right) \\ V_O &= V_{R2} - V_{R3} = V_{CC} \left(\frac{R_3}{R_3 + R4} - \frac{R_1}{R_1 + R2} \right) \end{aligned}$$

Or in another form:

$$\frac{V_O}{V_{CC}} = \frac{R_3/R_4}{R_3/R_4 + 1} - \frac{R_1/R_2}{R_1/R_2 + 1} \quad (5.1)$$

Equation 5.1 shows that the output voltage of the bridge is a function of the ratios of the resistances. Moreover, if $R_3/R_4 = R_1/R_2$ the output is zero which proves why resistances must be matched for a balanced output. Now if we place a resistor R_C in parallel with R_3 which is the added resistance of the strain gage and the matching resistor, the change in resistance of the arm becomes:

$$\Delta R = R_3 - \frac{R_3 R_C}{R_3 + R_C}$$

Or,

$$\frac{\Delta R}{R_3} = \frac{R_3}{R_3 + R_C} \quad (5.2)$$

However, unit resistance change is a function of strain, so if we re-express Equation 5.2 to reflect this, we can then extract a relationship between the simulated strain and the shunting resistance necessary to produce it. Unit resistance change is related to strain by:

$$\frac{\Delta R}{R_G} = F_G \varepsilon \quad (5.3)$$

Where R_G is the nominal resistance of the strain gage (obtained from Table 5.1), F_G is the gage factor, and ε is the material strain. Now, if we combine Equations 5.2 and 5.3, we can obtain:

$$\varepsilon_S = \frac{-R_3}{F_G(R_3 + R_C)} \quad (5.4)$$

Where ε_S is the compressive strain simulated by shunting R_3 with R_C ¹. Now, we already mentioned that the minimum bend radius of a multi-layer flex circuit should be of approximately 24 times the total thickness of the substrate, or in the case of the Skin Nodes $24 \times 0.0162in = 0.3888in = 0.987552cm$. If we take this to be the bending limit of the Skin Nodes, then the strains experienced by the gages will be extremely small. If we consider small strains and we solve for R_C from Equation 5.4 we can now find a resistance value that will produce a known strain which we can then use to calibrate the sensors:

$$R_C = \frac{R_3}{F_G \varepsilon_S} - R_3$$

Since we expect strains to be small, we can arbitrarily pick a relatively small strain value and calculate the resistance needed to produce it. For this case a value of 100^{-6} strain

¹Although these equations are specific to compressive strain, a similar method can be applied to find tensile strains by shunting R_4 instead of R_3

R_3	R_C
162 Ω	809838 Ω
165 Ω	824835 Ω
169 Ω	844831 Ω
174 Ω	869826 Ω
178 Ω	889822 Ω
180 Ω	899820 Ω
182 Ω	909818 Ω
187 Ω	934813 Ω

Table 5.2: Resistances needed to simulate 100 microstrain

units or 100 microstrain was picked. We also know that $F_G = 2.0$ which corresponds to the constantan gage factor²[16] and that $R_3 = R_{gage} + R_m$. We have all that we need to calculate the resistance values, however since the nominal resistances of the strain gages are not equal, and they were matched to 8 different values (which can be observed in Table 5.1), there are a total of 8 different results which are shown in Table 5.2.

Using these resistance values to shunt the strain gages would emulate a known strain, which can be directly mapped to a bridge output voltage. These values however, are not actually used because it would be difficult to find such commercially-available precision resistors; yet, this exercise serves to have an idea of how large resistor values should be to emulate a microstrain close to what we want. To actually calibrate the sensors, we do the reverse instead: we calculate the strain that corresponds to available resistors, which closely resemble these values, and then use the found strains as the calibration values. Table 5.3 shows the calibration values found with Equation 5.4 for $R_C = 812K\Omega$:

The negative values indicate a compressive strain, but since the gages are essentially located in the bending axis, compressive and tensile stresses are symmetric. This means that these values can be used to adjust tensile strains as well, with only a slight error margin (the constantan film is not exactly at the center). Several assumptions are being made though. First of all, since the bending range will be constrained to the calculated minimum bending radius, there will be no mechanical deformations, and we can assume there will be no

²Gage factor changes with temperature, but this will not be taken into account because the temperature range under which the system is expected to work (0°~ 80°C) has only a minimal effect on it

R_3	<i>Microstrain</i>
162 Ω	-99.73379695 μS
165 Ω	-101.5803439 μS
169 Ω	-104.0423853 μS
174 Ω	-107.1199029 μS
178 Ω	-109.5818897 μS
180 Ω	-110.812874 μS
182 Ω	-112.0438522 μS
187 Ω	-115.1212713 μS

Table 5.3: Emulated strain caused by shunting gages with an 812K Ω resistor

hysteresis. Second, we are also assuming that constantan is an isotropic material and that the film is so thin that the effects of *Poisson*, and *Shear* strains can be ignored.

The story would end here if all we were interested is the relationship between resistance change and strain however, we also need to find how the bridge output voltage changes with applied strain. To do this, we first record the output voltage when the gages are shunted with a reference resistor value, and then we shunt it again with a different resistor to record the change in output voltage. By doing this we effectively map a difference in simulated strain to a difference in output voltage. However, since we don't know if the relationship between these two is linear, we have to use more than two values to extract the relationship between them. In the actual calibration tests, 7 resistance values were used to calibrate each one of the two gages of a single node; the results are shown in Table 5.4.

The first column shows the shunting resistor used for the calibration, these were the actual values measured with a multimeter and not the one indicated by the resistor color code. The next four columns show the data for strain gages 1 and 2. For each gage, two columns are shown: the first one lists the strain values obtained with Equation 5.3 for each one of the shunt resistors used; the second one lists the voltage seen at the output of the bridge amplifier. Now we can extract the relationship between strain and output voltage by plotting the former as a function of the later using the previous data. Figure 5-3 shows the results obtained, notice that strain sign was ignored because it only indicates the type of strain. The relationship is actually pretty linear, however their curves ended up being displaced from one another, because resistance matching of the bridge branches is not perfect, and

R_C	Node #004 – 3			
	SG1 (matched to 169Ω)		SG2 (matched to 174Ω)	
	Strain	V_O	Strain	V_O
97000	-869	1.502	-895	1.671
107000	-788	1.492	-811	1.659
118000	-715	1.468	-736	1.646
127000	-664	1.466	-684	1.636
138000	-611	1.457	-629	1.621
148000	-570	1.454	-587	1.611
156000	-541	1.45	-557	1.605

Table 5.4: Calibration results

thus the zero-bias offset is slightly different for both of them.

There is still two more things to take into consideration. The first one is that these results only apply to the calibrated node, to have exact measurements for all nodes each one must be individually calibrated with this procedure; this was not done because it was not a project goal to extract precise measurements. The second one is that we have yet to extract the full sensor range by recording the output voltages experienced when gages are bent to their maximum allowable (set by the minimum bend radius). We do this because we are digitizing the output voltage with the microcontroller's ADC, and we need to figure out how to map the sampled values to an actual strain value. From the lab tests, Strain Gage 1 had a range of approximately $0.765V - -1.95V$ with a zero-bias offset of $1.3544V$; Strain Gage 2 had a range of $0.95V - -2 - 135V$ with a zero-bias offset of $1.54V$. This gives a full range for each gage of approximately $1.185V$, half of which is tensile and half compressive. Now, the ADC quantizes the output voltage into 8-bit samples, which means that if the full range of the sensors is of $1.185V$ then, each sampled bit will correspond to approximately $1.185V/256$ or roughly $4mV$. Now finally we can convert this to strain by using either one of the line equations shown on Figure 5-3, if we choose the first one, then each bit will correspond to: $5888.5 \times (4mV) - 7975.5 = 27.25\mu$. Therefore each bit corresponds roughly to 30 microstrain units.

One final note about gage calibration, the actual signal conditioning for the strain gages uses a sleep transistor to maintain power consumption down. This transistor causes a

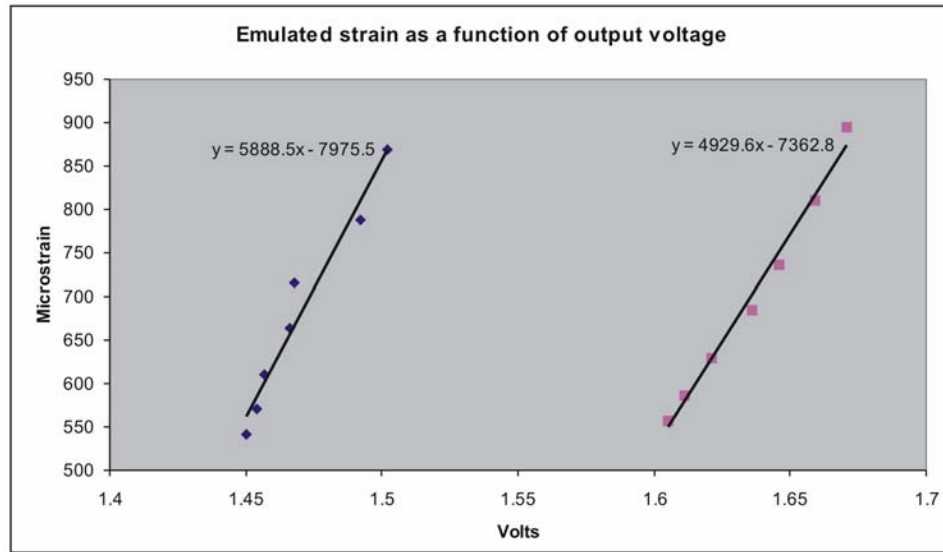


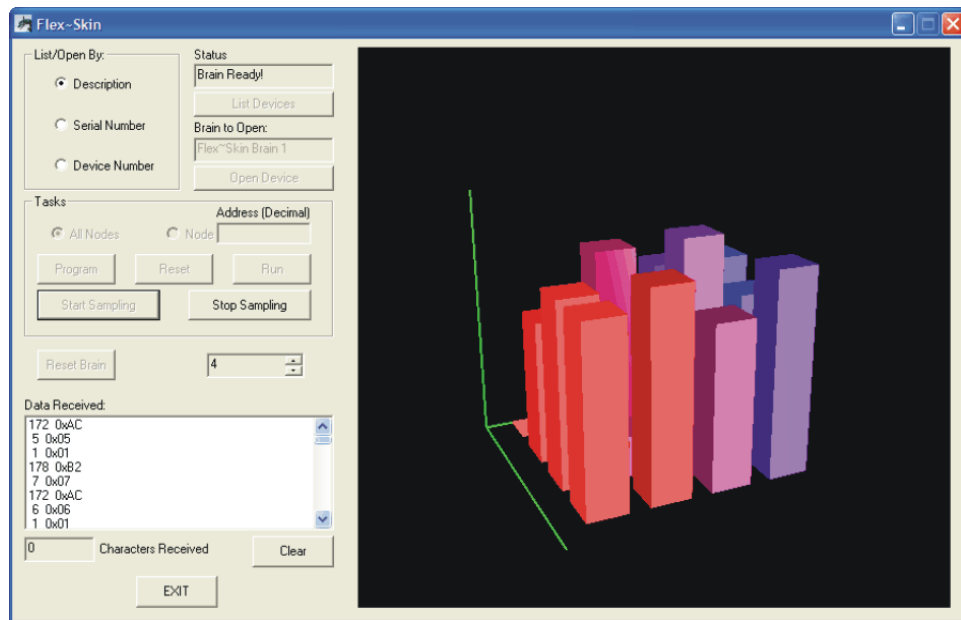
Figure 5-3: Strain Gage electronic calibration for gages 1 and 2 of node #004-3

voltage drop that decreases the total excitation voltage seen at the Wheatstone bridge and this effect was intentionally ignored. Also, if the system is to be used in a wide range of temperatures, then gages must be compensated for its effects; this is easily done though as each node is equipped with a temperature sensor.

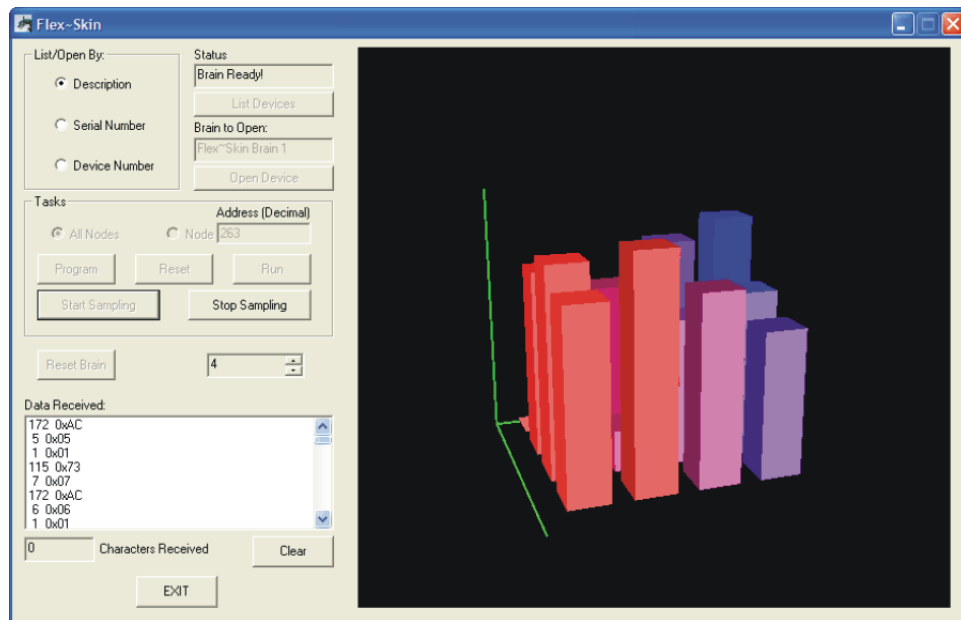
Data and Results

Once calibration is done, we can now proceed to show the data extracted from the skin. Figure 5-4 shows some snapshots taken when data from strain gages one and two were being sampled. Although no stimuli could be applied because of the mechanical problems previously mentioned, these are shown merely to demonstrate that raw data can be extracted from both strain gages. Figure 5-4(a) corresponds to data extracted from strain gage 1 of each node and Figure 5-5(c) corresponds to strain gage 2.

Although in the previous figures the strain gages were not submitted to a stimuli, their response can be visualized in Figure 5-5. These plots were extracted from the two strain gages of the node used for the calibration.

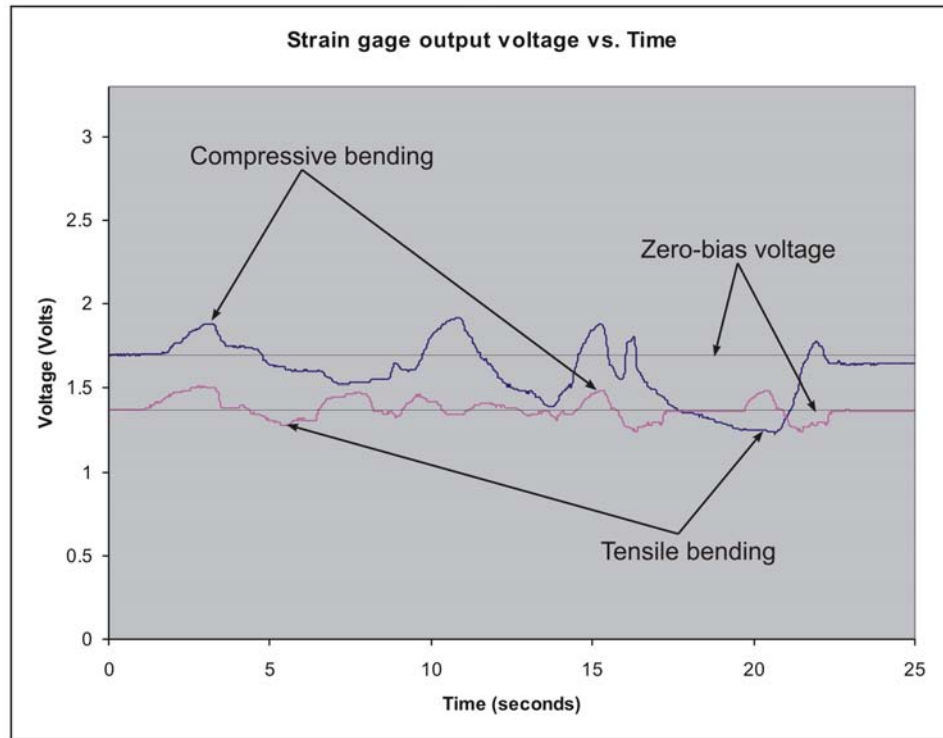


(a) Data from strain gage 1

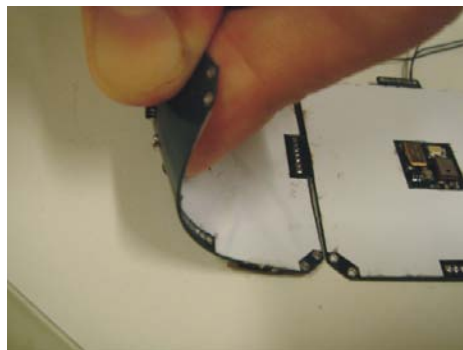


(b) Data from strain gage 2

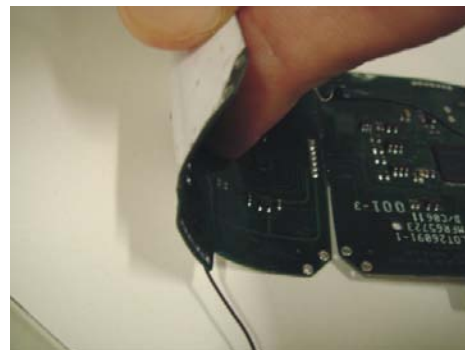
Figure 5-4: Real-time 3D visualization control showing offset from each one of the two strain gages of all nodes (no stimuli applied)



(a) Data from both strain gages



(b) Tensile bending



(c) Compressive bending

Figure 5-5: Strain gage data plots showing strain gage response

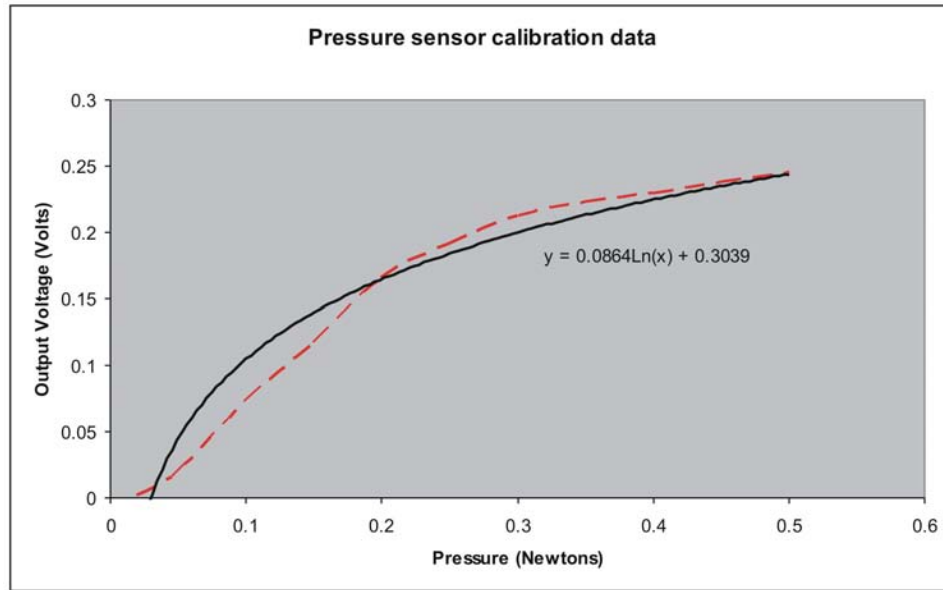


Figure 5-6: Pressure sensor calibration

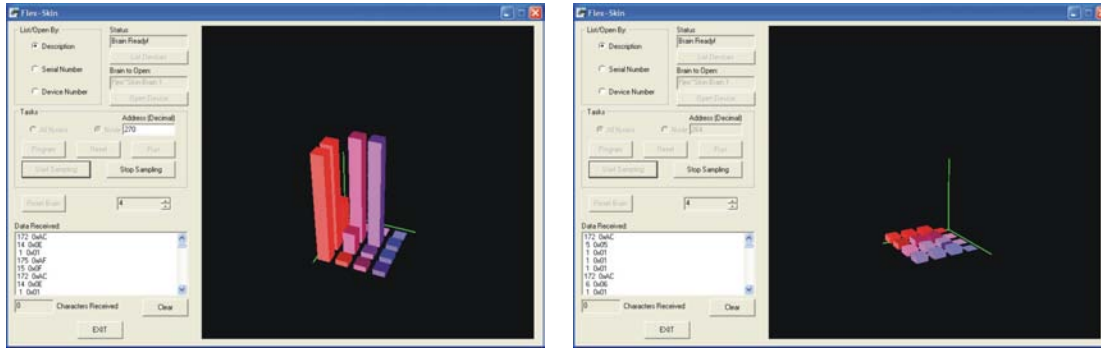
If strain is desired instead of the output voltage, this can be easily calculated using the procedure described before.

Pressure

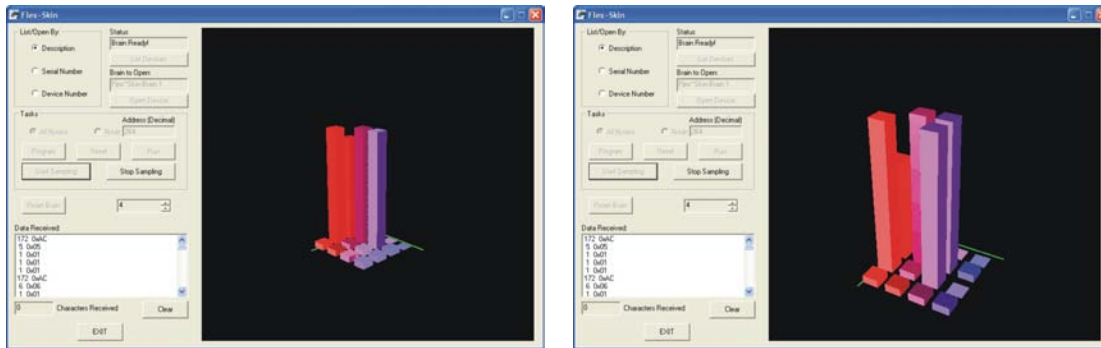
The second sensing modality that was also custom-designed was pressure. Pressure sensors were designed by using rigid board prototypes, because they could easily be fabricated at the lab. This was done mainly to observe the effect that trace width and length had over the sensitivity of the sensors. However, results showed that these factors had only an effect on the zero-bias resistance of the sensor and not their actual sensitivity.

Calibration of pressure sensors was much simpler than that of the strain gages because the instruments needed are easily obtained. In fact all that needed to be done was to apply known loads to the pressure sensors and record the output voltage seen at the output of the amplifier; to do this we only needed a calibrated scale. Figure 5-6 shows the data obtained when one of the pressure sensors was calibrated.

The red (dotted) line corresponds to the data extracted from the calibration measures,



(a) Pressure data being extracted from pressure channel 1 of all nodes (b) Pressure data being extracted from pressure channel 2 of all nodes

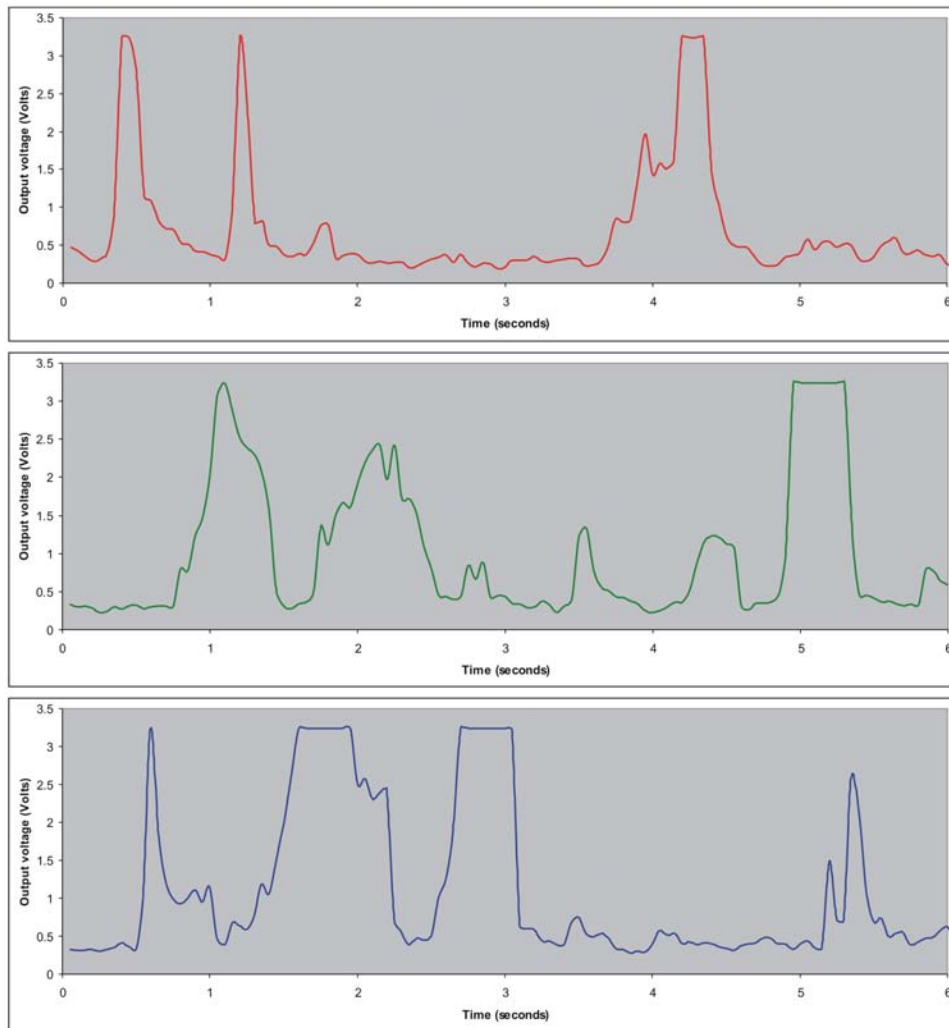


(c) Pressure data being extracted from pressure channel 3 of all nodes (d) Pressure data being extracted from pressure channel 4 of all nodes

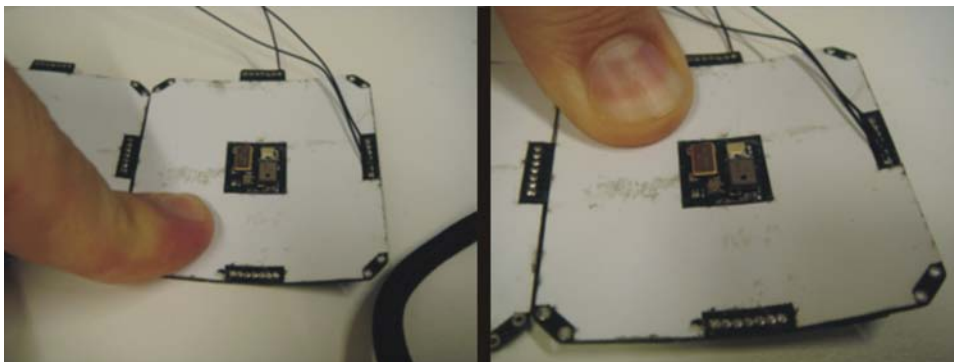
Figure 5-7: Real-time 3D visualization control showing data from each one of the four pressure channels of all nodes

and the black (solid) line is a curve fitted to the data. It is pretty evident that it has a logarithmic response which was actually expected, because as it was previously shown on Figure 3-16 the material resistance has an inverse exponential response to applied pressure. Since the signal conditioning circuit is a non-inverting amplifier, this inverse exponential is inverted and a logarithmic response was obtained. Also from the curve, it can be seen that the sensors are very sensitive, as only a slight touch is needed to generate a distinguishable output. The calibration procedure was done on each one of the four pressure sensors of one node, however this data is not presented because the results were almost identical to those presented in Figure 3-16.

Pressure data was also extracted from the Skin Patches, but as it was previously mentioned,



(a) Data from working pressure sensors and stimuli to generate them



(b) Pressure stimuli

Figure 5-8: Pressure data plots showing pressure sensor response

many of these did not work as expected because of some mechanical problems. Therefore, even though data was extracted from all of the sensors to illustrate how the 3D visualization chart displayed the information, data plots of the pressure sensors are only shown for some of those that actually worked as expected. Again data plots are shown with some pictures that show how the skin was stimulated to generate the data.

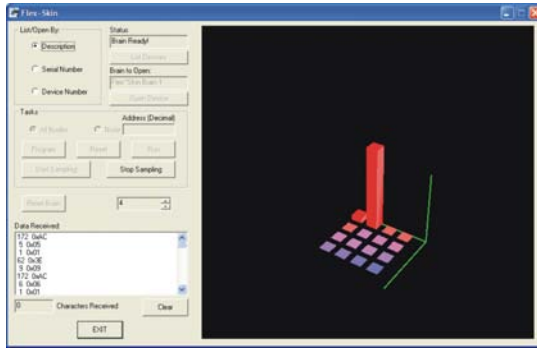
Figure 5-7 shows the real time data, while Figure 5-10(a) shows the data plots of some of the working pressure sensors. Only a few of them are shown though to illustrate their actual response to stimuli. In these plots the output voltage is plotted against time, however if a pressure value is desired it can be calculated using the logarithmic relationship shown above.

One final note on pressure sensing. Although there are multiple “dead” zones insensitive to pressure like the center part of the nodes and the intersection between them, this area only represents less than 10% of the total pressure area. There are many ways to overcome this limitation, some of which will be mentioned in the last chapter.

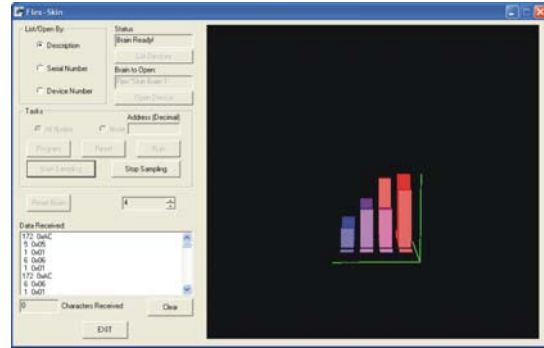
Ambient Light

Not much can be said about this sensing modality except that it was probably the best performing one according to the original expectations. The integrated sensor not only is compact and fully integrated, but it has a great sensitivity to all kinds of lighting conditions (incandescent and fluorescent) and it only consumes $620\mu A$. It was also extremely easy to stimulate all of the sensors of the Skin Patch at once.

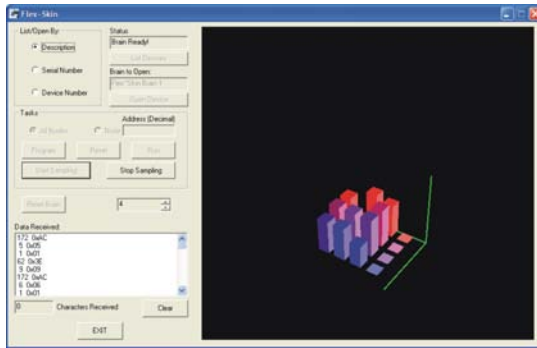
Several snapshots of the 3D visualization control were taken to show how different lighting conditions affected the skin. These can be observed in Figure 5-9. The first one shows the effect of a laser pointer aimed at the sensor when there was no other light source in the environment. The second one shows how a flashlight shining from the side generates a gradient. The last two show all of the sensors responding at the same time when the amount of ambient light changes.



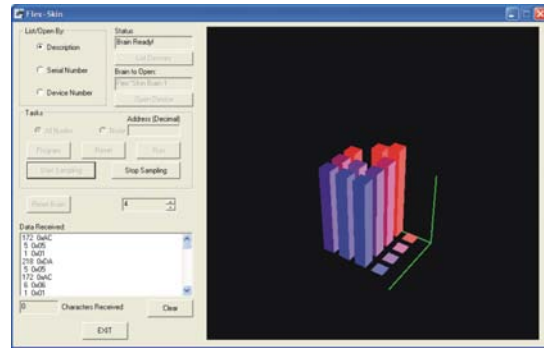
(a) No ambient light present; single node hit with a laser pointer



(b) No ambient light present; flashlight illuminating patch from the side



(c) Room with fluorescent ambient light



(d) Room with fluorescent light and flashlight shining on patch

Figure 5-9: Real-time 3D visualization control showing data from different lightning conditions.

Data plots were also extracted for all sensors and are shown with stimuli pictures in Figure 5-10

Finally, light sensors were not calibrated, because in this case the absolute light level was not of interest. Calibration is easily done though, as the manufacturer provides a curve that plots the output current vs. ambient light.

Temperature

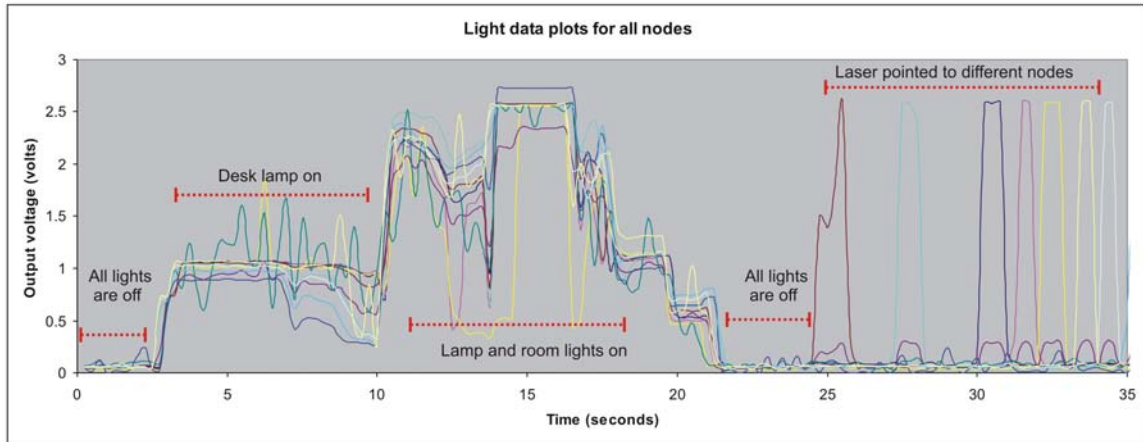
Temperature sensors worked in very much the same way as light sensors in the sense that stimuli could be applied without the need of physical handling of the patch. They also did not need calibration because the sensor datasheet[25] provides enough information to calculate the absolute temperature if this is needed.

The results are shown in a similar way as with the ambient light sensors. Still, since changing the temperature is not as easy as changing the ambient light, especially for just one node, only one general stimulus was applied to the patch to show the response of the sensors. To do this the Skin Patch was warmed with a hot air gun. Figure 5-11 shows the data extracted from all sensors by plotting temperature vs. time. Temperature was calculated by converting the output voltage using the formula provided in the datasheet.

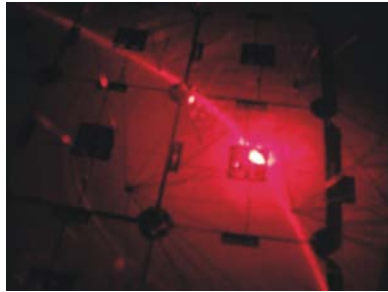
Sound

Sound was the most resource intensive sensing modality. First of all, it must be sampled at least 8Khz, with an 8-bit resolution if human voices or other sounds with a similar frequency range are to be recorded. Considerable processing power is also needed to calculate higher order features like it moving average and variance, and because of this it is also the most power consuming. Yet, also because of this, sound was the best way to push the limits on the system and see how well it performed.

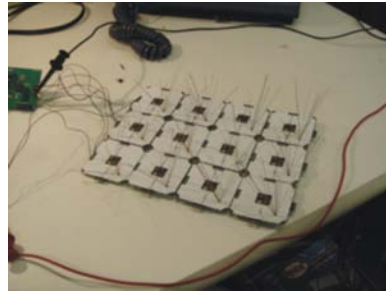
All the sensing modalities up to this point, have been presented in a very similar way: real time data, saved plots and stimuli; this is not done with sound. The reason for this is that



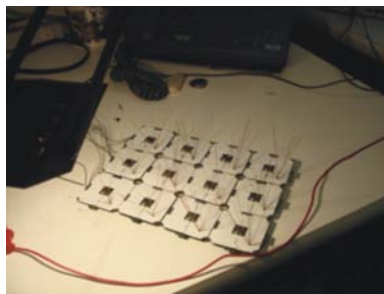
(a) Ambient Light sensor data from all nodes



(b) Laser pointed to a single node

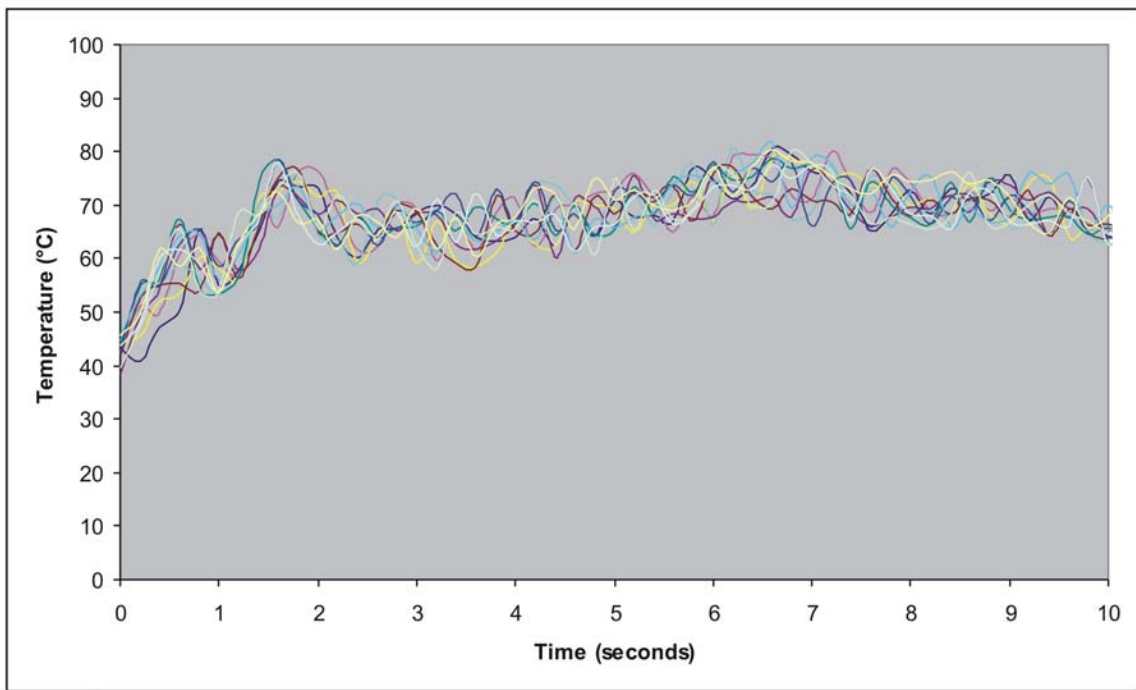


(c) Room lights on

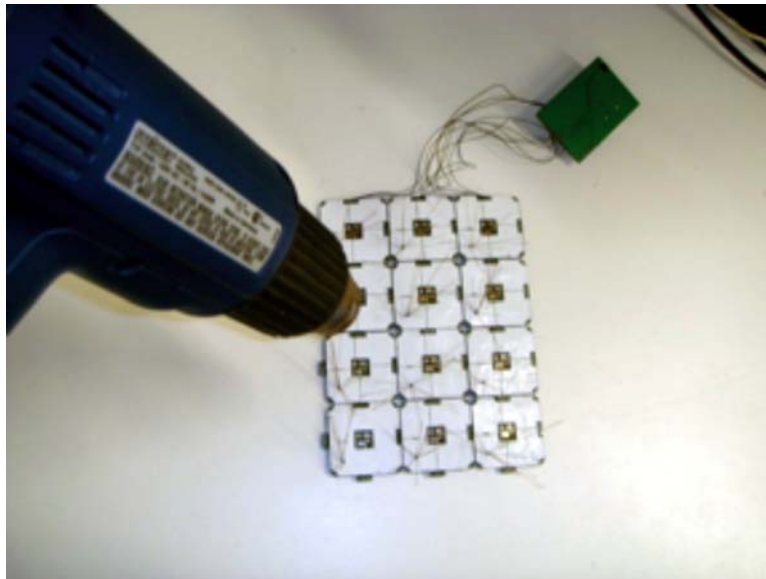


(d) Room lights on and desk lamp on

Figure 5-10: Light data plots showing ambient light sensor responses to different stimuli



(a) Temperature sensor data plots



(b) Hot air gun warming up the patch

Figure 5-11: Temperature sensor response

first of all this is highly undesirable because even a patch of skin with such a low node count (12) already produces a considerable amount of information: if each node is sampled at 8Khz with a 12-bit depth, each node will produce 12Kbits of information per second. That means that if we have 12 nodes, we will have to transfer 144Kbits bits every second, which is already almost half of the available I²C bandwidth (considered that it is run at 400Kbps).

From a functionality perspective, extracting full sound waves from every node does not make much sense either. Even for applications like sound localization, where sound signals are correlated to extract phase information, three microphones might be enough if they are correctly chosen. So why were microphones included into every node then? Well, first of all if we want to pick three microphones from the whole array, having one in each node gives more flexibility at the time of selecting them. Second, because even if data has to be sampled at high frequencies, it does not mean that it has to be transferred as it can be processed locally. So, as opposed to the raw data obtained from other sensors, when sound data is sampled with the GUI, what each node actually transmits is a feature extracted from the raw data, in this case its moving average.

The moving average of the sound signals is essentially the low-pass filtered version of the original one. This feature was chosen mainly because its simplicity but any other feature like its Timbre, Rhythm, Loudness, Spectrum, and Tonality can be calculated. These features, however, are generally more processing intensive which may cause the processor to be devoted only to this, which is another reason for which calculating them was left as a possible future application. Some sounds with their moving average were extracted from the Skin for illustrative purposes and these are shown in Figure 5-12.

In this case, both raw data and the feature are shown for illustrative purposes, however in a real-world scenario these features can be transferred instead of raw data which reduces the amount of bandwidth needed. Moving averages can also be resource intensive but any other filter can be implemented to further compress the information. A peak-detection algorithm for example could count the peaks in a certain frequency and report this instead.

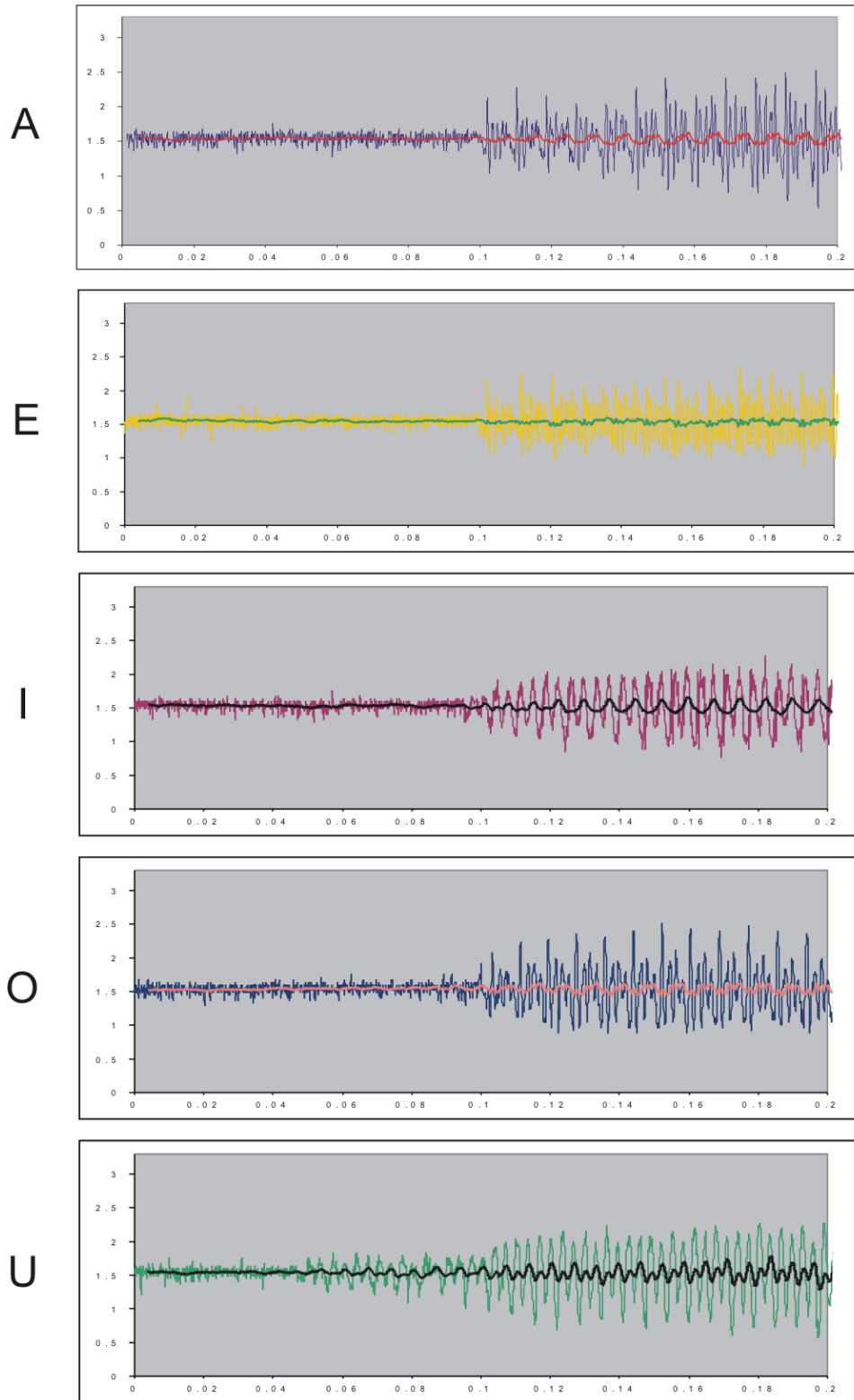


Figure 5-12: Raw microphone data with superimposed moving averages. Window size was 32 samples. Each plot corresponds to a vowel spoken in front of the microphone.

Proximity/Motion Sensing

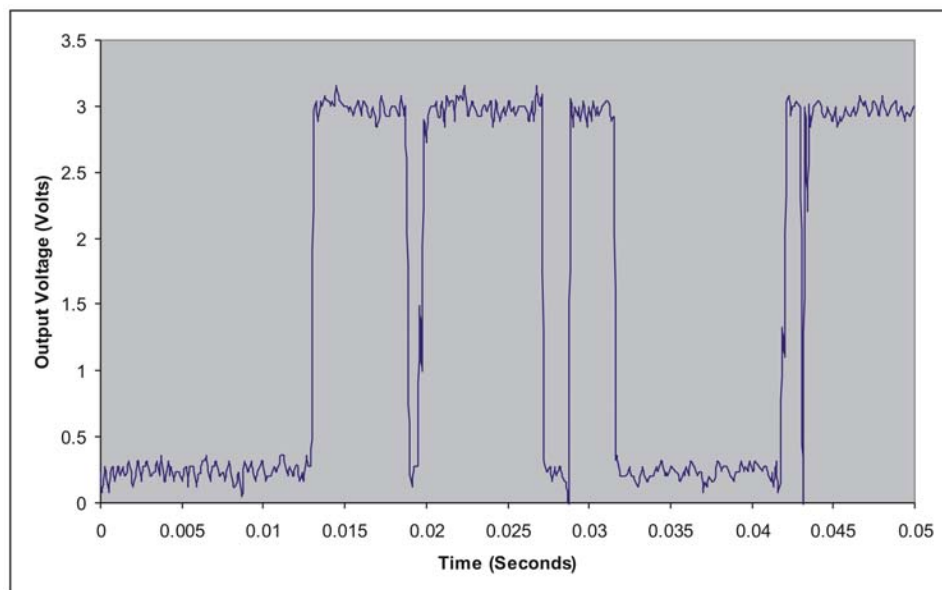
The last sensing modality for which results are shown are the whiskers. Whiskers can be seen as either motion/activity sensors or proximity sensors. Since whiskers are meant to indicate either the presence or absence of activity close to the skin, there is no need to quantize the information received from them as the nature of this information is inherently digital: presence/absence of activity. For this reason the whiskers were connected to interrupt-capable input pins, so that every time they are stimulated, an interrupt is generated, which can be then used to activate more sensors or simply increment a counter.

As it was mentioned in the Hardware chapter, whiskers were implemented with mini-sense piezo cantilevers to which some brush bristles were glued. When these are touched, the cantilever vibrates and it generates a train of impulses that are then detected by the microcontroller. This approach, although effective has two minor drawbacks: first, the cantilevers are mounted on a rigid substrate that hinders the flexibility of the node when this is soldered to it; and second, because the sensor detects the vibrations on the cantilever, there must be available space so that the cantilever can be vibrate freely or it will not work. An alternate method to create the whiskers using a PSAC shock sensor from Kyocera was also considered, but because these sensors were not available at the time the Skin Nodes were designed, they could not be used or tested.

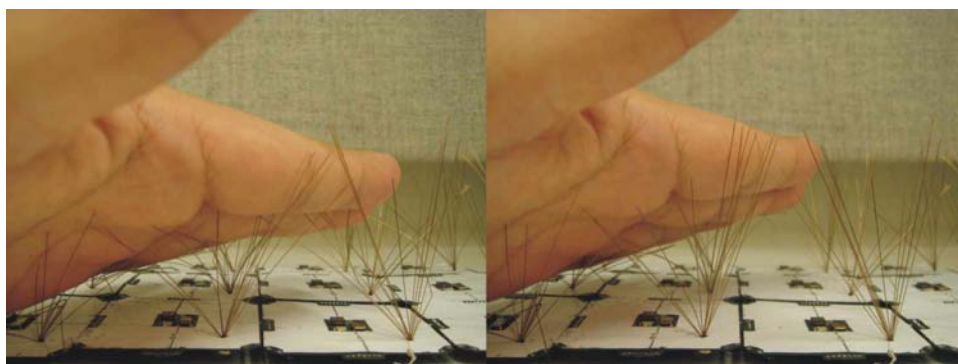
Figure 5-13 shows a plot of data illustrating the behavior of the sensor. Also shown on the figure is a picture that shows how the whiskers are stimulated.

5.2.2 Skin Patches as Stand-alone Devices

It was previously mentioned that Skin Patches can either be used to send data or work as stand-alone devices. The first case is useful if data needs to be further processed or used for another purpose in which case it needs to be extracted from the skin by a personal computer. The second case could be useful for applications where the patch can act like an autonomous device, for example if it is used like an interactive material, where each node is capable of sensing, processing and actuating.



(a) Activity sensor data



(b) Whiskers being stimulated

Figure 5-13: Activity sensor results

To demonstrate the functionality of the Skin Patches as stand-alone devices, a simple application that maps sensor data to the on-board LED was developed. This application samples the ambient light channel and uses the information to modulate the light on the output LED; the less light in the environment, the stronger the LED is lit and viceversa, thus creating an inverse feedback loop that depends on the amount of light in the environment. This application can be used for example, to do shadow tracking which can be seen in Figure 5-14

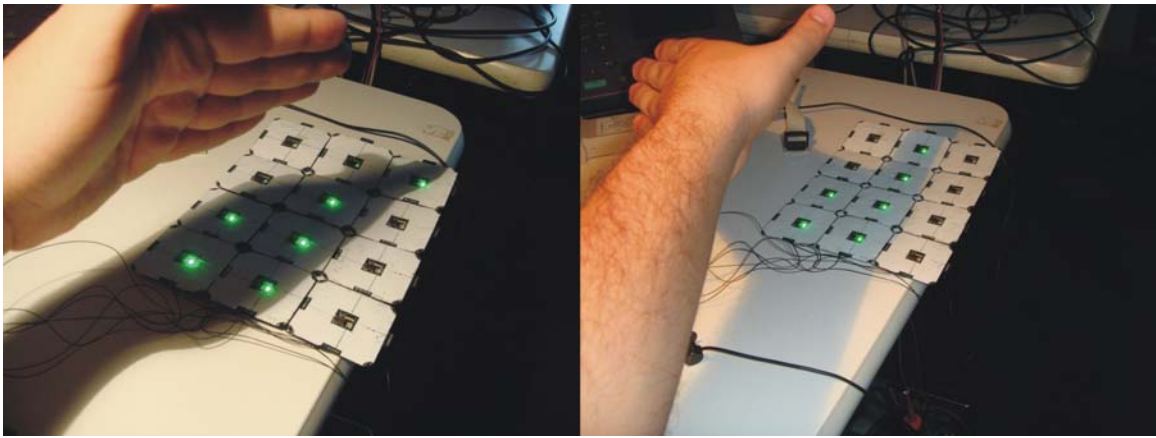


Figure 5-14: Patch used as a stand-alone device. LED's light according to the amount of ambient light

Since the only output device of the nodes is the RGB LED, applications would be probably limited to mapping sensor data to LED lights in different ways. Yet there are many circumstances in which this would be enough, for example if large patches are used to cover up a wall or floor to make it interactive, in fact, Sensor Net Skins covering interactive floors were explored by Richardson in [59]. Then again, the microcontroller has still several unused output pins to which other output devices like a speaker can be connected. This of course would need a redesign of the Skin Nodes so that different output devices can be connected to them, which is easily achieved by adding an extra header.

5.3 Performance Metrics

We have presented results for all the sensing modalities and modes of operation of a Skin Patch. Yet, these results although illustrative, provide little reference as to the overall performance of the project. This subsection will present some metrics that will grant a bit more insight into how well did the system performed against the design goals. In fact, the main goal was to demonstrate that by including processing power in each node, the necessary resources, in special bandwidth could be greatly reduced. The first metric analyzed is then the bandwidth needed to operate a Skin Patch network.

5.3.1 Network Performance

As the reader might recall, scalability is one of the main goals of the project, so ideally, we should be able to connect to a PC as many Skin Patches as possible and every patch of skin should be capable of growing to as many nodes as possible. In reality though these two limits were set by two of the three communications channels used: USB and I²C .

I²C Performance

Peer to peer is never a concern because only two elements are involved, however I²C and USB are shared buses that impose a limit on the amount of devices that can be connected at the same time. I²C sets a limit on the number of nodes per Skin Patch and USB sets it for the number of patches that can be connected to a computer at the same time. The reason for this is mainly bandwidth and network speed.

In the case of I²C , there are two factors that limit the amount of devices that can be connected to it: bus capacitance and network addresses. As we previously mentioned, I²C 10-bit addressing was chosen, which in theory limits the amount of nodes to 1023 ($2^{10} - 1$). However, the I²C bus specification restricts the rise and fall times of both signals to 300ns, and since this time is set by the RC constant of the circuit, the real limiting factors are the pull-up resistance value and the amount of capacitance in the bus.

Because the amount of capacitance in the bus depends on the amount of nodes connected to it, we have to set the resistor value as low as possible. An arbitrarily low value can't be chosen though, because the bus line current would increase and the MSP430 can only handle a maximum of 2mA. With a supply voltage of 3.3 volts, the minimum resistance that can be used is 1350Ωs. However in fast mode, this resistance limits the number of capacitance in the bus to about 300pF[55] instead of the maximum possible of 400pF. This decreases the amount of nodes that can be on the network and is why an active pull-up was used instead. Figure 5-15 shows how an active pull-up device eliminates the RC response of both bus lines (SDA and SCL) giving a speed increase.

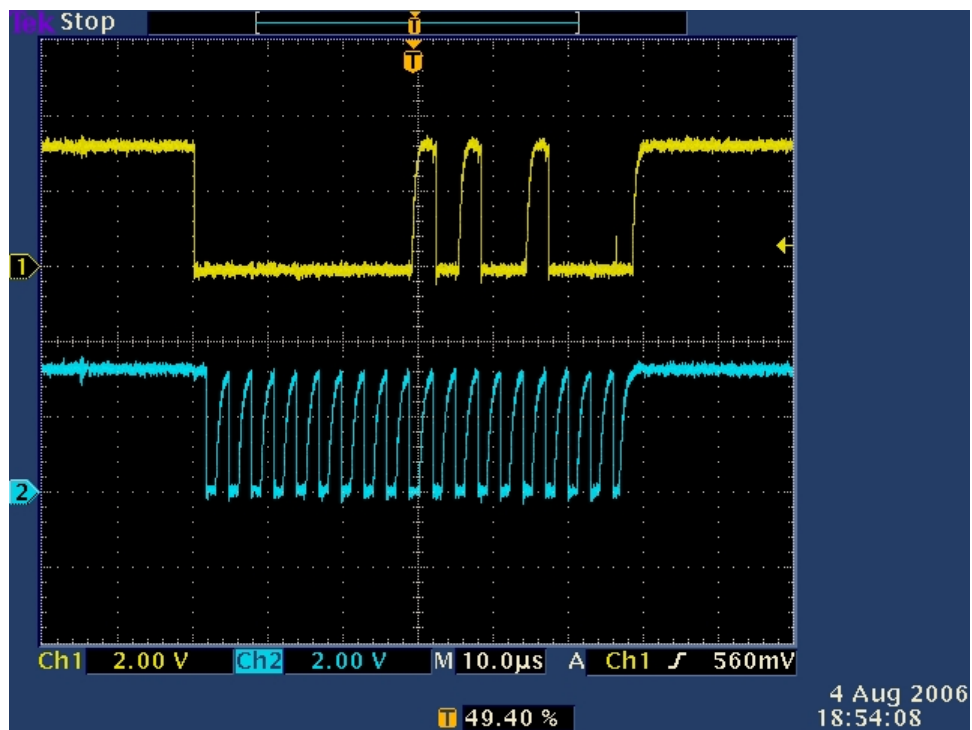
By using the active pull-ups, we can now use the 400pF allowed by the bus specification. The capacitance of the SDA and SCL lines was measured at 9.8pf and 9.6pF respectively with respect to ground, so the maximum number of nodes the bus can have is approximately 40. This is a very small number, yet no special drivers or a ground plane were used. If the driver mentioned in the hardware section is used, the 400pF limit increases to 4000pF. Furthermore if ground planes are used, the capacitance of the traces can be dramatically reduced. With these to improvements the number of nodes per patch can be easily brought to over 500. Once again, the reason why these features were not included were to reduce the amount of components and to keep the number of layers to a minimum. If specialized Skin Patches³ are designed though, it may make sense to include them.

USB Performance

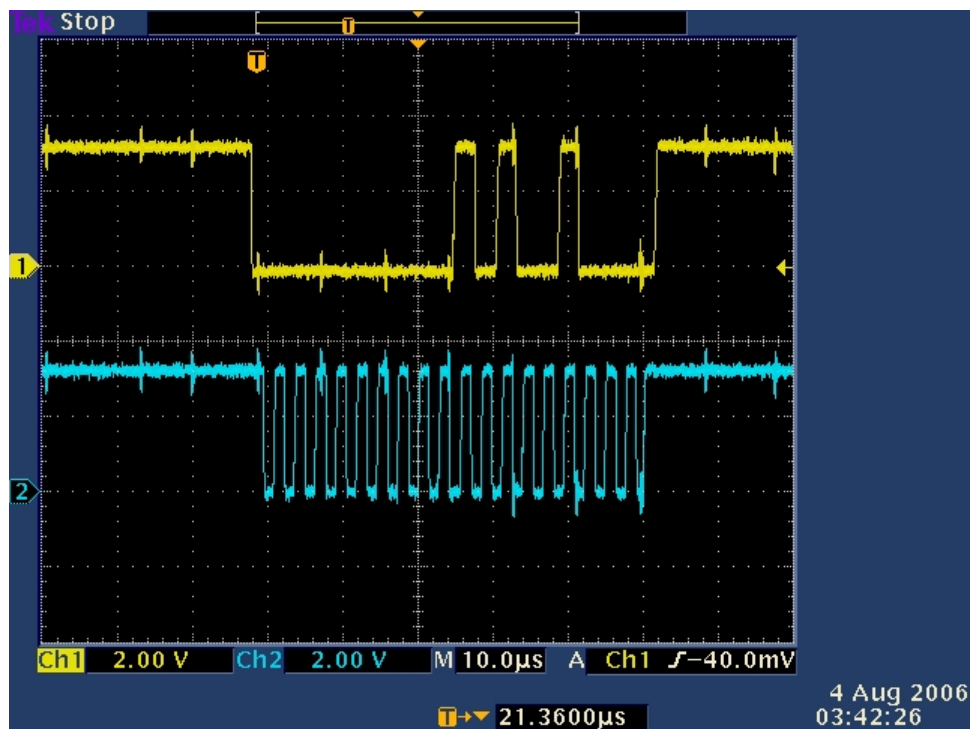
The second limiting factor for network size is the USB bandwidth. USB bandwidth limits the network size because this must be divided among the number of Skin Patches currently connected. This only makes sense if the Skin Patches are connected as data extraction devices, but it does illustrate why it was so important to make every node consume as little bandwidth as possible.

Considering that every node has 11 sensing channels, each one of which will be sampled at the rate and bit depth described in Table 4.3, each node will produce a total of 99800bps

³A specialized Skin Patch may sense only a subset of all sensing modalities included in this project



(a) I²C data when a 1500Ωs resistor was used as pull-up



(b) I²C when a current mirror was used as pull-up device

Figure 5-15: Difference in speed for both I²C lines when active and passive pull-up devices are used.

or 12475 bytes every second. The USB chip used has a data rate of 8Mbps or 1MB/s so a total of 84 nodes can be connected in different patches. Once again this number may seem extremely low, but it is only because we are extracting raw data at the full sampling rates. If higher order features are calculated and these are transferred instead of raw data, and if a USB 2.0 capable chip is used instead (480Mbps), this number can grow considerably.

To illustrate this point, let's assume that each node is programmed so that it can change the sampling rates dynamically⁴. Let's also assume that each sensing modality is sampled at 10Hz/8-bits, in a low-bandwidth/ultra-low-power mode. 11 sensing channels will produce a total of 880bps. If USB 2.0 is used and assuming that it is 70% efficient, we would have a total of $480Mbps \times 0.7 = 336Mbps$. With this bandwidth, it would be possible to have more than 380,000 nodes. This is why having processing power in each node is so important: it allows the network to adapt to different conditions, so power consumption and bandwidth requirements are minimized. All of this is in addition to any further gains of calculating higher order features so these are transmitted instead of raw data.

5.3.2 Power Consumption

Power consumption is the second metric used to evaluate the performance of the skin. Although the importance of a low power consumption might not be apparent at first, this becomes evident if Skin Patches with large numbers of nodes are created. Table 5.5 lists the quiescent current consumption of each component of the nodes:

With the data from the table the approximate power consumption can be now calculated. The first component, the microcontroller has a power consumption that depends on the speed at which it runs. Since data processing and transmission require full speed, the MCU is set to run at 8.000Mhz, for a total consumption of about 2.1mA. This however can be made as low as 300nA if deep sleep is used. In the case of the RGB LED's, a current-limiting resistor was added to each color to decrease power consumption, so if they are lit at full power, they consume a maximum of 2mA.

⁴Either by adapting to stimuli, or by receiving an instruction from a PC or Brain

Component	# per node	Current consumption
MSP430F1610	1	$300\mu A/MHz$
NCP553SQ33T1	1	$2.8\mu A$
LTST-C17FB1WT	1	2mA/color if lit
MAX4462	2	$700\mu A$
MAX4400	4	$320\mu A$
MAX4734	1	$4nA$
LM20CIM7	1	$10\mu A$
TPS851/52	1	$62\mu A$ (depending on lighting conditions)
SPM0102NE3	1	$175mA$ (average)
FDG6301N	1	$100nA$

Table 5.5: Power consumption of Skin Node components

Amplifiers were chosen with a bit more bandwidth than actually needed, so they consume more than could be actually be achieved. If the OPA349 from Texas Instruments was used instead the power consumption per amplifier could be brought down to $70\mu A$ per amplifier. Next, The ambient light sensor power consumption depends on the amount of ambient light present, but in regular indoor conditions under artificial lightning it consumes $62\mu A$.

And finally, since the MOSFET is used to gate the Wheatstone bridges used to excite the strain gages, only its leakage current is listed as power consumption. However if the MOSFET is turned on, the bridges will become active and they will consume a current depending on the resistance of their branches. So for example, if a node has a bridge with branches matched to 169Ω s and 174Ω s these will consume:

$$\begin{aligned}
I_{bridges} &= I_{B1} + I_{B2} \\
I_{bridges} &= \frac{3.3V - V_T}{169\Omega} + \frac{3.3V - V_T}{174\Omega} \\
I_{bridges} &= \frac{3.3V - 0.7V}{169\Omega} + \frac{3.3V - 0.7V}{174\Omega} \\
I_{bridges} &= 0.01538A + 0.014942A = 30.32mA
\end{aligned}$$

So in average, the strain gages consume a total of 30mA when turned on, which is why it was so important to gate them using the MOSFET. Total power consumption can be then as low or as high as:

$$\begin{aligned}
 \text{Low} \quad & 300nA + 2.8\mu A + 2(700\mu A) + 4(320\mu A) + 4nA + 10\mu A + 62\mu A + 175\mu A + 100nA = 2.927404mA \\
 \text{High} \quad & 2.4mA + 2.8\mu A + 2(700\mu A) + 4(320\mu A) + 4nA + 10\mu A + 620\mu A + 175\mu A + 3mA + 6mA = 14.887904mA
 \end{aligned}$$

In actual tests, maximum power consumption of one node with the MCU running at full speed, all LEDs on at full power, both strain gages on and a laser aimed at the light sensor, was of 41mA. When everything was turned off however it consumed less than 2mA. If we now combine this with the possible number of nodes in a Skin Patch, we can see that a Skin Patch with 40 nodes at full power would consume 1.64A of current, but this case would be rare. On average each node consumed a total power of less than 9mA in regular operation, so a total of 40 nodes would consume roughly 360mA.

Still, it is important to note that even though 9mA was the average current consumed, this is highly dependant on the application being run by the nodes since most of this will be dissipated by the LEDs. Their total current consumption can be easily brought down though, since they are driven by timer output pins, which means that they can be pulse-width modulated.

Another thing to note is that power dissipated by components does not have any measurable effect in temperature sensor readings. This is mainly because the amplifiers and RGB LED, which are the most power-hungry elements, are placed so far from it that most of their heat dissipates to the surrounding air rather than to the substrate. Moreover, Kapton is not a good heat conductor so it would be extremely rare to see any effects in the temperature readings caused by heat dissipated from nearby components.

Finally, since power is readily available for Brains, and their power consumption is negligible compared to the total power that a large Skin Patch could in theory consume, this was not an issue and was therefore not calculated.

5.3.3 Cost

The final metric used is the overall cost of the project. Cost was a big consideration in the overall design of the project because flex boards are expensive to fabricate and even more expensive to prototype, specially if multilayer boards and other fancy techniques are used. Without a doubt, the major cost component of the project was the fabrication of the node substrates which accounted for roughly two thirds of the total cost. 32 nodes were fabricated at a total cost of \$3,500, so each node cost \$110.

Component prices for nodes and Brains can be observed in the Bill of Materials included in Appendix B. Two prices are listed in this table: the price used for the project and a bulk price for each component. This was done with the intention of providing a comparison between the cost of a prototype project like this one and its possible cost with large-scale manufacturing. It can be seen that the components for each node add-up for a total of \$54 per node or about a third of the total cost. If these components are bought in large quantities though, the cost decreases to about half as much. Even substrates can be manufactured for about a tenth of the cost if they are fabricated in large numbers.

Brains are much cheaper because they use standard fabrication techniques and relatively cheap components. Also the price can be seen in the Bill of Materials.

Chapter 6

Conclusions and Future Work

“So long and thanks for all the fish.”

– *Doplhins to humans* (Douglas Adams)

We arrive to the last chapter, which presents the conclusions derived from the results presented before. First a summary of the work along with some general conclusions are presented. This is followed by a description of possible applications and future work.

6.1 Conclusions

A Dynamically Adaptable Artificial Sensate Skin was designed. Based on the design goals proposed, 32 nodes were fabricated with Flex circuit technology. Half of these were assembled into two patches of skin of different sizes to test the two modes in which they can operate. Two Brains were also designed and developed so that data could be extracted from one of the patches. Finally several software components were developed for the system. These include a GUI application to serve as a front end to the Skin Patch network and several firmware applications to test the functionality of the skin as a stand-alone device.

Generally speaking, several goals of the project were met. First, the goal of creating a device that emulates some of the functions of the human skin was successful, and it is represented by the two Skin Patches created to test the project. Second, it was demonstrated that having processing power on each node has several advantages:

1. Application code running in the Skin Patches can be changed at any time, either for a single node or an entire patch
2. Each node can adjust the sampling rate of its nodes depending on different criteria
3. Skin Patches can be operated at different power modes

Yet, even though the major goals of the project were met, there are several design choices that greatly reduced the performance of the project as a whole. First, the mechanical problems mentioned before had a great impact on the reliability of I²C communications. Second, because of the time frame of the project, it was not possible to develop enough application code to thoroughly test all the functionality available; this includes the Peer-to-peer communications channel, which in spite of being present, it is not exploited.

Yet, there are several measures that can be taken to correct most of the problems encountered throughout the design and implementation of this project. For example, the fact that the microcontroller could easily break off when the nodes were bent was caused because of its size and packaging; if a much smaller one with a leaded package¹ is chosen instead, this problem can be easily eliminated. Using a smaller microcontroller would also mean sacrificing functionality, which leads to the next point.

The vast majority of the problems found were due to the fact that the number of components in each node was significant. This can be avoided if specialized nodes are created instead. For example, because the MEMS microphone, ambient light sensor and temperature sensors had to be on the outer-facing layer of the skin, the area where these were placed was completely insensitive to pressure. If a pressure-only skin is designed though, the entire top

¹The leads in the package could absorb some of the stress caused by the node bending, and would therefore help to avoid any ruptures

surface can be used to sense pressure, and since functionality requirements are reduced, a smaller microcontroller can be then chosen.

Another one of the mechanical-caused problems was interconnect conductor cracking. Since the bending of the Skin Patches was mostly restrained to the flaps as previously mentioned, conductors cracked very easily. This can be corrected by making the flaps almost as large as the node itself.

In spite of all these problems though, all components of the project were functional as originally expected, and it was possible to demonstrate both modes of operation, (stand-alone and data extraction) successfully.

6.2 Possible Applications

So far we have extensively talked about the What's and How's but not the Why's. The last part of the chapter, and of this entire document, briefly outlines some of the possible applications of the project.

Given the Sensor Network nature of the Skin Patches, and given that they are equipped with a wide variety of sensing modalities, there are several applications that can be run on the platform. These are presented in the following list:

- Sound Localization: to do this, three or more “sound nodes” could be designated by the Brain. Once this is done, the Brain can then send a broadcast message indicating them to start sampling. After a certain period, samples are recovered by the Brain, and correlations are calculated. From these the direction of the source of the sound can be extracted. Similarly large patches of the skin can be used as an audio beam-forming array, at least for short snippets of skin
- Shape recognition: Basically each node records the amount of light it is receiving and it decides to report a status of either “shadowed” or “lit”, so when the Brain scans for the status of all nodes, it can determine the shape of the shadowing object.

- **Code Distribution:** a very simple means of code distribution was demonstrated in this project, however it can be as complex as needed. Some nodes might be designated as leaders, so that code has to be transferred only to them by the Brain. Once a low activity condition is detected, these would proceed to distribute the code recursively to their neighbors.
- **Proximity from shadows:** this would be trivial to implement. The average amount of ambient light can be calculated for an entire patch to serve as a reference point. Once this is done, proximity can be calculated from the amount of light blocked from either one or many sensors.
- **Pressure Gradients:** gathering data from neighbors, nodes can calculate the center of mass of an object placed on top of the skin.
- **Motion Sensing:** using the whiskers the skin can be used to detect the amount of wind.
- **Artistic displays:** Skin Patches can be used to wrap walls, floors or ceilings and make them interactive. A passer by could cast a shadow for example, and LEDs would light up, displaying its silhouette.

6.3 Future Work

There are several things that can be done to improve the functionality of the project. Several of these have already been mentioned before, however they are summarized in the following list. A brief description is also provided.

- **Larger Network:** a larger network would allow more tests and applications to be tested.
- **Improve mechanical design:** several mechanical characteristics of the design can be improved.

- Implement P2P Communications: currently no applications that use the Peer-to-peer communications channel have been implemented
- Implement an Operating System: a bootloader was implemented for this project, however if more complex tasks are needed, it may be a good idea to add hardware abstraction by implementing an OS.
- Increase Bootloader code size: the current bootloader can only handle a maximum code size of 4KB. This can be changed by modifying the bootloader code so that it reads multiple 4KB code blocks, instead of only one.
- Improve Brain by changing FTDI chip to newer version: there is now a new version of the FTDI chip that does not need any of the external components currently used by the FT245BM. Switching to this version would save on cost and Brain size.
- Create different kinds of skins with different capabilities: as was mentioned before, a better way to implement the Skin Patches would be to create specialized nodes instead of monolithic ones.
- Incorporate QTC Material into substrate or encase in silicon: to avoid the warping and bubbling of the QTC material when the nodes are bent, and to distribute the pressure evenly among the pressure channels, the entire skin could be covered in a silicon rubber. Another option would be to incorporate it into the material stack; this option would be possible if the nodes are specialized, since it would mean fewer components, and therefore less routing needed, which would leave space for an extra layer for the material.
- Increase current capacity of Brain to allow for a larger network: currently the Brain provides the current to the entire Skin Patch connected to it. If a larger Skin Patch is needed, the current capacity of the traces in the Brain responsible for this have to be enlarged.
- Network discovery protocol: this was already mentioned before in the software section. This would be necessary for the Skin to be dynamically reconfigurable so that

whenever the Skin Patch topology is changed, this can be detected by the Brain or PC.

- Multiple masters/slaves: currently the I²C bus is arbitrated by the Brains. No node ever uses the bus unless it is addressed by a Brain. This approach, though, can't be used if a node wants to start communications, so that it can for example report unsolicited data to the Brain. It also means that nodes can't use the line to address any arbitrary neighbor on the network.

It is with this list that we reach the end of the current work, but not before leaving a final note. Even though the goals of the project were broadly met, it was still far from emulating most of the characteristics of the human skin. The technology necessary to create an artificial device that has all the functional characteristics, electrical and mechanical, of our skin is still some years ahead. Much work has to be done yet to research the necessary materials and methods so that we can one day have a device as versatile and functional as our skin.

Appendix A

Abbreviations and Symbols

ADC	Analog to digital converter.
API	Application Programming Interface.
DC	Direct Current.
DCO	Digitally Controlled Oscillator.
DMA	Direct Memory Access.
FIFO	First-In First-Out.
FPC	Flexible Printed Circuits.
FSR	Force Sensitive Resistor.
GUI	Graphic User Interface
I2C	Inter-Integrated Circuit Bus.
I/O	Input/Output.
IDE	Integrated Development Environment.
IPC	Institute of Printed Circuits, now IPC.
JTAG	Joint Test Action Group.
KB	Kilobyte.
LED	Light-Emitting Diode.
MCU	Microcontroller Unit.
MEMS	Micro-electromechanical systems.

MIPS	Million Instructions Per Second.
PCB	Printed circuit board.
PDMS	Polydimethylsiloxane
PNP	A type of semiconductor (P-type, N-type, P-type).
PVDF	Polyvinylidene fluoride.
QFN	Quad flat package no leads.
QTC	Quantum Tunneling Composites.
RAM	Random Access Memory.
RISC	Rapid Instruction Set Computer.
RF	Radio frequency.
RGB	Red, green and blue.
RTD	Resistive Temperature Detector.
SMD	Surface Mount Device.
SNR	Signal to noise ratio.
SPI	Serial Peripheral Interface.
USART	Universal Synchronous-Asynchronous Receive Transmit.
USB	Universal Serial Bus.

Appendix B

Bill of Materials

Appendix C

Schematics and PCB Layouts

Node Sensing Suite

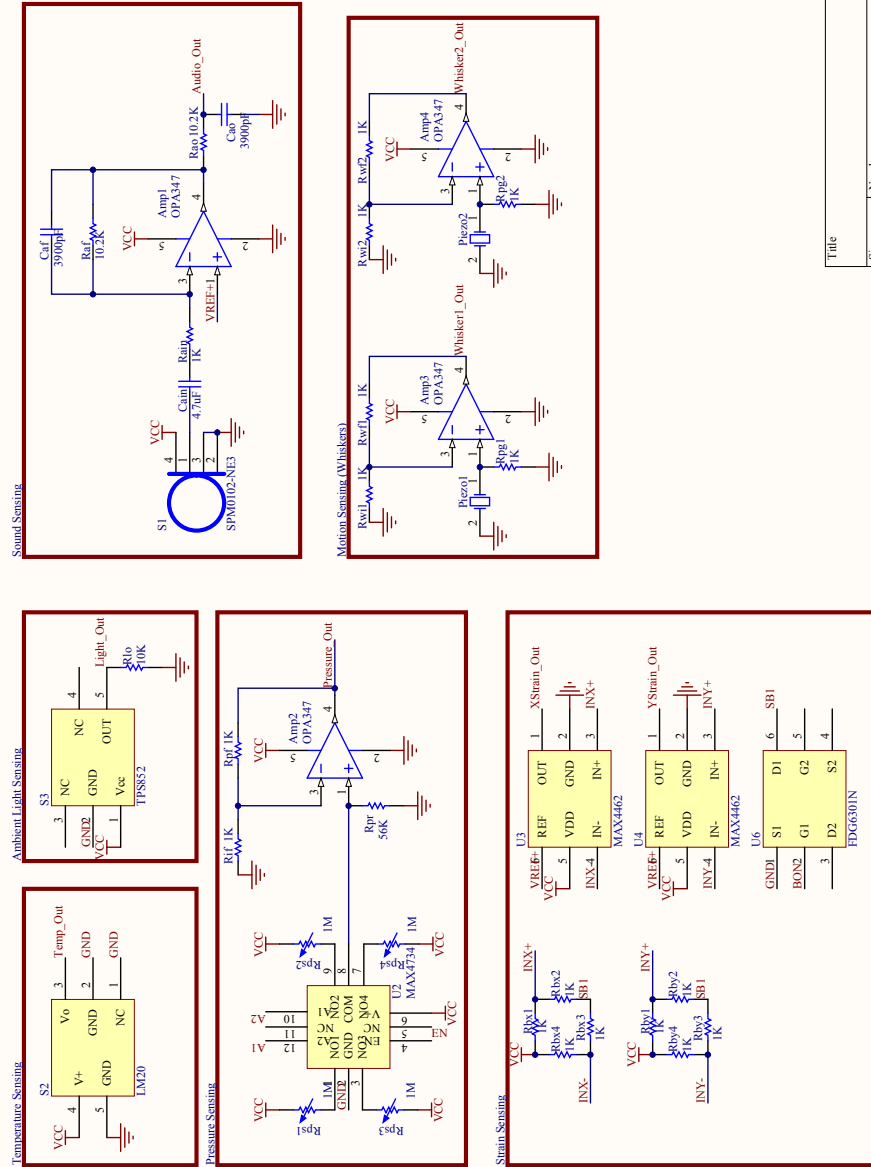


Figure C-1: Node Sensing Suite

Node Processing, Output and Mechanical

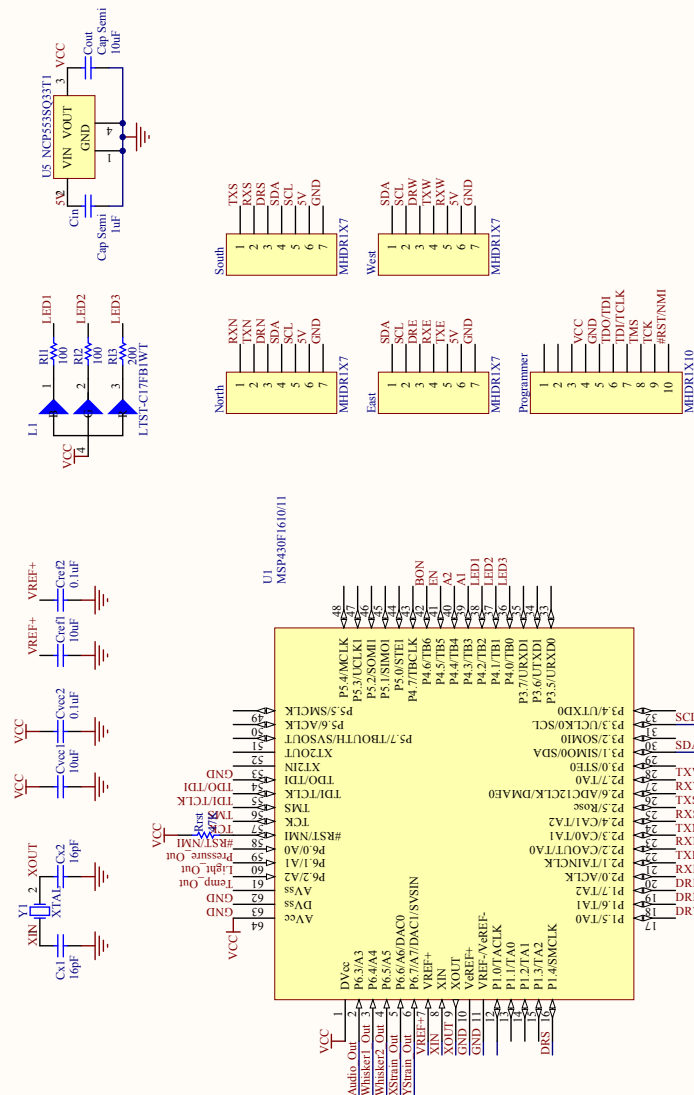


Figure C-2: Node Processing

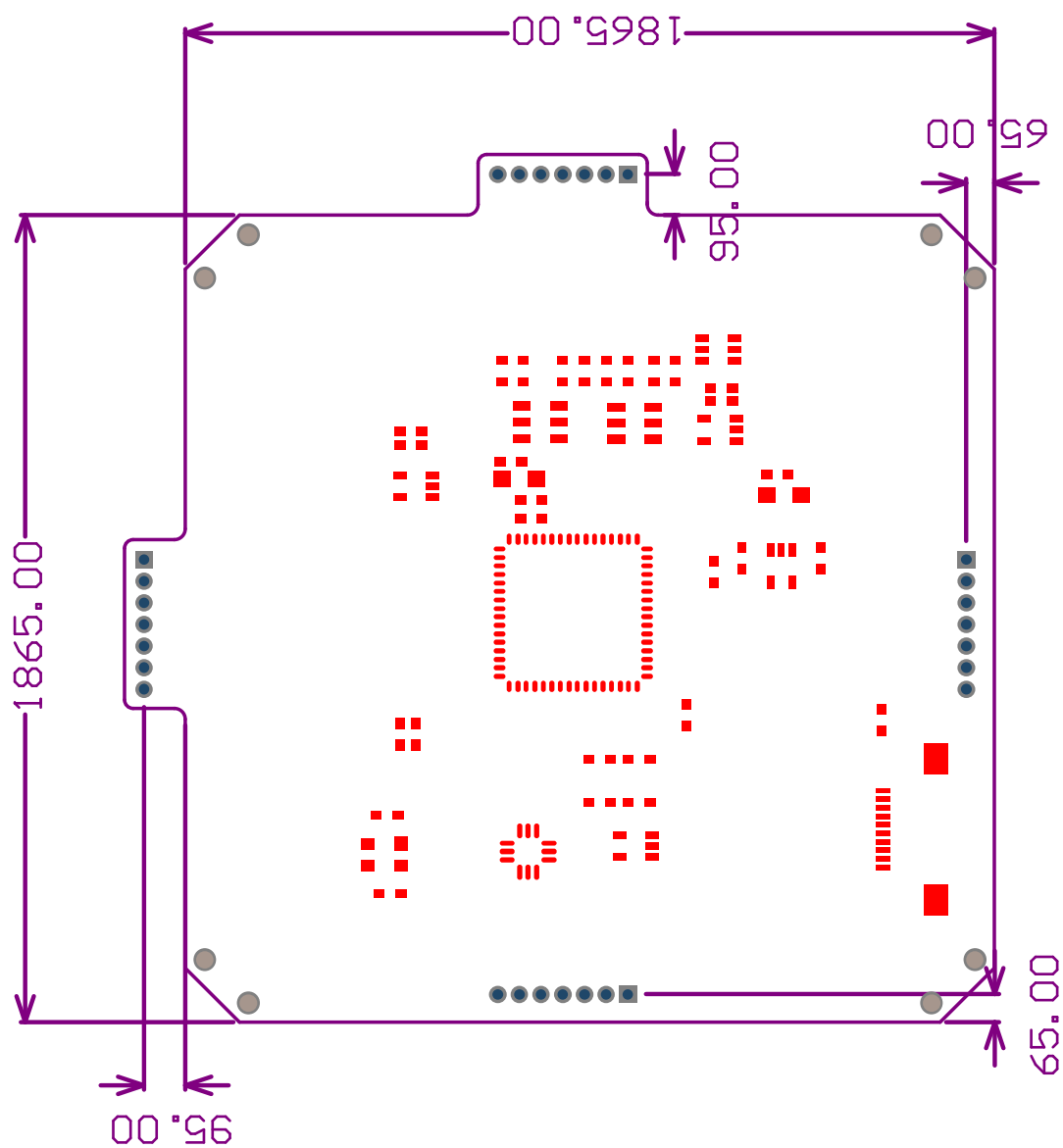


Figure C-3: Node Dimensions (mils)

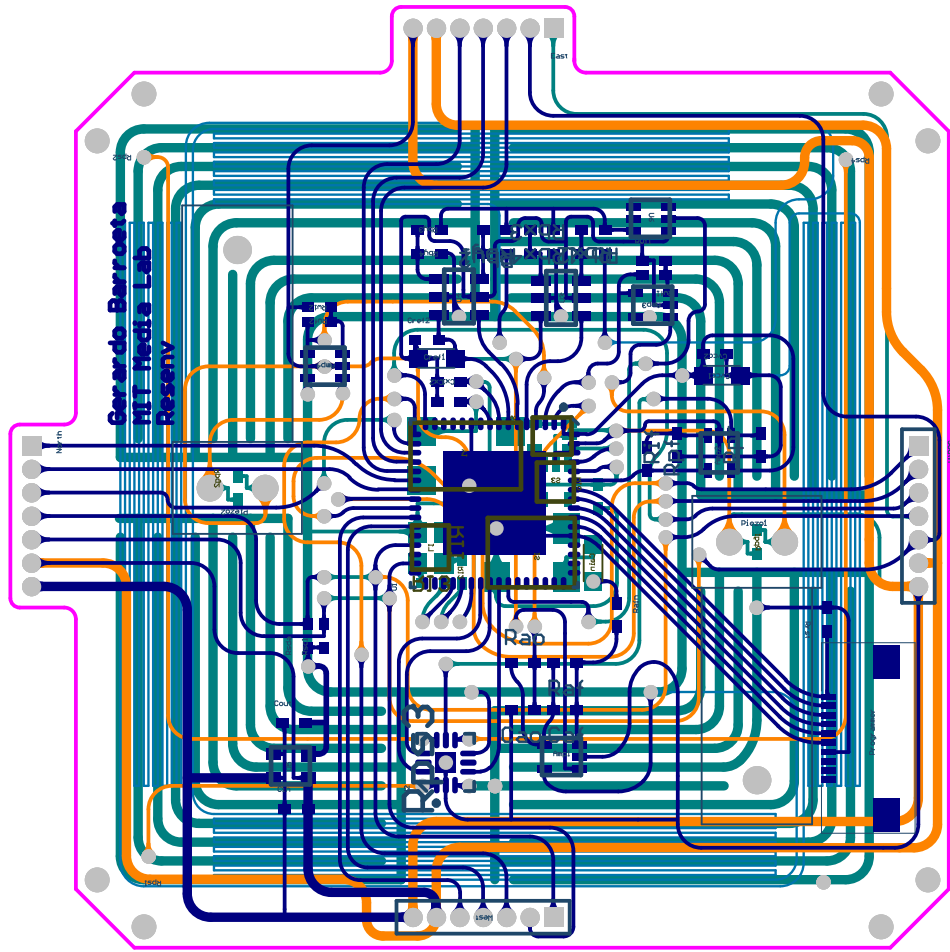


Figure C-4: Node Full Routing Stack

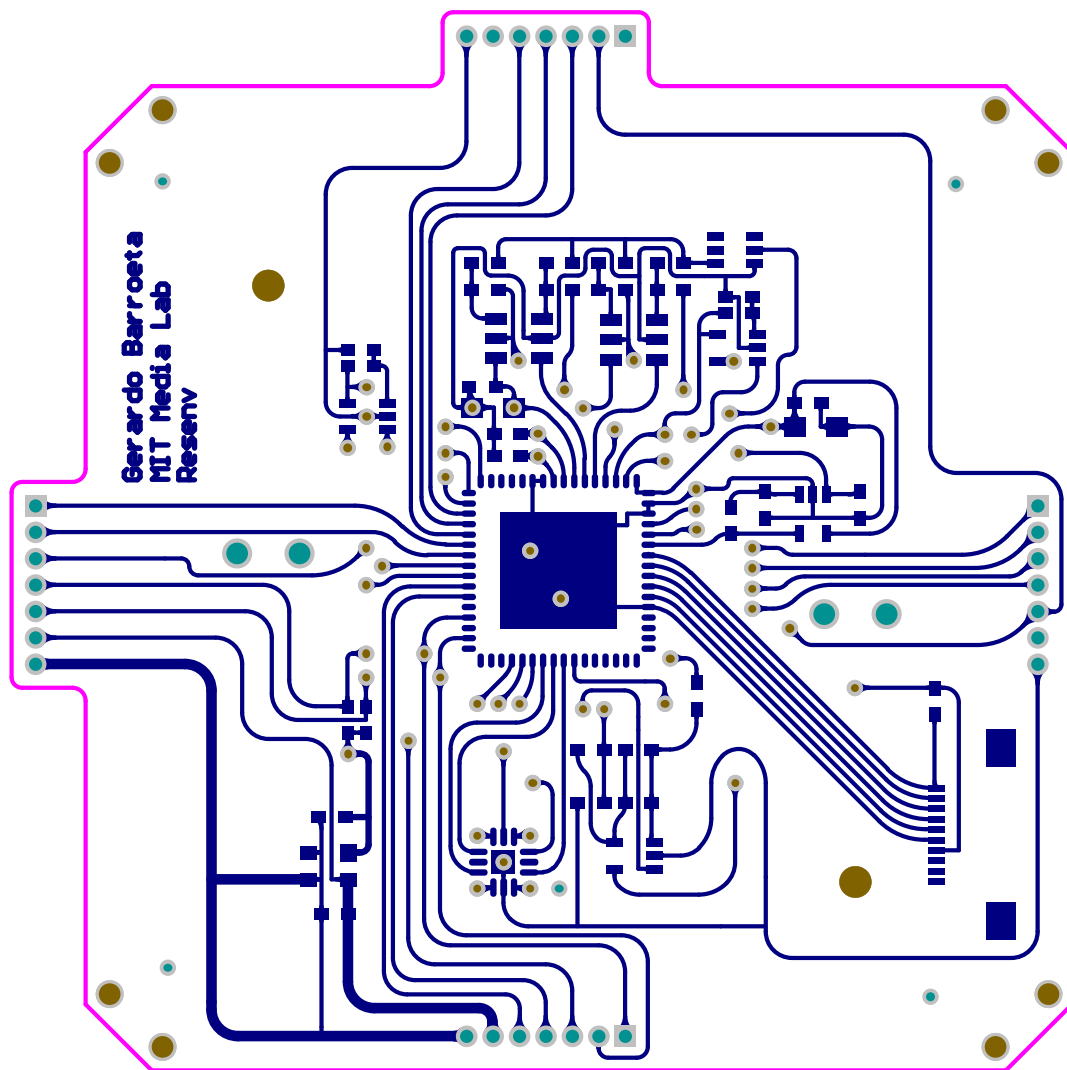


Figure C-5: Node Top Routing Layer

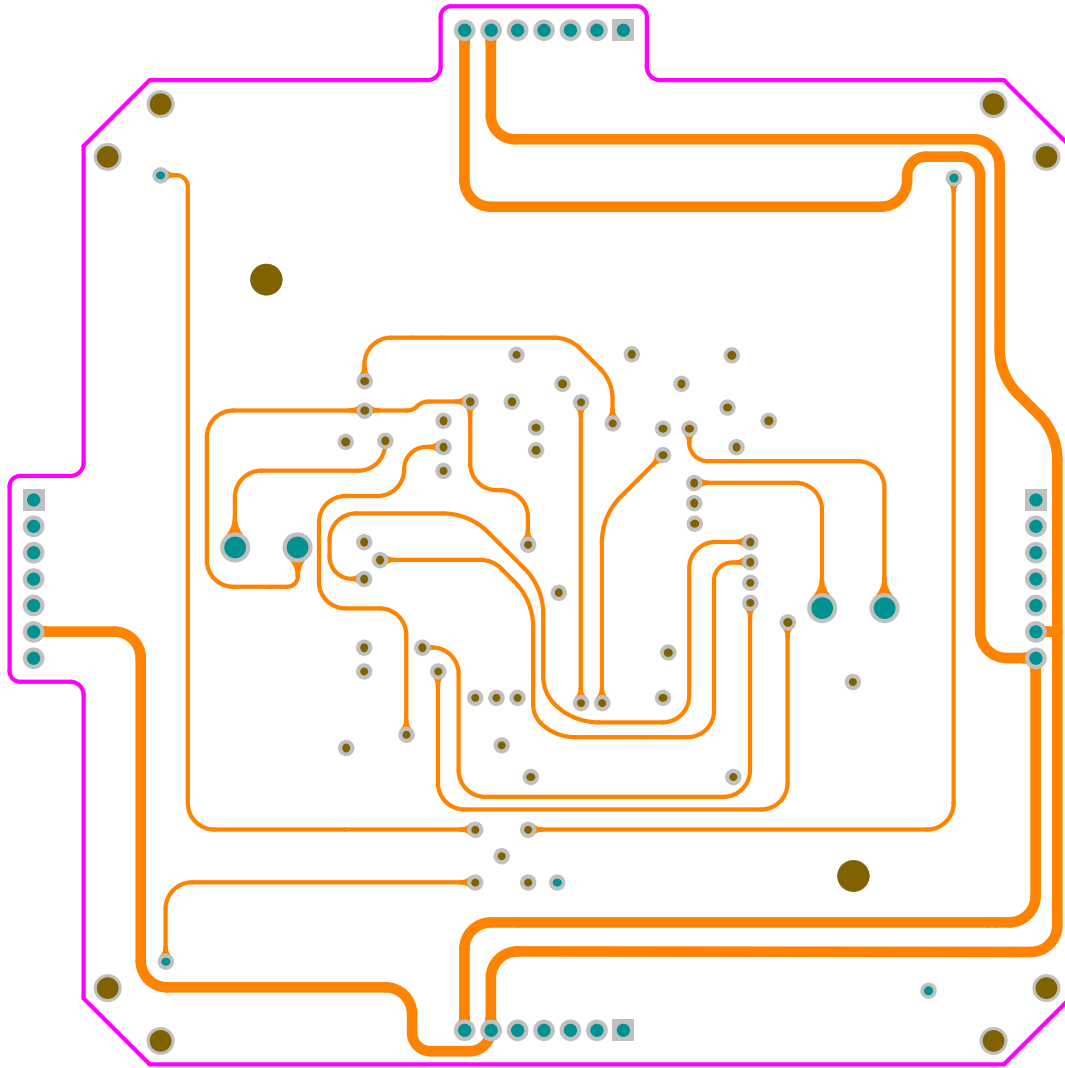


Figure C-6: Node Internal Layer 1

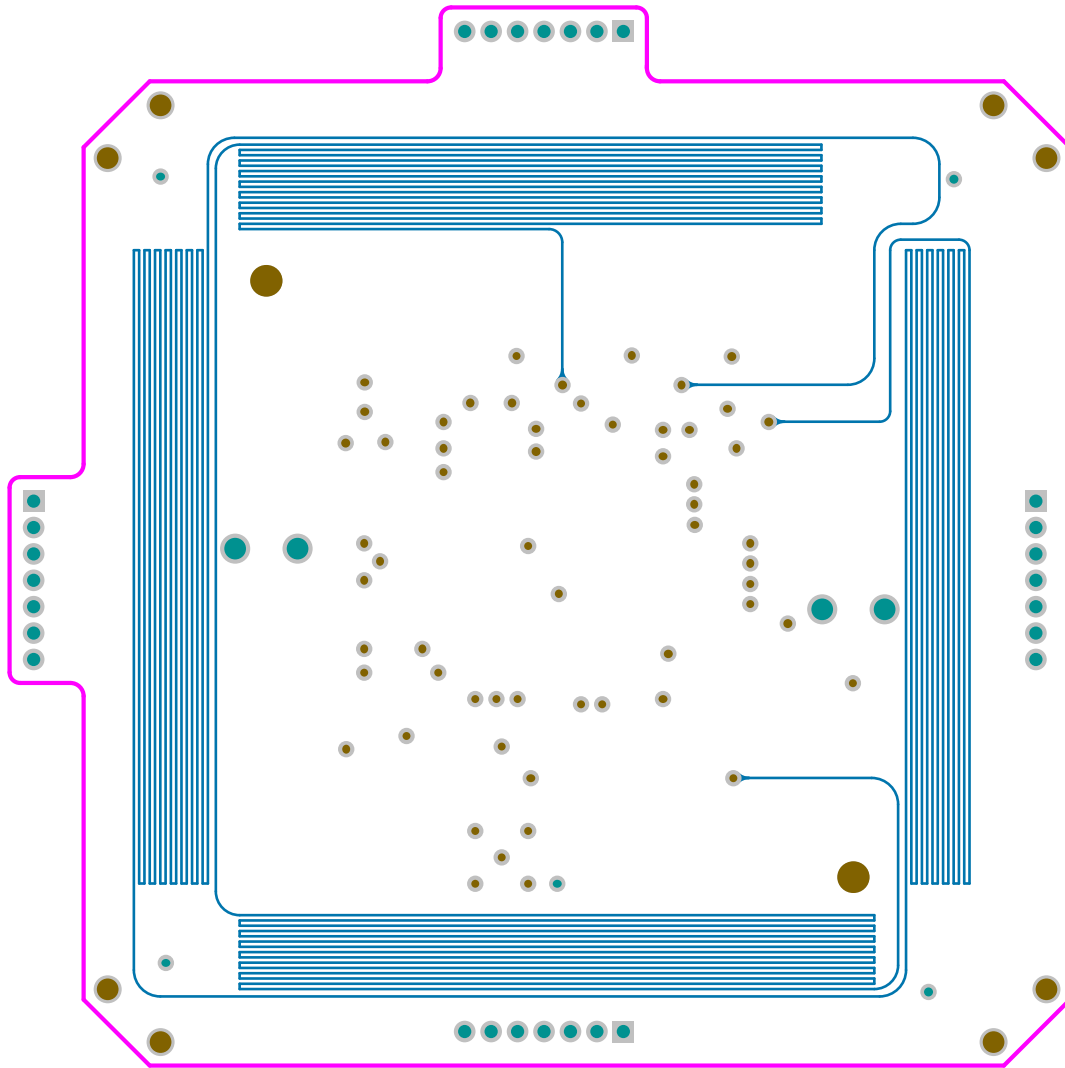


Figure C-7: Strain Gages (Internal Layer 2)

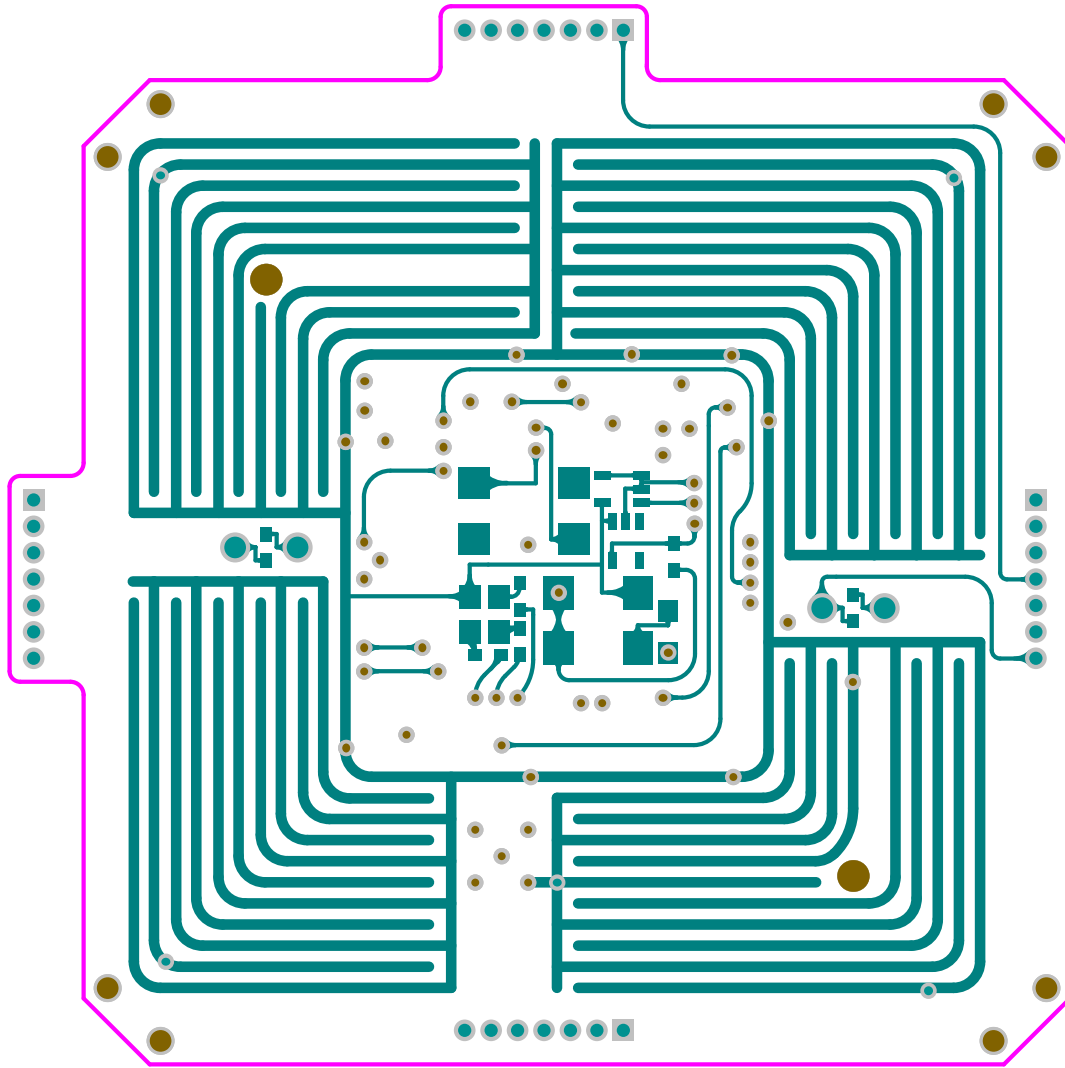


Figure C-8: Node Bottom Routing Layer

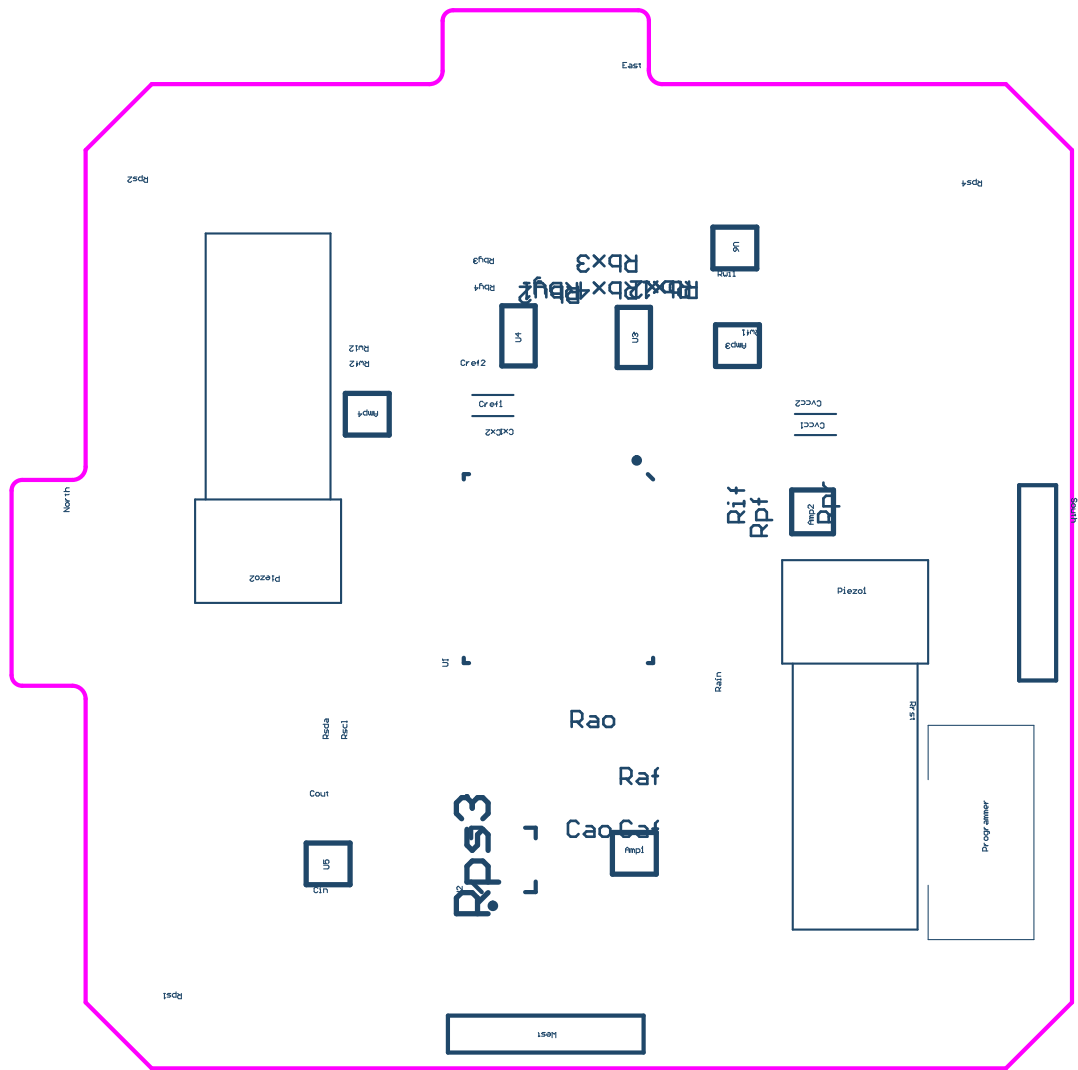


Figure C-9: Node Top Overlay

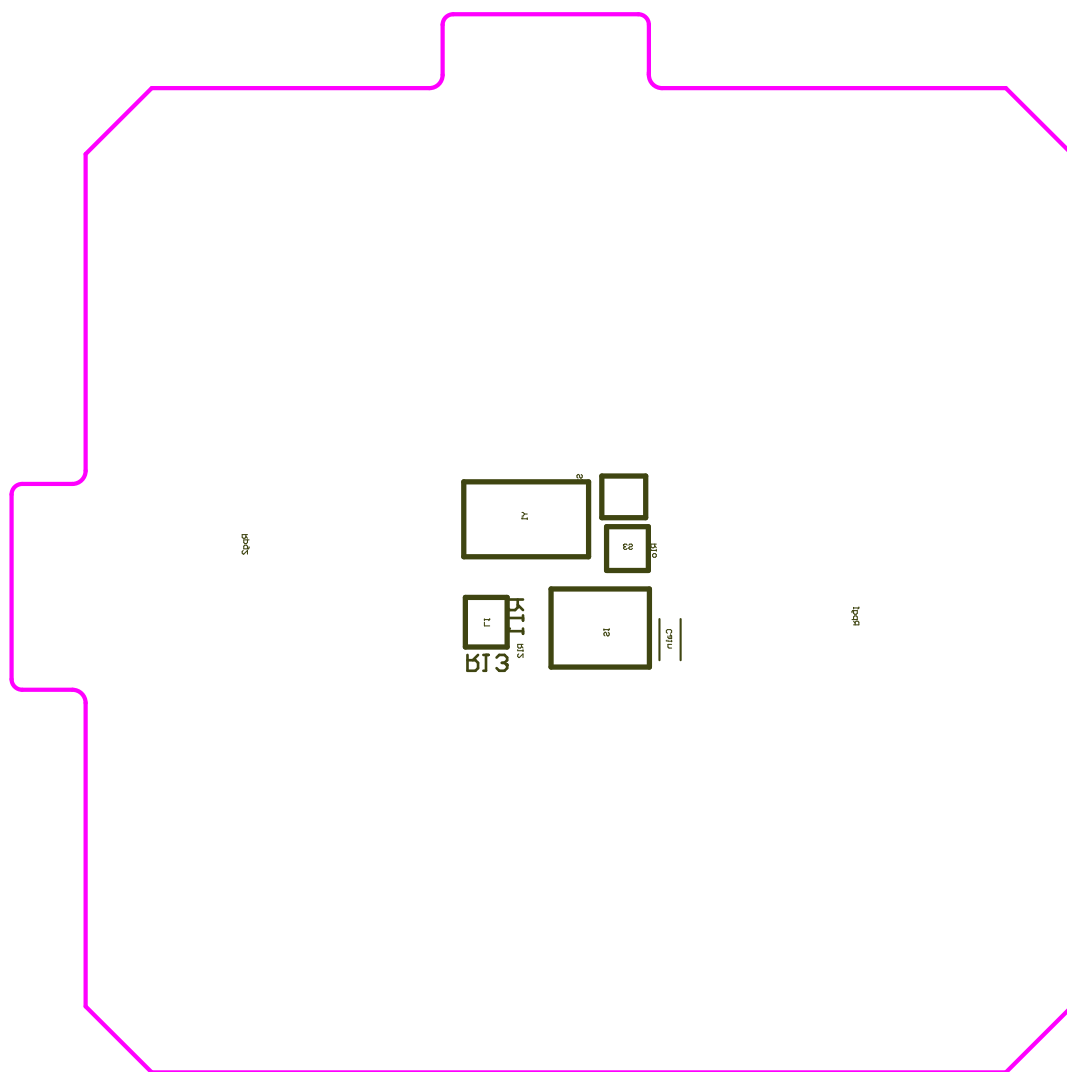


Figure C-10: Node Bottom Overlay

Brain Processing and Actuation

162

Brain Communications

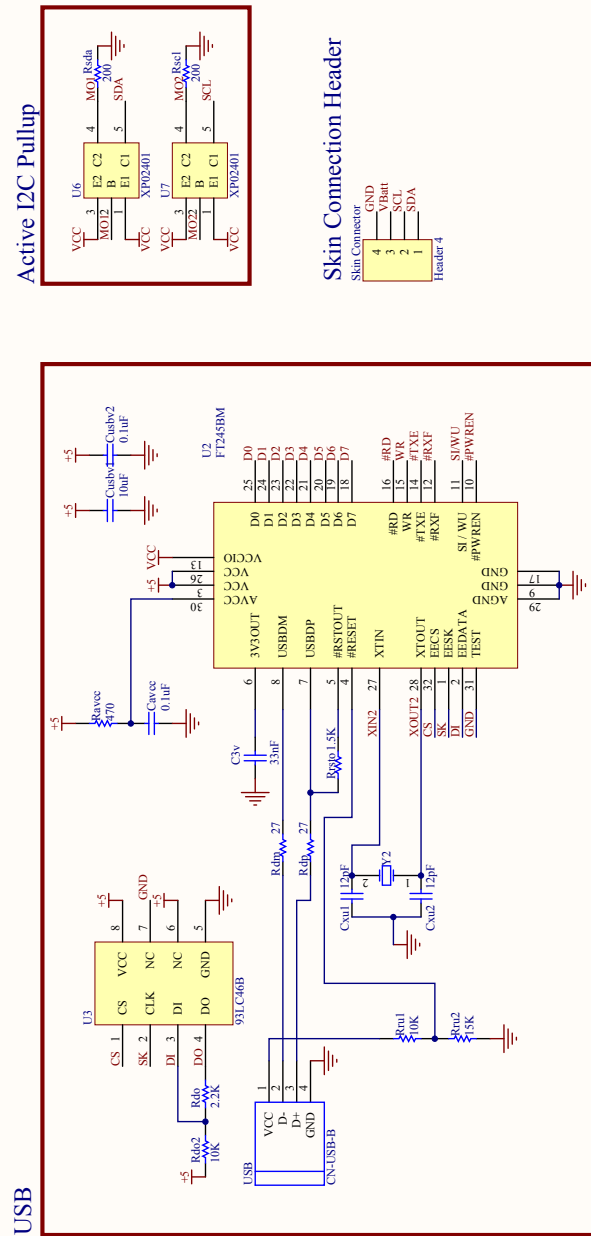


Figure C-12: Brain Communications

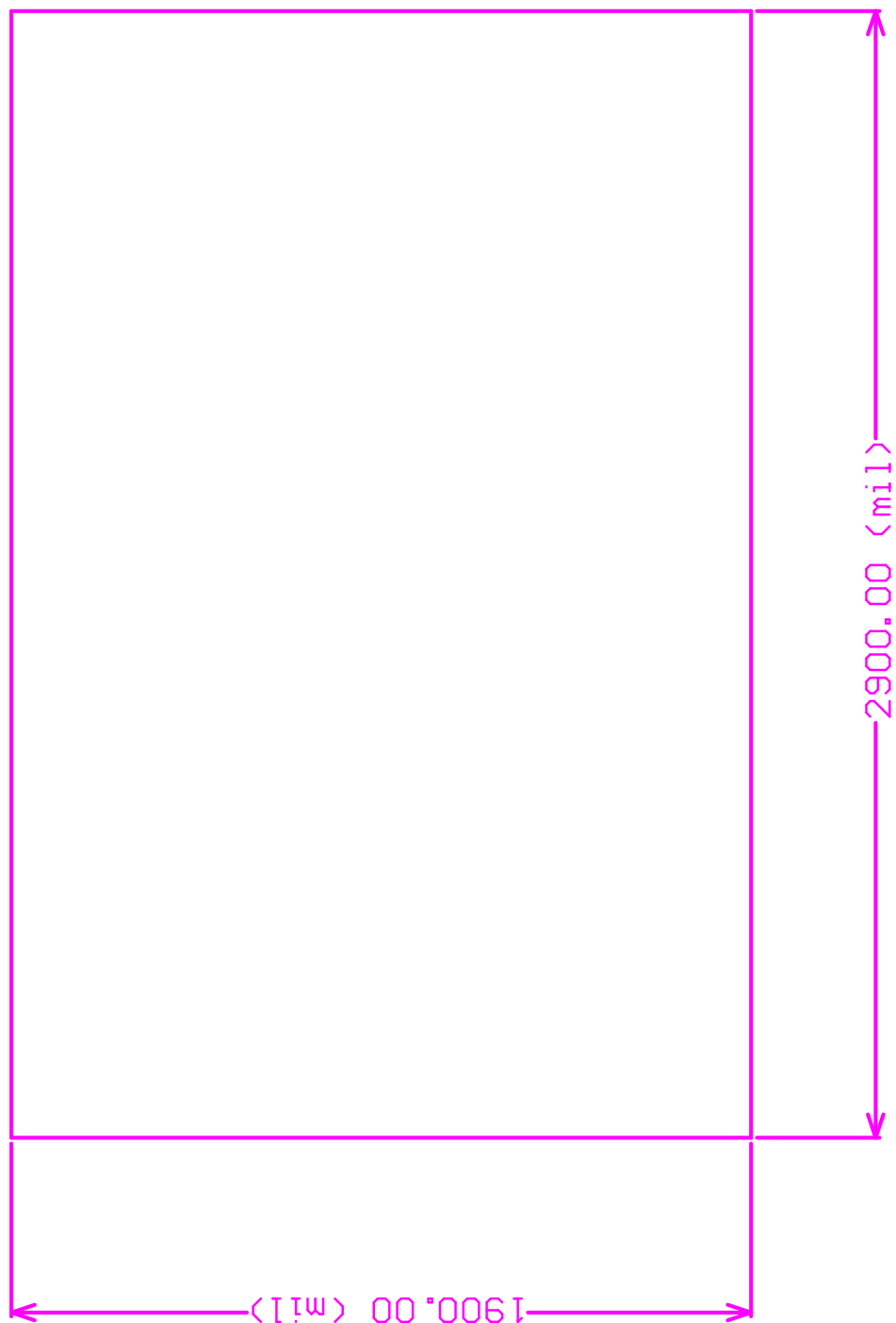


Figure C-13: Brain Dimensions (mils)

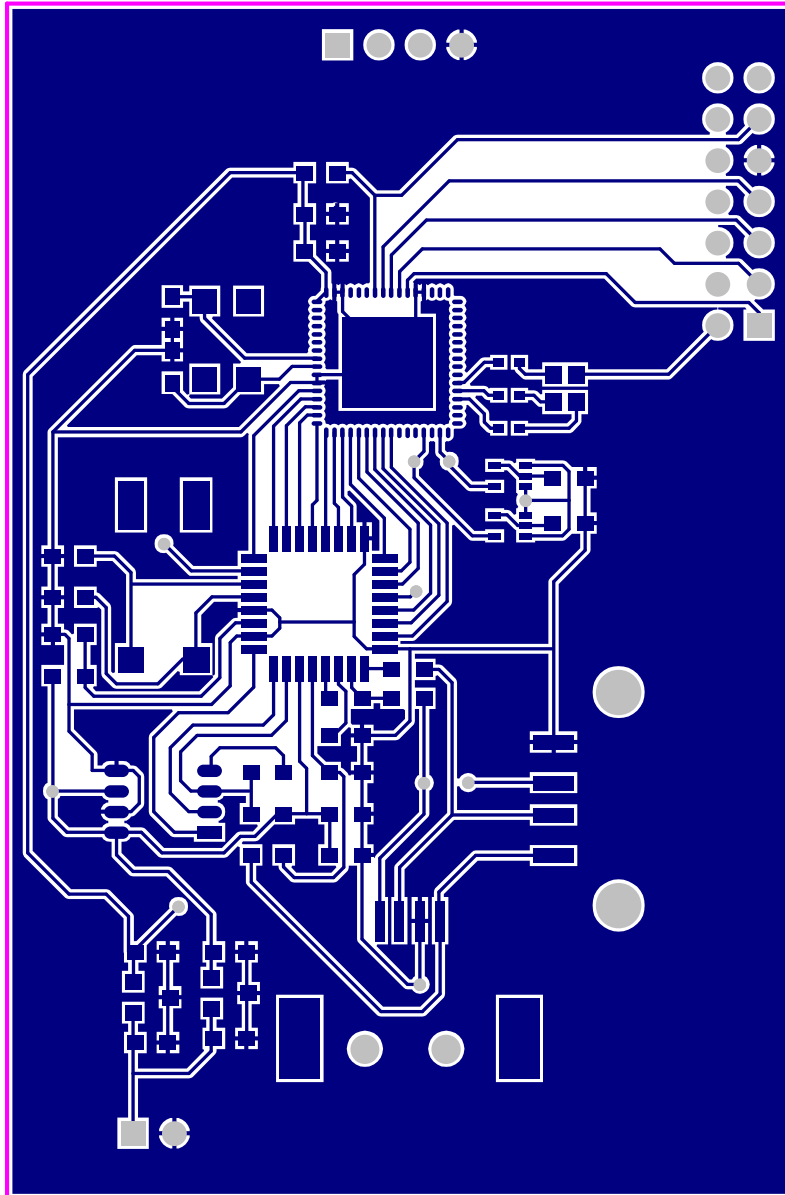


Figure C-14: Brain Top Layer

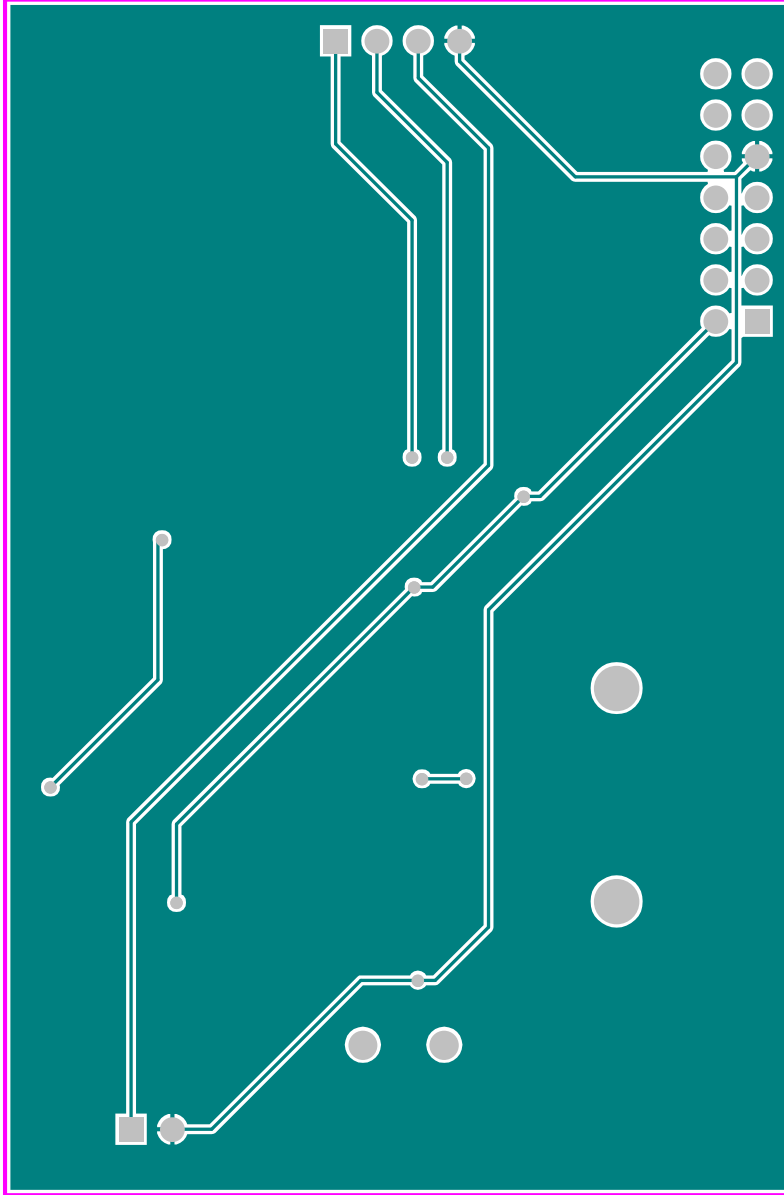


Figure C-15: Brain Bottom Layer

Appendix D

Firmware

C:\Documents and Settings\Gerardo\My Documents\Work\SM (MIT)\Thesis\Code\Firmware\BootLoader.s43

```

#include "map430c16x.h"      (0x000)
#define MAX_CODE_SIZE        (0x8000)
#define CODE_START_ADDR      (0x0A0)
#define REFRESH_INST         (0xA2)
#define RESET_BRAIN_INST     (0xA4)
#define RESET_NORE_INST      (0xA6)
#define EXECUTE_CODE_INST     (0xB1)
#define I2C_OWN_ADDRESS      (0x61)
;
;
ORG 1140h

filebuf DS MAX_CODE_SIZE
Address DB 2
nbyte DS 2
codeStartAddr DB 2
filesize DS 2
codeword DS 2
DataFlags DB 1
I2CFlags DB 1
;
;-----
RESET MOV W, #1130h,SP ; Initialize 'x'9x stackpointer
;
; /STOP WATCHDOG
MOV W, #WATCHDOG_HOLD, &WDTCTL ; stop watchdog
;
//INITIALIZE S/S
MOV B, #060h+PORN,&SVCTL ; S/S FOR enabled @ 2.6V
;
//INITIALIZE CRYSTAL (8.000 MHZ)
BIC B, #OSCOFF, SR
BIS B, #XTS, &BCSCTL1
;
L1 BIC B, #OPIFG,&IFG1 ; LFXU High-freq mode
; wait for crystal to stabilize
MOV W, #OFFF,R15 ; Clear OPIFG
; Delay
;
L2 DEC R15
JNG L2 ; Re-test OPIFG
BIS B, #OPIFG,&IFG1 ; Repeat test if needed
JNG L1
;
//INITIALIZE PORTS
RIS B, #OP70,&APDIR ; Set as outputs
MOV B, #0B5h,&PAOUT ; Turn off Strain gauges
;
//INITIALIZE I2C PORT
RIS B, #0Ah,&ISEL ; Select I2C pins
RIS B, #I2C-SNC-XA,&MUCTL ; Recommended init procedure
BIC B, #I2CN,&UMCTL ; Recommended init procedure
RIS B, #I2CSSEL0+I2CPM,&I2CTCTL; ACLK
MOV B, #7, &I2SCSH ; Set Band Rate to 400kHz

```

Page 1 of 6

C:\Documents and Settings\Gerardo\My Documents\Work\SM (MIT)\Thesis\Code\Firmware\BootLoader.s43

```

MOV.B #7, _12CSCL ; Set baud rate to 400KHz
MOV.B #12C, _12COWNADDRESS_&12COA ; Slave Address is 046h
BIS.B #12CEN_&0DCTL ; Enable TX

//INITIALIZE VARIABLES
MOV.W #0, fileBufPtr ; Init pointer
MOV.B #0, fileFlags ; Init flags
MOV.B #0, _12CFlags
CLR R6

MOV.W #130, R10 ; Delay to signal reset
CALL #DELAY ;
MOV.B #0B0F, &P4OUT ; Turn off led's
EINT ; Enable interrupts

MainLoop
MOV #1, R10 ; Wait until An instruction
CALL #12C_GBT_BYTE ; is received, and then decode it
BIT.B #1, &12CFlags ; If flag is set, nothing was received
JC MainLoop ; Jump back to main loop
BIT.B #0A1FG-&GCFG, &12CIFG

DecodeInstruction
CMP.B #REFLASH_INST, R5 ; If it is a reflash instruction
JZ ReflashSelf ; get file first, then reflash device
CMP.B #RPSSET_NODE_INST, R5 ; If the instruction is to reset
JZ ResetSelf ; Write invalid code to Watchdog for PIC
CMP.B #EXECUTE_CODE_INST, R5 ; If there is a code loaded and it
JZ ExecuteCode ; needs to execute, jump to its start address
JMP MainLoop ; Invalid instruction/data

ReflashSelf
MOV #200h, R10
CALL #12C_GBT_BYTE
MOV R5, R6
CALL #12C_GBT_BYTE
SWPB R5
XOR R6, R5
MOV R5, fileSize
MOV #01, _12CFlags
JNC GetFile
BIT.B #0F6, fileFlags
MOV #0FFh, R10
MOV.B fileFlags, R5
CALL #12C_SLAVE_READ
JMP MainLoop //777h, receive the file

GetFile
CALL #GBT_FILE
CALL #RPSFLASH_SELF
JMP MainLoop

ResetSelf
MOV #0, _WDCTL ; Invalidate watchdog write to cause PIC

ExecuteCode
MOV #01000h, R5 ; Load pointer
CMP #0, 01(R5) ; This address contains a flag indicating

```

Page 2 of 6

<pre> C:\Documents and Settings\Gerardo\My Documents\Work\SM (MIT)\Thesis\Code\Firmware\BootLoader.s43 JNZ MainLoop ; If there is a valid code programmed. MOV 2(R5), codeStartAdd MOV_B #0, &I2CIFG BIC_B #I2CEN,&I2CTL DINT BR ; codeStartAdd ; Jump to start address of flashed code I2C_SLAVE_READ ; Send a byte through I2C ; RET ; I2C_GET_BYTE ; Obtain a byte through I2C ; BIT_B #RXRDYIFG,&I2CIFG JC Get12Byte DEC_B R10 I2C_GET_BYTE JNZ I2C_GET_BYTE BIS_B #01h,&I2CFlags RET Get12Byte MOV_B &I2CDBR, R5 BIC_B #RXRDYIFG,&I2CIFG BIC_B #01h,&I2CFlags RET GET_FILE ; Gets a file through I2C ; MOV #0Fh, R10 CALL I2C_GET_BYTE BIT_B #I2CFlags JNZ SaveByte BIS_B #02h,&fileFlags RET SaveByte MOV fileBufPtr, R6 MOV_B R5, fileBuf(R6) INC R6 CMP #1000h, R6 JNZ NotFileSizeLimit CLR R6 BIS_B #04h,&fileFlags NotFileSizeLimit MOV R6, fileBufPtr MOV R6, nbytes DEC fileSize JZ R8, fileDone //MOV R8, fileSize JMP GET_FILE fileDone MOV nbytes, fileSize MOV #0, fileBufPtr BIS_B #1, &fileFlags </pre>	<pre> C:\Documents and Settings\Gerardo\My Documents\Work\SM (MIT)\Thesis\Code\Firmware\BootLoader.s43 REFLASH_SELF ; Burns a received code file into Flash memory ; //FIRST CALCULATE CHECKSUM FOR EVERY LINE, IF ANYTHING IS WRONG, ABORT. CLR fileBufPtr CLR codeSize CLR R5 MOV fileSize, R6 ChecksumLine CLR R7 MOV_B fileBuf(R5), R8 ; R7 Holds line Accumulator ; First byte contains # of data bytes ADD R8, codeSize ; Calculate total code size ; Accumulate SUB R8, R7 ; Decrease total bytes to process INC R5 ; Increment pointer ADD_B fileBuf(R5), R7 ; Accumulate address 1st byte INC R5 ; Increment pointer ADD_B fileBuf(R5), R7 ; Accumulate address 2nd byte INC R5 ; Increment pointer ADD_B fileBuf(R5), R7 ; Accumulate nth data byte DEC_B R8 ; Decrease data byte counter JNZ AddressByte ; Again ; Calculate checksum by ; taking the 2's complement INC R5 ; of the sum CMP_B fileBuf(R5), R7 ; compare to stored checksum JNZ Errors ; Was there an error? ; Increment pointer INC R4, R6 ; Are we done? SUB R4, R6 JNZ ChecksumLine ; Yes MOV_B fileBuf(R5), R6 ; Now calculate code Start Address INC R5 ; MOV_B fileBuf(R5), R7 ; SWPB R7 BIS R7, R6 MOV R6, codeStartAdd ; Save code Start Address ADD codeSize, R6 //EVERYTHING WAS CORRECT, REFLASH DEVICE CMP #1000h, codeSize ; Before doing that, is code bigger ; than the allowed limit? JGE FileTooBig CMP #0FA00h, R6 ; Is code size + code start add bigger than ; allowed? yes, abort JGE FileTooBig MOV #8000h, R5 ; Nope, move the start address to pointer MOV #WDTPW+WDTHOLD, &WDTCU ; stop watchdog DINT ; Disable Interrupts MOV_W #FWKEY+FSSEL_1, &FCTL2 ; Configure Flash controller MOV_W #FWKEY+FM4+FN1+FN0, &FCTL2 ; Configure Flash controller MOV_W #FWKEY,&FCTL3 ; Clear LOCK //ERASE FLASH MEMORY EXCEPT FOR BL SEGMENTS EraseNext MOV #FWKEY+ERASE,&FCTL1 ; Enable segment erase </pre>
--	--

```

CLR    R5                ; Dummy Write to erase
ADD    #200h, R5         ; Point to next segment
MOV    #0FA00h, R5       ; Stop when address equal to BL address
JNB    ErrorCS, ErrorCS  ; ErrorCS = 0, no error

; Erase interrupt vectors AND INFO MEMORY
MOV    #0FE00h, R5       ; Erase interrupt vectors
JNB    ErrorCS, ErrorCS  ; ErrorCS = 0, no error
MOV    #PKKEY+ERASE.&FCTL1
CLR    R5                ; Enable segment erase
MOV    #01000h, R5       ; Dummy Write to erase
CLR    R5                ; Enable segment erase
MOV    #01080h, R5       ; Dummy Write to erase
MOV    #PKKEY+ERASE.&FCTL1
CLR    R5                ; Enable segment erase
MOV    #0FFFEh, R5       ; Dummy Write to erase
MOV    #PKKEY+HRT.&FCTL1 ; Restore BL reset vector
MOV    #0FA00h, 0(R5)    ; Enable segment write
MOV    #0FA00h, 0(R5)    ; Dummy Write to restore RSSET vector

; NOW BURN CODE TO FLASH!
CLR    R5
MOV    codeSize, R9
FlashNextLine
MOV.B  fileBuf(R5), R8
INC    R5                ; Get # of data bytes of current line
MOV.B  fileBuf(R5), R6
INC    R5                ; Calculate address of line
MOV.B  fileBuf(R5), R7
SWPB   R6                ;
R7, R6                  ;
BIS    R8, R7            ;
MOV    #0FA00h, R6       ; Is it a valid address?
JNB    IVCheck           ;
JNB    FlashLine        ;
IVCheck
CMP     #0FFFEh, R8      ; Is it an interrupt vector?
JL     InvalidAddress   ;
CMP     #0FFFEh, R6      ; Is it the Reset vector?
JNB    FlashLine        ;
ADD     #3, R5           ; Nope, flash it as a regular line
JNB    DoneFlashing     ;
FlashNextLine
FlashLine
JNB    DoneFlashing
FlashLine
INC     R5
MOV     #PKKEY+HRT.&FCTL1 ; Enable segment write
MOV.B  fileBuf(R5), 0(R6) ; Write to Flash
INC     R6
DEC.B  R8
JNB    FlashLine
FlashLine
INC     R5
SUB     R7, R9
JNB    FlashNextLine
FlashNextLine
DoneFlashing
MOV     #1000h, R5
MOV     #PKKEY+HRT.&FCTL1 ; Indicate a successful write
MOV     #0, 0(R5)        ; Enable segment write
INCD   R5
MOV     codeStartAdd, 0(R5) ;

```

```

MOV     #1000h, R5
MOV     #I2C_ON_ADDRESS, 0(R5) ; Burn the I2C address in flash
MOV     #FWSET+LOCK, &FCTL3   ; Done Writing, see lock
JNB    ErrorCS, ErrorCS      ; ErrorCS = 0, no error
MOV     #0B0h, fileFlags
JNB    ErrorCS, ErrorCS      ; Indicate successful writing!
RET

ErrorsCS
BIS.B  #08, fileFlags
RET
FileToBig
BIS.B  #10h, fileFlags
RET
InvalidAddress
BIS.B  #20h, fileFlags
RET

RET

;
; DELAY ; Delay function (3n*2 + 4n + delay-9)
;
PUSH    R8
PUSH    R9
MOV     R10, R9
LoopDelay1
MOV     R10, R8
LoopDelay2
DEC     R8
JNZ    LoopDelay2
DEC     R9
JNZ    LoopDelay1
POP     R9
POP     R8
RET

;
; Interrupt Vectors Used MSP430x13x/14x/15x/16x
;
ORG     OFFFEh           ; MSP430 RESET Vector
DM      RSSET            ;
END

```

```

#include "mp430i6x.h"          (0x00)
#define RESET_PIN_INST         (0x02)
#define RESST_PIN_INST         (0x04)
#define EXECUTE_CODE_INST      (0x06)
#define DEEP_SLEEP             (0x08)

; Variables
;
; RAM VARIABLES
;-----
ORG 1140h
;-----
Packet EQU Pressure
Sound DS 1024
Light DS 256
Temp DS 8
Pressure DS 4
SoundAvg DS 2
SoundVar DS 2
XStrain DS 1
YStrain DS 1
LightValue DS 1
TempVar DS 1
SoundPtr DS 0,0,0
SoundPtrL DS 2
LightPtr DS 2
TempPtr DS 2
PressurePtr DS 2
PacketPtr DS 2
FlagSoundAdd DS 1
SoundAdd DS 1
SoundPtrL DS 1
;VALUES
LIGHT_MAX EQU 8800h

;-----
ORG 08000h ; Program Start
;-----
RESET
MOV.W #1120h,SP
; Initialize 'x169 stackpointer

;STOP WATCHDOG
MOV.W #WDTFR+WDTHOLD,&WDTCTL ; stop watchdog

;INITIALIZE SNS
MOV.B #060h+PORCH,&SVRCTL ; SNS FOR enabled @ 2.5V

;INITIALIZE CRYSTAL (8.000 MHZ)
BIC #SCOFF,SR ; Turn on osc.
BIS.B #MYS,&SCSCTL1 ; LPMCTL high-freq mode
; wait for crystal to stabilize
BIC.B #OFIFG,&IFG1 ; Clear OFIFG
MOV #0FFh,R15 ; Delay
L2
DEC R15

```

```

JNZ L2 ; Re-test OFIFG
BIS.B #OFIFG,&IFG1 ; Repeat test if needed
JNZ L1 ; Set XTCLK as source for MCLK
MOV.B #SEIM_3,&SCSCTL2 ; Set XTCLK as source for MCLK
BIS.B #SEIS,&SCSCTL2 ; select XTCLK as source for SMCLK

;INITIALIZE PORTS
BIS.B #7FH,&PDIR ; Set as outputs
MOV.B #0CB,&PSEL ; Enable A/D channel inputs
MOV.B #0AB,&PAOUT
BIS.B #07h,&PASEL

;INITIALIZE I2C
BIS.B #0AB,&P3SEL ; Select I2C pins
MOV.B #12Ch+SYNCR+XA,&AU0CTL ; Recommended init procedure
BIC.B #12CEN,&I2CCTL ; Recommended init procedure
MOV.B #12CSSEL0,&I2CCTL ; ACLK
MOV.B #07h,&I2CSCLR ; Set Baud Rate to 400KHz
MOV.B #07h,&I2CSCLL ; Set Baud Rate to 400KHz
BIS.B #RXDIVFG+GCIE,&I2CIE ; Activate I2C receive Interrupt
MOV #0107h,&I2COA ; Own Address is 1AAh
BIS.B #12CEN,&I2CCTL ; Enable I2C

;INITIALIZE ADC
MOV #ADC1ON+SHT0_3+REFON,&ADC12CTL0 ; Turn on ADC12, set MSC
MOV #SHP,&ADC12CTL1 ; Use samp. timer, single sequence
BIS.B #INCH0,&ADC12MCTL0 ; AVCC+ref+, channel=A0 (pressure channel)
BIS.B #INCH1,&ADC12MCTL1 ; AVCC+ref+, channel=A0 (light channel)
BIS.B #INCH2,&ADC12MCTL2 ; AVCC+ref+, channel=A0 (temperature channel)
BIS.B #INCH3,&ADC12MCTL3 ; AVCC+ref+, channel=A0
BIS.B #INCH4,&ADC12MCTL4 ; AVCC+ref+, channel=A0
BIS.B #INCH5,&ADC12MCTL5 ; AVCC+ref+, channel=A0
BIS.B #INCH6,&ADC12MCTL6 ; AVCC+ref+, channel=A0
BIS.B #INCH7,&ADC12MCTL7 ; AVCC+ref+, channel=A0
MOV #000h,&ADC12IE ; Activate Interrupts
BIS #SNC,&ADC12CTL0 ; Enable conversions

;INITIALIZE TIMERS
MOV.W #OUTMOD_4+CCIE,&TBCTL0 ; CCR1 reset/set
MOV.W #OUTMOD_4+CCIE,&TBCTL1 ; CCR1 reset/set
MOV.W #OUTMOD_4+CCIE,&TBCTL2 ; CCR1 reset/set
MOV.W #OUTMOD_4+CCIE,&TBCTL3 ; CCR1 reset/set
MOV.W #OUTMOD_4+CCIE,&TBCTL4 ; CCR1 reset/set
MOV.W #OUTMOD_4+CCIE,&TBCTL5 ; CCR1 reset/set
MOV.W #TBIE+TBSEL1+MC_2,&TBCTL ; ACLK, upmode

;INITIALIZE VARIABLES
MOV.W #0,SoundPtr
MOV.W #2,SoundPtrL
MOV.W #0,LightPtr
MOV.W #0,PressurePtr
MOV.W #0,TempPtr
MOV.W #0,SoundAvg
MOV.W #0,PacketPtr
BINT

MainLoop

```

```

JMP      MainLoop

```

```

;
DISABLE_TBCCR1Q / Disable TBCCR interrupts to allow sampling of ADC channel
;

```

```

BIC      #CCIE,ATBCCR1L1 / Disable all TBCCR IRQ's to allow ADC conv.
BIC      #CCIE,ATBCCR1L2 / Disable all TBCCR IRQ's to allow ADC conv.
BIC      #CCIE,ATBCCR1L3 / Disable all TBCCR IRQ's to allow ADC conv.
BIC      #CCIE,ATBCCR1L4 / Disable all TBCCR IRQ's to allow ADC conv.
BIC      #CCIE,ATBCCR1L5 / Disable all TBCCR IRQ's to allow ADC conv.
BIC      #CCIE,ATBCCR1L6 / Disable all TBCCR IRQ's to allow ADC conv.
RET

```

```

;
ENABLE_TBCCR1Q / ENABLE TBCCR interrupts to allow sampling of ADC channel
;

```

```

BIS      #CCIE,ATBCCR1L1 / Enable all TBCCR IRQ's to allow ADC conv.
BIS      #CCIE,ATBCCR1L2 / Enable all TBCCR IRQ's to allow ADC conv.
BIS      #CCIE,ATBCCR1L3 / Enable all TBCCR IRQ's to allow ADC conv.
BIS      #CCIE,ATBCCR1L4 / Enable all TBCCR IRQ's to allow ADC conv.
BIS      #CCIE,ATBCCR1L5 / Enable all TBCCR IRQ's to allow ADC conv.
BIS      #CCIE,ATBCCR1L6 / Enable all TBCCR IRQ's to allow ADC conv.
RET

```

```

;
DELAY / Delay function (3n*2 + 4n + delay-9)
;

```

```

PUSH     R8
PUSH     R9
MOV      R10, R9
LoopDelay1:
MOV      R10, R8
LoopDelay2:
DEC      R8
JNZ      LoopDelay2
JNZ      LoopDelay1
POP      R9
POP      R8
RET

```

```

;-----
ADC12ISR / Interrupt Service Routine for ADC12
;-----

```

```

ADD      #ADC12IV, PC / Add offset to PC 3
RETI
JMP      ADOVF / ADC Overflow
JMP      ADOVF / ADC Timing Overflow
JMP      ADM0 / ADC Mem0 ISR
JMP      ADM1 / ADC Mem1 ISR
JMP      ADM2 / ADC Mem2 ISR
JMP      ADM3 / ADC Mem3 ISR
JMP      ADM4 / ADC Mem4 ISR
JMP      ADM5 / ADC Mem5 ISR
JMP      ADM6 / ADC Mem6 ISR
JMP      ADM7 / ADC Mem7 ISR
JMP      ADM8 / ADC Mem8 ISR
JMP      ADM9 / ADC Mem9 ISR
JMP      ADM10 / ADC Mem10 ISR

```

```

JMP      ADM11 / ADC Mem11 ISR
JMP      ADM12 / ADC Mem12 ISR
JMP      ADM13 / ADC Mem13 ISR
JMP      ADM14 / ADC Mem14 ISR

```

```

ADM15 / Add ADC12MEM15 ISR code Here

```

```

JMP      ADC12ISR
;
//THIS INTERRUPT FIRMS WHEN PRESSURE CONVERSION IS DONE

```

```

ADM0 / Add ADC12MEM0 ISR code Here
MOV      #20h, &P4OUT / Move A0 result
CALL     #ENABLE_TBCCR1Q / Turn Off MUX

```

```

//Downsample to 8 bits

```

```

PRA      R5
PRA      R5

```

```

PRA      R5
PRA      R5

```

```

MOV.B    PressurePtr, R6

```

```

MOV.B    R5, Pressure (R6)

```

```

INC      R6

```

```

CMP.B    #4, R6

```

```

JNZ      DonePressure

```

```

MOV      #0, R6

```

```

DonePressure

```

```

MOV      R6, PressurePtr

```

```

CMP.B    #0F0h, R5

```

```

JGE      Lower

```

```

BIC.B    #01h, &P4OUT

```

```

JMP      EndPressure

```

```

BIS.B    #01, &P4OUT

```

```

EndPressure

```

```

RETI / Return from interrupt

```

```

//THIS INTERRUPT FIRMS WHEN LIGHT CONVERSION IS DONE
; Add ADC12MEM1 ISR code Here

```

```

ADM1 / Add ADC12MEM1 ISR code Here
MOV      #ADC12MEM1, R5
CALL     #ENABLE_TBCCR1Q

```

```

PRA      R5
PRA      R5

```

```

PRA      R5
PRA      R5

```

```

MOV      LightPtr, R6

```

```

MOV.B    R5, Light (R6)

```

```

MOV.B    R5, LightValue

```

```

INC      LightPtr

```

```

CMP.B    #255, LightPtr

```

```

JNZ      DoneLight

```

```

MOV      #0, LightPtr

```

```

DoneLight

```

```

RETI / Return from interrupt

```

```

//THIS INTERRUPT FIRMS WHEN TEMPERATURE CONVERSION IS DONE
; Add ADC12MEM2 ISR code Here

```

```

ADM2 / Add ADC12MEM2, R5
CALL     #ENABLE_TBCCR1Q

```

```

PRA      R5
PRA      R5

```

```

PRA      R5
PRA      R5

```

```

RETI

```

<pre> C:\Documents and Settings\Gerardo\My Documents\Work\SM (MIT)\Thesis\Code\Firmware\Node_Test.s43 R0A R5 R0A R5 R0A TempPtr, R6 MOV R5, TempPtr, R6 MOV R5, TempValue INC TempPtr CMP #8, TempPtr JNZ DoneTemp MOV #0, TempPtr DoneTemp RETI ; Return from Interrupt //THIS INTERRUPT FIRES WHEN SOUND CONVERSION IS DONE ; Add ADC12MNM3 ISR code Here ADM3 MOV SoundPtr, R6 MOV &ADC12MNM3, Sound(R6) CALL #ENABLE_TBCCRIRQ INCD SoundPtr CMP #1024, SoundPtr JNZ DoneSound MOV #0, SoundPtr DoneSound RETI ; Return from Interrupt ; Add ADC12MNM4 ISR code Here ADM4 MOV &ADC12MNM4, R5 RETI ; Return from Interrupt ; Add ADC12MNM5 ISR code Here ADM5 MOV &ADC12MNM5, R5 RETI ; Add ADC12MNM6 ISR code Here ADM6 MOV &ADC12MNM6, R5 RETI ; Add ADC12MNM7 ISR code Here ADM7 MOV &ADC12MNM6, R5 MOV R5, XStrain MOV &ADC12MNM7, R5 CALL #ENABLE_TBCCRIRQ MOV R5, YStrain BIC B BIC #40b, &40OUT BIC #ENC, &ADC12CTL0 BIS #NSC, &ADC12CTL0 BIS #ENC, &ADC12CTL0 RETI ADM8 RETI ADM9 RETI ADM10 RETI ADM11 RETI ADM12 RETI ADM13 RETI ADM14 RETI </pre>	<pre> C:\Documents and Settings\Gerardo\My Documents\Work\SM (MIT)\Thesis\Code\Firmware\Node_Test.s43 AD0V RETI AD0V ; Add ADC12 Overflow ISR code Here AD0V RETI AD0V ; Add ADC12 Timer Overflow ISR code Here ;----- ; Toggle P1.0 ;----- ADD.W #200, &TBCCR0 RETI ; Offset until next interrupt ;----- ; Common ISR for TBCCR1-6 and overflow ;----- TBX_ISR: ADD.W &TBIV, PC RETI JMP TBCCR1_ISR JMP TBCCR2_ISR JMP TBCCR3_ISR JMP TBCCR4_ISR JMP TBCCR5_ISR JMP TBCCR6_ISR TB_Over RETI TBCCR1_ISR BIT #ADC12BUSY, &ADC12CTL1 JC ; Generates frequency to sample audio ; Wait for ADC to finish conversions BIC #ENC, &ADC12CTL0 MOV #STARTADD_1+SHP, &ADC12CTL1 ; Turn off to configure BIS #ENC, &ADC12CTL0 CALL #DISABLE_TBCCRIRQ BIS #DISABED_TBCCRIRQ CALL #ADC12SC, &ADC12CTL0 ; Start conversions ADD.W #200, &TBCCR1 ; Offset until next interrupt (Sample sound @ 8 KHz) JMP TBX_ISR RETI TBCCR2_ISR BIT #ADC12BUSY, &ADC12CTL1 JC TBCCR2_ISR BIC #ENC, &ADC12CTL0 MOV #STARTADD_1+SHP, &ADC12CTL1; Specify channel to sample (light) BIS #ENC, &ADC12CTL0 CALL #DISABLE_TBCCRIRQ BIS #ADC12SC, &ADC12CTL0 ; Start conversions ADD.W #200, &TBCCR2 ; Offset until next interrupt (Sample light @ 200Hz) JMP TBX_ISR RETI TBCCR3_ISR BIT #ADC12BUSY, &ADC12CTL1 JC TBCCR3_ISR MOV B, PressurePtr, R6 ; get pointer MOV R6, R6 ; shift to set mux address MOV R6, R6 ; shift to set mux address MOV R6, R6 ; Turn on MDX CLR R7 </pre>
Page 5 of 8	Page 6 of 8


```

;*****
; MSP-FRTP30P140 Demo - Software Toggle P1.0
; Description: Toggle P1.0 by xoring P0.1
; ACLK = n/a, XCLK = SNCLK = default DCO = 800k
;*****
;
; MSP430P149
;
; /|\
; | |
; | | XIN /-
; | |
; | | XOUT /-
; | |
; | |
; | | P1.0 /->LED
; | |
;
; M. Bucci
; Texas Instruments, Inc
; January 2004
;*****
#include "mp430x16x.h"

#define REFLASH_ALL_INST (0xA0)
#define RESET_BRAIN_INST (0xA2)
#define RESET_SKIN_INST (0xA4)
#define EXECUTE_CODE_INST (0xA6)
#define SAMPLE_INST (0xA8)
#define LIGHT_MAX (0x0100)
#define I2C_OWN_ADDRESS (269)

; Variables
;
; RAM VARIABLES
;
;-----
ORG 1140h

Light DS 16
Temp DS 20
LightPtr DS 1
Flame DS 1
BootloaderAdd DS 1

;-----
ORG 08000h
; Program Start

RESET
MOV.W #1120h,SP
; Initialize 'x1s' stackpointer

;STOP WATCHDOG
MOV.W #WDTPW+WDTHOLD,&WDCTL ; stop watchdog

;*****
; INITIALIZE SNS
MOV.B #060h+PORCH,&SVSCTL ; SNS POR enabled @ 2.5V

;*****
; INITIALIZE CRYSTAL (8.000 MHZ)
BIC #SCCOFF,SR ; Turn on osc.
BIS.B #XTS,&ECSCTL1 ; LFXTL high-freq mode
; wait for crystal to stabilize
BIC.B #OFFG,&IFG1 ; Clear OFFG

```

```

;*****
; Delay
;*****
MOV #OFFH,R15
; Delay

L2
DEC R15
JNZ L2
; Re-test OFFG
BTFSC &IFG1
; Repeat test if needed
JNZ L1
; Select XT1 as source for MCLK
BIS.B #SEL3,&BCSCTL2
BIS.B #SEL5,&BCSCTL2
; select XT1CLK as source for SMCLK

;*****
; INITIALIZE PORTS
BIS.B #P4DIR ; Set as outputs
BIS.B #P4SEL ; Set as timer outputs for PWM
BIS.B #07B,&P4SEL ; Enable A/D channel inputs
MOV.B #0A7h,&P4OUT

;*****
//INITIALIZE I2C
BIS.B #0A0h,&P3SEL ; Select I2C pins
BIS.B #I2C+SYNCR+XA,&U0CTL ; Recommended init procedure
BIC.B #I2CEN,&U0CTL ; Recommended init procedure
MOV.B #I2CSSEL0,&I2CTCTL ; ACLK
MOV.B #07h,&I2CSCLH ; Set I2C Baud Rate to 400KHz
MOV.B #07h,&I2SCLL ; Set I2C Baud Rate to 400KHz
BIS.B #GCR+TXRDYIE,&I2CIE ; Activate I2C receive interrupt
MOV #I000h,R5 ; Get I2C address from flash (from BL)
MOV 0(R5),&I2COA ; Slave Address is 048h
BIS.B #I2CEN,&U0CTL ; Enable I2C

;*****
//INITIALIZE ADC
MOV #ADC12ON+SHUTL3+REFON,&ADC12CTL0 ; Turn on ADC12, set MSC
MOV #SHR,&ADC12CTL1 ; Use samp. timer, single sequence
BIS.B #INCH1,&ADC12MCTL0 ; AVCC-ref+, channel A0
MOV #BIT0,&ADC12IE ; Enable ADC12IFG.0 for ADC12MEM0
BIS #ENC,&ADC12CTL0 ; Enable conversions

;*****
//INITIALIZE TIMERS
MOV #LIGHT_MAX,&TRCRO ; PWM Period
MOV #UTPMOD.7,&TRCTLL ; CCP1 reset/set
MOV #TBSSSEL_1+MC_1,&TRCTL ; SMCLK, upmode
EINT

EINT
MOV #0,LightPtr
CLR R7

MainLoop
BIS #ADC12SC,&ADC12CTL0 ; Start conversions
MOV.W #20,R10 ; Delay
CALL #DELAY
MOV R5,&TRCCR1
JMP MainLoop

; Delay function (3n*2 + 4n + delay-9)
;
;
; Delay
PUSH R8
PUSH R9
MOV R10,R9
LoopDelay1
MOV R10,R8

```

```
LoopDelay2
    DEC R8
    JNZ LoopDelay2
    JNZ LoopDelay1
    POP R9
    POP R8
    RET

/-----
ADC12ISR      ; Interrupt Service Routine for ADC12
/-----
    MOV     &ADC12MEM0,R5
    MOV     LightPtr,R6
    MOV     R5,Light(R6)
    INC     LightPtr
    BIC.B   #0F0H,LightPtr
    CMP.W   #LIGHT_MAX,R5
    JNC     EndISR
    MOV.W   #LIGHT_MAX,R5
    RETI

EndISR

/-----
I2C_ISR;      Common ISR for I2C Module
/-----
    ADD     &I2CIV,PC
    RETI
    RETI
    RETI
    RETI
    JMP     RXRDY_ISR
    JMP     TXRDY_ISR
    JMP     GC_ISR
    RETI

RXRDY_ISR
    MOV.B   &I2CDBB,R6
    MOV.B   Light(R6),&I2CRRB
    RETI

TXRDY_ISR
    MOV     LightPtr,R6
    MOV.B   Light(R6),&I2CRRB
    BIC.B   #TXRDYIFG,&I2CIFG
    MOV.B   #0FFH,R5
    WaitTX

WaitTX
    DEC.B   R5
    JZ      EndI2CISR
    BIT.B   #TXRDYIFG,&I2CIFG
    JNC     WaitTX
    BIC.B   #TXRDYIFG,&I2CIFG
    INC     R6
    MOV.B   Light(R6),&I2CRRB
    //XOR.B #01,&F400T
    RETI
```

```
GC_ISR
    MOV.B   &I2CDBB,R6
    MOV.B   LightPtr,R6
    INC     LightPtr
    BIC.B   #0F0H,LightPtr
    CMP.W   #3500,R5
    JNC     EndI2CISR
    MOV     #0,0(R5)
    BIC.B   #GCIFG+RXRDYIFG,&I2CIFG
    MOV     #0,&MDCTL
    ; Yup, reset

EndI2CISR
    RETI

/-----
;      Interrupt Vectors Used MSP430x13x/14x/15x/16x
/-----
    ORG     OFFFH
    DW      RESET
    ORG     OFFFH
    DW      ADC12ISR
    ORG     OFFFH
    DW      I2C_ISR
    DW      I2C_ISR

END
```


<pre> C:\Documents and Settings\Gerardo\My Documents\Work\SM (MIT)\Thesis\Code\Firmware\Blink.s43 ;***** ; MSP-FRTP30P140 Demo - Software Toggle P1.0 ; Description: Toggle P1.0 By xoring P0.1 ; CLK = n/a, CLK = SCLK = default DCO = 800k ;***** ; MSP430P149 ;----- ; / \ ; ; -- NST ; ; P1.0 /-->LED ;----- ; ; M.Buccini ; Texas Instruments, Inc ; January 2004 ;***** #include "mp430x16x.h" #define REFLASH_ALL_INST (0xA0) #define RESET_BRNIN_INST (0xA2) #define RESET_SKIN_INST (0xA4) #define EXECUTE_CODE_INST (0xA6) ;***** ;----- ; ORG 01140h ; Program Start ;----- flag DS 1 ;----- ;VALUES LIGHT_MAX EQU 0800h ;----- ; ORG 0800h ; Program Start ;----- RESET MOV.W #120h,SP ; Initialize 'x169 stackpointer ;----- ;STOP WATCHDOG MOV.W WDTPW+WDTHOLD,&NDCTL ; stop watchdog ;----- ;INITIALIZE SWS MOV.B #060h+PORCN,&SVSCTL ; SWS POR enabled @ 2.5V ;----- ;SET MAX DCO FREQUENCY BIS.B #RSEL2+RSEL1+RSEL0,&RSCCTL1 ; BIS.B #DCO2+DCO1+DCO0,&DCOCTL ; Set max DCO frequency ;----- ;INITIALIZE CRYSTAL (8.000 MHZ) BIC #SCOFF,SR ; Turn on osc. BIS.B #MOS,&RSCCTL1 ; LPM1L high-freq mode ; wait for crystal to stabilize BIC.B #OFIF0,&IFG1 ; Clear OFIF MOV #0FFh,R15 ; Delay L1 DEC R15 UNZ L2 BIT.B #OFIF0,&IFG1 ; Re-test OFIF </pre>	<pre> C:\Documents and Settings\Gerardo\My Documents\Work\SM (MIT)\Thesis\Code\Firmware\Blink.s43 UNZ L1 BIS.B #SEM_3,&RSCCTL2 ; Repeat test if needed BIS.B #SIS,&RSCCTL2 ; Select XT1 as source for MCLK ; select XT1CLK as source for SCLKX ;----- ;INITIALIZE PORTS BIS.B #PFI,&PDIR ; Set as outputs BIS.B #07h,&PSEL ; Enable A/D channel inputs MOV.B #03h,&P4OUT ;----- ;INITIALIZE I2C BIS.B #0Ah,&P3SEL ; Select I2C pins BIS.B #I2C+SYNCR+XA,&U0CTL ; Recommended init procedure BIS.B #I2CEN,&U0CTL ; Recommended init procedure MOV.B #07h,&I2CSSEL0+I2CEN,&I2CTCTL ; ACLK MOV.B #07h,&I2CSCLH ; Set Baud Rate to 400KHz MOV.B #07h,&I2SCLL ; Set Baud Rate to 400KHz BIS.B #SCIE,&I2CIE ; Activate I2C receive Interrupt BIS.B #I2CEN,&U0CTL ; Enable I2C EINT MOV.B #0,flag MainLoop XOR.B #05h,&P4OUT MOV.W #450h,R10 ; Delay CALL #DELAY JMP MainLoop ;----- ; Delay function (3n^2 + 4n + delay-9) ;----- DELAY PUSH R8 PUSH R9 MOV R10,R9 LoopDelay1 MOV R10,R8 LoopDelay2 DEC R8 UNZ LoopDelay2 DEC R9 UNZ LoopDelay1 POP R9 POP R8 RET ;----- ;I2C_ISR, Common ISR for I2C Module ;----- ADD &I2CIV,PC ; Add I2C offset vector RETI ; No Interrupt RETI ; Arbitration Lost RETI ; No Acknowledge RETI ; Own Address RETI ; Register Access Ready JMP RXRDY_ISR ; Receive Ready RETI ; Transmit Ready </pre>
---	---

C:\Documents and Settings\Gerardo\My Documents\Work\BN (MIT)\Thesis\Code\Firmware\Blink.s43

```
JMP GC_ISR
RETI
; General Call
; Start Condition

RXRDY_ISR
    RETC.B #RXRDYIFG, &I2CIFG
    RETI

GC_ISR
    MOV.B &I2CDSB.R5
    RETC.B #GCIFG+RXRDYIFG, &I2CIFG
    ORC.B #RESET.SKIN_INST, R5
    JNZ EndI2CISR ; Is it a reset?
    JNZ EndI2CISR ; No
    MOV #0, &MD7CTL ; Yup, reset

EndI2CISR
    RETI

;----- Interrupt Vectors Used MSP430x13x/14x/15x/16x -----
;
ORG 0FFFFh ; MSP430 RESET Vector
IN RESET
ORG 0FFFF0h ; I2C Interrupt vector
IN I2C_ISR
END
```

<pre> C:\Documents and Settings\Gerardo\My Documents\Work\SM (MIT)\Thesis\Code\Firmware\I2C_Master.s43 #include "mp430x16x.h" #define RD_ (0x0001) #define WR_ (0x0002) #define TXE_ (0x0004) #define RXF_ (0x0008) #define ST_WU (0x0010) #define PHREN (0x0020) #define MAX_CODE_SIZE (0x0000) #define REFLASH_INST (0x00) #define RESET_SKIN_INST (0x02) #define EXECUTE_CODE_INST (0x04) #define REFLASH_LEV_INST (0x06) #define RESET_DEV_INST (0x08) #define START_SAMPLING_INST (0x0A) #define STOP_SAMPLING_INST (0x0E) #define I2C_BRAIN_ADDRESS (0x0100) #define DATA_BYTES (2) ; Variables ; ; RAM VARIABLES ORG 1140h USBBuf DS MAX_CODE_SIZE nBytes DS 2 Address DS 2 DataPacket DS 18 fileFlag DS 1 I2CFlags DS 1 ; ;----- ; Program Start RESET MOV.W #1130h,SP ; Initialize 'x169 stackpointer ;STOP WATCHDOG MOV.W #WDTPW+WDTHOLD,&NDCTL ; stop watchdog ;INITIALIZE SNS MOV.B #060h+PORCN,&SVSCTL ; SNS FOR enabled @ 2.6V ;INITIALIZE CRYSTAL (8.000 MHZ) BIC.B #SCOFF,SR ; Turn on osc. BIS.B #XTS,&ECCTL1 ; LEXTL high-freq mode ; wait for crystal to stabilize BIC.B #OFFG,&IFG1 ; Clear OFFG MOV #OFFH,R15 ; Delay DEC R15 JNZ L2 BIT.B #OFFG,&IFG1 ; Re-test OFFG JNZ L1 ; Repeat test if needed BIS.B #SELMO+SELM,&SCCTL2 ; Select XT1 as source for MCLK BIS.B #SELUS,&SCCTL2 ; select XTCLK as source for SMCLK </pre>	<pre> C:\Documents and Settings\Gerardo\My Documents\Work\SM (MIT)\Thesis\Code\Firmware\I2C_Master.s43 //INITIALIZE PORTS BIS.B #0FH,&P2OUT ; Set all pins to 1 BIS.B #0C~0B,&P2IN,&P2DIR ; Set P2 directions BIS.B #08h,&P2IE ; Enable interrupts BIS.B #08h,&P2IF ; Enable interrupt MOV.B #0FEh,&P4OUT ; Turn off LED's BIS.B #07h,&P4DIR ; Set as outputs //INITIALIZE I2C PORT BIS.B #70h,&P5SEL ; Select I2C pins BIS.B #0Ah,&P3SEL ; Recommended init procedure BIS.B #I2C+SYNC,&I0CTL ; Recommended init procedure BIS.B #I2CN,&I0CTL ; Recommended init procedure BIS.B #XA,&I0CTL ; ACLK BIS.B #I2CSSELO,&I2TCTL ; Set Baud Rate to 400KHz MOV.B #7,&I2CSCLH ; Set Baud Rate to 400KHz MOV.B #7,&I2CSCLL ; Enable I2C BIS.B #I2CN,&I0CTL //INITIALIZE VARIABLES MOV.B #0,&I2CFlags MOV.W #0,&USBBufPtr MOV.B #0,&fileFlag MOV.W #130,&R10 CALL #DELAY MOV.B #OFFh,&P4OUT CALL //CALL #I2C_RESET BINT MainLoop BIT.B #80h,&I2CFlags ; Wait here until a code file is transferred JNC MainLoop ; Is sampling on? ; Nope, don't do anything BIC.B #I2CN,&I0CTL ; Reconfigure I2C BIS.B #XA,&I0CTL ; Reconfigure I2C BIC.B #I2CN,&I2TCTL ; deactivate Repeat Mode MOV.B #DATA_BYTES,&I2CNTAT ; Read n bytes BIC.B #I2CTEX,&I2TCTL ; Read bytes BIS.B #I2CN,&I0CTL ; Recommended init procedure BIS.B #MST,&I0CTL ; Master mode //MOV #272,&Address ; Last node in network //Read sensor info from node X ReadNode MOV Address,&I2CSA CLR R6 MOV #DATA_BYTES,nBytes BIS.B #I2CST+I2CSTP,&I2TCTL ; Initiate transfer ReadByte MOV #0200h,&R10 ; Timeout for reception CALL #I2C_GET_BYTE ; Get byte CALL #USB_SEND ; Send it through USB //MOV.B R5,&DataPacket[R6] ; Save byte INC R6 DEC.B nBytes JNZ ReadByte //MOV #400,&R10 //CALL #DELAY </pre>
---	---

<pre> C:\Documents and Settings\Gerardo\My Documents\Work\SM (MIT)\Thesis\Code\Firmware\I2C_Master.s43 BIC.B #0h, I2CFlags JMP MainLoop SampleCode DEC Address CMP #257, Address JMP MainLoop ; not yet ; ; REFFLASH ; Updates firmware in all nodes ; ; ; BIT.B #04, fileFlag ; Are we reflashing one or all nodes? ; JC SingleDevice ; If not single device, broadcast code ; BIC.B #I2CEN, &I2CTCTL ; Reconfigure I2C ; BIC.B #XA, &U0CTL ; Reconfigure I2C ; BIC.B #I2CEN, &I2CTCTL ; Activate Repeat Mode ; BIC.B #I2CEN, &I2CTCTL ; Recommended init procedure ; MOV #0, &I2CSA ; Reflash all nodes ; CLR R6 ; JMP InitI2CTX SingleDevice ; BIC.B #I2CEN, &U0CTL ; Reconfigure I2C ; BIC.B #XA, &U0CTL ; Reconfigure I2C ; BIC.B #I2CEN, &I2CTCTL ; Activate Repeat Mode ; MOV #2, nBytes ; Recommended init procedure ; SUB R6 ; Decrease nBytes ; CLR R6 ; Read Address ; MOV USBuf(R6), R5 ; Broadcast Address ; MOV #2, R6 ; MOV nBytes, R7 ; InitI2CTX ; MOV nBytes, R7 ; ; Get number of bytes to transfer ; ; //Indicate a reflash to BootLoader ; BIC.B #NST, &U0CTL ; Master mode ; BIC.B #I2CSFT+I2CTX, &I2CTCTL ; Initiate transfer ; MOV.B #REFFLASH_INST, R5 ; Now indicate a reflash instruction ; CALL #I2C_SEND_BYTE ; Send instruction ; //Send code size to indicate length of transmission ; MOV nBytes, R5 ; Get code file size from memory ; CALL #I2C_SEND_BYTE ; Send low end of nBytes ; SWPB R5 ; Send High end of nBytes ; CALL #I2C_SEND_BYTE ; Send low end of nBytes ; ; //Send File! ; SendLoop ; MOV.B USBuf(R6), R5 ; Get byte from memory ; CALL #I2C_SEND_BYTE ; Send byte ; INC R6 ; Increment pointer ; MOV #0FFh, R5 ; WaitCk ; DEC R5 ; JZ #I2CSLOW, &I2CTCTL ; Is slave holding clock line low? ; JC WaitCk ; Yup, wait ; DEC R7 ; Decrease bytes to send </pre>	<pre> C:\Documents and Settings\Gerardo\My Documents\Work\SM (MIT)\Thesis\Code\Firmware\I2C_Master.s43 JNZ SendLoop ; Are we done? Stp MOV #0FFh, R5 BIS.B #I2CSFT, &I2CTCTL ; Issue STOP ChkSTP1 DEC R5 JZ EndReFlash BIT.B #I2CSFT, &I2CTCTL ; Check STP condition JNZ ChkSTP1 ; ; BIC.B #02, fileFlag ; File Processed! ; BIC.B #02, &P4OUT ; MOV #500h, R10 ; CALL #DELAY ; BIS.B #02, &P4OUT ; MOV #0, I2CFlags ; MOV #0, fileFlag ; MOV #0, fileStatus ; EndReFlash ; RET ; ; I2C_SEND_BYTE ; Sends a byte through I2C (byte in R5) ; ; MOV.B #0FFh, R10 ; Send timeout ; MOV.B R5, &I2CDBR ; Send byte ; WaitTX ; DEC R10 ; Nope ; JZ EndI2C_Send ; Enough tries? ; BIT.B #TXDDYIFG, &I2CIFG ; Done with transmission? ; JNC WaitTX ; Nope wait ; EndI2C_Send ; BIC.B #TXDDYIFG, &I2CIFG ; Clear flag ; RET ; ; I2C_GET_BYTE ; Sends a byte through I2C (byte in R5) ; ; BIT.B #RXDDYIFG, &I2CIFG ; Receive ready? ; JC GetByte ; Yep, get byte ; DEC R10 ; Nope ; JNZ I2C_GET_BYTE ; Enough tries? ; BIS.B #01h, I2CFlags ; Error receiving byte! ; RET ; GetByte ; MOV.B &I2CDBR, R5 ; Read I2C data ; BIC.B #RXDDYIFG, &I2CIFG ; Clear RX flag ; BIC.B #01h, I2CFlags ; Did we get something? ; RET ; ; I2C_RESET ; Sends a byte through I2C (byte in R5) ; ; BIC.B #0Ah, &P3SEL ; Deselect I2C pins ; TestSDA ; BIS.B #0Ah, &P3DIR ; Set as outputs ; BIS.B #02h, &P3OUT ; Bring SDA back up (Assert a 1) </pre>
---	---

```
BIC.B #02h, &PDIR
BIT.B #02h, &PIN
JC GenerateStop
;
BIC.B #08h, &P3OUT
BIC.B #08h, &P3OUT
BIC.B #08h, &P3OUT
JMP TestSDA

GenerateStop
BIS.B #08h, &P3DIR
BIS.B #08h, &P3OUT
BIC.B #02h, &P3SEL
RET

;
USB_GET ; Reads data from FTDI Chip
;
BIC.B #RxE_, &P2IFG ; Clear IFG
BIC.B #0FFh, &PDIR ; Set USB data port as input
BIC.B #RD_, &P2OUT ; Strobe RD line to read data
MOV.B &PIN, R5 ; Read data
BIS.B #RD_, &P2OUT ; Strobe RD line back
RET

;
USB_SEND ; Sends data to FTDI Chip
;
BIT.B #TxE_, &P2IN ; Is transfer buffer full?
JC ; Yes, wait
BIS.B #0FFh, &PDIR ; Set USB data port as output
BIS.B #WR_, &P2OUT ; Strobe write line
MOV.B R5, &P2OUT ; Echo data received
BIC.B #WR_, &P2OUT ; Strobe line down
RET

;
DELAY ; Delay function (3n*2 + 4n + delay-9)
;
PUSH R8
PUSH R9
MOV R10, R9
LoopDelay1
MOV R10, R8
LoopDelay2
DEC R8
JNZ LoopDelay2
DEC R9
JNZ LoopDelay1
POP R9
POP R8
RET

;-----
USB_TX_ISR ; USB Receive ISR
;-----
//Receive USB byte
CALL #USB_GET
//Echo byte to ack
CALL #USB_SEND
```

```
//THIS PART DECODES INSTRUCTIONS RECEIVED FROM USB PORT
DecodeInstructions
SUB.B #00Ch, R5
JMP EndUSB_TX_ISR
CMP.B #0FFh, R5
JGE EndUSB_TX_ISR
ADD R5, PC
JMP ReflashAll
JMP ResetBrain
JMP ResetSkin
JMP ExecuteSkinCode
JMP ReflashDev
JMP ResetDev
JMP StartSampling
JMP StopSampling
//Other instructions go here

//REFLASH_DEV / REFLASH_ALL INSTRUCTION
ReflashAll
MOV.B #01, fileFlag ; Indicate that data is on the line
JMP StoreByte
ReflashDev
MOV.B #05, fileFlag ; Indicate that data is on the line
StoreByte
CALL #USB_GET ; Get byte
CALL #USB_SEND ; Get pointer value
MOV USBBufPtr, R6 ; Store data
R6, USBBuf(R6) ; Increment pointer
INC ; Overflow?
CMP #MAX_CODE_SIZE, R6 ; No, store pointer value
JNZ StorePtr ; Overflowed pointer, reset
CLR R6 ; Indicate file size overflow
BIS.B #04h, fileFlag
StorePtr
MOV R6, USBBufPtr ; Store pointer
MOV R6, nbytes ; Store number of bytes
BIT.B #RxE_, &P2IN ; Is there more data to read?
JNC StoreByte ; Yep
XOR.B #03, fileFlag ; File waiting...
CLR USBBufPtr ; Clear pointer
CALL #REFLASH
RETI

//RESET BRAIN INSTRUCTION
ResetBrain
MOV.W #0, &WDCTL ; Write WDT with no password (RESET!)

//RESET SKIN/NOIR INSTRUCTION
ResetDev
ResetSkin
BIC.B #I2CEN,&U0CTL ; Reconfigure I2C
BIC.B #XA,&U0CTL ; Reconfigure I2C
BIC.B #I2CEN,&I2CCTL ; ACK
BIS.B #I2CEN,&U0CTL ; Recommended init procedure
MOV #0,&I2CSA ; RESET ALL NOISES!
MOV #1,&I2CNDAT
BIS.B #NST,&U0CTL ; Master mode
```

```
BIS.B #12GST+12GSTP+12CTRX, &12CTCTL ; Initiate transfer
MOV.B #RESET_SKIN_INST, R5 ; Indicate a refash instruction
CALL #I2C_SEND_BYTE ; Send instruction
RETI
```

//EXECUTE SKIN CODE INSTRUCTION

```
ExecuteskinCode
BIC.B #12CRN.&10CTL ; Reconfigure I2C
BIC.B #XA.&10CTL ; Reconfigure I2C
BIC.B #12CRM.&12CTCTL ; ACK
BIS.B #12CRN.&10CTL ; Recommended init procedure
MOV #0.&12CSA ; RESET ALL MODES!
MOV.B #1, &12NDMT ; Master mode
BIS.B #INST.&10CTL ; Master mode
BIS.B #12GST+12GSTP+12CTRX, &12CTCTL ; Initiate transfer
MOV.B #EXECUTE_CODE_INST, R5 ; Indicate a refash instruction
CALL #I2C_SEND_BYTE ; Send instruction
RETI
```

StartSampling

```
CLR R6
CALL #USB_GET ; Get byte
CALL #USB_SEND ; echo
MOV.B R5, Address(R6)
CALL #USB_GET ; Get byte
CALL #USB_SEND ; echo
R6
INC
MOV.B R5, Address(R6)
BIS.B #80h, I2CFlags
RETI
```

StopSampling

```
BIC.B #80h, I2CFlags
RETI
```

End_USB_TX_ISR

```
RETI
```

I2C_ISR: Common ISR for I2C Module

```
ADD #&12CIV, PC ; Add I2C offset vector
RETI ; No Interrupt
RETI ; Arbitration Lost
RETI ; No Acknowledge
RETI ; Own Address
RETI ; Register Access Ready
JMP RXRDY_ISR ; Receive Ready
RETI ; Transmit Ready
RETI ; General Call
RETI ; Start Condition
```

```
RXRDY_ISR
MOV.B #&12CDBR, R5 ; RX data in R5
BIC.B #LPM0, 0(SP) ; Clear LPM0
RETI
```

Interrupt Vectors Used MSP430x13x/4x/15x/16x

```
ORG 0xFFFF ; MSP430 RESET Vector
ORG 0xFFFF ;
ORG 0xFFFF ; P2 Interrupt vector
ORG 0xFFFF ; P2 Interrupt vector
ORG 0xFFFF ; I2C Interrupt vector
ORG 0xFFFF ;
ORG 0xFFFF ;
```

END

Appendix E

PC Code

```

1 //-----
2 //
3 // Copyright (C) Gerardo Barroeta, MIT Media Lab
4 //
5 //-----
6 //
7
8 #pragma once
9 #include <gl/gl.h>
10 #include <gl/glu.h>
11
12 typedef struct vertex_t
13 {
14     float x, y, z;
15 } vertex_t;
16
17 typedef struct vector_t
18 {
19     float x, y, z;
20 } vector_t;
21
22 typedef struct polygon_s
23 {
24     vertex_t v[3];
25 } polygon_t;
26
27
28 void normalize(vector_t *v);
29 void normal(vertex_t v[], vector_t *normal);
30
31 class CopengGLControl :
32 {
33 public:
34     /*****
35     ** PUBLIC MEMBERS **
36     *****/
37     // Timer
38     UINT_PTR m_unplimer;
39     CopengGLControl(void);
40 public:
41     ~CopengGLControl(void);
42 private:
43     /*****
44     ** PRIVATE MEMBERS **
45     *****/
46     // Window information
47     Copnd
48     HDC hdc;
49     HGLRC hrc;
50     int m_nPixelFormat;
51     int m_nRect;
52     Rect m_rect;
53     Rect m_oldWindow;
54     Rect m_rectOld;
55     float m_fRectX;
56     float m_fRectY;
57     float m_fRectZ;
58     float m_fRectX;
59     float m_fRectY;
60     float m_fRectZ;
61     float m_fPosX;
62     float m_fPosY;
63     float m_fPosZ;
64     float m_fZoom;
65     float m_XMatrix;
66     float m_YMatrix;
67     float m_Height[100][100];
68 }
69

```

```

68 public:
69     void oglCreate(GRect rect, CWnd parent);
70     void oglInitialize(void);
71     void oglDrawScene(void);
72     void setHeight(int x, int y, float height);
73     void setMatrixSize(int x, int y);
74     void setMatrixSize(int x, int y);
75     void public:
76     void afx_msg int OnCreate(LPCREATESTRUCT lpCreateStruct);
77     void afx_msg void OnPaint();
78     void afx_msg void OnTimer(CDC *pDC);
79     void afx_msg void OnDraw(CDC *pDC);
80     void afx_msg void OnWindowMove(UINT_PTR nHEvent);
81     void afx_msg void OnSize(UINT nType, int cx, int cy);
82     void afx_msg void OnMouseMove(UINT nFlags, CPoint point);
83     void public:
84     DECLARE_MESSAGE_MAP()
85     };
86 };
87

```



```

c:\Documents and Settings\Gerardo\My ... \SM (MT)\Thesis\Code\Example1\resource.h 1
1 //([NO_DEPENDENCIES])
2 // Microsoft Visual C++ generated include file.
3 // Used by USBtest.rc
4 //
5 #define IDM_ABOUTBOX 0x0010
6 #define IDD_ABOUTBOX 100
7 #define IDS_ABOUTBOX 101
8 #define IDD_USRTEST_DIALOG 102
9 #define IDR_MAINFRAME 128
10 #define IDC_BUTTON_SENDFILE 1004
11 #define IDC_SLIDER_WHITE_RATE 1006
12 #define IDC_EDIT_PORT_SELECTED 1014
13 #define IDC_EDIT_PORT_STATUS 1015
14 #define IDC_LIST1 1019
15 #define IDC_EDIT_NUM_REC'D 1021
16 #define IDC_BUTTON_CLEAR 1023
17 #define IDC_BUTTON_OPEN 1024
18 #define IDC_EDIT_ADDRESS 1025
19 #define IDC_EDIT_NAME_NUMBER 1026
20 #define IDC_RADIO_NAME_NUM 1027
21 #define IDC_RADIO_DEVNO 1028
22 #define IDC_RADIO_LIST 1029
23 #define IDC_BUTTON_LIST 1030
24 #define IDC_LIST2 1032
25 #define IDC_BUTTON_RESET 1037
26 #define IDC_BUTTON_RUN_NODES 1038
27 #define IDC_BUTTON_RS 1039
28 #define IDC_OPENGL 1041
29 #define IDC_RADIO_SINGLE_NODE 1043
30 #define IDC_RADIO_ALL_NODES 1044
31 #define IDC_BUTTON_START 1046
32 #define IDC_BUTTON_STOP 1047
33 #define IDC_EDIT1 1061
34 #define IDC_EDITSPIN 1061
35 #define IDC_SPIN 1063
36
37 // Next default values for new objects
38 //
39 #ifdef APSTUDIO_INVOKED
40 #ifndef APSTUDIO_READONLY_SYMBOLS
41 #define _APS_NEXT_RESOURCE_VALUE 130
42 #define _APS_NEXT_COMMAND_VALUE 32771
43 #define _APS_NEXT_CONTROL_VALUE 1064
44 #define _APS_NEXT_SYMED_VALUE 101
45 #endif
46 #endif
47

```

```

c:\Documents and Settings\GerardoWy...\SM (MT)\Thesis\Code\Example1\Stdafx.h 1
1 // stdafx.h : include file for standard system include files.
2 // or project specific include files that are used frequently, but
3 // are changed infrequently
4 //
5
6 #if !defined(APX_STDAFX_H_07909308_D75E_11D4_A644_93781B97CC41_INCLUDED_)
7 #define APX_STDAFX_H_07909308_D75E_11D4_A644_93781B97CC41_INCLUDED_
8
9 #if _MSC_VER > 1000
10 #pragma once
11 #endif // _MSC_VER > 1000
12
13 #define VC_EXTRALEAN // Exclude rarely-used stuff from Windows headers
14
15 #include <afxwin.h> // MFC core and standard components
16 #include <afxext.h> // MFC extensions
17 #include <afxdisp.h> // MFC Automation classes
18 #include <afxdtctl.h> // MFC support for Internet Explorer 4 Common Controls
19 #ifndef _AFX_NO_AFXCMN_SUPPORT
20 #include <afxcmn.h> // MFC support for Windows Common Controls
21 #endif // _AFX_NO_AFXCMN_SUPPORT
22
23
24 //{{AFX_INSERT_LOCATION}}
25 // Microsoft Visual C++ will insert additional declarations immediately before the
26 // previous line.
27 #endif // !defined(APX_STDAFX_H_07909308_D75E_11D4_A644_93781B97CC41_INCLUDED_)
28

```

```

c:\Documents and Settings\Gerardo\My ... \SM (MIT)\Thesis\Code\Example1\USBtest.h 1
1 //-----
2 //
3 // Copyright (C) Gerardo Barroeta, MIT Media Lab
4 //
5 //-----
6 //
7
8 // USBtest.h : main header file for the USBTEST application
9 //
10
11 #if !defined(AFX_USBTEST_H__07909304_D75E_11D4_A644_93781B97CC41__INCLUDED_)
12 #define AFX_USBTEST_H__07909304_D75E_11D4_A644_93781B97CC41__INCLUDED_
13
14 #if _MSC_VER > 1000
15 #pragma once
16 #endif // _MSC_VER > 1000
17
18 #ifndef _AFXWIN_H_
19 #error include 'stdafx.h' before including this file for PCH
20 #endif
21
22 #include "resource.h" // main symbols
23
24 ////////////////////////////////////////////////////
25 // CUSBTestApp:
26 // See USBtest.cpp for the implementation of this class
27 //
28
29 class CUSBTestApp : public CWinApp
30 {
31 public:
32     CUSBTestApp();
33
34 // Overrides
35 // ClassWizard generated virtual function overrides
36 //{{AFX_VIRTUAL(CUSBTestApp)
37 public:
38     virtual BOOL InitInstance();
39     //}}AFX_VIRTUAL
40
41 // Implementation
42
43 //{{AFX_MSG(CUSBTestApp)
44 // NOTE - the ClassWizard will add and remove member functions here.
45 // DO NOT EDIT what you see in these blocks of generated code !
46 //}}AFX_MSG
47     DECLARE_MESSAGE_MAP()
48 };
49
50 ////////////////////////////////////////////////////
51 //{{AFX_INSERT_LOCATION}}
52 // Microsoft Visual C++ will insert additional declarations immediately before the
53 // previous line.
54
55 #endif // !defined(AFX_USBTEST_H__07909304_D75E_11D4_A644_93781B97CC41__INCLUDED_)
56

```

```

c:\Documents and Settings\Gerardo\My ... (MIT)\Thesis\Code\Example\USSTestDlg.h 1
1 //-----
2 //
3 // Copyright (C) Gerardo Barroeta, MIT Media Lab
4 //
5 //-----
6 //
7 // USSTestDlg.h : header file
8 //
9
10 #if !definedAFX_USSTESTDLG_H_07909306_D75E_11D4_A644_93781B97CC41_INCLUDED_
11 #define AFX_USSTESTDLG_H_07909306_D75E_11D4_A644_93781B97CC41_INCLUDED_
12 #define GUID_CLASS_USB_DEVICE GUID_DEVINTERFACE_USB_DEVICE
13
14 #if _MSC_VER > 1000
15 #pragma once
16 #endif // _MSC_VER > 1000
17
18 #include "fd2xx.h"
19 #include "OpenSerialControl.h"
20 #include "Serial.h"
21 #include <str.h>
22 #include <intguid.h>
23 #include "afxwin.h"
24 #include "afxcmn.h"
25
26 UINT ThreadProc(LPVOID param);
27 const int OFF = 101;
28 const int ON = 101;
29 static GUID GUID_DEVINTERFACE_USB_DEVICE = { 0x5DC0B10L, 0x6530, 0x11D2, { 0x90, 0x1F,
    , 0x00, 0xC0, 0x4F, 0xB9, 0x51, 0x2D } };
30
31 // CUSSTestDlg dialog
32 class CUSSTestDlg : public CDialog
33 {
34 // Construction
35 public:
36     CUSSTestDlg(CWnd* pParent = NULL); // standard constructor
37     CUSSTestDlg(CUSSTestDlg* pOther): {} // copy constructor
38     FT_STATUS CUSSTestDlg::OpenBy(){}
39
40 // Dialog Data
41     ///{AFX_DATA(CUSSTestDlg)
42     enum { IDD = IDD_USSTEST_DIALOG };
43     CRect m_RectBox;
44     long m_NunRecd;ved;
45     int m_SerDesc;
46     int m_Nodes;
47     CString m_128status;
48     CString m_NameMbr;
49     CString m_PortStatus;
50     CString m_PortStatus;
51     COpenSerialControl m_ooglWindow;
52     CString m_EditSpin;
53     CSpinButtonCtrl m_Spin;
54
55     ///{AFX_DATA
56     // ClassWizard generated virtual function overrides
57 public:
58     afx_msg void OnVntItemchangedList2(NMHDR *pNMHDR, LRESULT *pResult);
59     afx_msg void OnClose();
60     afx_msg void OnEnable(BOOL bEnable);
61     afx_msg void OnSerialControl(NMHDR *pNMHDR, LRESULT *pResult);
62     FT_STATUS ReadLPVOID(DWORD, LPDWORD);
63     FT_STATUS ReadLPVOID(DWORD, LPDWORD);
64     FT_STATUS GetQueueStatus(LPWORD);
65     FT_STATUS Purge(ULONG);
66

```

```

c:\Documents and Settings\Gerardo\My ... (MIT)\Thesis\Code\Example\USSTestDlg.h 2
67 // Implementation, typedefs for DLL functions
68 #pragma:
69 HICON m_hIcon;
70 HMODULE m_hModule;
71 FT_HANDLE m_ftHandle;
72 void LoadDLL();
73 void RegisterNotification(HDEVNOTIFY *pDevNotify);
74 void UnregisterNotification(HDEVNOTIFY *pDevNotify);
75
76 typedef FT_STATUS (WINAPI *PfttOpen)(PVOID, FT_HANDLE *);
77 PfttOpen m_POpen;
78 FT_STATUS Open(PVOID);
79
80 typedef FT_STATUS (WINAPI *PfttOpenEx)(PVOID, DWORD, FT_HANDLE *);
81 PfttOpenEx m_POpenEx;
82 FT_STATUS OpenEx(PVOID, DWORD);
83
84 typedef FT_STATUS (MINAPI *PfttListDevices)(PVOID, PVOID, DWORD);
85 PfttListDevices m_ListDevices;
86 FT_STATUS ListDevices(PVOID, PVOID, DWORD);
87
88 typedef FT_STATUS (MINAPI *PfttClose)(FT_HANDLE);
89 PfttClose m_PClose;
90 FT_STATUS Close();
91
92 typedef FT_STATUS (MINAPI *PfttRead)(FT_HANDLE, LPVOID, DWORD, LPDWORD);
93 PfttRead m_PRead;
94 FT_STATUS Read(LPVOID, DWORD, LPDWORD);
95
96 typedef FT_STATUS (MINAPI *PfttWrite)(FT_HANDLE, LPVOID, DWORD, LPDWORD);
97 PfttWrite m_PWrite;
98 FT_STATUS Write(LPVOID, DWORD, LPDWORD);
99
100 typedef FT_STATUS (MINAPI *PfttResetDevice)(FT_HANDLE);
101 PfttResetDevice m_PResetDevice;
102 FT_STATUS ResetDevice();
103
104 typedef FT_STATUS (MINAPI *PfttPurge)(FT_HANDLE, ULONG);
105 PfttPurge m_PPurge;
106 FT_STATUS Purge(ULONG);
107
108 typedef FT_STATUS (MINAPI *PfttSetTimeouts)(FT_HANDLE, ULONG, ULONG);
109 PfttSetTimeouts m_PSetTimeouts;
110 FT_STATUS SetTimeouts(ULONG, ULONG);
111
112 typedef FT_STATUS (MINAPI *PfttGetQueueStatus)(FT_HANDLE, LPDWORD);
113 PfttGetQueueStatus m_PGetQueueStatus;
114 FT_STATUS GetQueueStatus(LPWORD);
115
116 // Generated message map functions
117 virtual BOOL OnInitDialog();
118 afx_msg void OnSysCommand(UINT nID, LPARAM lParam);
119 afx_msg void OnPaint();
120 afx_msg void OnKeyDown();
121 afx_msg void OnKeyUp();
122 afx_msg void OnButtonSendFile();
123 afx_msg void OnClose();
124 afx_msg void OnButtonClear();
125 afx_msg void OnTimer(UINT nIDEvent);
126 afx_msg void OnButtonOpen();
127 afx_msg void OnButtonClose();
128 afx_msg void OnRadioAllNodes();
129 afx_msg void OnRadioObvno();
130 afx_msg void OnRadioAllNodes();
131 afx_msg void OnRadioSingleNode();
132 afx_msg void OnRadioSingleNode();
133 afx_msg void OnRadioSingleNode();

```

```
134 afx_msg void OnChangeEditAddress();
135 afx_msg void OnButtonStart();
136 afx_msg void OnSelChangeList();
137 afx_msg void OnButtonReset();
138 afx_msg void OnButtonRe();
139 afx_msg void OnButtonRunNode();
140 afx_msg void OnButtonStart();
141 afx_msg void OnButtonStop();
142 //}}AFX_MSG
143 DECLARE_MESSAGE_MAP()
144
145 //}}AFX_VIRTUAL(CUSBTestDlg)
146 protected:
147 virtual void DoDataExchange(CDataExchange* pDX); // DDX/DDV support
148 virtual BOOL OnCommand(WPARAM wParam, LPARAM lParam);
149 //}}AFX_VIRTUAL
150 };
151
152 //}}AFX_INSERT_LOCATION}}
153 // Microsoft Visual C++ will insert additional declarations immediately before the
154 // previous line.
155 #endif // !defined(AFX_USBTESTDLG_H__07909306_D75E_11D4_A644_93781B97CC41__INCLUDED_)
156
```

```

1 //-----
2 //
3 // Copyright (C) Gerardo Barroeta, MIT Media Lab
4 //
5 //-----
6 //
7 #include "stdafx.h"
8 #include "OpenGLControl.h"
9 #include <math.h> // sqrt
10
11 OpenGLControl::OpenGLControl(void)
12 {
13     m_fPosX = 0.0f; // X position of model in camera view
14     m_fPosY = -10.0f; // Y position of model in camera view
15     m_fZoom = 80.0f; // Zoom on model in camera view
16     m_fRotX = -75.0f; // Rotation on model in camera view
17     m_fRotZ = 45.0f; // Rotation on model in camera view
18     m_nMatrix = 8;
19     m_nMatrix = 8;
20     for (int j=0; j<100; j++)
21     {
22         for (int k=0; k<100; k++)
23         {
24             //m_Height[j][k] = (float)j*(float)k;
25             m_Height[j][k] = 0;
26         }
27     }
28 }
29
30 OpenGLControl::~OpenGLControl(void)
31 {}
32
33 void OpenGLControl::oglCreate(CRect rect, CWnd *parent)
34 {
35     CString className = AfxRegisterWndClass(CS_HREDRAW |
36     CS_VREDRAW | CS_WNDCLASS, NULL,
37     (HBRUSH)GetStockObject(BLACK_BRUSH), NULL);
38
39     CreateEx(0, className, "OpenGL", WS_CHILD | WS_VISIBLE |
40     WS_CLIPCHILDREN | WS_CLIPSIBLINGS | WS_CLIPCHILDREN, rect, parent, 0);
41
42     // Set initial variables' values
43     m_oldWindow = rect;
44     m_originalRect = rect;
45
46     hWnd = parent;
47 }
48
49 BEGIN_MESSAGE_MAP(COpenGLControl, CWnd)
50 ON_WM_PAINT()
51 ON_WM_CREATE()
52 ON_WM_SIZE()
53 ON_WM_MOUSEMOVE()
54 ON_WM_MOUSEMOVE()
55 ON_WM_MOUSEMOVE()
56 END_MESSAGE_MAP()
57
58 int COpenGLControl::OnCreate(LPCREATESTRUCT lpCreateStruct)
59 {
60     if (CWnd::OnCreate(lpCreateStruct) == -1)
61         return -1;
62
63     // TODO: Add your specialized creation code here
64     oglInitialize();
65
66     return 0;
67 }

```

```

68 }
69
70 void COpenGLControl::OnPaint()
71 {
72     //CPaintDC dc(this); // device context for painting
73     // TODO: Add your message handler code here
74     // Paint all the controls. OnPaint() for painting messages
75     // Paint all the controls. OnPaint() for painting messages
76     ValidateRect(NULL);
77 }
78
79 void COpenGLControl::OnDraw(CDC *pDC)
80 {
81     // TODO: Camera controls.
82     glLoadIdentity();
83     glTranslatef(0.0f, 0.0f, -m_fZoom);
84     glRotatef(m_fPosX, m_fPosX, m_fPosY, 0.0f);
85     glRotatef(m_fRotX, 1.0f, 0.0f, 0.0f);
86     glRotatef(m_fRotZ, 0.0f, 0.0f, 1.0f);
87 }
88
89 void COpenGLControl::cgInitialize(void)
90 {
91     // Initial Setup:
92     static PIXELFORMATDESCRIPTOR pfd =
93     {
94         sizeof(PIXELFORMATDESCRIPTOR),
95         1,
96         PFD_DRAW_TO_WINDOW | PFD_SUPPORT_OPENGL | PFD_DOUBLEBUFFER,
97         TRUE,
98         32, //bit depth
99         0, 0, 0, 0, 0, 0, 0, 0,
100         16, // z-buffer depth
101         0, 0, 0, 0, 0, 0,
102         0, 0, 0, 0, 0, 0,
103     };
104
105     // Get device context only once.
106     hdc = GetDC() -> m_hDC;
107
108     // Pixel format.
109     ChoosePixelFormat(hdc, pfd);
110     SetPixelFormat(hdc, m_hPixelFormat, pfd);
111
112     // Create the OpenGL Rendering Context.
113     hrc = wglCreateContext(hdc);
114     wglMakeCurrent(hdc, hrc);
115
116     // Basic Setup:
117     // Set color to use when clearing the background.
118     glClearColor(0.0f, 0.0f, 0.0f, 1.0f);
119     glClearDepth(1.0f);
120
121     // Turn on backface culling
122     glFrontFace(GL_CW);
123     glCullFace(GL_BACK);
124
125     // Turn on depth testing
126     glEnable(GL_DEPTH_TEST);
127     glDepthFunc(GL_LESS);
128     glHint(GL_PERSPECTIVE_CORRECTION_HINT, GL_NICEST);
129     // Perspective Calculations
130
131     // Create light components
132     GLfloat ambientLight[] = { 0.0f, 0.0f, 0.0f, 1.0f };
133     GLfloat diffuseLight[] = { 0.2f, 0.2f, 0.2f, 1.0f };
134

```

```
134 GLfloat specularLight0[] = { 0.2f, 0.2f, 0.2f, 1.0f };
135 CreateLightComponents
136 GLfloat ambientLight[] = { 0.0f, 0.0f, 0.0f, 1.0f };
137 GLfloat diffuseLight[] = { 0.2f, 0.2f, 0.2f, 1.0f };
138 GLfloat specularLight[] = { 0.2f, 0.2f, 0.2f, 1.0f };
139 // Create light components
140 CreateLightComponents
141 GLfloat ambientLight2[] = { 0.0f, 0.0f, 0.0f, 1.0f };
142 GLfloat diffuseLight2[] = { 0.2f, 0.2f, 0.2f, 1.0f };
143 GLfloat specularLight2[] = { 0.2f, 0.2f, 0.2f, 1.0f };
144
145 GLfloat global_ambient[] = { 0.999f, 0.999f, 0.999f, 1.0f };
146
147 GLfloatModelfv(GL_LIGHT_MODEL_AMBIENT, global_ambient);
148
149 // Assign created components to GL_LIGHT0
150 glLightfv(GL_LIGHT0, GL_AMBIENT, ambientLight0);
151 glLightfv(GL_LIGHT0, GL_DIFFUSE, diffuseLight0);
152 glLightfv(GL_LIGHT0, GL_SPECULAR, specularLight0);
153 // Assign created components to GL_LIGHT1
154 glLightfv(GL_LIGHT1, GL_AMBIENT, ambientLight1);
155 glLightfv(GL_LIGHT1, GL_DIFFUSE, diffuseLight1);
156 glLightfv(GL_LIGHT1, GL_SPECULAR, specularLight1);
157 // Assign created components to GL_LIGHT2
158 glLightfv(GL_LIGHT2, GL_AMBIENT, ambientLight2);
159 glLightfv(GL_LIGHT2, GL_DIFFUSE, diffuseLight2);
160 glLightfv(GL_LIGHT2, GL_SPECULAR, specularLight2);
161
162 GLfloat position0[] = { 0, 200, 0, 1.0f };
163 GLfloat position1[] = { 50, 200, 0, 1.0f };
164 GLfloat position2[] = { -50, 200, 0, 1.0f };
165
166 // Assign light positions
167 glLightfv(GL_LIGHT0, GL_POSITION, position0);
168 glLightfv(GL_LIGHT1, GL_POSITION, position1);
169 glLightfv(GL_LIGHT2, GL_POSITION, position2);
170
171 glShadeModel(GL_SMOOTH);
172 glEnable(GL_Line_SMOOTH);
173
174 // Blending Function For Translucency Based On Source Alpha Value ( NEW )
175 //glBlendFunc(GL_SRC_ALPHA, GL_ONE);
176 //glEnable(GL_BLEND);
177 //glDisable(GL_DEPTH_TEST);
178
179 //Set up lighting model
180 glEnable(GL_LIGHTING);
181 glEnable(GL_LIGHT0);
182 glEnable(GL_LIGHT1);
183 glEnable(GL_LIGHT2);
184 // Send draw request
185 OnDraw(NULL);
186 }
187
188 void OpenGLControl::OnTimer(UINT nIDEvent)
189 {
190     switch (nIDEvent)
191     {
192     case 1:
193     {
194         // Clear color and depth buffer bits
195         glClear(GL_COLOR_BUFFER_BIT | GL_DEPTH_BUFFER_BIT);
196
197         // Draw OpenGL scene
198         oglDrawScene();
199
200         // Swap buffers
```

```
201 SwapBuffers(hdc);
202
203     break;
204 }
205
206 default:
207     break;
208 }
209
210 CWnd::OnTimer(nIDEvent);
211 }
212
213 void OpenGLControl::OnSize(UINT nType, int cx, int cy)
214 {
215     CWnd::OnSize(nType, cx, cy);
216
217     if (0 >= cx || 0 >= cy || nType == SIZE_MINIMIZED) return;
218
219     // Map the OpenGL coordinates.
220     glViewport(0, 0, cx, cy);
221
222     // Projection view
223     GLfloatModel(GL_PROJECTION);
224
225     glLoadIdentity();
226
227     // Set our current view perspective
228     gluPerspective(35.0f, (float)cx / (float)cy, 0.01f, 2000.0f);
229
230     // Model view
231     GLfloatModel(GL_MODELVIEW);
232
233     void OpenGLControl::oglDrawScene(void)
234 {
235     // Filled Mode
236     glPolygonMode(GL_FRONT_AND_BACK, GL_FILL);
237     glEnable(GL_DEPTH_TEST);
238     glEnable(GL_COLOR_MATERIAL);
239
240     //Set up material properties
241     float red=1.0f, green=0.0f, blue=0.0f, alpha=1.0f;
242     float mcolor[] = { red, green, blue, alpha };
243     GLfloat material[] = { GL_FRONT, GL_AMBIENT_AND_DIFFUSE, mcolor };
244     glFrontFace(GL_CW);
245     glColor3f(red, green, blue);
246
247     //Specular highlights
248     GLfloat specularReflection[] = { 0.4f, 0.4f, 0.4f, 1.0f };
249     GLfloat materialfv(GL_FRONT, GL_SPECULAR, specularReflection);
250
251     polygon_t face;
252     GLfloat a=-(3*M_XMatrix/2-1), b, offset;
253     vector_t vecNormal = { 0.0f, 0.0f, 0.0f };
254     for (int i=0; i<m_XMatrix; i++)
255     {
256         b=-(3*M_YMatrix/2-1);
257         for (int j=0; j<m_YMatrix; j++)
258         {
259             glBegin(GL_QUADS);
260             // Top Side
261             face.v[0].x=a-1.0f+a;
262             face.v[0].y=b-1.0f+b;
263             face.v[1].x=a-2.0f;
264             face.v[1].y=a-1.0f+a;
265             face.v[2].x=a-1.0f+a;
266             face.v[2].y=b-1.0f+b;
267             face.v[3].x=a;
268             face.v[3].y=b;
269             glEnd();
270         }
271     }
272 }
```

```

269 face.v[0].x=-1.0f+a;
270 face.v[0].y=1.0f+b;
271 face.v[0].z=0;
272 //Calculate normal vector
273 normal(face.v, &vecNormal);
274 //Paint the polygon
275 glVertex3f(1.0f+a, 1.0f+b, m_Height[i][j]);
276 glVertex3f(1.0f+a, 1.0f+b, 0.0f);
277 glVertex3f(-1.0f+a, 1.0f+b, 0.0f);
278 glVertex3f(-1.0f+a, 1.0f+b, m_Height[i][j]);
279 glNormal3f(face.v[0].x + vecNormal.x, face.v[0].y + vecNormal.y, face.z + vecNormal.z);
280
281 // Bottom Side
282 face.v[0].x=-1.0f+a;
283 face.v[0].y=-1.0f+b;
284 face.v[0].z=0;
285 face.v[1].x=1.0f+a;
286 face.v[1].y=1.0f+b;
287 face.v[1].z=0;
288 face.v[2].x=1.0f+a;
289 face.v[2].y=-1.0f+b;
290 face.v[2].z=2.0f;
291 //Calculate normal vector
292 normal(face.v, &vecNormal);
293 //Paint the polygon
294 glVertex3f(-1.0f+a, -1.0f+b, 0.0f);
295 glVertex3f(1.0f+a, -1.0f+b, 0.0f);
296 glVertex3f(1.0f+a, -1.0f+b, m_Height[i][j]);
297 glVertex3f(-1.0f+a, -1.0f+b, m_Height[i][j]);
298 glNormal3f(face.v[0].x + vecNormal.x, face.v[0].y + vecNormal.y, face.z + vecNormal.z);
299
300 // Front Side
301 face.v[0].x=1.0f+a;
302 face.v[0].y=1.0f+b;
303 face.v[0].z=2.0f;
304 face.v[1].x=1.0f+a;
305 face.v[1].y=1.0f+b;
306 face.v[1].z=2;
307 face.v[2].x=-1.0f+a;
308 face.v[2].y=-1.0f+b;
309 face.v[2].z=2.0f;
310 //Calculate normal vector
311 normal(face.v, &vecNormal);
312 //Paint the polygon
313 glVertex3f(1.0f+a, 1.0f+b, 1.0f+b, m_Height[i][j]);
314 glVertex3f(-1.0f+a, 1.0f+b, m_Height[i][j]);
315 glVertex3f(-1.0f+a, -1.0f+b, m_Height[i][j]);
316 glNormal3f(face.v[0].x + vecNormal.x, face.v[0].y + vecNormal.y, face.z + vecNormal.z);
317
318 // Back Side
319 face.v[0].x=-1.0f+a;
320 face.v[0].y=1.0f+b;
321 face.v[0].z=0;
322 face.v[1].x=-1.0f+a;
323 face.v[1].y=1.0f+b;
324 face.v[1].z=0;
325 face.v[2].x=1.0f+a;
326 face.v[2].y=1.0f+b;
327 face.v[2].z=0;
328 //Calculate normal vector
329 normal(face.v, &vecNormal);
330 //Paint the polygon
331 glVertex3f(-1.0f+a, -1.0f+b, 0.0f);

```

```

332 glVertex3f(-1.0f+a, 1.0f+b, 0.0f);
333 glVertex3f(1.0f+a, 1.0f+b, 0.0f);
334 glVertex3f(1.0f+a, -1.0f+b, 0.0f);
335 glNormal3f(face.v[0].x + vecNormal.x, face.v[0].y + vecNormal.y, face.z + vecNormal.z);
336
337 // Left Side
338 face.v[0].x=-1.0f+a;
339 face.v[0].y=-1.0f+b;
340 face.v[0].z=0;
341 face.v[1].x=-1.0f+a;
342 face.v[1].y=-1.0f+b;
343 face.v[1].z=2.0f;
344 face.v[2].x=1.0f+a;
345 face.v[2].y=1.0f+b;
346 face.v[2].z=2.0f;
347 //Calculate normal vector
348 normal(face.v, &vecNormal);
349 //Paint the polygon
350 glVertex3f(-1.0f+a, -1.0f+b, 0.0f);
351 glVertex3f(-1.0f+a, -1.0f+b, m_Height[i][j]);
352 glVertex3f(1.0f+a, -1.0f+b, m_Height[i][j]);
353 glVertex3f(-1.0f+a, 1.0f+b, 0.0f);
354 glNormal3f(face.v[0].x + vecNormal.x, face.v[0].y + vecNormal.y, face.z + vecNormal.z);
355
356 // Right Side
357 face.v[0].x=1.0f+a;
358 face.v[0].y=1.0f+b;
359 face.v[0].z=2.0f;
360 face.v[1].x=1.0f+a;
361 face.v[1].y=1.0f+b;
362 face.v[1].z=2.0f;
363 face.v[2].x=1.0f+a;
364 face.v[2].y=-1.0f+b;
365 face.v[2].z=0;
366 //Calculate normal vector
367 normal(face.v, &vecNormal);
368 //Paint the polygon
369 glVertex3f(1.0f+a, 1.0f+b, m_Height[i][j]);
370 glVertex3f(1.0f+a, -1.0f+b, m_Height[i][j]);
371 glVertex3f(1.0f+a, -1.0f+b, 0.0f);
372 glVertex3f(1.0f+a, 1.0f+b, 0.0f);
373 glNormal3f(face.v[0].x + vecNormal.x, face.v[0].y + vecNormal.y, face.z + vecNormal.z);
374 glEnd();
375
376 b+=3;
377 red -= 1/(m_YMatrix*m_XMatrix);
378 //Change the color
379 glColor3f(red, green, blue);
380 }
381 a++;
382 blue += 5/(m_YMatrix*m_XMatrix);
383 }
384 a=(3*m_XMatrix/2);
385 //Calculate reflection2[] = { 0.0f, 0.0f, 0.0f, 0.0f, 1.0f };
386 GLfloat reflection2[] = { 0.0f, 0.0f, 0.0f, 0.0f, 1.0f };
387 glMaterialfv(GL_FRONT_AND_BACK, GL_SPECULAR, &reflection2);
388
389 glBegin(GL_QUADS);
390 glColor4f(0.2f, 0.2f, 0.2f, 0.5f);
391 face.v[0].x=-1.0f;
392 face.v[0].y=-1.0f;
393 face.v[0].z=-1.0f;
394 face.v[1].x=a;
395 face.v[1].y=a+1.0f;
396 face.v[1].z=-1.0f;

```



```

396 face.v[2].x=a+1.0f;
397 face.v[2].z=a+2.0f;
398 face.v[2].z=a+2.0f;
399 //Calculate normal vector
400 normal(face.v, &vecNormal);
401 glVertex3f(-a-1.0f, a+1.0f, -1.0f);
402 glVertex3f(a, a+1.0f, -1.0f);
403 glVertex3f(-a-1.0f, 2.0f, 0);
404 glVertex3f(-a-1.0f, a+1.0f, 2.0f*a);
405 glNormal3f(face.v[0].x + vecNormal.x, face.v[0].y + vecNormal.y, face.v[0].z +
vecNormal.z);
406
407 face.v[0].x=a-1.0f;
408 face.v[0].y=a-1.0f;
409 face.v[0].z=-1.0f;
410 face.v[1].z=-a-1.0f;
411 face.v[1].y=a;
412 face.v[1].z=-1.0f;
413 face.v[2].x=a-1.0f;
414 face.v[2].z=-1.0f;
415 face.v[2].z=2.0f*a;
416 //Calculate normal vector
417 normal(face.v, &vecNormal);
418 glVertex3f(-a-1.0f, a+1.0f, -1.0f);
419 glVertex3f(-a-1.0f, -a, -1.0f);
420 glVertex3f(-a-1.0f, a+1.0f, 2.0f*a);
421 glNormal3f(face.v[0].x + vecNormal.x, face.v[0].y + vecNormal.y, face.v[0].z +
vecNormal.z);
422
423 face.v[0].x=a-1.0f;
424 face.v[0].y=a-1.0f;
425 face.v[0].z=-1.0f;
426 face.v[1].x=a;
427 face.v[1].y=a+1.0f;
428 face.v[1].z=-1.0f;
429 face.v[2].x=a;
430 face.v[2].z=-1.0f;
431 face.v[2].z=-1.0f;
432 face.v[2].z=-1.0f;
433 //Calculate normal vector
434 normal(face.v, &vecNormal);
435 glVertex3f(-a-1.0f, a+1.0f, -1);
436 glVertex3f(a, a+1.0f, -1);
437 glVertex3f(-a-1.0f, -a, -1);
438 glNormal3f(face.v[0].x + vecNormal.x, face.v[0].y + vecNormal.y, face.v[0].z +
vecNormal.z);
439
440 glEnd();
441
442 glLineWidth(1.0f);
443 offset = 0.9;
444 glBegin(GL_LINES);
445 glColor3f(0.0f, 1.0f, 0.0f);
446 glVertex3f(-a+offset, a+offset, -1);
447 glVertex3f(-a+offset, -a, -1);
448 glVertex3f(-a+offset, a+offset, -1);
449 glVertex3f(-a+offset, -a+offset, -1);
450 glVertex3f(-a+offset, a+offset, -1);
451 glVertex3f(-a+offset, a+offset, 2*a);
452 glEnd();
453
454 void COpenGLControl::OnMouseMove(UINT nFlags, CPoint point)
455 {
456     int diffX = (int)(point.x - m_flastX);
457     int diffY = (int)(point.y - m_flastY);
458     m_flastX = (float)point.x;

```

```

460 m_flastY = (float)point.y;
461
462 // Left mouse button
463 if (nFlags & MK_LBUTTON)
464 {
465     m_fRotX += (float)0.5f * diffY;
466     m_fRotZ += (float)0.5f * diffX;
467     if ((m_fRotX > 360.0f) || (m_fRotX < -360.0f))
468     {
469         m_fRotX = 0.0f;
470     }
471
472     m_fRotZ += (float)0.5f * diffY;
473     if ((m_fRotZ > 360.0f) || (m_fRotZ < -360.0f))
474     {
475         m_fRotZ = 0.0f;
476     }
477
478     // Right mouse button
479     else if (nFlags & MK_RBUTTON)
480     {
481         m_fZoom -= (float)0.1f * diffY;
482         m_fZoom = (float)0.1f * diffY;
483         m_fZoom = (float)0.1f * diffY;
484         m_fZoom = (float)0.1f * diffY;
485         m_fZoom = (float)0.1f * diffY;
486         // Middle mouse button
487         else if (nFlags & MK_MBUTTON)
488         {
489             m_fPeakX += (float)0.05f * diffX;
490             m_fPeakY -= (float)0.05f * diffY;
491             m_fPeakX = (float)0.05f * diffX;
492             m_fPeakY = (float)0.05f * diffY;
493             OnDraw(NULL);
494
495             CWnd::OnMouseMove(nFlags, point);
496         }
497
498         // On Mouse Move
499         OnDraw(NULL);
500
501 void COpenGLControl::setHeight(int x, int y, float height)
502 {
503     m_Height[x][y] = height;
504     m_Height[x][y] = height;
505 void COpenGLControl::setMatrixSize(int x, int y)
506 {
507     m_XMatrix=(float)x;
508     m_YMatrix=(float)y;
509     m_XMatrix=(float)y;
510 void normalize (vector_t *v)
511 {
512     // calculate the length of the vector
513     float len = (float)(sqrt((v->x * v->x) + (v->y * v->y) + (v->z * v->z)));
514     // avoid division by 0
515     if (len > 0.0f)
516     {
517         len = 1.0f;
518     }
519     // reduce to unit size
520     v->x /= len;
521     v->y /= len;
522     v->z /= len;
523
524 void normal (vertex_t v[3], vector_t *normal)
525 {
526

```

```
527 vector_t a, b;  
528 // calculate the vectors A and B  
529 // note that v[3] is defined with counterclockwise winding in mind  
530 // a  
531 a.x = v[0].x - v[1].x;  
532 a.y = v[0].y - v[1].y;  
533 a.z = v[0].z - v[1].z;  
534 // b  
535 b.x = v[1].x - v[2].x;  
536 b.y = v[1].y - v[2].y;  
537 b.z = v[1].z - v[2].z;  
538  
539 // calculate the cross product and place the resulting vector  
540 // into the address specified by vector_t *normal  
541 normal->x = (a.y * b.z) - (a.z * b.y);  
542 normal->y = (a.z * b.x) - (a.x * b.z);  
543 normal->z = (a.x * b.y) - (a.y * b.x);  
544 // normalize  
545 normalize(normal);  
546 }  
547  
548 }  
549
```

```

1 c:\Documents and Settings\GerardoWy ... \SM (MIT)\Thesis\Code\Example\USBtest.cpp 1
2 //-----
3 // Copyright (C) Gerardo Barroeta, MIT Media Lab
4 //
5 //-----
6 // USBtest.cpp : Defines the class behaviors for the application.
7 //
8 #include "stdafx.h"
9 #include "USBtest.h"
10 #include "USBtestDlg.h"
11 #ifdef _DEBUG
12 #define _AFXDBG_NEW
13 #define _AFXDBG_NEW
14 static char THIS_FILE[] = __FILE__;
15 #endif
16
17 //Globals
18
19 //-----
20 // CUSBTestApp
21
22 BEGIN_MESSAGE_MAP(CUSBTestApp, CWinApp)
23 //[[AFX_MSG_MAP(CUSBTestApp)
24 // NOTE - the ClassWizard will add and remove mapping macros here.
25 // DO NOT EDIT what you see in these blocks of generated code!
26 //]]AFX_MSG
27 ON_COMMAND(ID_HELP, CWinApp::OnHelp)
28 END_MESSAGE_MAP()
29
30 // CUSBTestApp construction
31
32 CUSBTestApp::CUSBTestApp()
33 {
34 // TODO: add construction code here,
35 // Place all significant initialization in InitInstance
36 }
37
38 // The one and only CUSBTestApp object
39
40 CUSBTestApp theApp;
41
42 CUSBTestApp::InitInstance()
43 {
44 // Standard initialization
45 // If you are not using these features and wish to reduce the size
46 // of your final executable, you should remove from the following
47 // the specific initialization routines you do not need.
48
49 #ifdef _AFXDLL
50 #include "AfxWinInit.h"
51 AfxWinInit(
52 // Call this when using MFC in a shared DLL
53 // Enable3dControlsStatic(); // Call this when linking to MFC statically
54 #endif
55
56 CUSBTestDlg dlg;
57 m_pMainWnd = &dlg;
58 int nResponse = dlg.DoModal();
59 if (nResponse == IDOK)
60 {
61
62
63
64
65
66
67

```

```

c:\Documents and Settings\GerardoWy ... \SM (MIT)\Thesis\Code\Example\USBtest.cpp 2
68 // TODO: Place code here to handle when the dialog is
69 // dismissed with OK
70 }
71 else if (nResponse == IDCANCEL)
72 {
73 // TODO: Place code here to handle when the dialog is
74 // dismissed with Cancel
75 }
76
77 // Since the dialog has been closed, return FALSE so that we exit the
78 // application, rather than start the application's message pump.
79 return FALSE;
80 }

```

```
// USbstestDlg.cpp : Implementation file
#include "stdafx.h"
#include "USbstest.h"
#include "USbstestDlg.h"
#include "fd2xx.h"
#include <stdio.h>

#ifdef _DEBUG
#define new DEBUG_NEW
#undef THIS_FILE
static char THIS_FILE[] = __FILE__;
#endif

#pragma region Definitions
#define BYTES_TO_READ 1000
#define BYTES_TO_SEND 45
#define SOF_BYTES 2
#define EOF_BYTES 2
#define REFLASH_ALL_INST 0xA0
#define REFLASH_INST 0xA1
#define RESET_SKIN_INST 0xA4
#define EXECUTE_CODE_INST 0xA6
#define REFLASH_DEV_INST 0xA8
#define RESET_DEV_INST 0xAA
#define START_SAMPLING_INST 0xAC
#define STOP_SAMPLING_INST 0xAE
#define BYTES_PER_LINE 2
#pragma endregion

#pragma region Globals
//Globals
bool m_bConnect=false;
bool m_bSampling=false;
DWORD numbevs;
CFile sampleFile;
int x=0, y=0;
int running;
int bConnectPresent;
int busBusy;
short R_Add;
HDEVNOTIFY *hdev=NULL;
int m_SpinValue;
CWinThread* pWinThread;
#pragma endregion

#pragma region AboutDlg
// AboutDlg dialog used for App About
class CAboutDlg : public CDialog
{
public:
    CAboutDlg();

// Dialog Data
    ///{{AFX_DATA(CAboutDlg)
    enum { IDD = IDD_ABOUTBOX };
    ///}}AFX_DATA

    // ClassWizard generated virtual function overrides
    protected:
    virtual void DoDataExchange(CDataExchange* pDX);    // DDX/DDV support
    ///}}AFX_VIRTUAL

    protected:
    // Implementation
    ///{{AFX_MSG(CAboutDlg)
    ///}}AFX_MSG
};
```

```
DECLARE_MESSAGE_MAP()
};

CAboutDlg::CAboutDlg() : CDialog(CAboutDlg::IDD)
{
    ///{{AFX_DATA_INIT(CAboutDlg)
    ///}}AFX_DATA_INIT
}

void CAboutDlg::DoDataExchange(CDataExchange* pDX)
{
    CDialog::DoDataExchange(pDX);
    ///{{AFX_DATA_MAP(CAboutDlg)
    ///}}AFX_DATA_MAP
}

BEGIN_MESSAGE_MAP(CAboutDlg, CDialog)
    ///{{AFX_MSG_MAP(CAboutDlg)
    ///}}AFX_MSG_MAP
END_MESSAGE_MAP()
#pragma endregion

//Application Constructor
CUSBtestDlg::CUSBtestDlg(CWnd* pParent /*=NULL*/)
{
    CDialog(CUSBtestDlg::IDD, pParent)
    ///{{AFX_DATA_INIT(CUSBtestDlg)
    ///}}AFX_DATA_INIT
    m_hDevice = NULL;
    m_Nodes = 0;
    m_Address = _T("");
    m_NodesDesc = _T("");
    m_NumRecd = 0;
    m_128status = _T("");
    m_NameMbr = _T("FTDI USB Chip.");
    m_SetDesc = _T("");
    m_NodesDesc = _T("");
    m_EditSpin = _T("8");
    m_SpinValue = 8;
    ///}}AFX_DATA_INIT
    // Note that Loadicon does not require a subsequent Destroyicon in Win32
    m_hIcon = AfxGetApp()->LoadIcon(IDR_MAINFRAME);
}

//Synchronize window values
void CUSBtestDlg::DoDataExchange(CDataExchange* pDX)
{
    CDialog::DoDataExchange(pDX);
    ///{{AFX_DATA_MAP(CUSBtestDlg)
    DDX_Control(pDX, IDC_EDIT1, m_EditSpin);
    DDX_Text(pDX, IDC_EDIT_PORT_STATUS, m_PortStatus);
    DDX_Text(pDX, IDC_EDIT_NUM_REC, m_NumRecd);
    DDX_Text(pDX, IDC_EDIT_NAME_NUMBER, m_NameMbr);
    DDX_Text(pDX, IDC_EDIT_ADDRESS, m_Address);
    DDX_Text(pDX, IDC_EDIT_NODES, m_NodesDesc);
    DDX_Text(pDX, IDC_EDIT1, m_EditSpin);
    DDX_Control(pDX, IDC_SPIN, m_Spin);
    ///}}AFX_DATA_MAP

    //Message map
    #pragma region Message_Map
    BEGIN_MESSAGE_MAP(CUSBtestDlg, CDialog)
        ///{{AFX_MSG_MAP(CUSBtestDlg)
        //ON_WM_DEVICECHANGE()
        ///}}
    END_MESSAGE_MAP()
    #pragma endregion
};
```

```
c:\Documents and Settings\Gerardo\My ... (MIT)\Thesis\Code\Example1\USCTestDlg.cpp
```

3

```
ON_WM_SYSCOMMAND()
ON_WM_PAINT()
ON_WM_QUEYDRAGICON()
ON_WM_TIMER()
ON_WM_CLOSE()
ON_WM_DEVICECHANGE()
ON_BN_CLICKED(IDC_BUTTON_SENDFILE, OnButtonSendFile)
ON_BN_CLICKED(IDC_BUTTON_CLEAR, OnButtonClear)
ON_BN_CLICKED(IDC_BUTTON_OPEN, OnButtonOpen)
ON_BN_CLICKED(IDC_BUTTON_RESET, OnButtonReset)
ON_BN_CLICKED(IDC_BUTTON_RS, OnButtons)
ON_BN_CLICKED(IDC_BUTTON_LN_NODES, OnButtons)
ON_BN_CLICKED(IDC_BUTTON_NAME_NODES, OnButtons)
ON_BN_CLICKED(IDC_RADIO_SERIAL, OnRadioSerial)
ON_BN_CLICKED(IDC_RADIO_SERNUM, OnRadioSernum)
ON_BN_CLICKED(IDC_RADIO_DEVNO, OnRadioDevno)
ON_BN_CLICKED(IDC_RADIO_ALL_NODES, OnRadioAllNodes)
ON_BN_CLICKED(IDC_RADIO_SINGLE_NODE, OnRadioSingleNode)
ON_BN_CLICKED(IDC_BUTTON_LIST, OnButtonList)
ON_BN_CLICKED(IDC_BUTTON_STOP, OnButtonStop)
ON_BN_CLICKED(IDC_BUTTON_STOP, OnButtonStop)
ON_EN_CHANGE(IDC_EDIT_NAME_NUMBER, OnChangeEdiNameNumber)
ON_EN_CHANGE(IDC_EDIT_ADDRESS, OnChangeEdiAddress)
ON_NOTIFY(LVN_ITEMCHANGED, IDC_LIST2, &CUSCTestDlg::OnVitemchangedList2)
END_MESSAGE_MAP()

#pragma endregion
//APPLICATION MESSAGE HANDLERS
//Window Messages
BOOL CUSCTestDlg::OnInitDialog()
{
    CDialog::OnInitDialog();

    CRect rect;

    // Get size and position of the picture control
    GetDlgItem(IDC_OPENB)->GetWindowRect(rect);

    // Convert screen coordinates to client coordinates
    ScreenToClient(rect);

    // Create OpenGL Control window
    m_opglWindow.Create(rect, this);

    // Setup the OpenGL Window's timer to render
    m_opglWindow.m_unpTimer = m_opglWindow.SetTimer(1, 1, 0);

    // Add "About..." menu item to system menu.
    // NOTE: The pointer to this menu item is stored in the system menu's range.
    ASSERT(IDM_ABOUTBOX & 0xF000 != IDM_ABOUTBOX);
    ASSERT(IDM_ABOUTBOX < 0xF000);

    CMenu* pSysMenu = GetSystemMenu(FALSE);
    if (pSysMenu != NULL)
    {
        CString strAboutMenu;
        strAboutMenu.LoadString(IDS_ABOUTBOX);
        if (!strAboutMenu.IsEmpty())
        {
            pSysMenu->AppendMenu(MF_SEPARATOR);
            pSysMenu->AppendMenu(MF_STRING, IDM_ABOUTBOX, strAboutMenu);
        }
    }

    // Set the icon for this dialog. The framework does this automatically
    // when the application's main window is not a dialog
}
```

```
c:\Documents and Settings\Gerardo\My ... (MIT)\Thesis\Code\Example1\USCTestDlg.cpp
```

4

```
SetIcon(m_hIcon, TRUE); // Set big icon
SetIcon(m_hIcon, FALSE); // Set small icon

// TODO: Add extra initialization here
Buttons(OFF);//turn em off till a port is active
GetDlgItem(IDC_EDIT_ADDRESS)->EnableWindow(FALSE);

bus busy=0;
board present=0;
SetTimer(15, 100, NULL);//check for new USB data in the buffer every 100ms
rand((unsigned)time(0));

//read the last settings from the registry
m_Desc = AfxGetApp()->GetProfileInt("MyUSCTestApp", "SerDesc", 0);//default to Description
m_Spin.SetRange(4, 8);

if(m_SerDesc==0)
    m_NameNmbr = AfxGetApp()->GetProfileString("MyUSCTestApp", "DescString", "FTDI USB Chip-");
if(m_SerDesc==1)
    m_NameNmbr = AfxGetApp()->GetProfileString("MyUSCTestApp", "SerialString", "FTDI USB Chip-");
if(m_SerDesc==2)
    m_NameNmbr = AfxGetApp()->GetProfileString("MyUSCTestApp", "DevNmbr", "FTDI USB Chip-");

UpdateData(FALSE);

//Load DLL
LoadDll();

//Register for device notification
CUSCTestDlg::RegisterNotification(hdn);

//List Devices
OnButtonList();

return TRUE; // return TRUE unless you set the focus to a control
}

void CUSCTestDlg::RegisterNotification(HDEVNOTIFY *hDevNotify)
{
    DEV_BROADCAST_DEVICEINTERFACE NotificationFilter={0};

    //ZeroMemory(&NotificationFilter, sizeof(NotificationFilter));
    NotificationFilter.cbSize = sizeof(NotificationFilter);
    NotificationFilter.dwClassid = GUID_DEVINTERFACE_USB_DEVICE;
    hDevNotify = (void **)&RegisterDeviceNotification(GetSafeHwnd(), &NotificationFilter, DEVICE_NOTIFY_WINDOW_HANDLE);
}

void CUSCTestDlg::UnregisterNotification(HDEVNOTIFY *hDevNotify)
{
    if(NULL != hDevNotify)
    {
        UnregisterDeviceNotification(hDevNotify);
        hDevNotify = NULL;
    }
    void CUSCTestDlg::OnOK()
    {
        UnregisterNotification(hdn);
        //terminate the thread
    }
}
```

c:\Documents and Settings\Gerardo\My ... (MIT)\Thesis\Code\Example1\USStestDlg.cpp

5

```
m_sampling=0;
CDialog::
FreeLibrary(m_hmodule);

CDialog::OnOK();
}

void CUSStestDlg::OnSysCommand(UINT nID, LPARAM lParam)
{
    if ((nID & 0xFFFF) == IDM_ABOUTBOX)
    {
        CAboutDlg dlgAbout;
        dlgAbout.DoModal();
    }
    else
    {
        CDialog::OnSysCommand(nID, lParam);
    }
}

void CUSStestDlg::OnPaint()
{
    if (IsIconic())
    {
        CPaintDC dc(this); // device context for painting

        SendMessage(WM_ICONERASEBKGND, (LPARAM) dc, GetSafeHdc(), 0);

        // Center icon in client rectangle
        int cxIcon = GetSystemMetrics(SM_CXICON);
        int cyIcon = GetSystemMetrics(SM_CYICON);
        GetClientRect(&rect);
        int x = (rect.Width() - cxIcon + 1) / 2;
        int y = (rect.Height() - cyIcon + 1) / 2;

        // Draw the icon
        dc.DrawIcon(x, y, m_hicon);
    }
    else
    {
        CDialog::OnPaint();
    }
}

HCURSOR CUSStestDlg::OnQueryDragIcon()
{
    return (HCURSOR) m_hicon;
}

void CUSStestDlg::OnTimer(UINT nIDEvent)
{
    unsigned char rx[600];
    DWORD ret_bytes;
    DWORD bytes_in_buf;
    FT_STATUS status;

    if (!board_present) return;

    //Don't interfere with another test
    if (bus_busy) return;

    //Is there data to read?
    status = GetQueueStatus(&bytes_in_buf);
    if (status != FT_OK)
    {
        UpdateData(TRUE);
    }
}
```

c:\Documents and Settings\Gerardo\My ... (MIT)\Thesis\Code\Example1\USStestDlg.cpp

6

```
m_PortStatus = _T("Device not Open yet");
CDialog::
BoardPresent=0;
UpdateData(FALSE);
UpdateWindow();

    bytes_in_buf = 0;

    //There is stuff to read, read it!
    if (bytes_in_buf)
    {
        status = Read(rx, bytes_in_buf<600 ? bytes_in_buf : 600, &ret_bytes);
        //Is there data to read?
        if ((status == FT_OK) || ((status == FT_IO_ERROR) && (ret_bytes > 0)))
        {
            if (ret_bytes)
            {
                CString str;
                str.Format("%d", ret_bytes);
                UpdateData(TRUE);
                for (DWORD x=0; x<ret_bytes; x++)
                {
                    m_NumRead++;
                    str.Format("%4d 0x%.2X", rx[x], rx[x]);
                    m_Received.AddString(str);
                }
            }
            UpdateData(FALSE);
            UpdateWindow();
        }
        /*if (m_sampling)
        {
            for (int x=0; x<m_SpinValue; x++)
            {
                for (int y=0; y<m_SpinValue; y++)
                {
                    height = 0.5f*rand()/(RAND_MAX + 1.0f);
                    m_oglWindow.setHeight(x, y, height);
                }
            }
        }*/
    }
    CDialog::OnTimer(nIDEvent);
}

void CUSStestDlg::OnClose()
{
    UnregisterHotNotification(hdn);
    OnOK();
}

BOOL CUSStestDlg::OnDeviceChange(UINT nEventType, DWORD_PTR dwData)
{
    switch(nEventType)
    {
        case DMT_DEVICEARRIVAL:
            // A device has been inserted and is now available.
            if ( ((DEV_BROADCAST_HDR *)dwData)->dbch_devicetype !=
                DMT_DEVTYPE_DEVICEINTERFACE )
            {
                break;
            }
            if ( ((DEV_BROADCAST_DEVICEINTERFACE *)dwData)->dbcc_classguid !=
                GUID_CLASS_USB_DEVICE )
            {
                break;
            }
            // set/reset connection flag
            OnButtonList();
    }
}
```

```

m_Connect = TRUE;
break;
case DFT_DEVICE_REMOVE_COMPLETE:
    // Device has been removed.
    // Confirm this notify derives from the target device
    if ( ((IDEV_BROADCAST_HDR *)dwData)->dbch_devicetype !=
        DFT_DEVTYPE_DEVICEINTERFACE )
        break;
    if ( ((IDEV_BROADCAST_DEVICEINTERFACE *)dwData)->dbcc_classguid !=
        GUID_CLASS_USB_DEVICE )
        break;
    // set/reset connection flag
    m_Connect = !m_Connect;
    default:
        break;
}
return TRUE;
}
//Control Event Message Handlers
UINT ThreadProc(LPVOID param)//count up thread
{
    //typecast the handle to the parent window
    CUSBtestDig *pMyHnd1 = (CUSBtestDig *)param;
    unsigned char *xbuf[15*20], txbuf[3] = {START_SAMPLING_INST};
    DWORD ret_bytes;
    FT_STATUS status;
    CString str;
    writeBuf;
    DWORD bytes_in_buf=0;
    int values=0, x=0, y=0;
    int s_Add=261;
    while(m_sampling)
    {
        if (pMyHnd1->m_Nodes)
        {
            txbuf[1]=(BYTE)s_Add;
            txbuf[2]=((char*)&s_Add+1);
        }
        else
        {
            txbuf[1]=(BYTE)s_Add;
            txbuf[2]=((char*)&s_Add+1);
        }
        status=pMyHnd1->Purge(FT_PURGE_RX || FT_PURGE_TX);
        status = pMyHnd1->Write(txbuf, 3, &ret_bytes);
        while(bytes_in_buf != 5) pMyHnd1->GetQueueStatus(&bytes_in_buf);
        status = pMyHnd1->Read(txbuf, 5, &ret_bytes);
        if (ret_bytes == 5)
        {
            value = txbuf[3]+256*txbuf[4];
            pMyHnd1->m_NumRecd+=ret_bytes;
            for (int i=0; i<ret_bytes; i++)
            {
                str.Format("%04.0x %2x", txbuf[i], txbuf[i+1]);
                pMyHnd1->m_Received.AddString(str);
            }
            itoa(value, valueBuf, 10);
            writeBuf=(CString)valueBuf+"\t";
            if(m_sampling) sampleFile.Write(writeBuf.GetBuffer(), writeBuf.GetLength());
            pMyHnd1->m_OsWindow.SetHeight(x,y, 20*value/4096);
            if (s_Add == 273) && (pMyHnd1->m_Nodes)
            {
                s_Add=261;
                if(m_sampling) sampleFile.Write("\n", strlen("\n"));
            }
        }
    }
}

```

```

{
    if (pMyHnd1->m_Nodes)
    {
        if (m_sampling) sampleFile.Write("\n", strlen("\n"));
    }
    if (pMyHnd1->m_Nodes)
    {
        x=(x+1)%4;
        if(x==0) y=(y+1)%3;
        //Sleep(100);
    }
    return 0;
}
void CUSBtestDig::Buttons(int onoff)
{
    if(onoff == OFF)
    {
        GetDlgItem(IDC_BUTTON_RS)->EnableWindow(FALSE);
        GetDlgItem(IDC_BUTTON_RESET)->EnableWindow(FALSE);
        GetDlgItem(IDC_BUTTON_SENDFILE)->EnableWindow(FALSE);
        GetDlgItem(IDC_BUTTON_START)->EnableWindow(FALSE);
        GetDlgItem(IDC_BUTTON_STOP)->EnableWindow(FALSE);
        GetDlgItem(IDC_BUTTON_EDIT_NAME)->EnableWindow(FALSE);
        GetDlgItem(IDC_BUTTON_RUN_NODES)->EnableWindow(FALSE);
        GetDlgItem(IDC_RADIO_ALL_NODES)->EnableWindow(TRUE);
        GetDlgItem(IDC_RADIO_SINGLE_NODE)->EnableWindow(FALSE);
    }
    if(onoff == ON)
    {
        GetDlgItem(IDC_BUTTON_RS)->EnableWindow(TRUE);
        GetDlgItem(IDC_BUTTON_RESET)->EnableWindow(TRUE);
        GetDlgItem(IDC_BUTTON_SENDFILE)->EnableWindow(TRUE);
        GetDlgItem(IDC_BUTTON_START)->EnableWindow(TRUE);
        GetDlgItem(IDC_BUTTON_STOP)->EnableWindow(TRUE);
        GetDlgItem(IDC_RADIO_SINGLE_NODE)->EnableWindow(TRUE);
        GetDlgItem(IDC_RADIO_ALL_NODES)->EnableWindow(FALSE);
    }
}
BOOL CUSBtestDig::OnCommand(WPARAM wParam, LPARAM lParam) //disable the ESC key
{
    if(wParam==2) return FALSE;
    return CDialog::OnCommand(wParam, lParam);
}
void CUSBtestDig::OnButtonClear()
{
    UpdateData(TRUE);
    m_NumRecd=0;
    m_Received.ResetContent();
    UpdateData(FALSE);
    UpdateWindow();
}
void CUSBtestDig::OnButtonOpen()
{
    unsigned char txbuf[3];
    int tries=0;
    DWORD ret_bytes=0;
    UpdateData(TRUE);
}

```

```

c:\Documents and Settings\Gerardo\My ... (MIT)\Thesis\Code\Example1\USTestDig.cpp 9

m_PortStatus = "(-reset-)";
UpdateData(FALSE);
UpdateWindow();

Close();

//open the device
FT_STATUS status = OpenBy();
if (status==0)
{
    m_PortStatus = _T("Brain not Found!");
    board_present=0;
}
else
{
    status=ResetDevice();
    status=Purge(FT_PURGE_RX || FT_PURGE_TX);
    status=ResetDevice();
    SetTimeouts(3000, 3000);//extend timeout while board finishes reset
    Sleep(150);

    //test for presence of board
    txbuf[0] = 0x80;
    Write(txbuf, 1, &ret_bytes);
    //Read(txbuf, 1, &ret_bytes);
    //if (ret_bytes==0) //no response maybe windows was busy... read it again
    //Read(txbuf, 1, &ret_bytes);

    m_PortStatus = _T("Brain Ready!");
    Buttons(ON);//turn em off till a port is active
    board_present=1;
}

SetTimeouts(300, 300);
UpdateData(FALSE);
UpdateWindow();
}

void CUSTestDig::OnButtonEndFile()
{
    DWORD ret_bytes;
    FILE *codeFile;
    unsigned char* instatBuf=txBuf;
    UINT lBytesRead=0, nBytes, address[2], data[16], checksum, i, index=1;
    unsigned char fileBuf[1000];

    //Ask user for the code file
    CFileDialog fileOpenDlg(TRUE, NULL, NULL, OFN_OVERWRITEPROMPT, "MSF430 Compiled Code (*.*)",
        NULL, NULL, CFileDialog::FD_OPEN);
    if (fileOpenDlg.DoModal() != IDOK)
        return;
    FileName = FileOpenDlg.GetFileName();

    if (lRet == IDOK)
    {
        m_Received.ResetContent();
        //Open The File
        codeFile = fopen(FileOpenDlg.GetPathName(), "r");
        if (m_Nodes)
        {
            fileBuf[1]=(BYTE)0;
            fileBuf[2]='*'+((char*)&R_Add+1);
            index+=2;
        }
        //Parse text file
    }
}

```

```

c:\Documents and Settings\Gerardo\My ... (MIT)\Thesis\Code\Example\USTestDig.cpp 10

while (fscanf(codeFile, "%*1s %2x %2x %*2x", &nBytes, &address[0], &address[1]) != EOF)
{
    if (nBytes != 0)
    {
        fileBuf[index]=(char)nBytes;
        fileBuf[index+1]=(char)&address[0];
        fileBuf[index+2]=(char)&address[1];
        index+=3;
        for (i=0; i < nBytes; i++)
        {
            lBytesRead = fscanf(codeFile, "%2x", &data[i]);
            fileBuf[index+i]=(char)data[i];
        }
        lBytesRead = fscanf(codeFile, "%2x", &checksum);
        fileBuf[index+i]=(char)checksum;
        index+=i+1;
    }
    else lBytesRead = fscanf(codeFile, "%*1x", &nBytes);
}
//Close file
fclose(codeFile);

//Configure File Buffer
if(m_Nodes) fileBuf[0]=REFLASH_DEV_INST;
else fileBuf[0]=REFLASH_ALE_INST;
//Flush Buffer
FT_STATUS status=Purge(FT_PURGE_RX || FT_PURGE_TX);
//Send frame
Write(fileBuf, index, &ret_bytes);
}

void CUSTestDig::OnButtonReset()
{
    DWORD ret_bytes;
    unsigned char txbuf[3];
    int txBytes=1;
    unsigned char* instatBuf=txBuf;
    unsigned char* instatBuf=txBuf;

    Purge(FT_PURGE_RX || FT_PURGE_TX);
    //Send Reset Instruction
    FT_STATUS status = Write(instatBuf, 1, &ret_bytes);
    if (status != FT_OK) MessageBox("Error Sending Instruction");
}

void CUSTestDig::OnButtonRes()
{
    DWORD ret_bytes;
    unsigned char txbuf[3];
    int txBytes=1;
    Purge(FT_PURGE_RX || FT_PURGE_TX);
    //Send Reset Instruction
    //if (m_Nodes)
    {
        txbuf[1]=(BYTE)0;
        txbuf[2]='*'+((char*)&R_Add+1);
        txbuf[0]=RESET_DEV_INST;
        txBytes = 3;
    }
    //else
    {
        txbuf[0]=RESET_SKIN_INST;
        FT_STATUS status = Write(txbuf, txBytes, &ret_bytes);
        if (status != FT_OK) MessageBox("Error Sending Instruction");
    }
    // TODO: Add your control notification handler code here
}

```



```

c:\Documents and Settings\Gerardo\My ... (MIT)\Thesis\Code\Example1\USBTestDlg.cpp
1
void USBTestDlg::OnButtonRunNodes()
{
    DWORD ret_bytes;
    unsigned char txBuf[EXECUTE_CODE_INST];
    unsigned char* txBufBuf=&txBuf;

    Purge(FT_PURGE_RX || FT_PURGE_TX);
    //Send Reset Instruction
    int i=3;
    while(i>0)
    {
        if (status != FT_OK) MessageBox("Error Sending Instruction: 0x24");
        //Send 3 times the instruction
        ret_bytes = Write(txBuf, 1, &ret_bytes);
        if (status != FT_OK) MessageBox("Error Sending Instruction: 0x24");
    }

    void USBTestDlg::OnButtonStart()
    {
        int nBytesLeft;
        CString fileName="";

        if (board_present)
        {
            //Open a file to write data read from nodes
            CFHidIoctl FILE_DEVICE_BINARY, FALSE, NULL, NULL, OPEN_OVERWRITEPROMPT, "Skin Sensor Data (*.*)";
            xla["*.xls"]all files (*.*) (*.*)";
            int iRet = FileOpenDlg.DoModal();
            if (iRet == FileOpenDlg.DoModal())
            {
                FileName = FileOpenDlg.GetFileName();
                if (FileName.Find(".xls") == -1) FileName += ".xls";

                if ((iRet == IDOK) && (FileName != ""))
                {
                    //Open the file
                    m_sampling = true;
                    bool file = sampleFile.Open(FileName, CFFile::modeCreate|CFFile::modeWrite);
                    if (file)
                    {
                        ButtonsOff();
                        GetDlgItem(IDC_BUTTON_LIST)->EnableWindow(FALSE);
                        GetDlgItem(IDC_BUTTON_OPEN)->EnableWindow(FALSE);

                        GetDlgItem(IDC_BUTTON_STOP)->EnableWindow(TRUE);
                        //Get the file
                        Purge(FT_PURGE_TX);
                        KillTimer(15);
                        OnButtonRunNodes();
                        pthread = AfxBeginThread(ThreadProc1, this);
                        //else MessageBox("Error Sending Instruction");
                        OnButtonClear();
                    }
                    else MessageBox("Error: file could not be created");
                }
            }
        }

        void USBTestDlg::OnButtonStop()
        {
            DWORD ret_bytes;
            unsigned char txBuf[3]={STOP_SAMPLING_INST};
            Purge(FT_PURGE_TX);

            m_sampling = false;
            //Send instruction to stop sampling
            FT_STATUS status = Write(txBuf, 1, &ret_bytes);

            //Close file
            sampleFile.Close();
            OnButtonClear();
            GetDlgItem(IDC_BUTTON_LIST)->EnableWindow(TRUE);
            GetDlgItem(IDC_BUTTON_OPEN)->EnableWindow(TRUE);
            GetDlgItem(IDC_BUTTON_STOP)->EnableWindow(TRUE);
        }
    }
}

```

```

c:\Documents and Settings\Gerardo\My ... (MIT)\Thesis\Code\Example\USBTestDlg.cpp
12
GetDlgItem(IDC_BUTTON_STOP)->EnableWindow(FALSE);
}
void CUSBTestDlg::OnRadioOnNameNum()
{
    CWinApp* pApp = AfxGetApp();
    //write the new setup to the registry
    pApp->WriteProfileInt("MyUSBTestApp", "SerDesc", 0);
    UpdateData(TRUE);
    m_NameNbr = AfxGetApp()->GetProfileString("MyUSBTestApp", "DevNbr", "FTDI USB Chip.
    .");
    UpdateData(FALSE);
    UpdateWindow();
}

void CUSBTestDlg::OnRadioSernum()
{
    CWinApp* pApp = AfxGetApp();
    //write the new setup to the registry
    pApp->WriteProfileInt("MyUSBTestApp", "SerDesc", 1);
    UpdateData(TRUE);
    m_NameNbr = AfxGetApp()->GetProfileString("MyUSBTestApp", "SerialString", "FTDI USB
    Chip.
    .");
    UpdateData(FALSE);
    UpdateWindow();
}

void CUSBTestDlg::OnRadioDevno()
{
    CWinApp* pApp = AfxGetApp();
    //write the new setup to the registry
    pApp->WriteProfileInt("MyUSBTestApp", "SerDesc", 2);
    UpdateData(TRUE);
    m_NameNbr = AfxGetApp()->GetProfileString("MyUSBTestApp", "DevNbr", "FTDI USB Chip.
    .");
    UpdateData(FALSE);
    UpdateWindow();
}

void CUSBTestDlg::OnRadioAllNodes()
{
    if (board_present)
    {
        GetDlgItem(IDC_BUTTON_START)->EnableWindow(TRUE);
        GetDlgItem(IDC_BUTTON_SENDFILE)->EnableWindow(TRUE);
        GetDlgItem(IDC_EDIT_ADDRESS)->EnableWindow(FALSE);
    }
}

void CUSBTestDlg::OnRadioSingleNode()
{
    if ((R_Add >= 1) && (R_Add <= 1023))
    {
        GetDlgItem(IDC_BUTTON_SENDFILE)->EnableWindow(TRUE);
        GetDlgItem(IDC_BUTTON_EDIT_ADDRESS)->EnableWindow(TRUE);
    }
    else
    {
        GetDlgItem(IDC_BUTTON_SENDFILE)->EnableWindow(FALSE);
        GetDlgItem(IDC_BUTTON_EDIT_ADDRESS)->EnableWindow(FALSE);
    }
}

void CUSBTestDlg::OnRadioSingleNode()
{
    if ((R_Add >= 1) && (R_Add <= 1023))
    {
        GetDlgItem(IDC_BUTTON_SENDFILE)->EnableWindow(TRUE);
        GetDlgItem(IDC_BUTTON_EDIT_ADDRESS)->EnableWindow(TRUE);
    }
    else
    {
        GetDlgItem(IDC_BUTTON_SENDFILE)->EnableWindow(FALSE);
        GetDlgItem(IDC_BUTTON_EDIT_ADDRESS)->EnableWindow(FALSE);
    }
}

```

```

}

void CUSTestDlg::OnButtonList()
{
    //search for Descriptions or Serial Numbers depending on the current mode
    FT_STATUS ftStatus;

    Clone(); //must be closed to perform the ListDevices() function
    UpdateData(TRUE);
    m_PortStatus = _T("Devices Closed.");
    m_NumDevs=0;
    m_NumDevs = 0;
    m_NumDevs = 0;
    UpdateData(FALSE);
    UpdateWindow();

    ftStatus = ListDevices(knumDevs, NULL, FT_LIST_NUMBER_ONLY);
    if (ftStatus == FT_OK)
    {
        // FT_ListDevices OK, show number of devices connected in list box
        CString str;
        str.Format("%d device(s) attached", (int)numDevs);
        m_Received.AddString(str);

        //if current mode is open "by device #" then list device numbers
        if (((m_SerDesc==2) && (numDevs>0))
        {
            for (DWORD d=1; d<=numDevs; d++)
            {
                str.Format("%s", d);
                m_Received.AddString(str);
            }
        }

        //if current mode is open "by description" then list descriptions of all connected
        devices
        if (((m_SerDesc==0) && (numDevs>0))
        {
            ftStatus = ListDevices(knumDevs, NULL, FT_LIST_NUMBER_ONLY);
            if (ftStatus == FT_OK)
            {
                char *BufPtrs[64]; // pointer to array of 64 pointer
                DWORD d=0;

                for (d=0; d<numDevs; d++){
                    BufPtrs[d] = new char[64];
                }
                BufPtrs[d] = NULL;

                ftStatus = ListDevices(BufPtrs, knumDevs, FT_LIST_ALL|
FT_OPEN_BY_DESCRIPTION);
                if (FT_SUCCESS(ftStatus))
                {
                    for (DWORD u=0; u<numDevs; u++)
                    {
                        str.Format("%s", BufPtrs[u]);
                        m_Received.AddString(str);
                    }
                }
                else
                {
                    str.Format("ListDevices failed");
                    m_Received.AddString(str);
                }
            }
        }
    }
}

```

```

//free ram to avoid memory leaks
for (d=0; d<numDevs; d++)
{
    delete BufPtrs[d];
}

//if current mode is open "by serial number" the list descriptions
//of all connected devices
if ((m_SerDesc==1) && (numDevs>0))
{
    //AFXMessageBox("by serial.");
    ftStatus = ListDevices(knumDevs, NULL, FT_LIST_NUMBER_ONLY);
    if (ftStatus == FT_OK)
    {
        DWORD d=0;
        for (d=0; d<numDevs; d++){
            BufPtrs[d] = new char[64];
        }
        BufPtrs[d] = NULL;

        ftStatus = ListDevices(BufPtrs, knumDevs, FT_LIST_ALL|
FT_OPEN_BY_SERIAL_NUMBER);
        if (FT_SUCCESS(ftStatus))
        {
            for (DWORD u=0; u<numDevs; u++)
            {
                str.Format("%s", BufPtrs[u]);
                m_Received.AddString(str);
            }
        }
        else
        {
            str.Format("ListDevices failed");
            m_Received.AddString(str);
        }

        //free ram to avoid memory leaks
        for (d=0; d<numDevs; d++)
        {
            delete BufPtrs[d];
        }
    }

    if (numDevs == 1)
    {
        AfxGetApp()->WriteProfileString("MyUSTestApp", "DescString", str);
        OnButtonOpen();
    }
    if (numDevs == 0)
    {
        Buttons (OFF);
        m_connect = FALSE;
    }
    else
    {
        Buttons (ON);
    }
}
else
{
    // FT_ListDevices failed
    AfxMessageBox("FT_ListDevices failed");
}
}

```

```

}

void CUSBTestDlg::OnChangeEditNameNumber()
{
    UpdateData(TRUE);
    //write the new setup to the registry
    if(m_SerDesc==0)
        AfxGetApp()->WriteProfileString("MyUSBTestAp", "DescString", m_NameNbr);
    if(m_SerDesc==1)
        AfxGetApp()->WriteProfileString("MyUSBTestAp", "SerialString", m_NameNbr);
    if(m_AfxGetApp()->WriteProfileString("MyUSBTestAp", "DevNbr", m_NameNbr);

    if(m_NameNbr.GetLength() < 1) m_SerDesc = 2;
    UpdateData(FALSE);
    UpdateWindow();
}

void CUSBTestDlg::OnChangeEditAddress()
{
    UpdateData(TRUE);
    if(m_pOpenEx == NULL)
        if (board_present)
        {
            if ((R_Add >= 1) && (R_Add <= 1023))
            {
                GetDlgItem(IDC_BUTTON_SENDFILE)->EnableWindow(TRUE);
                GetDlgItem(IDC_BUTTON_START)->EnableWindow(TRUE);
            }
            else
            {
                GetDlgItem(IDC_BUTTON_SENDFILE)->EnableWindow(FALSE);
                GetDlgItem(IDC_BUTTON_START)->EnableWindow(FALSE);
            }
        }
    UpdateData(FALSE);
}

void CUSBTestDlg::LoadDLL()
{
    m_hModule = LoadLibrary("Ftd2xx.dll");
    if(m_hModule == NULL)
    {
        AfxMessageBox("Error: Can't Load ftd245.dll");
        return;
    }
    m_pWrite = (PrtToWrite)GetProcAddress(m_hModule, "FT_Write");
    if(m_pWrite == NULL)
    {
        AfxMessageBox("Error: Can't Find FT_Write");
        return;
    }
    m_pRead = (PrtToRead)GetProcAddress(m_hModule, "FT_Read");
    if(m_pRead == NULL)
    {
        AfxMessageBox("Error: Can't Find FT_Read");
        return;
    }
    m_pOpen = (PrtToOpen)GetProcAddress(m_hModule, "FT_Open");
    if(m_pOpen == NULL)

```

```

{
    AfxMessageBox("Error: Can't Find FT_Open");
    return;
}

m_pOpenEx = (PrtToOpenEx)GetProcAddress(m_hModule, "FT_OpenEx");
if(m_pOpenEx == NULL)
{
    AfxMessageBox("Error: Can't Find FT_OpenEx");
    return;
}

m_pListDevices = (PrtToListDevices)GetProcAddress(m_hModule, "FT_ListDevices");
if(m_pListDevices == NULL)
{
    AfxMessageBox("Error: Can't Find FT_ListDevices");
    return;
}

m_pClose = (PrtToClose)GetProcAddress(m_hModule, "FT_Close");
if(m_pClose == NULL)
{
    AfxMessageBox("Error: Can't Find FT_Close");
    return;
}

m_pResetDevice = (PrtToResetDevice)GetProcAddress(m_hModule, "FT_ResetDevice");
if(m_pResetDevice == NULL)
{
    AfxMessageBox("Error: Can't Find FT_ResetDevice");
    return;
}

m_pPurge = (PrtToPurge)GetProcAddress(m_hModule, "FT_Purge");
if(m_pPurge == NULL)
{
    AfxMessageBox("Error: Can't Find FT_Purge");
    return;
}

m_pSetTimeouts = (PrtToSetTimeouts)GetProcAddress(m_hModule, "FT_SetTimeouts");
if(m_pSetTimeouts == NULL)
{
    AfxMessageBox("Error: Can't Find FT_SetTimeouts");
    return;
}

m_pGetQueueStatus = (PrtToGetQueueStatus)GetProcAddress(m_hModule, "FT_GetQueueStatus");
if(m_pGetQueueStatus == NULL)
{
    AfxMessageBox("Error: Can't Find FT_GetQueueStatus");
    return;
}

void CUSBTestDlg::OnSelchangeList1()
{
    UpdateData(TRUE);
    int pos = m_Received.GetCursel();
    m_Received.GetText(pos, m_NameNbr);
    UpdateData(FALSE);
    UpdateWindow();
    if(m_SerDesc==0)
        AfxGetApp()->WriteProfileString("MyUSBTestAp", "DescString", m_NameNbr);
}

```

c:\Documents and Settings\Gerardo\My ... (MIT)\Thesis\Code\Example1\USSTestDlg.cpp 17

```

if(m_SerDesc==1)
    AfxGetApp()->WriteProfileString("MyUSSTestAp", "SerialString", m_NameNbr);
if(m_SerDesc==2)
    AfxGetApp()->WriteProfileString("MyUSSTestAp", "DevNbr", m_NameNbr);
}

void CUSSTestDlg::OnVnItemchangedList2(NMHDR *pNMHDR, LRESULT *pResult)
{
    LPNMListView_PNMHV = reinterpret_cast<LPNMListView>(pNMHDR);
    *pResult = 0;
    // TODO: Add your control notification handler code here
}

void CUSSTestDlg::OnVScroll(UINT nSBCode, UINT nPos, CScrollBar* pScrollBar)
{
    // TODO: Add your control notification handler code here
    m_ScrollWindow.SetMaxSize(nPos, nPos);
    //OnVScroll(nSBCode, nPos, pScrollBar);
}

#pragma region USB_DLL_Functions
//USB Driver function Definitions
FT_STATUS CUSSTestDlg::Read(LPVOID lpvBuffer, DWORD dwBufferSize, LPDWORD lpdwBytesRead)
{
    if (m_pRead)
    {
        AfxMessageBox("FT_Read is not valid!");
        return FT_INVALID_HANDLE;
    }
    return (*m_pRead)(m_ftHandle, lpvBuffer, dwBufferSize, lpdwBytesRead);
}

FT_STATUS CUSSTestDlg::Write(LPVOID lpvBuffer, DWORD dwBufferSize, LPDWORD lpdwBytes)
{
    if (m_pWrite)
    {
        AfxMessageBox("FT_Write is not valid!");
        return FT_INVALID_HANDLE;
    }
    return (*m_pWrite)(m_ftHandle, lpvBuffer, dwBufferSize, lpdwBytes);
}

FT_STATUS CUSSTestDlg::Open(PVOID pvDevice)
{
    if (m_pOpen)
    {
        AfxMessageBox("FT_Open is not valid!");
        return FT_INVALID_HANDLE;
    }
    return (*m_pOpen)(pvDevice, &m_ftHandle);
}

FT_STATUS CUSSTestDlg::OpenEx(PVOID pArg1, DWORD dwFlags)
{
    if (m_pOpenEx)
    {
        AfxMessageBox("FT_OpenEx is not valid!");
        return FT_INVALID_HANDLE;
    }
}

```

c:\Documents and Settings\Gerardo\My ... (MIT)\Thesis\Code\Example1\USSTestDlg.cpp 18

```

    }
    return (*m_pOpenEx)(pArg1, dwFlags, &m_ftHandle);
}

FT_STATUS CUSSTestDlg::ListDevices(PVOID pArg1, PWORD pArg2, DWORD dwFlags)
{
    if (m_pListDevices)
    {
        AfxMessageBox("FT_ListDevices is not valid!");
        return FT_INVALID_HANDLE;
    }
    return (*m_pListDevices)(pArg1, pArg2, dwFlags);
}

FT_STATUS CUSSTestDlg::Close()
{
    if (m_pClose)
    {
        AfxMessageBox("FT_Close is not valid!");
        return FT_INVALID_HANDLE;
    }
    return (*m_pClose)(m_ftHandle);
}

FT_STATUS CUSSTestDlg::ResetDevice()
{
    if (m_pResetDevice)
    {
        AfxMessageBox("FT_ResetDevice is not valid!");
        return FT_INVALID_HANDLE;
    }
    return (*m_pResetDevice)(m_ftHandle);
}

FT_STATUS CUSSTestDlg::Purge(ULONG dwMask)
{
    if (m_pPurge)
    {
        AfxMessageBox("FT_Purge is not valid!");
        return FT_INVALID_HANDLE;
    }
    return (*m_pPurge)(m_ftHandle, dwMask);
}

FT_STATUS CUSSTestDlg::SetTimeouts(ULONG dwReadTimeout, ULONG dwWriteTimeout)
{
    if (m_pSetTimeouts)
    {
        AfxMessageBox("FT_SetTimeouts is not valid!");
        return FT_INVALID_HANDLE;
    }
    return (*m_pSetTimeouts)(m_ftHandle, dwReadTimeout, dwWriteTimeout);
}

FT_STATUS CUSSTestDlg::GetQueueStatus(LPDWORD lpdwAmountInQueue)
{
    if (m_pGetQueueStatus)
    {

```

```

c:\Documents and Settings\Gerardo\My ... (MIT)\Thesis\Code\Example1\USHtestDlg.cpp 19
    AfxMessageBox(FT_GetQueueStatus is not valid!");
    return FT_INVALID_HANDLE;
}

return (m_pGetQueueStatus(m_ftHandle, lpdwAmountInBQueue);
}
#pragma endregion
FT_STATUS CUSHtestDlg::OpenBy()
{
    UpdateData(TRUE);

    if (m_SerDesc==0)
        m_NameNbr = AfxGetApp()->GetProfileString("MyUSHtestApp", "DescString", "FTDI USB
    if (m_SerDesc==1)
        m_NameNbr = AfxGetApp()->GetProfileString("MyUSHtestApp", "SerialString", "FTDI
    USB Chip.");
    if (m_SerDesc==2)
        m_NameNbr = AfxGetApp()->GetProfileString("MyUSHtestApp", "DevNbr", "FTDI USB
    Chip.");
    if (m_NameNbr == "")
    {
        //highlight the descriptor/serial number to draw attention...
        CEdit *pEdit;
        pEdit = (CEdit *)GetDlgItem(IDC_EDIT_NAME_NUMBER);
        pEdit->SetFocus();
        pEdit->SetSel(0, -1, FALSE);
        AfxMessageBox("You must enter a valid Brain Description or Serial Number.");
        return FT_DEVICE_NOT_OPENED;
    }

    FT_STATUS status;
    ULONG x=0;
    if (m_SerDesc==0)
        status = OpenEx(PVOID)(LPCTSTR)m_NameNbr, FT_OPEN_BY_DESCRIPTION;
    if (m_SerDesc==1)
        status = OpenEx(PVOID)(LPCTSTR)m_NameNbr, FT_OPEN_BY_SERIAL_NUMBER;
    if ((m_SerDesc==2) || (m_SerDesc==1))//if open by device OR no method was selected
    {
        if (m_NameNbr.GetLength() < 1)//nothing entered - open default device 0
        {
            status = Open(PVOID)x;//load default device 0
        }
        else
        {
            if (m_NameNbr.GetLength() > 21//no Open() method selected...
            {
                AfxMessageBox("You must enter a valid Brain Description or Serial Number.");
                return FT_DEVICE_NOT_OPENED;
            }
        }

        //convert string to decimal number and open(x)
        char str[3]; (LPCTSTR)m_NameNbr);
        strcpy(str, str);
        if ((x<0) || (x>64))
        {
            AfxMessageBox("You must enter a valid Brain Description or Serial Number.");
            return FT_DEVICE_NOT_OPENED;
        }
        status = Open(PVOID)x;
    }
}

```

```

c:\Documents and Settings\Gerardo\My ... (MIT)\Thesis\Code\Example1\USHtestDlg.cpp 20
    }
    return status;
}

```


Bibliography

- [1] John C. Ansel. Skin – nervous system interactions. *Dermatology Foundation*, 1:198–204, 1996.
- [2] Jessica Banks. Design and control of an anthropomorphic robotic finger with multi-point tactile sensation. Master’s thesis, Massachusetts Institute of Technology, 2001. 60
- [3] Richard Barry. Freertos modules, 2006. 80
- [4] Shekar Bhansali, H. Thurman Henderson, and Steven B. Hoath. Probing human skin as an information-rich smart biological interface using mems-based informatics. In SPIE, editor, *Proceedings of SPIE–the international society for optical engineering*, volume 4235. SPIE, 2001.
- [5] Athanassios Boulis. Design and implementation of a framework for efficient and programmable sensor networks. *Proceedings of the 1st international conference on Mobile systems, applications and services*, 1:187–200, 2003. 80
- [6] William Butera. *Programming a Paintable Computer*. PhD thesis, Massachusetts Institute of Technology, 2002. 24
- [7] E. Catterall, K. Van Laerhoven, and M. Strohbach. Self organization in ad hoc sensor networks: An empirical study, 2002.
- [8] Loren P. Clare. Multipoint sensing by intelligent collectives. In *The First Annual Symposium on Autonomous Intelligent Networks and Systems*. AINS, May 8-9 2002.
- [9] Adam Dunkels. The contiki operating system 2.x, 2006. 80
- [10] EFunda. Strain gage: Theoretical background. 61
- [11] Jonathan Engel, Jack Chen, and Chang Liu. Development of a multi-modal, flexible tactile sensing skin using polymer micromachining. In *Proc. of The 12th International Conference on Solid State Sensors, Actuators and Microsystems*. IEEE, June 2003. 30, 37
- [12] FTDI. Ft245bm designers guide version 2.0, 2003. 76

- [13] Ken Gilleo. *Handbook of Flexible Cicuits*. Van Nostrand Reinhold, 1992. 32, 44
- [14] Franz Graf. Features of the msp430 bootstrap loader, January 2003. 81
- [15] Vishay Measurements Group. Shunt calibration of strain gage instrumentation. 110
- [16] Vishay Measurements Group. Strain gage thermal output and gage factor variation with temperature. 114
- [17] Mitsuhiro HAKOZAKI, Atsushi HATORI, and Hiroyuki SHINODA. A sensitive skin using wireless tactile sensing elements. In *TECHNICAL DIGEST OF THE 18TH SENSOR SYMPOSIUM*, 2001. 28
- [18] M.B. Haris. New design of robotic tactile sensor using dynamic wafer technology based on vlsi technique. In *Biomedical Research in 2001*, 2001. 44
- [19] Charles A. Harper. *High Performance Printed Circuit Boards*. McGraw-Hill, 1999. 44
- [20] Falke M. Hendriks. *Mechanical behaviour of human epidermal and dermal layers in vivo*. Technische Universiteit Eindhoven,, 2005. 17
- [21] Robert D. Howe. Tactile sensing and control of robotic manipulation. *Journal of Robotic Manipulation*, 8:245–61, 1994.
- [22] Dimitris Hristu. The performance of a deformable-membrane tactile-sensor: basic results on geometrically-defined tasks. *IEEE Internationall Conference on Robotics and Automation*, 1:508–513, 2000. 28, 60
- [23] Vishay Inc. Strain gage selection. 45
- [24] Vishay Inc. Strain gage selection criteria procedures recommendations. 63
- [25] National Instruments. Lm20 temperature sensor datasheet, October 2005. 125
- [26] Texas Instruments. MSP430F1611 DATASHEET. 56
- [27] Texas Instruments. *MSP430Fx1xx User’s Guide*, 2006. 56
- [28] Future Technology Devices International. D2xx programmer’s guide, 2006. 93, 104
- [29] IPC. Adhesive coated dielectric films for use as cover sheets for flexible printed circuitry and flexible adhesive bonding films. Technical report, IPC, 2002. 46
- [30] IPC. Flexible metal-clad dielectrics for use in fabrication of flexible printed circuitry. Technical report, IPC, 2002. 46
- [31] IPC. Sectional design standard for rigid organic printed boards. Technical report, IPC, 2002. 51
- [32] T.J.C. Jacob, C.S. Fraser, L. Wang, V.E. Walker, and S. O’Connor. Psychophysical evaluation of responses to pleasant and mal-odour stimulation in human subjects; adaptation, dose response and gender differences. *International Journal of Psychophysiology*, 48:67–80, 2003. 42

- [33] Joseph Jacobson, B Comiskey, C Turner, J Albert, and P Tsao. The last book. *IBM Systems Journal*, 36:457–463, 1997. 34
- [34] Rodolphe Koehly, Denis Curtil, and Marcelo M. Wanderley. Paper fsrs and latex/fabric traction sensors: Methods for the development of home.made touch sensors. In *Proceedings of the 2006 International Conference on New Interfaces for Musical Expression*, 2006. 61
- [35] Stéphanie P. Lacour. Design and performance of thin metal film interconnects for skin-like electronic circuits. *IEEE Electron Device Letters*, 25:179–181, 2004. 34, 44
- [36] PhD Laura E. Edsberg, PhD Robert E. Mates, PhD Robert E. Baier, and ME Mark Lauren. Mechanical characteristics of human skin subjected to static versus cyclic normal pressures. *Journal of Rehabilitation Research and Development*, 36:1–5, 1999. 17
- [37] M.H. Lee and H.R. Nicholls. Tactile sensing for mechatronics – a state of the art survey. *Mechatronics*, 9:1–31, 1999. 28
- [38] Philip Levis. Tinyos 2.0 overview. 80
- [39] Joshua H. Lifton. Pushpin computing: a platform for distributed sensor networks. Master’s thesis, Massachusetts Institute of Technology, 2002. 26, 70
- [40] Joshua H. Lifton. Pushpin computing system overview: A platform for distributed, embedded, ubiquitous sensor networks. *Proceedings of the First International Conference on Pervasive Computing*, 1:139–151, 2002. 26, 80, 90
- [41] Joshua H. Lifton. Distributed sensor networks as sensate skin. In *Sensors, 2003. Proceedings of IEEE*, 2003. 25, 69
- [42] D. Um; V. Lumelsky. Fault tolerance via component redundancy for a modularized sensitive skin. In *Proceedings of the 1999 IEEE International Conference on Robotics & Automation*, 1999.
- [43] Vladimir J. Lumelsky. Sensitive skin. *IEEE Sensors Journal*, 1:41–51, 2001. 18, 28, 37
- [44] Sergio Maximilian. A textile based capacitive pressure sensor. *Sensor Letters*, 2:153–160, 2004. 30, 60
- [45] Claudio Melchiorri. Tactile sensing for robotic manipulation. *The International Journal of Robotics Research*, 0:25–36, 1990. 28
- [46] Minco. Flex-circuit design guide. 11, 34, 47, 49
- [47] Minco. Flex circuits. web, December 2002. 44
- [48] Omega. The strain gage. 62
- [49] T.V. Papakostas. A large area force sensor for smart skin applications. In *Proceedings of the 1st IEEE Sensors Conference*, 2002. 30, 44

- [50] Joseph A. Paradiso, Joshua Lifton, and Michael Broxton. Sensate media multimodal electronic skins as dense sensor networks. *BT Technology Journal*, 22:32–44, 2004. 18
- [51] Joseph A. Paradiso, Joshua Lifton, and Michael Broxton. Sensate media: Multimodal electronic skins as dense sensor networks. *BT Technology Journal*, 22:32–44, 2004.
- [52] Peratech. 11, 66
- [53] Peratech. Integration guide. 67
- [54] Philips. The i2c-bus specification. Technical report, Philips, January 2000. 40
- [55] Philips. The i2c-bus and how to use it (including specifications), April 2001. 134
- [56] Seppo Pohja. Survey of studies on tactile senses. Technical report, European Research Consortium for Informatics and Mathematics at SICS, 2001. 18, 59
- [57] Niels Reijers. Efficient code distribution in wireless sensor networks. *Proceedings of the 2nd ACM international conference on Wireless sensor networks and applications*, 2:60–67, 2003. 80
- [58] Jun Rekimoto. Smartskin: an infrastructure for freehand manipulation on interactive surfaces. In *Proceedings of the SIGCHI conference on Human factors in computing systems: Changing our world, changing ourselves*, 2002. 28
- [59] Bruce Richardson, Krispin Leydon, Mikael Fernstrom, and Joseph A. Paradiso. Z-tiles: building blocks for modular, pressure-sensing floorspaces. In *CHI '04: CHI '04 extended abstracts on Human factors in computing systems*, 2004. 132
- [60] Doug Richardson. Smart skins and structures. *Armada International*, 22:50–56, 1998.
- [61] D. De Rossi. Electroactive fabrics for distributed, conformable and interactive systems. *Sensors, 2002. Proceedings of IEEE*, 2:1608–1613, 2002. 60
- [62] Takao Someya. Integration of organic field-effect transistors and rubbery pressure sensors for artificial skin applications. In *Electron Devices Meeting IEDM '03 Technical Digest.*, 2003. 30
- [63] Measurement Specialties. Piezo film sensors technical manual, 1999. 70
- [64] Thomas H. Stearns. *Flexible Printed Circuitry*. McGraw-Hill, 1995. 44
- [65] W.D. Stiehl, Lalla L., and Cynthia. Breazeal. A "somatic alphabet" approach to "sensitive skin". In *Robotics and Automation, 2004. Proceedings. ICRA '04. 2004 IEEE International Conference on*, 2004. 26
- [66] Johan Tegin and Jan Wikander. Tactile sensing in intelligent robotic manipulation. *The Industrial robot*, 32:64–70, 2005.
- [67] Toshiba. Tps851 datasheet, 2004. 71

- [68] Vilis Tutis. The physiology of the senses transformations for perception and action. web. 42
- [69] D. Um, B. Stankovic, K. Giles, T. Hammond, and V. Lumelsky. A modularized sensitive skin for motion planning in uncertain environments. In *Proceedings of the 1998 IEEE International Conference on Robotics & Automation*, 1998. 28, 37, 49
- [70] Shawna Vogel. Smart skin. *Discover*, 11:26, 1990.
- [71] Ravindra Wijesiriwardana. Inductive fiber-meshed strain and displacement transducers for respiratory measuring systems and motion capturing systems. *IEEE SENSORS JOURNAL*, 6:571–579, 2006. 60
- [72] Adrian C Williams. *Transdermal and Topical Drug Delivery*. Pharmaceutical Press, 2003. 17
- [73] Tom Woznicki. Flex circuits news. 46
- [74] Yong Xu, Yu-Chong Tai, Adam Huang, and Chih-Ming Ho. Ic-integrated flexible shear-stress sensor skin. In *Solid-State Sensor, Actuator and Microsystems Workshop*, 2002. 30
- [75] Kouichi Yamada, Kenji Goto, Yoshiki Nakajima, and Nobuyoshi Koshida. A sensor skin using wire-free tactile sensing elements based on optical connection. *SICE -ANNUAL CONFERENCE*, 41:131–134, 1999. 28, 60
- [76] Yamada Yoji, Takashi Maeno, Isao Fujimoto, Tetsuya Morizono, and Yoji Umetani. Identification of incipient slip phenomena based on the circuit output signals of pvdf film strips embedded in artificial finger ridges. *TRANSACTIONS - Society of Instruments and Control Engineers*, 40:648–655, 2004. 60